Universidade do Minho
Escola de Engenharia

Pedro Ferreira da Costa

Development of advanced cell/tissue culture systems, based on enhanced polymeric scaffolds and sophisticated bioreactors, for tissue engineering applications

dezembro de 2013

Development of advanced cell/tissue culture systems, based on enhanced polymeric scaffolds and sophisticated bioreactors, for tissue engineering applications
Pedro Ferreira da Costa
UMinho | 2013

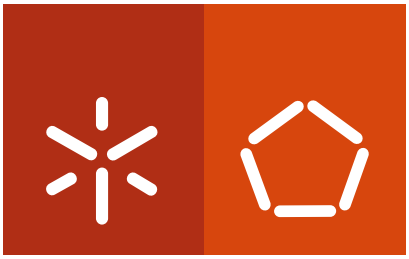

Universidade do Minho
Escola de Engenharia

Pedro Ferreira da Costa

Development of advanced cell/tissue culture systems, based on enhanced polymeric scaffolds and sophisticated bioreactors, for tissue engineering applications

Programa Doutoral em Engenharia Biomédica

Trabalho realizado sob a orientação do
Professor Doutor Rui L. Reis
e da
Professora Doutora Manuela E. Gomes

dezembro de 2013

In loving memory of my mother

Acknowledgements

During the course of my PhD, several people have contributed to the accomplishment of this thesis, both professionally and personally.

First of all, I would like to acknowledge my thesis supervisor, Professor Rui Reis, for giving me the oportunity to work in such a renowned research group as the 3B's. I would like to thank him for showing me that science can be much more than just having good ideas and that it doesn't necessarily need to be confined to a conventional research lab. I would like to thank him for expanding my horizons to other realities such as industry, business and intelectual property.

I would also like to acknowledge my co-supervisor at 3B's, Professor Manuela Gomes for her guidance, reviewing criticism and support despite her very busy agenda, in particular during the final stage of the preparation of this thesis.

Furthermore, I would also like to thank my supervisor in Australia, Professor Dietmar Hutmacher, for hosting me in his lab as part of his team. Working on the other side of the world can be tough sometimes but due to his kindness I have been able to feel at home and part of a big family. I am deeply grateful to him for showing me that, despite being very competitive, science can still be humane and fun.

In particular, I would like to deeply thank Dr. Cédryck Vaquette and Dr. Albino Martins who, apart from being my truthful friends, have been crucial in the development of the work described in this PhD thesis. Either in Australia or Portugal I have always been able to count on their unconditional support, guidance and friendly advice.

I would also like to acknowledge all the co-authors in the publications described in this thesis for their scientific input and for their contributions into improving the quality of the work described in this thesis.

During my stay at Materialise (Belgium) I have also been lucky enough to meet fantastic people who, despite distance and time, I will always remember. Dr. Erik Boelen has been my direct supervisor during that time and from whom I've learned so much about medical image processing, rapid prototyping, business development and product development in industrial environment. I also aknowledge his patience since that was the first time I worked for an extended time both abroad and in an industrial environment. I would also like to thank Jeroen Dille and Dr. Roel Wirix-Speetjens for their guidance and support. I also want to dedicate a special thank to my colleagues and friends at Materialise's sofware division namely Patricia Lopes, Bart Veeckmans, Dimitri Vanlessen, Davy Willems,

Wim Claassen and in particular my friends Sophie Lauwers and Thomas Van Mechelen who have made my stay at Materialise very pleasant and amusing.

Also, a special thank to my colleagues and friends at Queensland University of Technology (Australia), namely Christina Theodoropoulos, Toby Brown, Ferry Melchels, Anna Taubenberger, Laure Thibaudeau, Jana Wrobel, Fabio Volpato, Anna Slotosch and Jeremy Baldwin who have made my life in the lab (and also outside the lab) so much easier and fun.

To finalize my professional acknowledgements, I would like to dedicate a special thank to the present and former colleagues at the 3B's group.

I should also acknowledge the Portuguese Foundation for Science and Technology (FCT) for my PhD grant SFRH/BD/62452/2009, the North Portugal Regional Operational Programme (ON.2 – O Novo Norte), under the National Strategic Reference Framework (NSRF), through the European Regional Development Fund (ERDF) and the HIPPOCRATES (NMP3-CT-2003-505758), DISC REGENERATION (NMP3-LA-2008-213904) and MARIE CURIE ALEA JACTA EST (MEST-CT-2004-008104) european projects for funding.

At a personal level, I would also like to show my deepest appreciation for some people. First of all, my father and my brother who have been so important throughout my growth and with whom I've had the priviledge to share the best and worst moments of my life. A special thank to my mother who has strongly molded my personality and taught me to never give up.

Also, my good friends Vitor Martins and Filipe Noronha who despite following separate paths have always kept close and always made me feel that my life and work are meaningful.

Last but not least, a special thank to Ana, my better half, who has made my life so much happier and has supported me so much ever since I met her.

Development of advanced cell/tissue culture systems, based on enhanced polymeric scaffolds and sophisticated bioreactors, for tissue engineering applications

Abstract

In a typical tissue engineering approach, cells are collected from the patient and then seeded into a three-dimensional scaffold where they proliferate to generate a tissue-like substitute to be re-implanted back into the defect site. However, human tissues possess various degrees of complexity which often makes them impossible to be reproduced in such a simplified way. In fact, many tissues such as bone, for example, exhibit specific architectures and shapes, mechanical properties and cellular content that are very challenging to reproduce, in particular when combined together into a single construct. In order to overcome the limitations found in the generation of complex tissues such as bone and bone interfaces with other tissues, various automated technologies have been adopted by tissue engineering approaches to help generate viable tissue substitutes in a time- and cost-effective way.

Bioreactors are automated systems where cell-seeded scaffolds can be cultured under highly controlled conditions to generate replacement tissues. They improve the mobility of nutrients and avoid cell death in internal regions of constructs and influence cellular development through biomechanical stimuli. Bioreactors show the potential to generate constructs in a more standardized, traceable, cost-effective, safe and regulatory-compliant way.

Additive manufacturing is another highly automated technology which has more recently been introduced into tissue engineering. Its main use has been in producing 3D scaffolds with highly defined architectures by layer-by-layer deposition of materials. Herein we proposed the utilization of additive manufacturing to build simultaneously and concomitantly a 3D scaffold and bioreactor chamber, from different materials, as a single object. This would allow to produce scaffolds readily contained into bioreactor chambers, reducing the necessity for assembling, hence reducing production time and cost as well as the contamination risk due to the significantly decreased manipulation of both the scaffold and bioreactor.

In a first approach we aimed at applying this concept to the generation of tailor-made constructs for defect- and patient-specific applications. By resorting to medical imaging, a 3D model of a tibia bone tissue section was obtained and utilized as a template for generating a porous tissue replica scaffold as well as an enclosing culture chamber tightly fitting the outer shape of the porous scaffolds. The device showed to be able to homogenously distribute cells throughout the scaffold and to keep them viable along a 6 weeks culture period.

In a second approach, the same concept was used to simultaneouslly seed and culture multiple scaffolds contained into one single upscalable perfusion culture device. Additionally, the device was used for coating the scaffolds contained in its interior with a calcium phosphate layer in order to enhance their

osteoinductivity upon implantation. Cultured scaffolds showed homogeneous cell distribution and high cell viability throughout a 4 weeks culture period and calcium phosphate-coated scaffolds resulted in a significant increase in cell number. Such device may also find applications in the high throughput screening of combinations of multiple variable factors such as the selected biomaterials, scaffold architectures, cell types and culture regimes. Furthermore, this device might be applicable in the simultaneous generation of large amounts of tissue substitutes in a scenario of widespread adoption of tissue engineering-based therapies.

Additive manufacturing was also applied to a specific tissue engineering application that requires the development of a biphasic construct, targeting the generation of bone-periodontal ligament-teeth interfaces in a guided tissue regeneration strategy. In this case additive manufacturing was combined with the electrospinning technology to fabricate the biphasic construct, that is potentially able to accommodate a bone and a periodontal ligament tissue construct in separate cavities. The additively manufactured 3D scaffold was treated by means of a calcium phosphate coating in order to increase its osteoinductivity and then attached to a fine electrospun fibrilar mesh. First the additively manufactured part of the scaffold was seeded with osteoblasts and later the electrospun part was used for depositing cell sheets of periodontal ligament acting as a biomechanical support. After further culture, the complex constructs were finally attached to dentin blocks simulating the surface of teeth and subcutaneously implanted into rats. After 8 weeks of implantation, increased bone formation was observed when comparing to non-coated scaffolds. Histological analysis revealed that the large pore size of the periodontal compartment permitted the vascularization of the periodontal cell sheets and the formation of a tissue similar to native periodontal ligament tissue at the interface with dentin. Given the promising results achieved, this new and complex biphasic scaffold represents therefore a new hope in the regeneration of complex tissue defects resulting from serious forms of periodontitis.

Finally, a study was performed to evaluate the feasibility of cryopreservation-based storage and later off-the-shelf utilization of cell/scaffold constructs showing that cell and scaffold properties can be maintained upon cryopreservation and that the architecture of porous scaffolds may favor the retention and viability of construct's cellular content.

In summary, the work performed in this thesis resulted in significant advances towards automation and mass production of tailor-made and off-the-shelf tissue engineered products that might facilitate the widespread clinical adoption of tissue engineering strategies holding the promise to revolutionize the treatment of damaged tissues.

Desenvolvimento de sistemas avançados de cultura celular/tecidular, com base em estruturas de suporte melhoradas e bioreactores sofisticados, para aplicações de engenharia de tecidos

Resumo

Numa típica abordagem de engenharia de tecidos, são recolhidas células de um paciente e utilizadas para colonizar um suporte tridimensional poroso onde proliferam e geram um substituto tecidular a ser reimplantado no local danificado. No entanto, a maior parte dos tecidos humanos possui variados graus de complexidade que impossibilitam a sua reprodução de um modo tão simplificado. Muitos tecidos, tais como o osso, exibem arquitecturas e formas, propriedades mecânicas e conteúdos celulares difíceis de reproduzir, particularmente quando combinados num único substituto tecidular. De modo a superar as limitações encontradas na geração de tecidos complexos, tais como o osso e suas interfaces com outros tecidos, várias tecnologias automatizadas têm sido adoptadas em estratégias de engenharia de tecidos de modo a gerar tecidos viáveis de um modo eficiente em termos de tempos e custos de produção.

Bioreactores são sistemas automatizados onde estruturas de suporte celularizadas podem ser cultivadas sob condições muito controladas de modo a originarem substitutos tecidulares. Melhoram também a difusão de nutrientes reduzindo a morte celular nas regiões internas dos substitutos tecidulares e influenciam o desenvolvimento celular por aplicação de estimulação biomecânica. Os bioreactores têm potencial para gerar substitutos tecidulares de modo standardizado, rastreável, rentável e seguro, de acordo com as normas aplicáveis.

A fabricação aditiva é outra tecnologia altamente automatizada que foi recentemente introduzida na engenharia de tecidos, principalmente na produção de suportes celulares 3D com arquitecturas altamente definidas por deposição de materiais camada-sobre-camada. Nesta tese, propôs-se portanto a utilização de fabricação aditiva para construir simultânea e concomitantemente uma estrutura de suporte celular 3D e uma câmara de bioreactor, a partir de materiais diferentes, como um objecto único. Isto permitiria produzir estruturas de suporte contidas em câmaras de bioreactor reduzindo a necessidade de montagem, o tempo e custo de produção e o risco de contaminação decorrente da manipulação. Numa primeira abordagem o objectivo principal consistiu na aplicação deste conceito à geração de substitutos tecidulares personalizados de acordo com defeitos variáveis em pacientes. Um modelo 3D de uma secção de tibia foi obtido por imagiologia médica e utilizado para gerar um suporte celular poroso replicando a estrutura do osso assim como uma câmara de cultura ajustada à forma exterior do suporte celular. O dispositivo foi capaz de distribuir células homogeneamente pelo suporte celular continuando viáveis durante 6 semanas.

Numa segunda abordagem, o mesmo conceito foi utilizado para colonizar e cultivar simultâneamente multiplos suportes celulares contidos num único dispositivo expansível de cultura de perfusão. Adicionalmente, o dispositivo foi usado para recobrir as estruturas de suporte celular com uma camada de

fosfato de cálcio de modo a aumentar a sua osteoindutividade após implantação. Tal dispositivo pode ser aplicável na triagem de alta produtividade envolvendo multiplas variáveis tais como o biomaterial, arquitectura do suporte celular, tipos celulares e regimes de cultura utilizados. Este dispositivo pode também ser aplicável na geração simultânea de grandes quantidades de substitutos tecidulares num cenário de adopção generalizada de terapias de engenharia de tecidos. Os suportes celulares cultivados revelaram distribuição celular homogénea, alta viabilidade celular e um significativo aumento do conteúdo celular durante 4 semanas particularmente quando revestidos com fosfato de cálcio.

A fabricação aditiva foi também aplicada especificamente na geração de interfaces osso-ligamento periodontal-dente por meio de um substituto tecidular bifásico desenvolvido numa estratégia de regeneração tecidular guiada. Neste caso, a fabricação aditiva foi combinada com tecnologia de electrospinning para fabricar um substituto tecidular bifásico potencialmente capaz de acomodar substitutos ósseos e periodontais em cavidades separadas. O suporte celular 3D fabricado aditivamente foi recoberto com fosfato de cálcio para aumentar a sua osteoindutividade e ligado a uma fina malha fibrilar produzida por electrospinning. Primeiramente, a parte fabricada aditivamente foi colonizada com osteoblastos e mais tarde na malha produzida por electrospinning foram depositadas camadas celulares de ligamento periodontal actuando como um suporte biomecânico. Após cultura, os complexos substitutos tecidulares foram justapostos a blocos de dentina simulando a superfície dentária e implantados subcutâneamente em ratos. Após 8 semanas de implantação, uma acentuada formação de osso foi observada quando comparando com suportes celulares não recobertos. Análises histológicas revelaram também que os largos poros do compartimento periodontal permitiram a vascularização das camadas celulares periodontais e a formação de tecido semelhante ao ligamento periodontal nativo no interface com a dentina. Tendo em conta os bons resultados obtidos, este novo e complexo scaffold bifásico representa assim uma nova esperança na regeneração de defeitos em casos extremos de periodontite.

Finalmente, foi feito um estudo para avaliar a exequibilidade do armazenamento por criopreservação e posterior utilização de estruturas de suporte com células demonstrando que as propriedades das células e scaffolds podem ser mantidas após criopreservação e que a arquitectura de estruturas porosas podem favorecer a retenção do conteúdo celular e sua viabilidade.

Em resumo, o trabalho desenvolvido no âmbito desta tese resultou em avanços significativos no sentido de automatizar a produção em massa por engenharia de tecidos de produtos customizados prontos a usar e assim facilitar a aplicação clínica generalizada de estratégias de engenharia de tecidos que prometem revolucionar o tratamento de tecidos danificados.

Table of contents

List of abbreviations and nomenclature

0-1

2D - two-dimensional

3D - three-dimensional

A

ABS - acrylonitrile butadiene styrene

ALP - alkaline phosphatase

AM - additive manufacturing

B

BMSC - bone marrow mesenchymal stem cells

Brushite - highly soluble calcium phosphate phase

C

CAD - computer-aided design

CaP - calcium phosphate

CNC - computerized numerical control

CT - computerized tomography

D

DAPI - 4′-6-diamidino-2-phenylindole

DCPD - di-Calcium Phosphate Dihydrate

DMEM - dulbecco's modified Eagle's medium

DNA - deoxyribonucleic acid

dsDNA - double-stranded DNA

E

EDTA - ethylenediaminetetraacetic acid

F

FBS - fetal bovine serum

FDA - food and drug administration

FDA - fluorescein diacetate

FDM - fused deposition modelling

G

GTR - guided tissue regeneration

H

H&E - haematoxylin and eosin

HA - hydroxyapatite

HTS - high throughput screening

M

α-MEM - minimum essential medium alpha

Micro-CT or μ-CT - micro-computerized tomography

MRI - magnetic resonance imaging

MTT - 3-(4,5-dimethylthiazol-2-yl)-2,5-diphenyltetrazolium bromide

N

NaOH - sodium hydroxide

P

PBE - phosphate buffered EDTA

PBS - phosphate buffer saline

PCL - polycaprolactone

PDL - periodontal ligament

PFA - paraformaldehyde

PGA - poly-glycolic acid

PI - Propidium iodide

PLA - poly(lactic acid)

R

RNA - ribonucleic acid

RP - rapid prototyping

S

SBF - simulated body fluid

SEM - scanning electron microscopy

SLS - selective laser sintering

ssDNA - single-stranded DNA

T

TEC - tissue-engineered construct

β-TCP - β-tricalcium phosphate

TMJ - temporomandibular joint

List of figures

Chapter 1 - Automating the processing steps for obtaining bone tissue engineered substitutes: from imaging tools to bioreactors

Chapter 3 - Bioreactor composed of watertight chamber and internal matrix for the generation of cellularized medical implants

List of tables

Short curriculum vitae

Pedro Ferreira da Costa graduated in Applied Biology at the University of Minho (Portugal) in 2007. He started working in the field of tissue engineering and regenerative medicine in 2005, when he joined the 3B's Research Group for preparing his final year graduation thesis. Right after graduation, he was hired as a researcher at the 3B's Research Group in the scope of the European research project Hippocrates for continuing his work on developing novel dynamic culture systems for tissue engineering applications. In January 2008, Pedro Costa started his PhD under the supervision of Professor Rui Reis and co-supervision of Professor Manuela Gomes, intending to combine cell/tissue culture technologies and advanced 3D manufacturing technologies for developing substitutes for large complex tissues.

In July 2008, Pedro Costa received a Marie Curie Alea Jacta Est mobility scholarship to develop part of his PhD research work in the fields of CT and MRI data acquisition, 3D modelling and additive manufacturing in Belgium at Materialise NV (a world leading company in providing software and rapid prototyping solutions for biomedical and industrial applications) and where he also assumed the roles of business developer and product developer within the field of tissue engineering and regenerative medicine. The experience in business and industry shows the application-driven nature of Pedro Costa's research in an effort to develop tangible products for the tissue engineering and regenerative medicine field.

From 2010 to 2012, Pedro Costa also had the opportunity to work as a visiting PhD student at the Institute of Health and Biomedical Innovation, Queensland University of Technology, Australia, as a result from a strong collaboration with Professor Dietmar Hutmacher, Professor and Chair in regenerative Medicine in the same university and one of the pioneers in applying additive manufacturing within the field of tissue engineering and regenerative medicine.

Pedro Costa has been involved in the preparation of several national (Portuguese Foundation for Science and Technology) and European (7th Framework Program) grant proposals as also in the organization of conferences such as the 2008 TERMIS-EU conference held in Porto, Portugal.

Finally, Pedro Costa is author and co-author in 7 papers submitted and/or published in international refereed journals, 6 national and international patent applications and 1 book chapter. Furthermore, he has participated in some of the most relevant conferences in his research field in the form of 10 oral communications and 7 poster communications and received several awards in recognition of his work.

List of publications

The work performed under the scope of this PhD thesis resulted in the publications listed below.

Publications in International Refereed Journals

1- Costa P.F., Hutmacher D.W., Theodoropoulos C., Gomes M.E., Reis R.L., Vaquette C., 2013, Additive manufacturing for high throughput screening of 3D tissue engineered constructs in dynamic culture, *Nature Materials*, Submitted.

2- Costa P.F., Martins A., Neves N.M., Gomes M.E., Reis R.L., 2013, Automating the processing steps for obtaining bone tissue engineered substitutes: from imaging tools to bioreactors, *Tissue Engineering Part B: Reviews*, Submitted.

3- Costa P.F., Vaquette C., Baldwin J., Gomes, M.E., Reis R.L., Theodoropoulos C., Hutmacher D.W., 2013, Biofabrication of customized bone grafts by combination of additive manufacturing and bioreactor technologies, *Biofabrication*, Submitted.

4- Costa P.F., Vaquette C., Zhang Q., Reis R.L., Ivanovski S., Hutmacher D.W., 2013, Advanced tissue engineering scaffold design for regeneration of the complex hierarchical periodontal structure, *Journal of Clinical Periodontology*, Accepted for publication.

5- Costa P.F., Dias A., Reis R.L., Gomes M.E., 2012, Cryopreservation of cell/scaffold tissue engineered constructs, *Tissue Engineering Part C: Methods*, 18(11): 852-858.

6- Gonçalves M.A., **Costa, P. F.**, Rodrigues M.T., Dias I.R., Reis R.L. and Gomes M.E., 2011, Effect of flow perfusion conditions in the chondrogenic differentiation of bone marrow stromal cells cultured onto starch based biodegradable scaffolds, *Acta Biomaterialia*, 7(4):1644-1652.

7- Alves da Silva M.L., Martins A., Costa-Pinto A. R., **Costa, P. F.**, Faria S., Gomes M.E., Reis R.L. and Neves N.M., 2010, Cartilage tissue engineering using electrospun PCL nanofiber meshes and MSCs, *Biomacromolecules*, 11 : 3228–3236.

Patents

1- Costa P.F., Martins A., Vaquette C., Neves N.M., Gomes M.E., Hutmacher D.W., Reis R.L., Single-step method and device for the generation of stratified tubular tissue substitutes, World Patent Application WO2013/085404.

2- Costa P.F., Martins A., Vaquette C., Melchels F.P., Neves N.M., Gomes M.E., Hutmacher D.W., Reis R.L., Bioreactor composed of watertight chamber and internal matrix for the generation of cellularized medical implants. World Patent Application WO 2013/103306.

3- Costa P.F., Martins A., Vaquette C., Melchels F.P., Neves N.M., Gomes M.E., Hutmacher D.W., Reis R.L., Bioreactor composto por câmara estanque e matriz interna para geração de implantes médicos celularizados. Portuguese Patent Application 2012/106083.

4- Costa P.F., Martins A., Vaquette C., Neves N.M., Gomes M.E., Hutmacher D.W., Reis R.L., Dispositivo e método simplificado para a geração de substitutos tecidulares tubulares estratificados. Portuguese Patent Application 2011/106046.

5- Costa P.F., Martins A., Gomes, M.E., Neves N.M., Reis R.L., Multichamber bioreactor with bidirectional perfusion integrated in culture system for tissue engineering strategies. European Patent Application 2009/09009863.

6- Costa P. F., Martins A., Gomes M.E., Neves N. M., Reis R. L., Bioreactor multi-câmara com perfusão bidireccional para aplicação em estratégias de engenharia de tecidos. Portuguese Patent Application 2008/104155.

Book Chapters

1- Coutinho D.F., **Costa P.F.**, Neves N.M., Gomes M.E. and Reis R.L., 2010, Micro and Nano Technology in Tissue Engineering, In The Tissue Engineering Book: State of the art, Visions and Limitations, eds. Pallua N, Springer.

Oral Communications

1- Costa P.F., Vaquette C., Theodoropoulos C., Gomes M.E., Reis R.L., Hutmacher D.W., Additive manufacturing technologies applied to tissue engineering strategies, ESB Annual Meeting, Madrid, Spain, September 2013.

2- Costa P.F., Vaquette C., Theodoropoulos C., Gomes M.E., Reis R.L., Hutmacher D.W., Application

of rapid prototyping to high throughput screening of 3D dynamic environments, SFB Annual Meeting, Boston, USA, April 2013.

3- Costa P.F., Vaquette C., Gomes M.E., Reis R.L., Hutmacher D.W., All-in-one rapid-prototyped bioreactor/implant for semi-automated generation of tailor-made critical size bone tissue substitutes, TERMIS-WC, Vienna, Austria, September 2012.

4- Rodrigues A.I., **Costa P.**, Gomes M.E., Leonor I.B., Reis R.L., In vitro evaluation of osteogenic starch based scaffolds using a flow perfusion bioreactor, TERMIS-EU, Granada, Spain, June 2011.

5- Costa P.F., Martins A., Neves N.M., Gomes M.E. and Reis R.L., Rapid prototyping tools and strategies for tissue engineering applications, Young Persons' World Lecture Competition (YPWLC), Kuala Lumpur, Malaysia, September 2010.

6- Costa P.F., Martins A., Neves N.M., Gomes M.E. and Reis R.L., Rapid prototyping tools and strategies for tissue engineering applications, Young Persons' Portuguese Lecture Competition (YPLC), Guimarães, Portugal, June 2010.

7- Costa-Pinto A. R., Correlo V.M., Sol P.C., Battacharya M., Martins A., **Costa, P.F**., Reis R.L. and Neves N.M., The Culture of Human Mesenchymal Stem Cells on Chitosan based Scaffolds in a Multi-Chamber Flow Perfusion Bioreactor for Bone Tissue Engineering, 2nd TERMIS World Congress in conjunction with 2009 Seoul Stem Cell Symposium, Seoul, Korea (south), September 2009.

8- Costa-Pinto A. R., Correlo V.M., Sol P.C., Battacharya M., Martins A., **Costa, P.F.**, Reis R.L. and Neves N.M., Scaffold Composition Conditions the Osteogenic Differentiation in Flow Perfusion Culture of Human Mesenchymal Stem Cells , 2nd TERMIS World Congress in conjunction with 2009 Seoul Stem Cell Symposium , Seoul, Korea (south), September 2009.

9- Costa, P.F., Gardel L.S., Rada T., Gomes M.E. and Reis R.L., Stimulating adult stem cells from different origins for bone TERM approaches, IX International Symposium on Experimental Techniques, Vila Real, Portugal, October 2008.

10- Alves da Silva M.L., Martins A., **Costa, P.F.**, Correlo V.M., Sol P.C., Bhattacharya M., Rougier N., Reis R.L. and Neves N.M., Cartilage tissue engineering using a flow perfusion bioreactor, TERMIS-EU, Porto, Portugal, June 2008.

Poster Communications

1- Vaquette C., **Costa P.**, Hamlet S., Reis R., Ivanovski S., Hutmacher D.W., A calcium phosphate coated biphasic scaffold for periodontal complex regeneration, TERMIS-WC, Vienna, Austria, September 2012.

2- Martins A., Pinho E.D., **Costa P.F.**, Marques A.P., Reis R.L. and Neves N.M., Osteogenic Differentiation of Human Bone Marrow Mesenchymal Stem Cells on Nanofiber Reinforced Microfibrous Composite Scaffolds, TERMIS-WC 2009, Seoul, Korea (south), August 2009.

3- Costa P.F., Dias A.F., Dias I.R., Gomes M.E. and Reis R.L., Evaluation of the effect of cryopreservation over the functionality of bone-generating cell/tissue constructs, 2nd Meeting of the Institute for Biotechnology and Bioengineering, Braga, Portugal, October 2010.

4- Costa, P.F., Gomes M.E. and Reis R.L., Automated generation of three-dimensional scaffold architectures with multiple levels of organized randomness for rapid prototyping-based tissue engineering applications, Week of Engineering School at University of Minho, Guimarães, Portugal, October 2009.

5- Costa-Pinto A. R., Correlo V.M. , Sol P.C., Battacharya M., Martins A., **Costa P.F.** and Neves N.M., The Culture of Human Mesenchymal Stem Cells on Chitosan based Scaffolds in a Multi-Chamber Flow Perfusion Bioreactor for Bone Tissue Engineering , 2nd TERMIS World Congress in conjunction with 2009 Seoul Stem Cell Symposium, Seoul, Korea (south), August 2009.

6- Costa P.F., Martins A., Neves N.M., Gomes M.E. and Reis R.L., Innovative Perfusion-Based Dynamic Culture System for the Generation of Improved Tissue Engineered Constructs, TERMIS World Congress, Seoul, South Korea, August 2009.

7- Costa P.F., Martins A., Neves N.M., Gomes M.E. and Reis R.L., A novel bioreactor design for enhanced stem cells proliferation and differentiation in tissue engineered constructs, TERMIS-EU, Porto, Portugal, June 2008.

Awards

The work performed under the scope of this PhD thesis also resulted in the following awards.

1- 3rd prize in the SYIS oral presentation competition held at the 3rd World Tissue Engineering and Regenerative Medicine International Society's Conference (TERMIS), in September 2012, Vienna, Austria.

2- Young Investigator Travel Award to attend the 3rd World Tissue Engineering and Regenerative Medicine International Society's Conference (TERMIS), in August 2012, Vienna, Austria.

3- Finalist in the Young Persons' World Lecture Competition (YPWLC), in September 2010, Kuala Lumpur, Malaysia, organized by IOM3 - Institute of Materials, Minerals and Mining.

4- Winner of the Young Persons' Portuguese Lecture Competition (YPLC), June 2010, in Guimarães, Portugal, organized by IOM3 - Institute of Materials, Minerals and Mining.

Structure of the thesis

The present thesis is divided into 8 chapters, organized according to the defined aims, the nature of the experiments performed and the results obtained. Furthermore, an annex section was added to this thesis to include additional work performed during the course of the PhD, namely one patent, which for reasons detailed bellow was not directly incorporated in the work presented here. The sub-division in chapters is based in a series of related papers and patents published in international journals or submitted for publication, which are identified in the front page of each chapter. Therefore, each thesis chapter corresponds to a published or submitted manuscript with minor format changes for ensuring an homogenous style and consistent structure combining the various thesis chapters.

The first chapter consists of a comprehensive and detailed literature review about currently available tools and methodologies which have the potential to increase the level of automation involved in the process of generating tissue-like constructs, and which were explored in the experimental sections of this thesis.

The second chapter of the thesis includes a detailed description of the materials used, the processing technologies and the techniques used for the scaffolds physicochemical characterization. The biological tests, including the used cellular sources and assays performed to characterize the cell-seeded/cultured constructs are also described.

The third chapter describes a patent application related with a new type of perfusion-based bioreactor produced by a fabrication process of additive manufacturing. This new bioreactor concept is further explored and applied in chapters 4 and 5.

The fourth chapter reports the development of an innovative methodology which, by resorting to additive manufacturing is able to build accurate tissue replicas readiliy contained into optimized bioreactor chambers according to obtained medical images, for further seeding and culture of cells.

The fifth chapter reports the application of the concept described in chapter 3 to the high throughput screening of cell-biomaterial dynamic environments by developing an up-scalable device capable of culturing multiple constructs simultaneously in a reduced space. This device was also presented as a way to facilitate the serial treatment of scaffolds with superficial biomimetic coatings by perfusion with solutions prior to cell culture.

The sixth chapter describes the combination of additive manufacturing with melt electrospinning to generate a biomimetically coated biphasic scaffold able to more efficiently regenerate bone-periodontal ligament-tooth interfaces. This scaffold was tested both in *in vitro* and *in vivo* conditions.

Chapter seven describes a study on the feasibility of cryopreservation-based long term storage of constructs composed of scaffolds previously seeded and cultured with cells since such strategy would enable the storage of mass produced tissue substitutes and its later off-the-shelf utilization. In this thesis we have focused on strategies that can decrease the production time of tissue engineered constructs and thus also contribute for shortening the waiting time of patients that require treatment with such therapies. Nevertheless, the cryopreservation of tissue engineered constructs should be further explored in the future when mass utilization of tissue engineered constructs becomes a reality.

Chapter eight of this thesis, the final chapter, contains the overall conclusions obtained from the performed research work and discusses the future perspectives and lines of research to be followed.

Furthermore, in annex 1, is described an additional patent related with a novel device and method for facilitating the generation of stratified tissue substitutes composed of multiple types of cells in segregated layers, such as blood vessels. Vascularization is essential for the generation of large tissue substitutes and by utilizing the described device and the electrospinning technologies previously applied in chapter 6, such structures would be achievable in shorter periods of time due the simplicity of the process and to the intrinsically enhanced mechanical properties of the generated constructs.The concept described in this patent was not fully explored under the scope of this thesis and therefore is not sufficiently correlated to the other works presented, but is relevant for further development of the strategies described/proposed and for this reason it was included as an annex.

Section I

General introduction

Chapter 1

Automating the processing steps for obtaining bone tissue engineered substitutes: from imaging tools to bioreactors

Abstract

Bone diseases are highly incapacitating and result in a high demand for tissue substitutes with specific biomechanical and structural features. Tissue engineering has already proven to be effective in regenerating bone tissue but has not yet been able to become an economically viable solution due to the complexity of the tissue which is very difficult to be replicated, eventually requiring the utilization of highly labour-intensive processes. Process automation is seen as the solution for mass production of cellularized bone tissue substitutes at an affordable cost by being able to reduce human intervention as well as reducing product variability. The combination of various tools which are currently used in tissue engineering shows potential to generate automated production ecosystems which will in turn enable the generation of commercially available products with clinical widespread application.

This chapter is based on the following publication:

Costa P.F., Martins A., Neves N.M., Gomes M.E., Reis R.L., 2013, Automating the processing steps for obtaining bone tissue engineered substitutes: from imaging tools to bioreactors, *Tissue Engineering Part B: Reviews*, Submitted.

1. Introduction

Bone is a dense and specialized form of connective tissue responsible for supporting and protecting the body and its organs. Its complex architecture is built from type I collagen and calcium phosphate in the form of hydroxyapatite resulting in unique biomechanical properties which are difficult to mimic artificially. Bone diseases are therefore highly incapacitating and are increasingly becoming a major socioeconomic issue [1]. More than 2.2 million bone grafting procedures take place annually worldwide to ensure adequate bone healing in many skeletal problems [2] at an estimated cost of 2.5 billion US dollars [3]. Auto-transplantation employing bone harvested from patient's donor sites is the most common procedure due to its inherent histocompatibility and non-immunogenicity [4]. However, the sourcing of grafts in the patient's body enhances tissue morbidity, blood loss, risk of infection and fracture, operative time and cost and results in long immobilization periods and post-operative pain. To eliminate these drawbacks, synthetic products such as Ostim® (Aap Implantable AG, Germany), Kasios® and Jectos® (Kasios, France) and Pro Osteon® (Biomet Inc, USA) composed of hydroxyapatite and/or calcium phosphates and natural products of xenogeneic origin such as Bio-Oss® (Geistlich Pharma, Switzerland) have been introduced in the market. However, these products have high production cost and are mainly provided in the form of granules or pastes showing reduced ability to repair complex and/or high load demanding defects.

Over the last two decades, tissue engineering has shown great promise in regenerating human tissues by employing exogenously generated substitutes. Since then, various types of tissue substitutes, such as bone [5], cartilage [6] or skin [7], have been successfully generated *in vitro*. Despite initial projections (80 billion USD market by 2012) and extensive corporate investment, the translation of these ground-breaking technologies from the lab to a clinical widespread application revealed to be modest. The most commercially successful tissue engineered product so far was a skin substitute produced by Organogenesis Inc. which, despite its proven effectiveness and relative simplicity, reached a very small part of its potential market given its labour-intensive and costly production process [8]. Being bone tissue more complex and difficult to regenerate than skin, mainly due to its structural and biomechanical properties, the task of creating commercially viable tissue engineered bone replacement products becomes therefore even more arduous. Automation is probably one of the key issues for enabling the generation of bone substitutes with enhanced complexity in a time- and cost-effective manner, allowing an effective shift from labour-intensive production to mass production.

In this paper we review several production steps of the process for the generation of bone substitutes focusing on the available options that rely on automated tools and strategies which are currently applied in tissue engineering, namely 3D medical imaging, computer-aided design (CAD), additive manufacturing and bioreactor technologies (Figure 1.1).

2. Imaging tools for design

Technological advancement has enabled the visualization of human tissues and organs to levels of detail as never seen before and, by doing so, it became possible to understand the structure-function relationship at the level of cells, tissues and organs. With the advent of tissue engineering and regenerative medicine, it becomes now possible to not only observe but as well to mimic those same structures in such a way that the replacement and regeneration of damaged tissues and organs is possible.

Currently existing technologies for non-invasive imaging allow for body parts or whole bodies to be analysed without any damage to the target tissues. Technologies such as magnetic resonance imaging (MRI) and in particular computerized tomography (CT), enable the collection of data from bone tissue sites which need to be repaired. Given the high degree of resolution provided by such technologies it becomes possible to obtain not only information related to the defect's and organ's outer shape but also information related to their more complex inner porosity, density and micro structure. This data can even be used for indirectly assessing other tissue parameters, such as mechanical properties, by comparison with calibration phantoms [9].

Softwares such as Mimics (Materialise NV, Belgium), the CTAn+CTVol package (SkyScan NV, Belgium) [10] or Invesalius (Renato Archer Technology of Information Center, Brazil) [11] are specialized into converting raw CT/MRI data (in the form of sequential 2D images made of density-based grayscale-coloured pixels) into 3D models by combining these 2D images into 3D stacks. According to a desired density threshold, density-based shapes and volumes can therefore be defined in 3D and selected out of the 3D stack. Finally, the obtained shapes are used to generate a volume, a 3D model, consisting of the volume contained in its interior (Figure 1.1A). The analysis of parameters such as densities, volumes and porosities may differ according to the software-specific algorithms, the scanning equipment and contrasting agents used. Bone tissue also exhibits very irregular outer shapes which are difficult to mimic by other means than CT or MRI imaging. In a work by Grayson et al. [12] medical CT was used to scan a bovine temporomandibular joint (TMJ) condylar bone and then fabricate an atomically shaped scaffold replica by computerized numerically controlled (CNC) milling of a bone

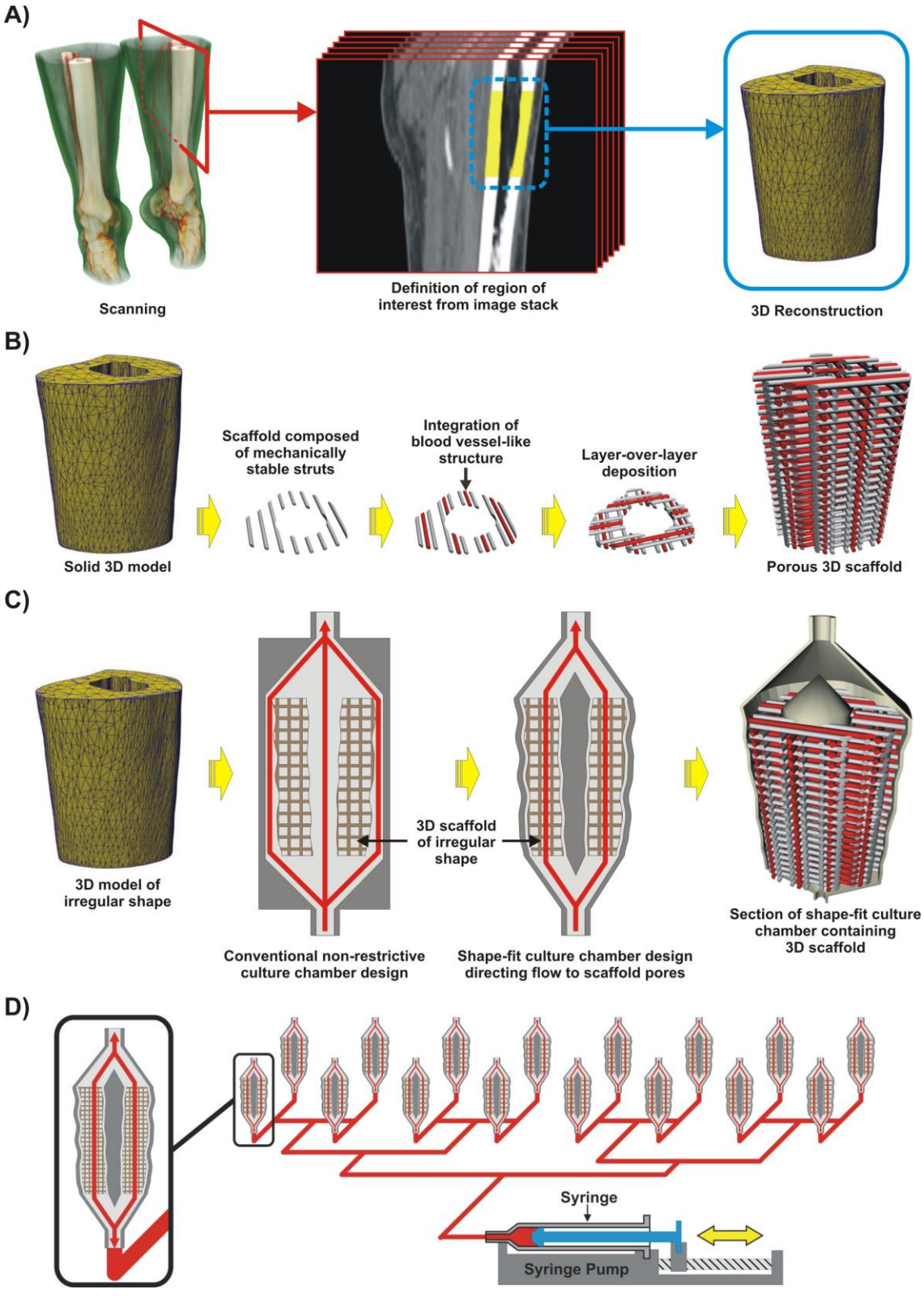

Figure 1.1 –Schematic representation of process for mass production of personalized bone substitutes. The process starts with a 3D reconstruction obtained by medical imaging A) which allows to produce scaffolds replicating the shape and structure of the target tissues B) as well as shape-specific culture chambers C) into which scaffolds are optimally seeded and cultured with cells in large scale D).

explant block. This solution was very successful in generating a tailor-made functional bone substitute despite of the above mentioned drawbacks associated with bone explants.

3. Design by replication of real tissue models

Apart from replication, current technological development allows to improve on the natural design of tissues and organs and maximize the functionality of *de novo* generated substitutes as well as facilitating their manufacture.

The replication of tissue parts by reconstruction of CT or MRI scans usually involves a certain extent of design modifications which are applied to CT- or MRI-generated 3D models (such as reorientation, edge smoothing and mesh simplification operations) in order to facilitate and accelerate the 3D model manipulation, fabrication and integration within the target site. The reconstructed 3D model can as well be manually redesigned or combined with other 3D models (CT/MRI-originated or CAD-designed) to improve their functionality. Otherwise, in cases where there is a complete or substantial lack of tissue to be scanned and reconstructed it becomes necessary to resort to other reference tissues possessing similar shape and properties in order for their 3D models to be adapted to the target site by reverse engineering [13].

The most simple way of using a CT/MRI-generated 3D model for generating tissue substitutes is by simply converting the reconstructed 3D model (which is initially solid) into a model containing repeating porosity patterns (which will later originate a porous implant). Porosity and pore interconnectivity are crucial parameters in the efficiency of tissue engineered implantable devices since they allow pre-seeded cells to proliferate and populate the inner parts of the device while receiving sufficient nutrition as well as neovascularization and tissue ingrowth coming from the native tissues surrounding the device upon implantation [14-16]. Porosity, together with pore's interconnectivity and architecture can also be greatly responsible for other features such as the device's mechanical properties. The mechanical properties of scaffolds can as well be adjusted according to numerically generated models to meet desired requirements [17].

Porosity patterns can be generated by using design-based methods [18] and/or fabrication-based methods [19] either by simple repetition of predetermined subunits [20] or generated by means of mathematical models developed by analysis of the target tissue structure [21, 22] (Figure 1.2). Design-based methods imply further manipulation and modification of the 3D model and rely on the generation of a regular 3D matrix which overlaps the 3D model. This 3D matrix is populated by subunits

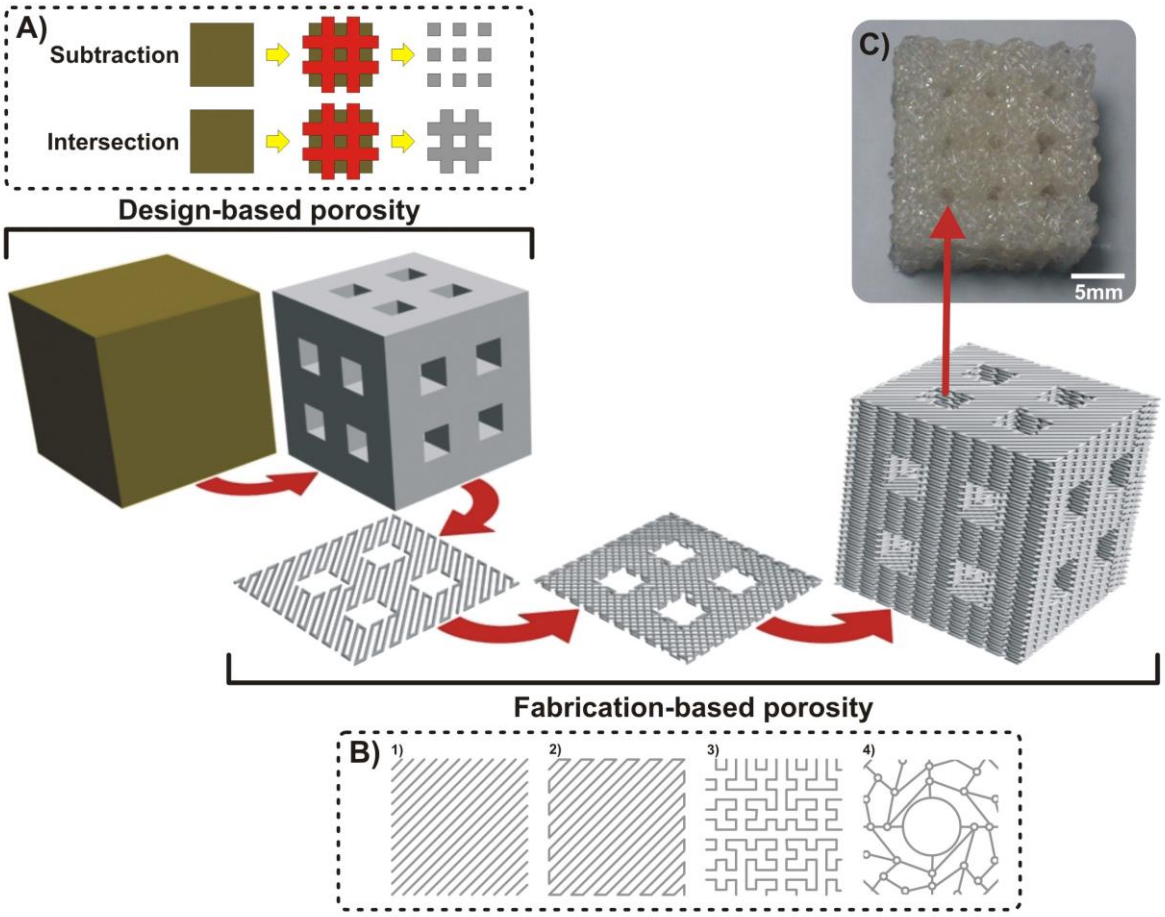

Figure 1.2 – Schematic representation of generation of porosity into a 3D model by means of design- and fabrication-based methods. A) Boolean operations employed in design-based porosity generation. B) Examples of patterns of varied complexity employed in fabrication-based porosity generation. C) Scaffold possessing design- and fabrication-based porosity. B4 modified with permission from [21].

possessing predetermined geometries which are used for locally performing either intersection or subtraction boolean operations over the 3D model (Figure 1.2A). A boolean object resulting from an intersection operation will contain only the volume that was common to both original objects (3D model and subunits) while a boolean object resulting from a subtraction operation will consist of the volume of the original object (3D model) with the intersection volume (subunits) subtracted from it. The main restriction in the design of these subunits is that they must be able to adjacently intersect with each other at some point. In the case of intersection Boolean operations, this feature becomes crucial since, upon fabrication, this allows for the device to maintain its structural and mechanical integrity. When performing subtraction Boolean operations, this feature is mostly important in keeping the interconnectivity of pores. Fabrication-based methods on the other hand imply the manipulation of operating parameters utilized in the process of fabrication itself. When ready for fabrication, the 3D

model is horizontally sliced and each of the slices filled with patterned lines which are then used by the fabrication machine-controlling software as guiding pathways for activating and moving the machine's tools. Pattern types can vary from just simple sets of parallel lines to more complex mathematically calculated patterns (Figure 1.2B). Slice thickness and line spacing are other common examples of simple parameters that can be easily manipulated to substantially change the amount, size and interconnectivity of pores. Such as in design-based methods, the only vital requirement in the generation of these patterns is that upon fabrication, all the patterned layers are attached to each other at some point and forming a single object capable of maintaining its structural and mechanical integrity. Both design-based and fabrication-based methods provide an enormous array of possibilities when developing tissue engineering devices. Furthermore, the combination of design-based and fabrication-based methods is also an option and can generate an even more immense array of design possibilities. The combination of both can i.e. be used for generating distinct but integrated types of porosity into one single device (Figure 1.2C).

4. Fabrication with accuracy and reproducibility

In order to be able to fabricate structures as complex as tissues and organs, high precision tools need to be employed. These tools must allow to accurately position cell and material building blocks but also enable the three-dimensional positioning necessary to generate fully functional three-dimensional constructs.

Additive manufacturing is a highly automated layer-by-layer process which, unlike subtractive rapid prototyping, involves the sequential building of layers of material by deposition of new layers on top of previously laid layers of material. The first main application of additive manufacturing in the medical field was in helping to plan surgeries. By building real size models accurately mimicking tissue features contained in the interior of the body it was possible for surgeons to better plan surgical procedures [23]. Furthermore, surgical guides for tool orientation were also built by additive manufacturing enabling as well a better execution of the surgical procedure itself [24, 25].

In general, an additive rapid prototyping material must be convertible to a more versatile form, such as a liquid, a colloidal or a powder form, (typically by applying high temperatures or solvents) in order to be selectively and accurately added to layers. After deposition, the chosen material must be able as well to directly or indirectly attach back together in order for adjacent layers to be efficiently joined together during the layer-by-layer process.

Despite the existence of a wide array of materials able to be used in the additive manufacturing of bone scaffolds, polycaprolactone (PCL) and poly(lactic acid) (PLA) are the most commonly used materials (either alone or combined with other materials) due to their biodegradability and adequate mechanical properties as well as their approval for medical implantation. Another material of great interest for fabricating bone scaffolds is hydroxyapatite which is a natural constituent of bone. Hydroxyapatite can be utilized in additive manufacturing by applying significantly higher processing temperatures than PCL or PLA when directly deposited. Alternatively, hydroxyapatite scaffolds can as well be indirectly fabricated by casting into sacrificial moulds fabricated by additive manufacturing [26].

The array of specialized materials which can be utilized in additive rapid prototyping, although not as wide as in subtractive rapid prototyping, is still quite large and is constantly evolving given that there is currently a wide range of additive rapid prototyping technologies and that each one utilizes materials with specific properties for adequate processing. Fused deposition modelling (FDM) and selective laser sintering (SLS) are the most commonly used additive manufacturing technologies in bone tissue engineering applications mostly due to the possibility of manufacturing objects which possess mechanical properties similar to the ones found in native bone while at the same time maintaining a high degree of control over the outer and inner architecture of the manufactured object. SLS results from the fusion of particles contained in a powder layer by means of directed laser radiation [27]. A thin layer of powder is first spread over a flat surface and then irradiated by a laser beam which is oriented to selected locations of the powder layer. As a result, the irradiated powder particles are fused together forming two-dimensional patterns. The laser beam is then stopped and a new layer of powder is spread over the precedent layer by means of a mechanical roller. The patterned fusion process is then repeated resulting in the fusion of the new patterned layer with the layer beneath. In the end of the process, the excess powder is removed uncovering the manufactured object (Figure 1.3A). On the other hand, FDM consists on the extrusion of molten material from a heated extruder forming a thin filament which is laid down over a deposition surface which moves over three axis relatively to the extrusion nozzle [28]. By coordinating the movement of the deposition table and the extrusion in the nozzle, highly detailed patterns of thermoplastic material can be created over the deposition surface. When the deposition of one layer of material is finished, the extrusion is stopped while the deposition table is slightly moved away from the extruder tip. The extrusion is then restarted and a new patterned layer is deposited over the precedent layer to which it adheres (Figure 1.3B). FDM and SLS technologies may however need to be complemented with other additive manufacturing technologies, such as bioprinting,

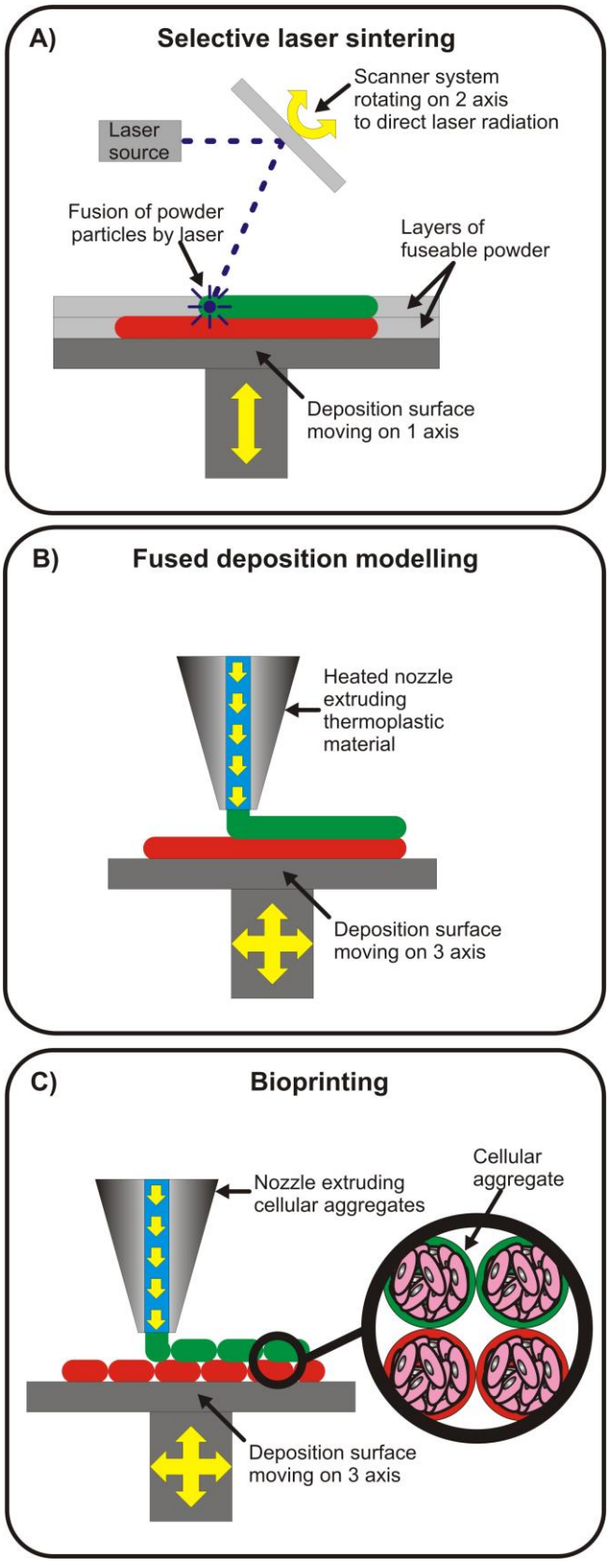

Figure 1.3 – Schematic representation of the mode of operation of selective laser sintering A), fused deposition modeling B) and bioprinting C).

in order to replicate specific features contained into the bone tissue structure. Bioprinting results from the extrusion of material from a nozzle but unlike fused deposition modelling it does not involve heating. Therefore, the extrusion process can involve sensitive materials such as gels and cellular aggregates [29]. Typically, the process is started with the patterned deposition of a gel filament which forms a grooved layer. This gel layer then allows for further deposition of a second material which is composed of small cellular aggregates. The deposition of those aggregates into the grooves formed by the gel layer insures that the cellular aggregates are kept in their exact positions. This process is repeated layer over layer generating three-dimensional shapes composed of cellular aggregates which during further maturation fuse together and generate continuous masses of cells possessing a pre-determined shape (Figure 1.3C). A particular application of bioprinting is in the formation of blood vessel networks contained into bone. Blood vessel networks are flexible and delicate structures which possess mechanical properties very different from the surrounding tissue. These structures have so far been mimicked by applying gel-based or even scaffold-free printing technologies which are able to lay down intricate patterns of cells which later generate vessel-like structures. An example of that is shown in a work by Norotte et al. [30], where bioprinting was utilized to concomitantly lay down aggregates of various cell types according to predefined patterns which during further maturation fused together and generated stratified three-dimensional vessel-like structures. Furthermore, previous works show as well that soft materials such as gels can be further integrated into the structure of more stiff thermoplastic scaffolds resulting in scaffolds possessing optimal mechanical properties [31, 32]. By using a similar strategy, and applying design principles mimicking the natural organization of blood vessels [33-35], the concomitant integration of bioprinted blood vessels into the structure of more mechanically stable scaffolds produced by technologies such as FDM or SLS would potentially enable the generation of mechanically stable vascularized bone tissue substitutes (Figure 1.1B).

5. Culturing cells in 3D templates

Despite being highly labour intensive and expensive, static culture is still the most widely used cell culture technique in tissue engineering strategies. This culturing technique is often characterized by non-homogenous cell distribution, being the majority of seeded cells confined to the outer surfaces of the scaffold, which in turn results in non-homogenous distribution of the *in vitro*-generated extracellular matrix. Furthermore, static culturing conditions are far from mimicking the dynamic environment found *in vivo* which is responsible for many signals/stimuli that trigger cell development. Dynamic cell culture

has been shown to avoid cell death in the construct's core by improving the mobility of nutrients into these most central regions as well as influencing cellular development [36-39]. Hence, many dynamic culture devices possessing varying degrees of automation have so far been developed in order to overcome the limitations found in static culture. These systems are able to culture tissue engineered constructs into highly controlled environments while providing a wide array of biomechanical stimuli (Figure 1.4).

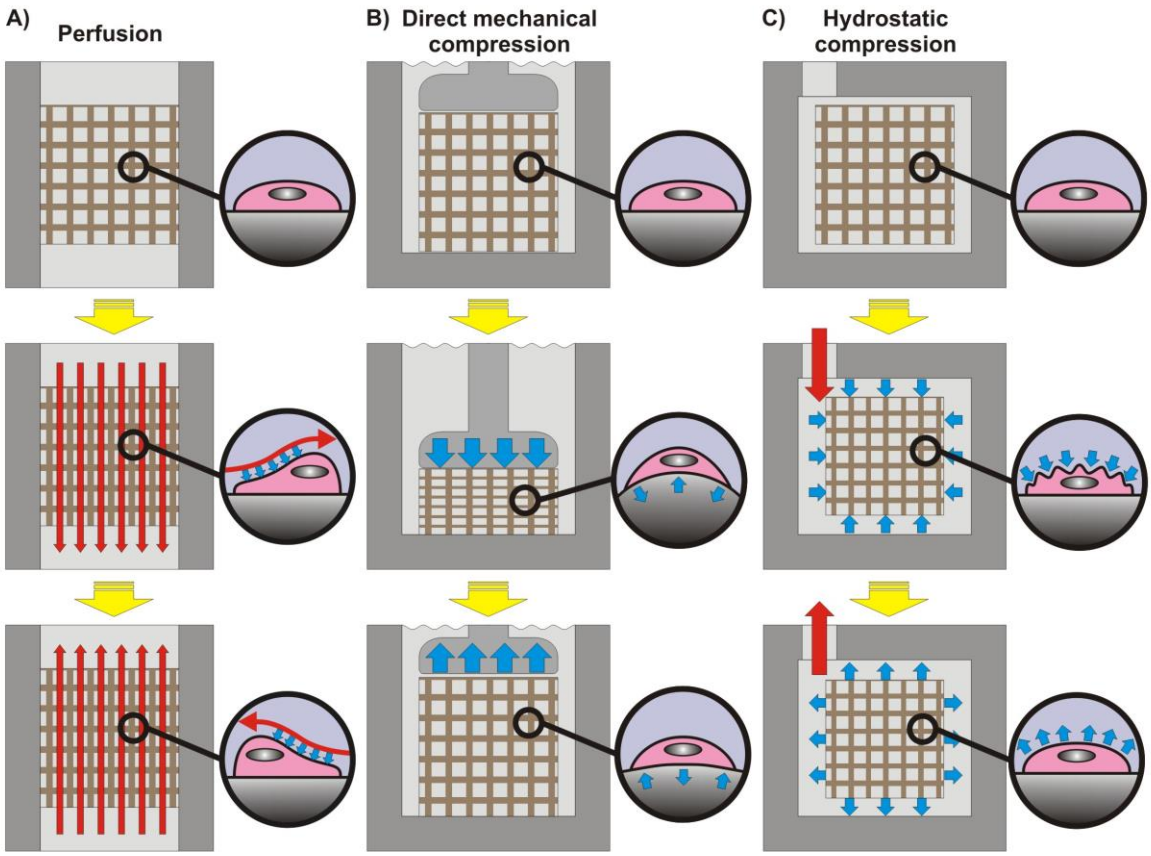

Figure 1.4 – Scheme showing how perfusion, mechanical compression and hydrostatic compression bioreactors are able to mechanical deform cells in order to stimulate their development. Red Arrows indicate fluid movement and blue arrows indicate mechanical forces.

Stimulatory signals applied in bone tissue engineering such as perfusion-based shear stress [40, 41], direct mechanical compression [42] and hydrostatic compression [43] have shown to be effective in improving the quality of generated constructs. In fact, such results would be expectable since such stimuli can be found influencing bone development in a similar way when applied *in vivo* [44, 45]. Bioreactors are able to modulate cellular development through a mechanism of mechanotransduction which consists on triggering intracellular biochemical signals by means of mechanical deformation of

the cellular structure [46]. Perfusion bioreactors employ pumps to continuously perfuse culture medium through the interconnected porous networks of cell-seeded scaffolds. Shear stress resulting from the movement of fluid over the surface of cells in the scaffolds results in the deformation of the structure of cells and triggers mechanotransductive downstream reactions (Figure 1.4A). Given their simplicity, flow perfusion bioreactors enable seeding and culture of cells into scaffolds with a high degree of automation. In a different way, bioreactors performing direct mechanical compression are inspired by the mechanical compressive forces felt by tissues in their natural environment during movement. Cells contained into porous scaffolds are stimulated by the deformation that occurs in the scaffold's structure during compression/relaxation (Figure 1.4B). Shear stress can as well occur as a result from the movement of fluids from/to the interior of the scaffold's pores during deformation. Finally, in hydrostatic pressure bioreactors, mechanical forces act directly over the wall of cells contained into porous scaffolds by means of a fluid. When the pressure of the fluid (culture medium) contained in the bioreactor (and into the scaffold's pores) is increased/decreased it acts upon the cellular wall by causing a compression/relaxation deformation (Figure 1.4C). Apart from being able to simplify and automate the process of construct culture, bioreactors in general show as well the potential to generate constructs in a more standardized, traceable, cost-effective, safe and regulatory-compliant way [47, 48]. Bioreactors must also be versatile, being able to adapt to various kinds of constructs possessing variable degrees of complexity and aimed at diverse applications. This is why bioreactors, as well as their fabrication process, must be easily adjustable to specific conditions and requirements on the fly. Recent work addressed this requirement by resorting to additive manufacturing not only to fabricate scaffolds but as well to simultaneously fabricate their enclosing culture chamber [49]. In this way, complex-shaped constructs could be produced to replicate the shape of CT-scanned bone parts while contained into a culture chamber optimally designed for that specific construct (Figure 1.1C).

Another aspect which is important for the applicability of tissue engineering into the clinic is process scalability. In a scenario of widespread adoption of tissue engineering-based therapies, significant amounts of sufficiently large constructs would need to be simultaneously produced in order to fulfil clinical demands (Figure 1.1D). Many scalable and modular systems have been developed to address this requirement by resorting to various fabrication processes in order to enable the simultaneous culture of multiple and/or large constructs [38, 50-52]. A specific application where this is already visible (although usually at a smaller construct scale) is in the high throughput screening of biomaterials where cells contained into multiple simplified 3D constructs are submitted to varying culture environments in order to fully understand and optimize their development [53, 54].

Such as the human body, bioreactors must as well be able to continuously sense and accordingly react to all the events occurring in the construct and its surrounding environment during culture. Many kinds of sensors and analytical techniques have been so far integrated into bioreactor-based procedures. The most common ones are based on electrochemical and optical principles and are usually applied in either an invasive, non-invasive or shunt configuration [55]. Some of them are commonly used in other types of fully up-scaled cultures such as the culture of yeasts or bacterial microorganisms for mass production of food and drug compounds as well as in clinical and physiological monitoring [56]. A very interesting type of bioreactor with particular utility for bone tissue engineering is able to perform non-invasive high resolution analysis of bone constructs under perfusion culture by means of micro-CT scanning [57, 58]. In this way, tissue constructs do not need to be removed from its culture chamber every time a scan is performed hence reducing human labour as well as minimizing the possibility of contamination.

6. Implant

The most common tissue engineering strategies assume that in order to regenerate or replace a damaged tissue, one must collect cells from the patient and then seed and culture them *ex vivo* onto a material support in combination with biochemical factors in order to generate a construct which then can be implanted back into the patient's body through common surgical procedures. Despite the popularity of *ex vivo* strategies, alternative tissue engineering strategies consider that tissue replacements can be generated inside the patient's own body by using the concept of "*in vivo* bioreactors". This strategy consists on the creation and manipulation of artificial spaces in the patient's body into which an external material can be inserted and cultured. In this strategy, the patient's body becomes the bioreactor since it dynamically provides all the necessary biomechanical and biochemical conditions for cells directly recruited from the patient's own body to generate a new tissue inside the "*in vivo* bioreactor" [59-64].

Given the high complexity and sensitivity of the body, *in vivo* bioreactors can be considered the apex of tissue culture since they are naturally capable of continuously sensing the changing needs required by a developing tissue and accurately providing all the necessary biomechanical and biochemical signals. On the other hand, this kind of strategy also shows evident disadvantages in comparison to *ex vivo* strategies since it requires additional surgical procedures namely for the creation of the *in vivo* bioreactor cavity as well as for the collection of the generated tissue to be applied into damaged sites.

7. Off-the-shelf storage of tissue engineered constructs by cryopreservation

Given that tissue engineered products are expected to have a growing number of applications in the regeneration of human tissues, and that their fabrication process can require long time spans [65-69], resulting in excessively long incapacitation of patients, the ability to properly store large amounts of these products for later off-the-shelf utilization is seen as a promising possibility but also as a demanding challenge.

The utilization of cryopreservation has been evaluated as a solution for long term storage of such live tissue substitutes [70-75]. Cryopreservation is based on the principle that chemical, biological and physical processes are effectively "suspended" at cryogenic temperatures [76] and therefore becomes more advantageous than commonly used preservation techniques, such as refrigeration or continuous tissue culture, which show drawbacks such as limited shelf-life, high cost, risk of contamination and genetic drift. Such strategy of cryopreserving tissue engineered substitutes would involve cells previously seeded and cultured onto scaffolds. This would be a way to generate a reliable source of readily available and ready to implant engineered constructs, greatly reducing the incapacitation time of patients.

8. Concluding remarks and future directions

The automation of tissue engineering is becoming a reality. Important advancements in this area allowed so far to mostly create and identify the basic enabling technologies necessary for the proper development of this field. Nonetheless, and given the high complexity of bone tissue, it becomes necessary to develop equally complex development strategies, but these must result in simpler methodologies and technologies that enable automation and thus, easier processing into industrial viable products that can reach large scale clinical applicability. The rapid development in computer and automation technologies as well as the achievement of higher resolution powers in analysis and fabrication processes increasingly enables tissue engineers to more closely mimic the complex and highly dynamic environments found in native tissues. The convergence of these technologies allied to an increasingly better understanding of the mechanisms at the basis of tissue development will in the future allow for the generation of tissue replicas possessing similar or even improved features. Equally

important is the training of highly skilled hybrid scientists capable of mastering and combining all the involved technologies into generating mass produced, tailor-made, patient-specific solutions.

9. Acknowledgments

We would like to acknowledge the partial support by the European Network of Excellence EXPERTISSUES (NMP3-CT-2004-500283). Pedro Costa would also like to acknowledge the Portuguese Foundation for Science and Technology for his PhD grant (SFRH/BD/62452/2009).

10. References

1. Brooks PM. The burden of musculoskeletal disease - a global perspective. Clin Rheumatol.25:778-81. 2006.
2. Giannoudis PV, Dinopoulos H, Tsiridis E. Bone substitutes: An update. Injury.36:20-7. 2005.
3. Desai BM. Osteobiologics. American journal of orthopedics (Belle Mead, NJ).36:8-11. 2007.
4. Damien CJ, Parsons JR. Bone-Graft and Bone-Graft Substitutes - a Review of Current Technology and Applications. J Appl Biomater.2:187-208. 1991.
5. Quarto R, Mastrogiacomo M, Cancedda R, Kutepov SM, Mukhachev V, Lavroukov A, et al. Repair of large bone defects with the use of autologous bone marrow stromal cells. New Engl J Med.344:385-6. 2001.
6. Brun P, Dickinson SC, Zavan B, Cortivo R, Hollander AP, Abatangelo G. Characteristics of repair tissue in second-look and third-look biopsies from patients treated with engineered cartilage: relationship to symptomatology and time after implantation. Arthritis Res Ther.10. 2008.
7. Eaglstein WH, Falanga V. Tissue engineering and the development of Apligraf(R), a human skin equivalent. Clin Ther.19:894-905. 1997.
8. Mason C. Automated tissue engineering: a major paradigm shift in health care. Medical device technology.14:16-8. 2003.
9. Shefelbine SJ, Simon U, Claes L, Gold A, Gabet Y, Bab I, et al. Prediction of fracture callus mechanical properties using micro-CT images and voxel-based finite element analysis. Bone.36:480-8. 2005.
10. Tuan HS, Hutmacher DW. Application of micro CT and computation modeling in bone tissue engineering. Comput Aided Design.37:1151-61. 2005.

11. Silva DN, De Oliveira MG, Meurer E, Meurer MI, Da Silva JVL, Santa-Barbara A. Dimensional error in selective laser sintering and 3D-printing of models for craniomaxillary anatomy reconstruction. J Cranio Maxill Surg.36:443-9. 2008.

12. Grayson WL, Frohlich M, Yeager K, Bhumiratana S, Chan ME, Cannizzaro C, et al. Engineering anatomically shaped human bone grafts. Proceedings of the National Academy of Sciences of the United States of America.107:3299-304. 2010.

13. Reiffel AJ, Kafka C, Hernandez KA, Popa S, Perez JL, Zhou S, et al. High-Fidelity Tissue Engineering of Patient-Specific Auricles for Reconstruction of Pediatric Microtia and Other Auricular Deformities. Plos One.8. 2013.

14. Kang TY, Kang HW, Hwang CM, Lee SJ, Park J, Yoo JJ, et al. The realistic prediction of oxygen transport in a tissue-engineered scaffold by introducing time-varying effective diffusion coefficients. Acta biomaterialia.7:3345-53. 2011.

15. Otsuki B, Takemoto M, Fujibayashi S, Neo M, Kokubo T, Nakamura T. Pore throat size and connectivity determine bone and tissue ingrowth into porous implants: Three-dimensional micro-CT based structural analyses of porous bioactive titanium implants. Biomaterials.27:5892-900. 2006.

16. Mavrogenis AF, Dimitriou R, Parvizi J, Babis GC. Biology of implant osseointegration. J Musculoskel Neuron.9:61-71. 2009.

17. Eshraghi S, Das S. Micromechanical finite-element modeling and experimental characterization of the compressive mechanical properties of polycaprolactone-hydroxyapatite composite scaffolds prepared by selective laser sintering for bone tissue engineering. Acta biomaterialia.8:3138-43. 2012.

18. Hollister SJ, Levy RA, Chu TM, Halloran JW, Feinberg SE. An image-based approach for designing and manufacturing craniofacial scaffolds. Int J Oral Max Surg.29:67-71. 2000.

19. Tellis BC, Szivek JA, Bliss CL, Margolis DS, Vaidyanathan RK, Calvert P. Trabecular scaffolds created using micro CT guided fused deposition modeling. Mat Sci Eng C-Bio S.28:171-8. 2008.

20. Wettergreen MA, Bucklen BS, Starly B, Yuksel E, Sun W, Liebschner MAK. Creation of a unit block library of architectures for use in assembled scaffold engineering. Comput Aided Design.37:1141-9. 2005.

21. Chen Z, Su Z, Ma S, Wu X, Luo Z. Biomimetic modeling and three-dimension reconstruction of the artificial bone. Comput Meth Prog Bio.88:123-30. 2007.

22. Yasar O, Lan SF, Starly B. A Lindenmayer system-based approach for the design of nutrient delivery networks in tissue constructs. Biofabrication.1. 2009.

23. Kermer C, Rasse M, Lagogiannis G, Undt G, Wagner A, Millesi W. Colour stereolithography for planning complex maxillofacial tumour surgery. J Cranio Maxill Surg.26:360-2. 1998.

24. Chow J, Hui E, Lee PKM, Li W. Zygomatic implants - Protocol for immediate occlusal loading: A preliminary report. J Oral Maxil Surg.64:804-11. 2006.

25. Ran W, Liu XZ, Guo B, Shu DL, Tan ZM. Removal of a foreign body from the skull base using a customized computer-designed guide bar. J Cranio Maxill Surg.38:279-83. 2010.

26. Chu TMG, Halloran JW, Hollister SJ, Feinberg SE. Hydroxyapatite implants with designed internal architecture. J Mater Sci-Mater M.12:471-8. 2001.

27. Williams JM, Adewunmi A, Schek RM, Flanagan CL, Krebsbach PH, Feinberg SE, et al. Bone tissue engineering using polycaprolactone scaffolds fabricated via selective laser sintering. Biomaterials.26:4817-27. 2005.

28. Zein I, Hutmacher DW, Tan KC, Teoh SH. Fused deposition modeling of novel scaffold architectures for tissue engineering applications. Biomaterials.23:1169-85. 2002.

29. Jakab K, Norotte C, Marga F, Murphy K, Vunjak-Novakovic G, Forgacs G. Tissue engineering by self-assembly and bio-printing of living cells. Biofabrication.2. 2010.

30. Norotte C, Marga FS, Niklason LE, Forgacs G. Scaffold-free vascular tissue engineering using bioprinting. Biomaterials.30:5910-7. 2009.

31. Schuurman W, Khristov V, Pot MW, van Weeren PR, Dhert WJA, Malda J. Bioprinting of hybrid tissue constructs with tailorable mechanical properties. Biofabrication.3. 2011.

32. Jetze V, Benjamin P, Thijs JB, Jelle B, Wouter JAD, Ferry PWM, et al. Biofabrication of multi-material anatomically shaped tissue constructs. Biofabrication.5:035007. 2013.

33. Lemon G, Howard D, Tomlinson MJ, Buttery LD, Rose FRAJ, Waters SL, et al. Mathematical modelling of tissue-engineered angiogenesis. Math Biosci.221:101-20. 2009.

34. Manoussaki D. A mechanochemical model of angiogenesis and vasculogenesis. Esaim-Math Model Num.37:581-99. 2003.

35. Merks RMH, Koolwijk P. Modeling Morphogenesis in silico and in vitro: Towards Quantitative, Predictive, Cell-based Modeling. Math Model Nat Pheno.4:149-71. 2009.

36. Bancroft GN, Sikavitsast VI, van den Dolder J, Sheffield TL, Ambrose CG, Jansen JA, et al. Fluid flow increases mineralized matrix deposition in 3D perfusion culture of marrow stromal osteloblasts in a dose-dependent manner. P Natl Acad Sci USA.99:12600-5. 2002.

37. Cartmell SH, Porter BD, Garcia AJ, Guldberg RE. Effects of medium perfusion rate on cell-seeded three-dimensional bone constructs in vitro. Tissue Eng.9:1197-203. 2003.

38. Grayson WL, Bhumiratana S, Cannizzaro C, Chao PHG, Lennon DP, Caplan AI, et al. Effects of Initial Seeding Density and Fluid Perfusion Rate on Formation of Tissue-Engineered Bone. Tissue Eng Pt A.14:1809-20. 2008.

39. Sikavitsas VI, Bancroft GN, Mikos AG. Formation of three-dimensional cell/polymer constructs for bone tissue engineering in a spinner flask and a rotating wall vessel bioreactor. J Biomed Mater Res.62:136-48. 2002.

40. Sikavitsas VI, Bancroft GN, Holtorf HL, Jansen JA, Mikos AG. Mineralized matrix deposition by marrow stromal osteoblasts in 3D perfusion culture increases with increasing fluid shear forces. Proceedings of the National Academy of Sciences of the United States of America.100:14683-8. 2003.

41. Goldstein AS, Juarez TM, Helmke CD, Gustin MC, Mikos AG. Effect of convection on osteoblastic cell growth and function in biodegradable polymer foam scaffolds. Biomaterials.22:1279-88. 2001.

42. Endres S, Kratz M, Wunsch S, Jones DB. Zetos: A culture loading system for trabecular bone. Investigation of different loading signal intensities on bovine bone cylinders. J Musculoskel Neuron.9:173-83. 2009.

43. Henstock JR, Rotherham M, Rose JB, El Haj AJ. Cyclic hydrostatic pressure stimulates enhanced bone development in the foetal chick femur in vitro. Bone.53:468-77. 2013.

44. Srinivasan S, Weimer DA, Agans SC, Bain SD, Gross TS. Low-magnitude mechanical loading becomes osteogenic when rest is inserted between each load cycle. J Bone Miner Res.17:1613-20. 2002.

45. Allison SJ, Folland JP, Rennie WJ, Summers GD, Brooke-Wavell K. High impact exercise increased femoral neck bone mineral density in older men: A randomised unilateral intervention. Bone.53:321-8. 2013.

46. Sikavitsas VI, Temenoff JS, Mikos AG. Biomaterials and bone mechanotransduction. Biomaterials.22:2581-93. 2001.

47. Martin I, Smith T, Wendt D. Bioreactor-based roadmap for the translation of tissue engineering strategies into clinical products. Trends Biotechnol.27:495-502. 2009.

48. Gardel LS, Serra LA, Reis RL, Gomes ME. Use of Perfusion Bioreactors and Large Animal Models for Long Bone Tissue Engineering. Tissue Engineering Part B: Reviews. 2013.

49. Costa PF, Martins A, Vaquette C, Melchels FP, Neves NM, Gomes ME, et al. Bioreactor composed of watertight chamber and internal matrix for the generation of cellularized medical implants. 2013.

50. Koch MA, Vrij EJ, Engel E, Planell JA, Lacroix D. Perfusion cell seeding on large porous PLA/calcium phosphate composite scaffolds in a perfusion bioreactor system under varying perfusion parameters. J Biomed Mater Res A.95A:1011-8. 2010.

51. Janssen FW, van Dijkhuizen-Radersma R, Van Oorschot A, Oostra J, de Bruijn JD, Van Blitterswijk CA. Human tissue-engineered bone produced in clinically relevant amounts using a semi-automated perfusion bioreactor system: a preliminary study. J Tissue Eng Regen M.4:12-24. 2010.

52. Costa PF, Martins A, Neves NM, Gomes ME, Reis RL. Multichamber bioreactor with bidirectional perfusion integrated in culture system for tissue engineering strategies. European Patent Application 090098632009.

53. Rotenberg MY, Ruvinov E, Armoza A, Cohen S. A multi-shear perfusion bioreactor for investigating shear stress effects in endothelial cell constructs. Lab on a Chip.12:2696-703. 2012.

54. Figallo E, Cannizzaro C, Gerecht S, Burdick JA, Langer R, Elvassore N, et al. Micro-bioreactor array for controlling cellular microenvironments. Lab on a Chip.7:710-9. 2007.

55. Rolfe P. Sensing in tissue bioreactors. Meas Sci Technol.17:578-83. 2006.

56. Santoro R, Krause C, Martin I, Wendt D. On-line monitoring of oxygen as a non-destructive method to quantify cells in engineered 3D tissue constructs. J Tissue Eng Regen M.6:696-701. 2012.

57. Porter BD, Lin ASP, Peister A, Hutmacher D, Guldberg RE. Noninvasive image analysis of 3D construct mineralization in a perfusion bioreactor. Biomaterials.28:2525-33. 2007.

58. Hagenmuller H, Hitz M, Merkle HP, Meinel L, Muller R. Design and validation of a novel bioreactor principle to combine online micro-computed tomography monitoring and mechanical loading in bone tissue engineering. Rev Sci Instrum.81. 2010.

59. Holt GE, Halpern JL, Dovan TT, Hamming D, Schwartz HS. Evolution of an in vivo bioreactor. J Orthop Res.23:916-23. 2005.

60. Han D, Dai K. Prefabrication of a Vascularized Bone Graft With Beta Tricalcium Phosphate Using an In Vivo Bioreactor. Artificial Organs. 2013.

61. Stevens MM, Marini RP, Schaefer D, Aronson J, Langer R, Shastri VP. In vivo engineering of organs: The bone bioreactor. Proceedings of the National Academy of Sciences of the United States of America.102:11450-5. 2005.

62. Terheyden H, Knak C, Jepsen S, Palmie S, Rueger DR. Mandibular reconstruction with a prefabricated vascularized bone graft using recombinant human osteogenic protein-1: an experimental study in miniature pigs. Part 1: Prefabrication. Int J Oral Max Surg.30:373-9. 2001.

63. Terheyden H, Warnke P, Dunsche A, Jepsen S, Brenner W, Palmie S, et al. Mandibular reconstruction with prefabricated vascularized bone grafts using recombinant human osteogenic protein-1: an experimental study in miniature pigs. Part II: Transplantation. Int J Oral Max Surg.30:469-78. 2001.

64. Warnke PH, Springer ING, Wiltfang J, Acil Y, Eufinger H, Wehmoller M, et al. Growth and transplantation of a custom vascularised bone graft in a man. Lancet.364:766-70. 2004.

65. Fleming JE, Jr., Cornell CN, Muschler GF. Bone cells and matrices in orthopedic tissue engineering. Orthop Clin North Am.31:357-74. 2000.

66. Hutmacher DW. Scaffolds in tissue engineering bone and cartilage. Biomaterials.21:2529-43. 2000.

67. Kim BS, Mooney DJ. Development of biocompatible synthetic extracellular matrices for tissue engineering. Trends Biotechnol.16:224-30. 1998.

68. Perka C, Sittinger M, Schultz O, Spitzer RS, Schlenzka D, Burmester GR. Tissue engineered cartilage repair using cryopreserved and noncryopreserved chondrocytes. Clin Orthop Relat Res.245-54. 2000.

69. Vacanti CA, Bonassar LJ. An overview of tissue engineered bone. Clin Orthop Relat Res.S375-81. 1999.

70. Miyoshi H, Ehashi T, Ohshima N, Jagawa A. Cryopreservation of Fibroblasts Immobilized Within a Porous Scaffold: Effects of Preculture and Collagen Coating of Scaffold on Performance of Three-Dimensional Cryopreservation. Artificial Organs.34:609-14. 2010.

71. Yin H, Cui L, Liu G, Cen L, Cao Y. Vitreous cryopreservation of tissue engineered bone composed of bone marrow mesenchymal stem cells and partially demineralized bone matrix. Cryobiology.59:180-7. 2009.

72. Rupf T, Ebert S, Lorenz K, Salvetter J, Bader A. Cryopreservation of Organotypical Cultures Based on 3D Scaffolds. Cryoletters.31:157-68. 2010.

73. Bernemann I, Kuberka M, Glasmacher B. 71. Adapted freezing and thawing procedures to improve the cryopreservation of cell seeded scaffolds. Cryobiology.53:397-8. 2006.

74. Kofron MD, Opsitnick NC, Attawia MA, Laurencin CT. Cryopreservation of tissue engineered constructs for bone. Journal of Orthopaedic Research.21:1005-10. 2003.

75. Costa PF, Dias AF, Reis RL, Gomes ME. Cryopreservation of Cell/Scaffold Tissue-Engineered Constructs. Tissue Eng Part C-Me.18:852-8. 2012.

76. Karlsson JO, Toner M. Long-term storage of tissues by cryopreservation: critical issues. Biomaterials.17:243-56. 1996.

Section II

Detailed description of experimental testing and materials

Chapter 2

Materials and methods

This chapter provides a general overview and detailed information on all the techniques used and biological assays performed under the scope of this thesis. Although described in the materials and methods section of each experimental chapter, herein the objective is to contextualize and justify the selection of materials and methodologies applied throughout the thesis and complement information given on each chapter.

1. Materials

Throughout the work described in this thesis various materials have been utilized for the development of scaffolds. The selection of each material was performed according to the specific requirements of each device and application to be addressed in each of the experimental chapters. Polycaprolactone is a very commonly utilized and well accepted material in implantation-based biomedical applications either alone, blended with other polymers or in a composite with ceramic materials. Poly(lactic) acid is an equally common and accepted material in such applications with the additional advantage of also being one of the most commonly utilized materials in additive manufacturing by fused deposition modelling. Another advantage of these two materials is that their mechanical and biochemical properties can be easily tailored to meet required properties. Another material commonly utilized in fused deposition modelling is ABS, which, despite being more utilized in industrial applications, possesses the advantage of being inert and so becoming suitable for the fabrication of non-implantable devices (in this case cell culture chambers).

1.1. Polycaprolactone

Polycaprolactone (PCL) is a biodegradable polyester obtained by chemical synthesis from crude oil and can be synthesized by a ring opening polymerization of a cylic lactone monomer. PCL is an hydrophobic and semi-crystalline polymer with a melting point of around 60 °C and a glass transition temperature of about -60 °C. Its degradation by hydrolysis of ester bonds in physiological conditions [1, 2] along with good biocompatibility and ability to form blends and copolymers have made it very suitable for application as a biomaterial becoming approved by the Food and Drug Administration (FDA) for use in the human body in forms such as drug delivery devices and sutures [3-5]. The medical grade PCL used in this work was purchased from Lactel (USA) and was utilized in chapter 6 for producing fiber meshes by melt electrospinning.

1.2. Polycaprolactone - β-tricalcium phosphate

β-tricalcium Phosphate (β-TCP) is a bioactive and biocompatible ceramic similar to the amorphous inorganic phase of bone which can be produced synthetically by calcination of either precipitated hydroxyapatite or a mixture of dicalcium phosphate dihydrate with precipitated

hydroxyapatite [6]. It is degradable by osteoclastic activity, has the ability to bind directly to bone and is osteoinductive while eliciting minimal immunologic reactions. β-TCP is commonly used in the form of granules and blocks as a bone substitute. The integration of β-TCP and polymers such as polycaprolactone into composite scaffolds is able to combine properties of both the polymer and the ceramic resulting in enhanced mechanical, biocompatibility and osteoconductivity properties as well as increased degradation rate [7]. Given the known osteoinductive properties of polycaprolactone - β-tricalcium Phosphate, blends composed of medical grade PCL and 20% wt β-TCP were purchased from Osteopore Inc. (Singapore) and were used in the work described in chapter 6 of this thesis for producing 3D scaffolds by additive manufacturing.

1.3. Poly(lactic) acid

Poly(lactic) acid (PLA) is an hydrophobic aliphatic polyester belonging to the α-hydroxy group which is among the most popular and most widely used materials in tissue engineering [8, 9]. It is usually synthesized by ring-opening polymerization of the cyclic diester lactide [10]. PLA exists in either isomeric forms D or L, or in its racimic form D,L. The PLLA form is the most commonly used since it is preferentially metabolized in the body [11]. PLA is a degradable polymer which undergoes hydrolytic scission to its monomeric form, lactic acid, which in turn is eliminated from the body by incorporation into the tricarboxylic acid cycle. The principal elimination path for lactic acid is respiration, and it is primarily excreted by the lungs as CO2 [12]. Such as PCL, PLA is among the few biodegradable polymers which are approved by the FDA for human clinical use in the form of implantable materials and/or devices. The commercially available PLA used in this work was Ingeo 4043D from NatureWorks LLC (USA). Given the widespread use/study of PLA in biomedical applications, in particular for replacing hard tissues such as bone, it was used in the works described in chapters 4 and 5 for producing 3D scaffolds by additive manufacturing. Furthermore, PLA is one of the most commonly used polymers in fused deposition modelling-based additive manufacturing.

1.4. Acrylonitrile butadiene styrene (ABS)

Acrylonitrile–butadiene–styrene (ABS) is a copolymer synthesized via graft copolymerization of styrene and acrylonitrile monomers onto polybutadiene chains, which provides advantageous mechanical properties, such as increased toughness and a higher impact and chemical resistance [13]. Given its

characteristics, ABS has become a commonly used thermoplastic for making light, rigid, molded everyday products. Moreover, ABS has also become the most commonly used polymer in additive manufacturing given its high availability and low price. Due to its inert nature, ABS was used in the work described in chapters 4 and 5 for additively manufacturing bioreactor chambers with optimized geometries. The ABS utilized was purchased from Makerbot industries (USA).

1.5. Starch-Polycaprolactone blend (SPCL)

Starch is a polysaccharide carbohydrate made of glucose units joined together by glycosidic bonds, which in turn are made of amylose, a linear polymer of several thousand glucose residues, and amylopectin, a highly branched glucose-based polymer. Starch-based materials have attracted great attention in tissue engineering applications due to the advantages of being non-cytotoxic, having good mechanical properties and being processed by various methodologies as well as being able to reduce costs and increase biodegradability when combined with various synthetic polymers [14-17].

Starch-based scaffolds obtained from a blend of corn starch and polycaprolactone (SPCL) have for a long time been proposed in multiple studies from our group as candidates for bone tissue engineering applications showing its suitability in terms of cell viability, proliferation and maturation of osteoblastic cells or differentiation of bone marrow stromal cells [18, 19] as well as limited adverse immune response when tested *in vivo* [20-22]. For these reasons, the 30:70 (wt.%) SPCL blend was post-processed into either disk-shaped samples by injection molding or into fiber mesh structures by melt-spinning and fiber bonding, in order to be utilized in the work described in chapter 7. The polymeric blend was obtained from Novamont (Novara, Italy).

2. Fabrication of Culture devices and Scaffolds

2.1. Device Design

The general bioreactor design methodology employed in chapter 4 began with the generation of a 3D numerical model for any tissue or organ by micro-computed tomography (micro-CT) imaging which was then converted into a three-dimensional replica with pre-determined porosity. An outer shell, referred herein as bioreactor chamber, possessing inlets/outlets was then designed around the replica in order to manufacture, in one step, an anatomically shaped device comprising of an anatomically-optimized

scaffold inserted into a customized bioreactor chamber. This allowed for the perfusion of the resulting scaffold during *in vitro* culture, while better controlling the flow and shear stress in the system. In this way, a 3 cm ovine tibia section was scanned by micro-CT to create a numerical 3D model which was subsequently imported into 3Ds Max (Autodesk, USA) software. The 3D model was vertically re-oriented and both extremities of the tibial model were trimmed for obtaining horizontal flat surfaces and resulted in the final model having a total length of 2.5 cm. The 3D design tool, extrusion, was then used to generate a shell wall around the lateral and top outer surfaces of the 3D model. The generated wall was 1 mm thick and 1 mm-spaced from the 3D scaffold model's outer surfaces. The top part of the shell was converted to a tubular conical shape possessing a slope angle of 55° in order to be self-supportive. This part of the shell was designed to enable an adequate fluid flow on the interior of the device, and to provide sufficient space for containing extra culture medium. The top end of this conical medium reservoir had a slope angle of 90° creating an inlet/outlet structure with an inner diameter of 2mm onto which tubing could be connected. The bottom corners of the chamber were additionally chamfered by 2 mm with a slope angle of 45° to improve the hydrodynamic design. On the bottom part of the device, a plate containing a 1 mm-wide mini channel was designed, allowing connectivity of the centre of the plate to a lateral 2 mm diameter inlet/outlet. Furthermore, by using the same extrusion design tool, a plain column was also generated for filling the empty space located in the centre of the tibia-shaped model.

On the other hand, the device intended for high throughput screening applications utilized in chapter 5 was required to contain multiple samples for simultaneous testing and facilitated handling. The device utilised in chapter 5 was designed to be modular and to allow for scaling-up according to the number of scaffolds required for the experiment. The device was therefore designed to simultaneously accommodate 8 cubical scaffolds (8 mm width) composed of 400 µm diameter struts horizontally spaced by 1.5 mm in a 0-90 degree orientation. The device design was performed in 3Ds Max (Autodesk, USA) software and consisted in building individualised bioreactor chambers by placing 1 mm thick walls around each of the 8 scaffolds, which were organised in a rectangular 2 by 4 configuration. The walls were positioned at 1 mm from the scaffolds and were 10 mm taller than the scaffolds in order to create a reservoir for the culture medium. The top of every 4 chambers was covered by a pyramidal structure ending by a 2 mm diameter outlet utilised for attaching sterile filters during subsequent cell culture. A symmetrical mini-fluidic channel network was designed for homogenously distributing the culture medium through the various individual chambers and allowing connectivity to a lateral 2 mm diameter inlet/outlet.

2.2. Additive manufacturing of devices and scaffolds by fused deposition modelling (FDM)

Additive manufacturing is a highly automated layer-by-layer process which involves the sequential building of layers of material by deposition of new layers of material on top of previously laid layers of material. In tissue engineering, additive manufacturing is mainly used for the production of scaffolds according to very defined structures generated through computer aided design (CAD) [23, 24].

In the work described in chapters 3, 4 and 5 of this thesis, the developed 3D CAD structures were obtained either by simple design using geometrical shapes in the 3Ds Max (Autodesk, USA) software or by means of the utilization of medical imaging data obtained by micro computerized tomography analysis (Micro-CT).

The specific technology of fused deposition modelling, which was utilized in the work described in this thesis, consists on the extrusion of molten material from a heated extruder forming a thin filament which is laid down over a deposition surface which moves over three axis relatively to the extrusion nozzle. By coordinating the movement of the deposition table and the extrusion in the nozzle, highly detailed patterns of thermoplastic material can be created over the deposition surface. When the deposition of one layer of material is finished, the extrusion is stopped while the deposition table is slightly moved away from the extruder tip. The extrusion is then restarted and a new patterned layer is deposited over the precedent layer to which it adheres.

Prior to the actual manufacturing, the 3D CAD models of the developed devices were first sliced and converted to a G-Code file, which is the type of programming language commonly used to control additive manufacturing machines. The open source software Reprap (Reprap Online Community) was utilized in order to convert the plain volumes corresponding to the scaffolds designed in chapters 4 and 5 into porous structures by slicing into 0.27mm layers composed of deposition pathlines with a spacing of 1.5mm. The volumes corresponding to the outer chamber devices designed in chapters 4 and 5 were sliced and converted to G-Code through the open source software ReplicatorG (ReplicatorG Online Community) using 2 shells, a slice thickness of 0,27mm, an object infill of 100%, a feed rate of 20 mm/s and a travel feed rate of 55 mm/s as parameters. Both G-Codes generated through RepRap and ReplicatorG were finally merged together generating one single G-Code file. The devices were then manufactured using a dual extrusion Replicator (Makerbot Industries, USA) prototyping machine. Poly(lactic) acid (PLA) Ingeo 4043D (NatureWorks LLC, USA) was used for building the porous scaffolds

and acrylonitrile butadiene styrene (ABS) (Makerbot industries, USA) for building the enclosing devices. The temperature used for fusing both materials in their corresponding nozzles was 220°C. Both materials were deposited during the same print job through coordinated and alternating operation of the nozzles. The additive manufacturing by fused deposition modelling performed in the work described in chapter 6 was similar to the one described above for the generation of scaffolds but instead utilizing a PCL-β-TCP composite as deposition material.

2.3. Melt Electrospinning

Unlike randomly deposited fibers in solution electrospinning, molten polymers in melt electrospinning possess higher viscosities and lower conductivities but can still be electrostatically drawn over relatively large distances and their behavior and pathway can be controlled to a greater extent [25]. Melt electrospun fibers tend as well to be larger than the solution electrospun fibers and as a result generating meshes with greater pore size and interconnectivity facilitating cellular penetration.

The apparatus used in melt electrospinning apparatus is very similar to the ones utilized in solution electrospinning, being essentially composed of a high voltage power supply with an electrode connected to the needle of a syringe (containing the polymer) mounted onto a syringe pump and a ground metallic collector placed at a defined distance from the tip of the metallic needle. The main distinguishing characteristic of melt electrospinning is that the polymer contained into the syringe reservoir is in a solid form (usually as pellet or powder) and in turn is heated by a thermal element surrounding the syringe which in turn melts the polymer by heat transmission allowing it to be extruded through the syringe needle. When the polymer exits the syringe needle, the electrostatic forces generated by the power supply draw the polymer to the ground collector causing stretching and narrowing of the resisting fiber. The polymer processed through melt electrospinning in the work described in chapter 6 of this thesis (medical grade PCL from Lactel, (USA)) was electrospun using an in-house melt electrospinning device. Medical grade pellets were loaded into a 2 mL syringe and electrospun at a temperature of 80°C at a feed rate of 20 μL/h, at 7 kV and at a 4 cm tip to collector distance. Circular membranes with roughly 8 mm diameter were produced by electrospinning the molten PCL for periods of 4 min onto aluminum foil-covered glass slides placed over the collector. The architectural and mechanical properties of melt electrospun meshes were found to be ideal for being applied in the work described in chapter 6 since they would act as robust yet soft biomechanical

supports for the deposition of several layers of cell sheets without inducing any disruptive damage to those same cell sheets.

2.4. Biomimetic coating of the FDM scaffolds

In the early nineties Kokubo et al. developed a solution called Simulated Body Fluid (SBF) which could be utilized for depositing biomimetic calcium phosphate (CaP) coatings on the surface of devices and implants [26, 27]. This technique has demonstrated its efficacy at increasing bone related gene expression in various cell types [28-32] and at enhancing ectopic bone formation in rat models [33]. Given the osteoinductive properties of this kind of coating, the same was applied to the surface modification of two types of scaffolds involved in the work described in chapters 5 and 6 of this thesis.

The PCL FDM scaffolds utilized in chapter 6 were submitted to a calcium phosphate coating process by successive immersion into specific reagents and solutions. The procedure consisted of the following steps: immersion in 100% ethanol for 15 minutes under vacuum, immersion in sodium hydroxide 2 M for 30 min at 37°C, multiple rinse-immersions in ultrapure water until a water pH of 7 was reached, immersion in a 10x simulated body fluid (SBF) solution for 30 min at 37°C and immersion in a 0.5 M sodium hydroxide solution for 30 min at 37°C. Finally the coated scaffolds were rinsed with ultrapure water and stored in a desiccator until use.

In chapter 5, a similar coating method was employed for improving the surface properties of the utilized scaffolds. In this case however the utilized scaffolds were made of PLA and were contained into an enclosed device requiring a slightly modified procedure. Given the hydrophobic nature of PLA used for manufacturing the scaffolds, which could hinder appropriate and homogeneous fluid perfusion through the device, an alkaline etching was performed using a 2M sodium hydroxide (NaOH) solution. The devices were pre-wetted in 100% ethanol solution under vacuum for a period between 15 min and one hour. Thereafter, the ethanol was removed and the sodium hydroxide solution was perfused though the device until the bioreactor was entirely filled and 30 min vacuum treatment at room temperature was performed prior to placing the device at 37°C for 60 min. Finally, the devices were washed four times with distilled water prior to the further deposition of a calcium phosphate biomimetic coating on the PLA filaments. The deposition of the calcium phosphate coating was performed by filling the chambers with a total of 8 ml of 10x Simulated Body Fluid (SBF) solution at pH 6 for 30 min at 37°C and followed by perfusion with a 0.5 M sodium hydroxide solution for 30 min at 37°C. Finally the coated scaffolds were rinsed with ultrapure water and air-dried.

2.5. Fiber bonding

Fiber bonding is a very simple and straightforward processing methodology which consists of binding individual fibers, either woven or knitted, into three-dimensional patterns of variable pore size. The advantageous characteristic features of fiber meshes produced in this way are a large surface area for cell attachment and a good interconnectivity among pores that usually favors the flow of nutrients and therefore enhances cellular survival and proliferation [34-37]. A drawback of these scaffolds, when comparing to scaffolds fabricated by other methodologies such as additive manufacturing, is the difficulty to accurately control their architecture and porosity [34, 36, 37].

The porous scaffolds utilized in the work described in chapter 7 were produced through a pre-established fiber bonding methodology [38, 39]. Briefly, a selected amount of fibers obtained by melt spinning was placed in a glass mould and heated in an oven at 150°C. Immediately after removal of the mould from the oven, the fibers were slightly compressed with a Teflon cylinder. After bonding, the fiber meshes were cut into 8 mm diameter and 3.5–4 mm thick samples by punching.

2.6. Injection molding

In chapter 7 injection molding was employed to produce SPCL nonporous discs. This methodology has been utilized for producing scaffolds for tissue engineering applications, however it has mostly been explored in combination with blowing agents which, when exposed to high temperatures, expand and form pores into the molded polymer and therefore generating porous structures [40, 41]. In the work described in chapter 7, however, our aim was to obtain injection molded structures without any porosity and therefore no blowing agent was used. These discs were produced in a Klockner Ferromatic FM-20 machine using a mould that allowed obtaining discs with 8 mm diameter and 3 mm thickness. The produced injection molded discs were later seeded with cells and cryopreserved to assess the effect of this process on the surface properties of the materials and also to compare with porous scaffolds that underwent the same procedure, namely to analyze the effect of porosity in the maintenance of the survival of seeded/cultured cells upon cryopreservation.

3. Scaffolds Characterization

3.1. Morphological Characterization

3.1.1. Scanning Electron Microscopy

Scanning electron microscopy (SEM) is a commonly used microscopic method for analyzing the morphology of materials and structures given its high magnifications capacity. SEM is mainly used for studying the three-dimensional topography of specimens down to sub-micron scales. In order to increase the degree of magnification, polymeric samples are usually coated with conductive materials such as gold or carbon by sputtering prior to analysis.

SEM characterization was employed in all experimental chapters of this thesis, for assessment of the morphology and porous architectures of the developed scaffolds and also for assessing the interaction of cells with their surfaces. In the studies where materials and scaffolds were seeded/cultured with cells (chapters 4 to 7).the resulting samples were removed from culture, washed with PBS and fixed in 3% glutaraldehyde. Afterwards the cell-scaffolds samples were immersed in 0.1 M cacodylate buffer, 1 % osmium tetroxide in cacodylate buffer, rinsed in ultrapure water and then dehydrated by immersion into increasingly higher concentration ethanol solutions. Finally, samples were immersed in hexamethyldisilazane for 60 min, air dried, mounted onto stubs and gold coated. Samples were observed on a FEI Quanta 200 Environmental SEM operating at 10 kV.

3.1.2. Micro computerized tomography

Currently existing technologies for non-invasive imaging allow for body parts or whole bodies to be analyzed without any damage to tissues themselves. Technologies such as micro computerized tomography (micro-CT) enable the collection of data from damaged tissue sites which need to be repaired. Given the high degree of resolution provided by such technologies it becomes possible to obtain not only information related to the defect's and organ's outer shape but also information related to their more complex inner porosity, density and micro structure.

Micro computerized tomography makes use of an X-ray source to obtain cross-sectional images of three-dimensional objects which are then combined to reconstruct a three-dimensional numerical model of the analyzed object [42].

In the work described in chapters 4 to 6 of this thesis, samples were analyzed by Micro-CT (μCT40, SCANCO Medical AG, Brüttisellen, Switzerland) at a resolution of 12 μm, a voltage of 55 kVp and at a current of 175 μA. In chapter 7, a SkyScan 1072 equipment was used, where the x-ray source was set up to 40KV, 248μA with a magnification of 23.29x and an exposure time of 1.8 seconds which resulted in a resolution of about 11.32 μm/pixel. Three-dimensional images were reconstructed from the scans by the micro-CT system software. In chapters 4 and 5, this analysis allowed to evaluate characteristics such as the device's inner architecture and the effect of post-treatment modification in PLA scaffolds while in chapter 5 it allowed to assess the morphology and calculate both the volumes and densities of *de novo* generated bone tissue in the biphasic scaffolds. In chapter 7, micro-ct was mainly used to assess if the porosity of the scaffolds used was altered by cryopreservation.

3.1.3. Computational fluid flow modelling

Homogenous fluid velocities and absence of stagnant zones are among the main features defining an optimal culture system which can greatly determine the fate of cultured cells and tissues. The control over the fluid pattern within perfused scaffolds is essential for achieving efficient in vitro culture conditions. Computational fluid dynamics is a mathematically generated simulation tool which is able to predict the behavior of fluids with selected properties along spaces with predetermined sizes and shapes.

Computational fluid dynamics was used to optimize the flow pattern in the culture chambers developed under chapters 4 and 5. For this purpose, various chamber designs diverging in several parameters were tested with regard to the homogeneity of the flow pattern. Given the high complexity of the device's architecture, simplified two-dimensional sections of the devices were created in Design Modeler 13.0 (Ansys) software. The profile corresponding to the section of an 8 mm wide cubic porous scaffold surrounded by a 10 mm wide bioreactor chamber was considered in chapter 5. On the other hand, in chapter 4, a profile corresponding to a section of a tubular scaffold with a length of 2.5 cm, an outer diameter of 13 mm and an inner diameter of 6 mm was considered. The thickness of the studied simplified sections was 0.1 mm and the maximum face size of the generated model mesh was $2x10^{-4}$ mm. The fluid flow velocity profiles were calculated using Fluent 13.0 (Ansys, USA) software, within Ansys Workbench 13.0 platform. The pressure at the device's outlets was assumed to be zero and the scaffold and the bioreactor chamber were considered rigid and impermeable. We assumed that the

viscosity and the density of the culture media at 37°C were $\eta = 1.45 \bullet 10{-}3Pa.s$) and ($\rho$ = 1000 kg.m−3) respectively.

3.1.4. Atomic Force Microscopy (AFM)

Atomic force microscopy is a technique which allows to obtain very small surface roughness profiles in the surface of samples by means of a cantilever probe. The surface roughness of the SPCL discs utilized in chapter 7 was measured by AFM, in order to assess the effect of the cryopreservation process in this surface property. AFM was not performed on the SPCL scaffolds utilized in that chapter since their surfaces were not sufficiently flat for this methodology to be reliably employed. The analysis was performed on 3 samples per study group/condition on at least three spots per sample using tapping mode in a multimode scanning probe microscope (Veeco, USA) connected to a NanoScope III (Veeco, USA) with non-contacting silicon nanoprobes (ca. 300 kHz, setpoint 2–3 V) (Nanosensors, Switzerland). All images were fitted to a plane using the 1st degree flatten procedure included in NanoScope software version 4.43r8.

3.2. Mechanical characterization

In chapter 7, SPCL scaffolds and discs were submitted to compression tests before and after cryopreservation for determining their compressive modulus, using a universal tensile testing machine (Instron 4505 Universal Machine). The aim was to assess the effect of cryopreservation over the mechanical properties of the utilized scaffolds and discs. The tests were performed under compression loading using a crosshead speed of 2 mm/min until 60% strain was reached. The compressive modulus was determined in the most linear region of the stress–strain curve using the secant method. A total of 10 samples per study group/condition were used for this analysis.

3.3. X-Ray diffraction

X-ray diffraction is an important technique for qualitative and quantitative analyses as well as for fundamental studies of the properties and structures of materials. The particularly useful feature of this technique is that it enables the identification of specific compounds contained into samples.

Furthermore, it is a nondestructive technique hence allowing to obtain large amounts of information about relatively small material samples [43]. In a simplified way, x-ray diffraction acts by exposing materials to x-ray beams. The analysis of the angle and intensity of resulting diffracted beams can then be analyzed and a diffraction pattern obtained. The diffraction pattern of a pure material is unique hence resulting as a fingerprint. By comparison with diffraction patterns stored into databases it becomes then possible to identify the specific compounds composing a certain sample. This technique was utilized in chapter 6 of this thesis to analyse the calcium phosphate layer deposited onto the surface of the PCL-β-TCP scaffolds. Samples were characterised by using a PANalytical X'Pert MPD Powder X-ray Diffractometer, a Cobalt anode and a 2 theta step size of 0.001.

4. Biological assays

4.1. Harvest, Isolation and culture of primary osteoblasts

Freshly isolated osteoblasts were used for the studies carried out in the chapters 4, 5 and 6, aiming to assess the functionality of the developed devices for bone regeneration applications. The primary osteoblasts cultures were as well isolated from different locations in the body according to the bone tissue that they were intended to replace, namely from the hip in chapters 4 and 5 and from the mandible in chapter 6.

In the work described in chapters 4 and 5, where materials under study targeted applications in the replacement of long bones, human osteoblasts were collected from patients experiencing reconstructive hip surgery. Ethics approval for the use of human osteoblasts in this experiment was granted from The Prince Charles Hospital ethics committee (ethics clearance number: EC2310) and Queensland University of Technology ethics committee (ethics clearance number 0600000232). The osteoblasts were expanded in basal alpha MEM modified medium (Gibco, USA) supplemented with 10% fetal calf serum and 1% penicillin/streptomycin and used at passage 2. When reaching confluence, the cells were trypsinized for further seeding over scaffolds.

In the work described in chapter 6, where the material under study targeted the regeneration of jaw bone, cells were isolated from compact bone samples collected under sterile conditions from the mandible of Merino sheep (ovis aries). Animal ethics approval for this study was granted by the Animal Ethics Committee of the Queensland University of Technology. This procedure was performed under general anesthesia with a trephine drill (5 mm diameter). The extracted samples were then minced,

washed with phosphate buffered saline (PBS) and vortexed 5 times. Bone samples were then incubated with 10 mL of 0.25% trypsin/EDTA for 3 min at 37°C in a 5% CO2 atmosphere. After trypsin inactivation, samples were washed once again with PBS and transferred in basal culture media (DMEM containing 10% FBS, 1% of penicillin/streptomycin) into 175 cm2 tissue culture flasks. Outgrowth of osteoblasts was observed after 5-7 days. Cells were expanded and used at the third passage (P3) for seeding scaffolds.

4.2. Harvest, isolation and culture of primary periodontal ligament cells

In the study described in chapter 6, primary periodontal ligament cells were utilized, considering the relevance of assessing the materials specifically designed for the regeneration of periodontal ligament.

In this case, cells were isolated from two incisors teeth extracted from Merino sheep (ovis aries). Animal ethics approval for this study was granted by the Animal Ethics Committee of the Queensland University of Technology. The teeth were then placed into a 50 mL tube containing DMEM with 2% penicillin/streptomycin and 4 µg/mL fungizone. The middle third of the periodontal ligament (PDL) was subsequently gently removed from the root surface with a scalpel and further sectioned into approximately 1x1 mm^2 pieces. The PDL tissues were placed into a 25 cm^2 culture flask which was left standing upright in an incubator at 37°C and 5% CO2 atmosphere for 30 min to allow tissue adhesion. After this incubation period, 3 mL of DMEM containing 10% FBS, 1% of penicillin/streptomycin and 0.1 µg/mL fungizone were added and the flask was carefully laid down in the incubator. The first media change occurred 4 days post extraction. After one week of culture, cells started migrating outwards from the PDL tissues and reached confluence after 2-3 weeks of culture. The cells were passaged using 0.25% trypsin and further expanded until P3.

4.3. Periodontal ligament cell sheets

Cell sheet technology consists on the generation of multicellular tissues without the utilization of a support scaffold. Cells are typically cultured to near confluence onto temperature-responsive culture surfaces which as a consequence of temperature change promote the detachment of cells. As a result, the cultured cells which still maintain their cell-cell connections can be collected in the form of thin sheets of cells. This technology has before been applied to the generation of periodontal ligament cell

sheet by Akizuki et al. in order to form new cementum and promote periodontal attachment by placing various periodontal cell sheets onto the surfaces of teeth roots [44]. However, this technology can be simplified to a certain extent by replacing the temperature-responsive culture surface by simple culture wells from which cell sheets naturally detach when sufficient maturity is reached. Therefore, in the work described in chapter 6, periodontal ligament cells were seeded at 10,000 cells/cm^2 in a 24-well plate. The cells were cultured in osteogenic media and as the cell sheet matured (after 7 days of culture), it started to contract and detach from the well. The cell sheets were then collected by direct application onto the surface of melt electrospun meshes.

4.4. Harvest, Isolation and culture of goat bone marrow stromal cells

Stromal stem cells have become highly valued cell sources for cell-based therapeutics and regenerative medicine [45]. This can be explained by their high potential of expansion and self-renewal as well as their possible application in autologous tissue engineering strategies, which makes them more desirable than many other cell sources. Furthermore, when cultured with appropriated supplemented culture media and specific environments, stromal stem cells can be differentiated into a wide variety of tissues such as bone, cartilage, fat, muscle and tendon.

In chapter 7, bone marrow stromal cells were harvested from goats (GBMSC) given the similarity of such animal model to humans in terms of metabolism and dimensions. GBMSCs were harvested from the iliac crest of adult goats and isolated as described elsewhere [46] and then expanded in low-glucose Dulbecco's modified essential medium (DMEM; Sigma Chemical Co., St. Louis, MO, USA) supplemented with 1% antibiotic/antimycotic (Sigma) and 10% fetal bovine serum (FBS; Sigma). When confluence was reached, cells were trypsinized and ressuspended (at passage 4).

4.5. Perfusion culture

Perfusion bioreactors are able to improve mass transfer at the interior of three-dimensional scaffolds. This type of bioreactor uses a pump to perfuse medium continuously through the interconnected porous network of seeded scaffolds. The fluid path must be confined so as to ensure the flow path is through the scaffold, rather than around the edges. The perfusion bioreactor offers enhanced transport of nutrients because it allows medium to be transported through the interconnected pores of the scaffolds. Besides cell culture, flow perfusion bioreactors can also be used for seeding cells

into scaffolds. A variety of scaffolds can be effectively and reproducibly seeded in an automated and controlled process using this straightforward concept into a simply designed bioreactor. Additionally, perfusion seeding can be readily integrated into a perfusion bioreactor system capable of automatically performing both seeding and subsequent culture of the construct. Stimulatory signals such as shear stress applied by bioreactors have shown to be effective in improving the quality of generated constructs [47, 48] given their similarity to stimuli which are naturally applied to cells and tissues *in vivo* [49, 50].

Perfusion cell culture was employed in the work described in chapters 4 and 5 and took place over up to 6 weeks in a bi-directional perfusion mode into the specifically designed culture devices described in section 2. To this end, a 1ml sterile syringe mounted on a multi-syringe adapter placed on an Aladdin syringe pump (World Precision Instruments, USA) was connected to the device's medium inlet using sterile silicone tubing. The devices (each with a dedicated syringe) were simultaneously cultured in this system. The devices were first sterilized by perfusion with 50% ethanol solution for 20 minutes and dried in a sterile hood for 2 hours. The devices were then manually filled with basal medium and bi-directionally perfused overnight at a flow rate of 0.4 ml/min and flow direction inversion every 100 seconds using the syringe system. This hydration step aimed at promoting the pre-adsorption of proteins to the scaffold's surfaces and hence facilitating subsequent cell attachment. In order to ensure the sterility of the device over the culture period while still allowing gas exchange with the incubator's environment, a 0.2 μm pore size filter (13 mm diameter) (Pall, USA) was connected to the outlet positioned at the top of the device. Cell suspensions were injected into the devices through silicone tubes. The devices were bidirectionally perfused for 24 hours at a flow rate of 0.4 ml/min in order to allow cell attachment. The perfusion direction was automatically inverted every 100 seconds utilizing an external microcontroller connected to the syringe pump. After 24 hours, the culture medium was replaced by fresh medium and the flow rate was increased to 0.8 ml/min whereas the flow inversion frequency was reduced to 50 seconds. The medium was changed weekly until scaffolds collection. According to the performed fluid flow modelling studies, the resulting local fluid flow rate was in agreement with optimal flow rates reported in other studies [51, 52].

4.6. Confocal microscopy

Confocal microscopy allows to selectively control the depth of field eliminating out-of-focus information and enables to collect serial optical sections from thick specimens. Furthermore, sequential imaging can be applied to samples stained with specific agents which allow to distinguish elements of

the samples such as cells and tissues. In this way, confocal microscopy is a valuable tool for analyzing three-dimensional constructs since it allows to obtain high resolution 3D representations of irregularly shaped samples composed of differentially stained elements.

In chapters 4 to 6 of this thesis, the morphology, orientation and viability of cells located onto the surface of scaffolds were assessed by confocal laser microscopy using a confocal microscope (SP5, Leica). According to the specific features to be analyzed, different staining procedures were employed.

For assessing cellular morphology and orientation, samples were washed in PBS and fixed overnight in 4% (w/v) paraformaldehyde (PFA)/PBS. Samples were then washed in PBS and permeabilized with 0.2 % Triton X100/PBS for precisely 5 minutes and again washed twice with PBS. F-actin filaments and nuclei were then stained for 45 minutes with 0.8 U/mL rhodamine 415-conjugated phalloidin and 5 μg/mL 4′-6-diamidino-2-phenylindole (DAPI) respectively in PBS. Immunofluorescence was visualized and z-stacks acquired.

When constructs were analyzed for assessing cellular viability a live/dead assay was employed. For this purpose, the constructs were washed twice in PBS, incubated for 5 min at 37°C in PBS containing 0.67 μg/ml fluorescein diacetate (FDA) and 5μg/ml propidium iodide (PI) (both Invitrogen) and washed again in PBS. A semi-quantitative analysis of the cellular viability was also performed using the ImageJ software to quantify living cells and dead cells (in different colors) from the images obtained by confocal laser microscopy. A total of seven images from multiple areas of the constructs were captured and analyzed for each time point.

4.7. Metabolic activity staining (MTT)

MTT staining is a very straightforward colorimetric method which allows to qualitatively analyze the metabolic activity, and indirectly the viability of cells in culture. This method is based on the utilization of yellow 3-(4,5-Dimethylthiazol-2-yl)-2,5-diphenyltetrazolium bromide (MTT) which is reduced to purple formazan in the mitochondria of living cells. This reduction takes place only when mitochondrial reductase enzymes are active, and therefore the color change observed in cells can be directly related to their metabolic activity and viability.

In chapters 4 and 5, metabolically active cells were visualized by using a 1mg/ml 3-(4,5-dimethylthiazol-2-yl)-2,5-diphenyltetrazolium bromide (MTT) solution. Following collection, constructs were washed in PBS and then immersed into MTT solution for 30 minutes. A total of seven images from multiple areas of the constructs were captured and analyzed for each time point. Images showing

purple cells onto the surface of scaffolds were captured by a digital camera mounted on an Eclipse TS100 microscope (Nikon, Tokyo, Japan).

4.8. Metabolic activity quantification (MTS assay)

In chapter 7, cellular viability was quantitatively assessed by the MTS, 3-(4,5-dimethylthiazol-2-yl)-5-(3-carboxymethoxyphenyl)-2-(4-sulfophenyl)-2H-tetrazolium, assay (Promega, Madison, USA). Briefly, this assay is based on the bioreduction of a tetrazolium compound, 3-(4,5-dimethylthiazol-2-yl)-5-(3-carboxymethoxyphenyl)-2-(4-sulfofenyl)-2H-tetrazolium (MTS), into a brown formazan product that is soluble in water. This conversion is accomplished by the production of nicotinamide adenine dinucleotide phosphate (NADPH) or nicotinamide adenine dinucleotide (NADH) by the dehydrogenase enzymes existing in metabolically active cells. The absorbance relative to the quantity of formazan product is directly proportional to the number of living cells in culture, and was measured at 490 nm in a microplate reader (Bio-Tek, model Synergie HT; USA). Culture medium without FBS and phenol red was mixed with MTS in a ratio of 5:1 and added to wells containing the constructs to be analyzed. The constructs were incubated in this solution for 3 hours at 37°C in a 5% CO2 atmosphere. After the incubation period, the optical density (OD) was read in a microplate reader (Bio-Tek, Synergie HT, USA) at 490 nm. A total of 9 samples per study group/condition were analyzed being measurements made in triplicate. The obtained results were normalized to the surface area of each type of sample used (discs or scaffolds).

4.9. Cell proliferation assay

Cell proliferation is usually assessed by quantifying the synthesis of DNA at different time points during a certain culture period. In the work described in chapters 4 to 7 of this thesis, cell proliferation was quantified by the total amount of double-stranded DNA (dsDNA) using an ultrasensitive fluorescent nucleic acid stain, during the culturing periods. Quant-iT™ PicoGreen® dsDNA reagent was selected for this assay since it enables to quantify as little as 25 pg/mL of dsDNA (50 pg dsDNA in a 2 mL assay volume) with a standard spectrofluorometer and fluorescein excitation and emission wavelengths. Additionally, dsDNA can be quantified in the presence of equimolar concentrations of ssDNA and RNA with minimal effect on the quantitative results obtained.

Briefly, after collection of the samples and freezing at -80 °C for at least 48 hours, the analyzed constructs were placed in 1.5 mL Eppendorf tubes containing 500 µL of Proteinase K (Invitrogen) (Proteinase K/phosphate buffered EDTA (PBE) 0.5 mg/ml), at 60°C for 12 hours. The solution was thereafter diluted at a ratio of 1/50 in Phosphate Buffered EDTA PBE, and 100 µL was aliquoted in triplicates into black 96-well plates, and 100 µL of PicoGreen (P11496, Invitrogen) working solution was added. After 5 min incubation in the dark, the fluorescence (excitation 485 nm, emission 520 nm) was measured using a fluorescence plate reader (Benchmark PlusTM microplate spectrophotometer, BIO RAD). A standard curve of known λ DNA concentrations ranging from 10 ng/ml to 1 µg/mL was used to calculate the final DNA content of the sample.

4.10. Alkaline Phosphatase Quantification (ALP)

Alkaline phosphatase is a cell surface protein bound to the plasma membrane through phosphatidylinositol phospholipid complexes whose high activity is associated with the active formation of mineralized matrix, in particular during bone healing. ALP activity is also a commomly used marker of the osteogenic phenotype both in primary osteoblasts and differentiating stem cells. In chapter 6 of this thesis, ALP activity was measured from the media in triplicate at different time-points (2, 4 and 6 weeks) after a 24 hours release period. Briefly, samples were first immersed for 5 min in DMEM without phenol red and this was repeated three times. They were then transferred to a new 24-well plate and 1000 µL of this media was added before the samples were placed back in the incubator for precisely 24 hours. ALP activity was measured using a SigmaFASTTM kit, as per the manufacturer's instructions. 100 µL of p-Nitrophenyl phosphate (which is hydrolysed by the alkaline phosphatase produced by the cells) in Tris-base buffer was added to 100 µL of the culture media in a 96-well plate, and incubated at 37°C and 5% CO2 for another 24 hours. At the end of the second incubation period, the plate was brought back to ambient temperature (20 °C) for 5 min and the absorbance was read at 405 nm using a plate reader (Benchmark PlusTM microplate spectrophotometer, BIO RAD). The ALP absorbance was normalized by the DNA content of each sample.

5. *In vivo* model

The performance of a biphasic scaffold in achieving periodontal regeneration including simultaneous bone, periodontal ligament and cementum regeneration was assessed ectopically in a rat

model, under chapter 6. The osteoblast loaded scaffolds were cultured for 6 weeks and then 3 previously cultured PDL ligament cell sheets were placed onto the PCL mesh comprising the periodontal compartment. The following sections describe the preparation of the implant and surgical implantation procedure.

5.1. Dentin slices and scaffold assembly

In order to simulate the interaction of the PDL compartment with teeth, dentin slices were attached to the periodontal side of the biphasic constructs. To do so, one millimeter thick dentin slices were prepared from sheep teeth and adjusted to the size of the biphasic scaffolds. The assembly of the biphasic scaffolds onto dentin blocks was performed under sterile conditions and sutures were used to keep the biphasic scaffold on top of the dentin slice. Thereafter the samples were immersed in media for 2 hours in order to allow for cell sheet adhesion onto the dentin surface. Notches on the dentin slides were created in order to prevent the sutures from sliding off, thus ensuring high stability of the scaffold.

5.2. Subcutaneous implantation into nude rats

Ideally, models for studying new tissue engineering strategies should be based on the target tissue to be restored. However, in order to reduce the variables involved in the process as well as the number of tested animals, simpler models are usually adopted. The animal model utilized in the *in vivo* study described in chapter 6 - rats – is relatively easy to maintain and handle as well as less expensive than other larger models. Furthermore, the performed subcutaneous implantations enabled the implantation of multiple constructs into a reduced number of animals.

For performing this study, animal ethics approval for the use of athymic nude rats was granted by the Animal Ethics Committee of Griffith University. Five 8-week old male rats (Animal Resources Centre, Canning Vale, WA, Australia) were used. The animals were anaesthetized with isoflurane. Six small incisions were made longitudinally along the central line of the shaved dorsal area, approximately 2 cm apart, and subcutaneous pockets were made with surgical scissors. Six different groups of biphasic scaffolds were implanted. Biphasic scaffolds combined with three cell sheet (n=5) or without cell sheet (n=5), biphasic scaffold with osteoblasts cultured in basal media (n=5) or in osteogenic media (n=5), CaP-coated scaffold with osteoblasts cultured in basal media (n=5) or in osteogenic media (n=5)

were implanted for 8 weeks. Each individual pocket held one scaffold and the incisions were closed with surgical sutures. The animals were sacrificed after eight weeks and the implants were retrieved and fixed in 4% paraformaldehyde in PBS at pH 7.4 for further analysis.

5.3. Histological analysis of implanted constructs

In order to study the morphology of the constructs subcutaneously implanted into rats in chapter 6, samples were decalcified in 10% EDTA at pH 7.4 for 3 months at 4 °C with a weekly change of solution and subsequently embedded in paraffin. Sections near the central area of the implants were used for the haematoxylin and eosin (H&E) and immunological stainings.

6. Seeding, cryopreservation and thawing of cell-seeded porous scaffolds and nonporous discs

In chapter 7, In order to compare the effect of cryopreservation on different structures seeded with cells, special measures were taken in the seeding procedure. Given the difference in surface area available for cell attachment in the scaffolds and discs utilized in chapter 7, two different cellular concentrations were prepared for seeding in each kind of structure, namely one cell suspension to seed $5x10^5$ cells in 300 µl volumes, for the scaffolds, and another in order to seed $1x10^5$ cells in volumes of 200 µl onto the surface of SPCL discs. The rationale used for the cell seeding density used in this work was based in previously performed studies [46] which showed that a ratio of 5:1 was appropriate for being able to seed a similar amount of these cells per surface area in both porous and nonporous scaffolds and allowing for the formation of extracellular matrix and osteoblastic differentiation. All the scaffolds/discs were placed in 24 well non-adherent plates in order to perform the seeding. After seeding, these samples were carefully transferred into the incubator and left there for three hours, before adding 1,5 ml of DMEM basal medium. The samples were cultured for 7 days, being the medium changed every 2 or 3 days. Scaffolds and discs without cells were kept in the same conditions to be used as experimental controls.

After 7 days of culture, half of the previously seeded constructs, as well as unseeded scaffolds and discs, were collected for characterization assays, namely MTS, DNA quantification, SEM, micro-CT and mechanical analysis while the other half of the constructs was cryopreserved, along with some more unseeded scaffolds and discs. For the cryopreservation step, a cryopreservative solution composed of

DMSO and FBS was used for suspending the seeded and unseeded scaffold and discs. The concentration of DMSO to use in the cryoprotective solution was determined by estimating the amount of cells in the scaffolds after 7 days of culture, using data obtained in previous studies [53]. A period of 7 days of cryopreservation was chosen taking into consideration previous studies performed in the field which state that the duration of the storage in liquid nitrogen (-196ºC) has a negligible impact on constructs. Those studies used even shorter cryopreservation periods (less than one day) [54].Thus, for each million of cells, a 10% concentration of DMSO was added to the cryopreservative solution. All seeded and unseeded scaffolds and discs were suspended in cryoprotective solution inside standard cryovials and placed inside a Statebourne Biosystem 24 cryogenic tank. After 7 days of cryopreservation, the constructs and unseeded scaffolds/discs were removed from the cryogenic tank and partially thawed in a 37°C waterbath, removed from the cryovials and placed in 24 well non-adherent plates. To each sample, a volume of cold DMEM basal medium with 20% FBS was added. The samples were further cultured for 9 days being the medium changed every 2 or 3 days in order to allow cells to recover from the cryopreservation step. Cells alone and tissues that are submitted to cryopreservation always require a certain time to recover. Studies found in the literature have shown that, after thawing, cellular viability tends to decrease for a period of at least 7 days before stabilizing [55]. This recovery culture period also allowed for a more prolonged and more efficient leaching of toxic DMSO's residues, in particular from the porous constructs. The recovery culture period was not prolonged for longer than 9 days since the strategy involved in a medically oriented usage of these constructs would consist of applying these constructs into tissue defects as quickly as possible after thawing in order to reduce patient's immobilization time.

After each culturing period, the collected cell-seeded cells/scaffolds samples were washed at least twice with 1ml of sterile PBS. In the case of the cells/scaffolds constructs to be used in DNA quantifications, each sample was transferred to a sterile tube with 1ml of ultra-pure water. After this procedure, the tubes with samples were kept at a temperature of -80°C until further analysis, namely MTS, DNA quantification, SEM, micro-CT and mechanical analysis, which were performed following the procedures described in the previous sections..

7. Statistical Analysis

Statistical Analysis was performed in all the experimental chapters of this thesis using GraphPad Prism software (version 5.00 for Windows). The statistical analysis was performed using a

Shapiro-Wilk normality test and one-way ANOVA followed by a Tukey HSD post-hoc test. $p < 0.05$ was considered as statistically significant.

8. References

1.Pitt, C.G., et al., *Aliphatic Polyesters .2. The Degradation of Poly(Dl-Lactide), Poly(Epsilon-Caprolactone), and Their Copolymers Invivo.* Biomaterials, 1981. **2**(4): p. 215-220.

2.Tsuji, H. and Y. Ikada, *Blends of aliphatic polyesters .2. Hydrolysis of solution-cast blends from poly(L-lactide) and poly(epsilon-caprolactone) in phosphate-buffered solution.* Journal of Applied Polymer Science, 1998. **67**(3): p. 405-415.

3.Bezwada, R.S., et al., *Monocryl(R) Suture, a New Ultra-Pliable Absorbable Monofilament Suture.* Biomaterials, 1995. **16**(15): p. 1141-1148.

4.Darney, P.D., et al., *Clinical-Evaluation of the Capronor Contraceptive Implant - Preliminary-Report.* American Journal of Obstetrics and Gynecology, 1989. **160**(5): p. 1292-1295.

5.Allen, C., et al., *Polycaprolactone-b-poly(ethylene oxide) copolymer micelles as a delivery vehicle for dihydrotestosterone.* Journal of Controlled Release, 2000. **63**(3): p. 275-286.

6.Bohner, M., *Calcium orthophosphates in medicine: from ceramics to calcium phosphate cements.* Injury-International Journal of the Care of the Injured, 2000. **31**: p. S37-S47.

7.Lam, C.X.F., S.H. Teoh, and D.W. Hutmacher, *Comparison of the degradation of polycaprolactone and polycaprolactone-(beta-tricalcium phosphate) scaffolds in alkaline medium.* Polymer International, 2007. **56**(6): p. 718-728.

8.Agrawal, C.M. and R.B. Ray, *Biodegradable polymeric scaffolds for musculoskeletal tissue engineering.* Journal of Biomedical Materials Research, 2001. **55**(2): p. 141-150.

9.Athanasiou, K.A., G.G. Niederauer, and C.M. Agrawal, *Sterilization, toxicity, biocompatibility and clinical applications of polylactic acid polyglycolic acid copolymers.* Biomaterials, 1996. **17**(2): p. 93-102.

10.Gilding, D.K. and A.M. Reed, *Biodegradable Polymers for Use in Surgery - Polyglycolic-Poly(Actic Acid) Homopolymers and Copolymers .1.* Polymer, 1979. **20**(12): p. 1459-1464.

11.Gunatillake, P.A., R. Adhikari, and N. Gadegaard, *Biodegradable synthetic polymers for tissue engineering.* European Cells and Materials, 2003. **5**: p. 1-16.

12.Brady, J.M., et al., *Resorption Rate, Route of Elimination, and Ultrastructure of Implant Site of Polylactic Acid in Abdominal-Wall of Rat.* Journal of Biomedical Materials Research, 1973. **7**(2): p. 155-166.

13.Pisuttisap, A., et al., *ABS modified with hydrogenated polystyrene-grafted-natural rubber.* Journal of Applied Polymer Science, 2013. **129**(1): p. 94-104.

14.Bastioli, C., et al., *Physical State and Biodegradation Behavior of Starch-Polycaprolactone Systems.* Journal of Environmental Polymer Degradation, 1995. **3**(2): p. 81-95.

15.Koenig, M.F. and S.J. Huang, *Biodegradable Blends and Composites of Polycaprolactone and Starch Derivatives.* Polymer, 1995. **36**(9): p. 1877-1882.

16.Vikman, M., et al., *Morphology and enzymatic degradation of thermoplastic starch-polycaprolactone blends.* Journal of Applied Polymer Science, 1999. **74**(11): p. 2594-2604.

17.Yavuz, H. and C. Babac, *Preparation and biodegradation of starch/polycaprolactone films.* Journal of Polymers and the Environment, 2003. **11**(3): p. 107-113.

18.Gomes, M.E., et al., *Starch-poly(epsilon-caprolactone) and starch-poly(lactic acid) fibre-mesh scaffolds for bone tissue engineering applications: structure, mechanical properties and degradation behaviour.* Journal of Tissue Engineering and Regenerative Medicine, 2008. **2**(5): p. 243-252.

19.Gomes, M.E., et al., *Effect of flow perfusion on the osteogenic differentiation of bone marrow stromal cells cultured on starch-based three-dimensional scaffolds.* Journal of Biomedical Materials Research Part A, 2003. **67A**(1): p. 87-95.

20.Marques, A.P., R.L. Reis, and J.A. Hunt, *An in vivo study of the host response to starch-based polymers and composites subcutaneously implanted in rats.* Macromolecular Bioscience, 2005. **5**(8): p. 775-785.

21.Santos, T.C., et al., *Vascular Endothelial Growth Factor and Fibroblast Growth Factor-2 Incorporation in Starch-Based Bone Tissue-Engineered Constructs Promote the In Vivo Expression of Neovascularization Mediators.* Tissue Engineering Part A, 2013. **19**(7-8): p. 834-848.

22.Santos, T.C., et al., *In vivo short-term and long-term host reaction to starch-based scaffolds.* Acta Biomaterialia, 2010. **6**(11): p. 4314-4326.

23.Peltola, S.M., et al., *A review of rapid prototyping techniques for tissue engineering purposes.* Annals of Medicine, 2008. **40**(4): p. 268-280.

24.Yeong, W.Y., et al., *Rapid prototyping in tissue engineering: challenges and potential.* Trends in Biotechnology, 2004. **22**(12): p. 643-652.

25.Brown, T.D., P.D. Dalton, and D.W. Hutmacher, *Direct Writing By Way of Melt Electrospinning.* Advanced Materials, 2011. **23**(47): p. 5651-+.

26.Kokubo, T., et al., *Ca, P-rich layer formed on high-strength bioactive glass-ceramic A-W.* Journal of Biomedical Materials Research, 1990. **24**(3): p. 331-343.

27.Kokubo, T., H. Kushitani, and S. Sakka, *Solutions able to reproduce in vivo surface-structure changes in bioactive glass-ceramic A-W3.* Journal of Biomedical Materials Research, 1990. **24**: p. 721-734.

28.Al-Munajjed, A.A., et al., *Development of a biomimetic collagen-hydroxyapatite scaffold for bone tissue engineering using a SBF immersion technique.* Journal of Biomedical Materials Research - Part B Applied Biomaterials, 2009. **90**(2): p. 584-591.

29.Arafat, M.T., et al., *Biomimetic composite coating on rapid prototyped scaffolds for bone tissue engineering.* Acta Biomaterialia. **7**(2): p. 809-820.

30.Araujo, J.V., et al., *Surface controlled biomimetic coating of polycaprolactone nanofiber meshes to be used as bone extracellular matrix analogues.* Journal of Biomaterials Science, Polymer Edition, 2008. **19**(10): p. 1261-1278.

31.Liu, Y., et al., *Influence of calcium phosphate crystal assemblies on the proliferation and osteogenic gene expression of rat bone marrow stromal cells.* Biomaterials, 2007. **28**(7): p. 1393-1403.

32.Lu, Z., et al., *Bone biomimetic microenvironment induces osteogenic differentiation of adipose tissue-derived mesenchymal stem cells.* Nanomedicine: Nanotechnology, Biology and Medicine, 1999. **8**(4): p. 507-515.

33.Vaquette, C., et al., *Ectopic bone formation in tissue–engineered calcium phosphate coated polymeric construct: effect of coating and culture conditions.* Biomaterials, 2013. **to be submitted**.

34.Thomson, R.C., et al., *Biodegradable polymer scaffolds to regenerate organs.* Biopolymers Ii, 1995. **122**: p. 245-274.

35.Langer, R., *Selected advances in drug delivery and tissue engineering.* Journal of Controlled Release, 1999. **62**(1-2): p. 7-11.

36.Lu, L.C. and A.G. Mikos, *The importance of new processing techniques in tissue engineering.* Mrs Bulletin, 1996. **21**(11): p. 28-32.

37.Maquet, V. and R. Jerome, *Design of macroporous biodegradable polymer scaffolds for cell transplantation.* Porous Materials for Tissue Engineering, 1997. **250**: p. 15-42.

38.Mendes, S.C., et al., *Evaluation of two biodegradable polymeric systems as substrates for bone tissue engineering.* Tissue Eng, 2003. **9 Suppl 1**: p. S91-101.

39.Gomes, M.E., et al., *Influence of the porosity of starch-based fiber mesh scaffolds on the proliferation and osteogenic differentiation of bone marrow stromal cells cultured in a flow perfusion bioreactor.* Tissue Eng, 2006. **12**(4): p. 801-809.

40.Gomes, M.E., et al., *A new approach based on injection moulding to produce biodegradable starch-based polymeric scaffolds: morphology, mechanical and degradation behaviour.* Biomaterials, 2001. **22**(9): p. 883-889.

41.Neves, N.M., A. Kouyumdzhiev, and R.L. Reis, *The morphology, mechanical properties and ageing behavior of porous injection molded starch-based blends for tissue engineering scaffolding.* Materials Science & Engineering C-Biomimetic and Supramolecular Systems, 2005. **25**(2): p. 195-200.

42.Ho, S.T. and D.W. Hutmacher, *A comparison of micro CT with other techniques used in the characterization of scaffolds.* Biomaterials, 2006. **27**(8): p. 1362-1376.

43. Ryland, A.L., *X-ray diffraction.* Journal of Chemical Education, 1958. **35**(2): p. 80.

44.Akizuki, T., et al., *Application of periodontal ligament cell sheet for periodontal regeneration: a pilot study in beagle dogs.* Journal of Periodontal Research, 2005. **40**(3): p. 245-251.

45.Satija, N.K., et al., *Mesenchymal stem cells: Molecular targets for tissue engineering.* Stem Cells and Development, 2007. **16**(1): p. 7-23.

46.Rodrigues, M.T., et al., *Tissue-engineered constructs based on SPCL scaffolds cultured with goat marrow cells: functionality in femoral defects.* Journal of Tissue Engineering and Regenerative Medicine, 2011. **5**(1): p. 41-49.

47.Sikavitsas, V.I., et al., *Mineralized matrix deposition by marrow stromal osteoblasts in 3D perfusion culture increases with increasing fluid shear forces.* Proceedings of the National Academy of Sciences of the United States of America, 2003. **100**(25): p. 14683-14688.

48.Goldstein, A.S., et al., *Effect of convection on osteoblastic cell growth and function in biodegradable polymer foam scaffolds.* Biomaterials, 2001. **22**(11): p. 1279-1288.

49.Srinivasan, S., et al., *Low-magnitude mechanical loading becomes osteogenic when rest is inserted between each load cycle.* Journal of Bone and Mineral Research, 2002. **17**(9): p. 1613-1620.

50.Allison, S.J., et al., *High impact exercise increased femoral neck bone mineral density in older men: A randomised unilateral intervention.* Bone, 2013. **53**(2): p. 321-328.

51.Alvarez-Barreto, J., et al., *Flow Perfusion Improves Seeding of Tissue Engineering Scaffolds with Different Architectures.* Annals of Biomedical Engineering, 2007. **35**(3): p. 429-442.

52.Goncalves, A., et al., *Effect of flow perfusion conditions in the chondrogenic differentiation of bone marrow stromal cells cultured onto starch based biodegradable scaffolds.* Acta Biomaterialia, 2011. **7**(4): p. 1644-1652.

53.Gomes, M.E., et al., *Effect of flow perfusion on the osteogenic differentiation of bone marrow stromal cells cultured on starch-based three-dimensional scaffolds.* J Biomed Mater Res A, 2003. **67**(1): p. 87-95.

54.Wen, F., et al., *Vitreous cryopreservation of nanofibrous tissue-engineered constructs generated using mesenchymal stromal cells.* Tissue Engineering - Part C: Methods, 2009. **15**(1): p. 105-114.

55.Lübke, C., et al., *Cryopreservation of Artificial Cartilage: Viability and Functional Examination after Thawing.* Cells Tissues Organs, 2001. **169**(4): p. 368-376.

Section III

Experimental

Chapter 3

Bioreactor composed of watertight chamber and internal matrix for the generation of cellularized medical implants

Abstract

The present invention relates to a bioreactor for the generation of medical implants which comprises an external chamber, which can be unicompartmented 1 (preferably possessing two tubular structures 8) or multicompartmented, and watertight containing in its interior one or more matrices 7, the bioreactor's internal matrices 7 and external chamber 1 being simultaneously manufactured, preferably through a rapid prototyping process; and also characterized by an external chamber 1 possessing a shape adapted to the shape of the implant to be cellularized (internal matrix) enabling a greater efficiency in the cellular colonization and culture of the implant, and by the implants being removed from the inside of the bioreactor by cutting the external chamber 1 in locations defined by grooves 9 right before implantation, allowing a greater sterility of the implant.

This chapter is based on the following publication:

Costa P.F., Martins A., Vaquette C., Melchels F.P., Neves N.M., Gomes M.E., Hutmacher D.W., Reis R.L., Bioreactor composed of watertight chamber and internal matrix for the generation of cellularized medical implants. World Patent Application WO 2013/103306 A1.

1. Object of the invention

The present invention relates to a bioreactor composed of a watertight chamber and one or more matrices contained in its interior, which are simultaneously manufactured, whose matrix can be bi-dimensional or three-dimensional, with variable porosity and delineated by simple or complex shapes, is capable of supporting the seeding and culture of cells for, after removal of the watertight chamber, originating cellularized medical implants for the replacement/regeneration of animal or human tissues or organs previously damaged by trauma or disease.

2. State of the art

In the replacement or regeneration of tissues or organs after physical damage caused by trauma or disease auto-, alio- or xenografts are currently used in clinical practice. However, these medical grafts have limitations such as the low availability of healthy tissue, immunocompatibility problems or cross infection between different animal species. To overcome these restrictions on its use in the current clinic practice, Tissue Engineering emerged as a promising alternative. This strategy includes the development of bi- or three-dimensional porous matrices that support cellular colonization and culture, the ex vivo culture of cells and the presence of growth factors that induce cellular growth and/or differentiation. These factors may be used independently, in groups of two or three in order to allow tissue regeneration.

Being the development of bi- or three-dimensional porous matrices a key step in the success of a Tissue Engineering strategy, these matrices must comprise a set of physicochemical properties (e.g. porosity, interconnectivity, roughness, surface area, mechanical properties, hydrophilicity) that allow cellular adhesion, migration, proliferation and differentiation. The maintenance of cells in culture within these bi- or three-dimensional porous matrices can be achieved through the use of static or dynamic culture systems. It has been demonstrated that the culture of cells in an appropriate biochemical environment and in the presence of mechanical stimuli may promote the generation of cellularized medical implants. Therefore, there is a great interest to replicate in vitro the physiological environment of a target tissue, through the use of dynamic simulation biomechanics systems, scientifically known as bioreactors . These bioreactors not only provide the cells in culture within bi- or three-dimensional porous matrices with equal concentrations of nutrients and oxygen, but also allow the removal of byproducts resulting

from their metabolic activity. Besides these features, bioreactors also allow a more uniform colonization of the bi- or three-dimensional porous matrices by the cells. Therefore, these dynamic culture systems constitute a better quantitative control method over the parameters of cell culture, and can provide an unlimited number of cellularized medical implants.

The present invention aims at the development of cellularized medical implants with improved biomechanical properties, by developing methods of cellular colonization and culture on bi- or three-dimensional porous matrices. Implicit is the development of a bioreactor which contains, in itself, one or more bi- or three-dimensional porous matrices, allowing minimal handling of the cellularized medical implant (s) in order to minimize the risk of contamination during ex vivo cell culture.

3. Description of the invention

The present invention refers to a bioreactor which can be utilized in the colonization and culture of cells into support matrices contained into their interior, originating cellularized medical implants for the substitution/regeneration of animal or human tissues or organs, such as bone, cartilage, skin and muscle.

The bioreactor is mainly composed of one or more matrices, with variable porosity, three-dimensional or bi-dimensional, contained into a unicompartmented or multicompartmented watertight chamber.

The culture chamber as well as the matrix contained in its interior are simultaneously manufactured through a rapid prototyping process, from one or multiple materials. These materials can be biodegradable or not, inert or not, polymeric or composite, transparent, translucent or opaque, such as polycaprolactone (PCL) , polylactic acid (PLA) or polyglycolic acid (PGA) .

During the manufacture of the bioreactor and its internal matrix an extra water-soluble support material can be used, which is as well deposited during the rapid prototyping process. This material acts only as a support for the deposition of the deposited material or materials during the manufacture of the chamber and its matrix, being afterwards removed by immersion into water or aqueous solution .

The architecture of the chamber and its internal matrix should preferably be designed to be self-supportive, not being necessary the utilization of an additional support material.

The chambers and their inner matrices can be sterilized by several methods according to the materials utilized. They can be sterilized by immersion into ethanol, by exposure to ultraviolet radiation or exposure to ethylene oxide, in case none of the utilized materials show any adverse reactivity, or even by autoclaving, when the utilized materials are sufficiently stable when exposed to high temperatures.

In case the external chamber is prototyped from one or more transparent or translucid materials it becomes even possible to analyze its interior by optical means. In case the internal matrix is also prototyped from transparent or translucid materials the interior of the internal matrix can also be analyzed by optical means.

In order to improve the performance of the internal matrix contained into the chamber it is possible to perform coatings of its surfaces by filling or perfusing the interior of the chamber, through the internal matrix, with solutions or gases able to generate those coatings.

The internal matrix can be designed using as an initial reference simple shapes such as cuboid, cylindrical, tubular or other shapes, or as well from complex shapes obtained from the analysis of tissues or organs by means of computerized tomography or magnetic resonance techniques.

The design of the external chamber is performed having as initial reference the shape of the internal matrix and by extrusion of its external surfaces.

To the external chamber' s design are added at least two tubular structures which are intended to connect the interior of the chamber to the exterior and allowing the entry and exit of fluids and/or gases from/to the interior of the chamber. The location of these tubular structures should be determined taking into account the best possible efficiency in draining the fluids inserted into the chamber as well as the improvement of the fluid flow dynamic into the chamber.

The bioreactor can be integrated into a perfusion culture system which allows to circulate culture medium through the interior of the external chamber and through the pores of the bioreactor' s internal matrix.

The culture medium is supplied to the chamber through the tubular structures for entry/exit of medium, preferably located at the extremities of the culture chamber, and circulated from and to an aired culture medium reservoir by means of a peristaltic pump.

When integrated into a perfusion culture system, the bioreactor is able to perform continuous perfusion of expansion or differentiation culture medium, improving the mass transport of cells into the previously cellularized matrix. The continuous perfusion of culture medium performed by the culture system is able to act as a stimulus over the cells, being able to regulate or increase the proliferation and differentiation of cells. The perfusion of medium through the cellularized matrices can be performed both unidirectionally or bidirectionally.

After culture, the cellularized matrix can be removed from the interior of the bioreactor by cutting the external chamber in specifically designed locations, using surgical tools.

4. Brief description of the drawings

Figure 3.1 shows a longitudinal section of the device containing a simple three-dimensional porous structure in its interior.

Figure 3.2 shows a longitudinal section of the device containing a bi-dimensional porous structure in its interior.

Figure 3.3 shows a longitudinal section of the device containing a double three-dimensional porous structure in its interior.

Figure 3.4 shows a longitudinal section of the device containing a tubular three-dimensional porous structure in its interior.

Figure 3.5 shows a longitudinal section of the device containing a complex tubular three-dimensional porous structure, manufactured using a three-dimensional model obtained from computerized tomography or magnetic resonance analysis of a tissue or organ.

Figure 3.6 shows the device in isometric view.

Figure 3.7 shows a longitudinal section of the device.

Figure 3.8 shows a partial section of the device in isometric view.

Figure 3.9 shows an implant after removal of the external enclosure in isometric view.

Figure 3.10 shows the device described in figures 3.6 and 3.9 integrated into a dynamic perfusion cell culture system.

5. Detailed description of the invention

The following description relates to a preferential configuration of the invention resorting to the figures in this document in order to allow a better understanding of the invention.

The bioreactor is essentially composed of one unicompartmented 1 or multicompartmented 2 watertight chambers containing in its interior one or more matrices, possessing porosity which can be uniform or variable, homogenous or heterogenous, present in the whole matrix 3,5,6,7 or part of the matrix 4, three-dimensional 3,4,6,7 or bi-dimensional 5, possessing simple 3, 4, 5, 6 or complex 7 shapes.

The matrix's external simple shape design 3,4,5,6 can be achieved by using simple shapes as initial references such as cuboidal, cylindrical, tubular or other shapes, while the design of the complex 7 internal matrix' s external shape is achieved by resorting to complex shapes obtained from analysis performed on tissues or organs using technologies such as computerized tomography or magnetic resonance. The internal matrix's 3,4,5,6,7 internal pores can be generated by manually or automatically adding pores into the internal matrix's 3,4,5,6,7 design or as well later automatically

added by defining specific properties for the deposition of material during the conversion of the final three-dimensional design into commands for controlling the equipment which will manufacture the internal matrix 3,4,5,6 by rapid prototyping.

The design of the external chamber 1,2 is in turn performed taking as initial reference the external shape of the internal matrix 3,4,5,6,7 and by modifying, through extrusion of the external faces, a simplified replica of that same internal matrix 3,4,5,6,7, in such a way that the device's designed internal walls 1,2 are very close to the external walls of the internal matrix's design 3,4,5,6,7 but also sufficiently apart so that they do not - touch each other. This feature enables that, after simultaneous prototyping of the internal matrix 3,4,5,6 and external chamber 1,2, the media for cell seeding, culture and differentiation used afterwards in its interior are more efficient in seeding, feeding and stimulating the cells which will adhere to the internal and external surfaces of the internal matrix 3,4,5,6,7 when circulated through them, inside the external chamber 1,2, since all the employed culture medium will be permanently kept in close contact with the cells adhered to the internal and external surfaces of the internal matrix 3,4,5,6,7.

Given this feature, and despite being simultaneously prototyped, the internal matrix 3,4,5,6,7 and external chamber 1,2 are not bound together at any point, facilitating the removal of the internal matrix 3,4,5,6,7 from the interior of the external chamber 1,2 where the cell seeding and culture period took place.

To the external chamber's design 1,2 are preferably added two tubular structures 8 which connect the interior of the chamber 1,2 to the exterior and allow the entry and exit of fluids and gases from/to the interior of the chamber 1,2. The location of these tubular structures 8 should be determined taking into account the best possible efficiency in draining the fluids inserted into the chamber as well as the improvement of the fluid flow dynamic into the chamber 1,2.

To the design of the external chamber 1,2, are also added grooves 9, which will be later used for facilitating its precise cutting in predetermined locations, and so facilitating the removal of the matrix 3,4,5,6,7 from the interior of the external chamber 1,2.

The culture chamber 1,2 as well as the internal matrix 3,4,5,6,7 contained in its interior are simultaneously manufactured, through a rapid prototyping process from one or multiple materials. These materials can be biodegradable or not, inert or not, polymeric or composite, transparent, translucent or opaque.

When employing a rapid prototyping process for manufacturing the bioreactor, which is composed of a culture chamber 1,2 and an internal matrix 3,5,6,7, an extra water-soluble support material can be utilized, which is as well deposited during the prototyping process. This material's sole purpose is to support the deposition of the material or materials from which the chamber and matrix will be made of, and can afterwards be removed by immersion into water or aqueous solution.

Preferably, the architecture of the chamber 1,2 and its internal matrix 3,5,6,7 should be designed in a way to be self supportive, eliminating the need for an additional support material.

When the external chamber is prototyped from one or multiple transparent or translucid materials, it becomes also possible to analyze the interior of the chamber by optical means. If the internal matrix 3,4,5,6,7 located inside the chamber is also prototyped from transparent or translucid materials it becomes also possible to analyze the interior of that matrix 3,4,5,6,7.

Chambers 1,2 and their internal matrices 3,4,5,6,7 can be sterilized by various methods according to the utilized materials. They can be sterilized by immersion into ethanol, by exposure to ultraviolet radiation or to ethylene oxide, in case of absence of any adverse reactivity, or even by autoclaving, in case the utilized materials are sufficiently stable when exposed to high temperatures.

In order to improve the performance of the internal matrix 3,4,5,6,7 contained into the chamber 1,2 it is possible to perform coatings over its surfaces by filling and/or perfusing the interior of the chamber, through the matrix's pores, with solutions or gases which are able to generate those coatings. Additional coatings can also be performed over the chamber's outer walls 1,2 for various purposes, such as increasing the chamber's 1,2 watertightness .

The bioreactor can be integrated into a culture system illustrated in figure 3.10. This system is composed by the bioreactor in one of its possible configurations, which comprises an external chamber

1,2 containing one of various kinds of internal matrices 3,4,5,6,7, connected to a culture medium reservoir 10 by tubes connected to its tubular structures 8. Apart from the two medium inlets/outlets, the reservoir 10 possesses also an additional connection for the entry and exit of gases which are purified by an air filter 11.

The culture medium is collected from the culture medium reservoir 10, pumped by a peristaltic pump 12 into the external chamber 1,2, perfused through the internal matrix's 3,4,5,6,7 pores and finally pumped by the same peristaltic pump 12 back into the culture medium reservoir 10. This process and circuit is repeated for each individual culture cavity.

For the circulation of culture medium, tubings made from formulations such as silicone should be preferably used since they are highly permeable to gases such as carbon dioxide and oxygen, increasing the gas exchange between circulating medium and surrounding atmosphere.

This culture system can be used not only for culture but as well for the seeding of cells onto the matrix' s 3,4,5,6,7 internal and external surfaces for cellular growth. Given its small internal volume this device requires very low volumes of culture medium. For this reason, it is possible to perform dynamic seeding procedures using highly concentrated cell suspensions without using extremely large amounts of cells. In this way, cells have a greater chance to adhere to the matrix' s 3,4,5,6,7 internal and external surfaces since they are highly concentrated and are circulated more often through it, making the seeding process more efficient.

When integrated into the perfusion culture system described in figure 3.10, this bioreactor is capable of improving the cellular mass transport through the cellularized matrix 3,4,5,6,7. The continuous culture medium perfusion provided by the culture system can act as a stimulus over cells, resulting in the regulation or increase of cellular proliferation and differentiation.

Apart from enabling cell seeding and culture by means of a perfusion-based method, this device also allows to use other methodologies such as static or agitated seeding. When performing static seeding, a cell suspension is injected inside the chamber filling all its inner void spaces and in particular the internal matrix's 3,4,5,6,7 pores. After sealing the tubular structures 8 with lids, the cell suspension is kept inside the chamber 1,2 and the matrix's 3,4,5,6,7 pores for a sufficient period of time for cells

contained in the cell suspension to adhere to the internal matrix 3,4,5,6,7. During that seeding, the device can be kept in static conditions or as well under agitation in order to increase the possibility for cells to get into contact with multiple matrix's 3,4,5,6,7 surfaces and so increase the possibility of adhesion as well as enabling a more homogenous distribution of adhered cell on the matrix's 3,4,5,6,7 surface.

After the seeding period, the cell suspension containing non adhered cells is removed from the interior of the device and replaced by fresh expansion and/or differentiation medium. Likewise, during the expansion and/or differentiation period, the device containing expansion and/or differentiation medium in its interior can be kept in static conditions or alternatively submitted to agitation.

In order to keep a sterile environment, with stable and adequate temperature and humidity, the bioreactor, integrated or not into a perfusion system, is placed inside a cell culture incubator.

6. Claims

1. A bioreactor for the generation of cellularized medical implants characterized in that it comprises an external watertight unicompartmented (1) or multicompartmented (2) external chamber containing in its interior one or more matrices (3,4,5,6,7), these interior matrices (3,4,5,6,7) and the bioreactor' s external chamber (1,2) being simultaneously manufactured, preferably through a process of rapid prototyping; in that the external chamber (1,2) possesses a shape adapted to the implant shape to be cellularized (internal matrix) , and in that it allows the implants to be removed from the interior of the bioreactor by cutting the external chamber (1,2) in locations possessing grooves (9) right before implantation, enabling a greater sterility of the implant.

2. A bioreactor for the generation of cellularized medical implants according to the previous claim, characterized in that it allows a unitary or modular manufacturing.

3. A bioreactor for the generation of cellularized medical implants according to the previous claims, characterized in that one or more matrices possess uniform or variable porosity, homogenous or heterogenous, present in the whole matrix (3,5,6,7) or part of the matrix (4), are three-dimensional (3,4,6,7) or bi-dimensional (5), possessing simple (3,4,5,6) or complex (7) shapes.

4. A bioreactor for the generation of cellularized medical implants according to the previous claims, characterized in that the external chamber (1,2) as well as the internal matrix (3,4,5,6,7) are manufactured by biodegradable materials or not, inert or not, polymeric or composite, transparent, translucent or opaque, biocompatibles, such as polycaprolactone, polylactic acid or polyglycolic acid.

5. A bioreactor for the generation of cellularized medical implants according to the previous claims, characterized in that the culture chamber (1,2) and the internal matrices (3,5,6,7) are auto-supported, although allowing the use of an extra support material, also deposited during the prototyping process, which can afterwards be removed by immersion into water or aqueous solution.

6. A bioreactor for the generation of cellularized medical implants, according to the previous claims, characterized in that the matrix's external simple shape design (3,4,5,6) is achieved by using simple shapes as initial references such as cuboidal, cylindrical, tubular or other shapes, while the design of the complex (7) internal matrix's external shape is achieved by resorting to complex shapes obtained from tissues or organs analysis performed by technologies such as computerized tomography or magnetic resonance .

7. A bioreactor for the generation of cellularized medical implants according to the previous claims, characterized in that the design of the external chamber (1,2) has as initial reference the external shape of the internal matrix (3,4,5,6,7) in order to the device's designed internal walls (1,2) are very close to the external walls of the internal matrix's design (3,4,5,6,7) with a spacing similar to the pore diameter of the inner matrix, which diameter lies preferably between 0.25mm and 3mm.

8. A bioreactor for the generation of cellularized medical implants according to the previous claims, characterized in that the internal walls of the external chamber (1,2) are very close to the external walls of the internal matrix (3,4,5,6,7) forming a cavity, whose inner filler volume ensures submersion of the internal matrix, by which can be circulated culture media and/or solutions or gases.

9. A bioreactor for the generation of cellularized medical implants according to the previous claims, characterized in that it allows to perform coatings over its surfaces by filling and/or perfusing the

interior of the chamber, through the pores of the internal matrix, with solutions or gases which are able to generate those coatings.

10. A bioreactor for the generation of cellularized medical implants according to the previous claims, characterized in that the external chamber has at least two tubular structures (8) which connect the interior of the external chamber (1,2) .

11. A bioreactor for the generation of cellularized medical implants according to the previous claims, characterized in that it is manufactured from one or multiple transparent or translucid materials.

12. A bioreactor for the generation of cellularized medical implants according to the previous claims, characterized in that the cells/tissues incorporated into the internal matrices (3,4,5,6,7) cultured in the interior of the bioreactor can be submitted to static or dynamic conditions by integration of the bioreactor into a agitation and/or perfusion system.

13. A bioreactor for the generation of cellularized medical implants according to the previous claims, characterized in that the internal matrices (3,4,5,6,7) are perfused uni- or bi-directionally.

14. Culture system for the generation of cellularized medical implants characterized in that it comprises a bioreactor for the generation of cellularized medical implants, an external chamber (1,2) containing one of the various kinds of internal matrices (3,4,5,6,7), connected to a culture medium reservoir (10) by tubes connected to its tubular structures (8) and an additional connection for the entry and exit of gases which are purified by an air filter (11) .

7. Amended claims

1. A bioreactor for the generation of cellularized medical implants characterized in that it comprises an external watertight unicompartmented (1) or multicompartmented (2) external chamber containing in its interior one or more matrices (3,4,5,6,7), these interior matrices (3,4,5,6,7) and the bioreactor' s external chamber (1,2) being simultaneously manufactured, preferably through a process of rapid prototyping; in that the external chamber (1,2) possesses a shape adapted to the implant shape to be cellularized (internal matrix), and in that it allows the implants to be removed from the interior of the

bioreactor by cutting the external chamber (1,2) in locations possessing grooves (9) right before implantation, enabling a greater sterility of the implant.

2. A bioreactor for the generation of cellularized medical implants according to the previous claims, characterized in that the culture chamber (1,2) and the internal matrices (3,5,6,7) are auto-supported, although allowing the use of an extra support material, also deposited during the prototyping process, which can afterwards be removed by immersion into water or aqueous solution.

3. A bioreactor for the generation of cellularized medical implants, according to the previous claims, characterized in that the simple matrix's external shape design (3,4,5,6) is achieved by using simple shapes as initial references such as cuboidal, cylindrical, tubular or other shapes, while the design of the internal complex matrix's (7) external shape is achieved by resorting to complex shapes obtained from tissues or organs analysis performed by technologies such as computerized tomography or magnetic resonance.

4. A bioreactor for the generation of cellularized medical implants according to the previous claims, characterized in that the design of the external chamber (1,2) has as initial reference the external shape of the internal matrix (3,4,5,6,7) in order to the device's designed internal walls (1,2) are sufficiently apart so that they do not touch the external walls of the internal matrix's design (3,4,5,6,7) with a spacing similar to the pore diameter of the inner matrix, which diameter lies preferably between 0.25mm and 3mm .

5. A bioreactor for the generation of cellularized medical implants according to the previous claims, characterized in that the internal walls of the external chamber (1,2) are sufficiently apart so that they do not touch the external walls of the internal matrix (3,4,5,6,7) forming a cavity, whose inner filler volume ensures submersion of the internal matrix, by which can be circulated culture media and/or solutions or gases.

6. A bioreactor for the generation of cellularized medical implants according to the previous claims, characterized in that it allows to perform coatings over its surfaces by filling and/or perfusing the interior of the chamber, through the pores of the internal matrix, with solutions or gases which are able to generate those coatings.

7. A bioreactor for the generation of cellularized medical implants according to the previous claims, characterized in that the external chamber has at least two tubular structures (8) which connect the interior of the external chamber (1,2) .

8. A bioreactor for the generation of cellularized medical implants according to the previous claims, characterized in that it is manufactured from one or multiple transparent or translucid materials.

9. A bioreactor for the generation of cellularized medical implants according to the previous claims, characterized in that the cells/tissues incorporated into the internal matrices (3,4,5,6,7) cultured in the interior of the bioreactor can be submitted to static or dynamic conditions by integration of the bioreactor into a agitation and/or perfusion system.

10. A bioreactor for the generation of cellularized medical implants according to the previous claims, characterized in that the internal matrices (3,4,5,6,7) are perfused uni- or bi-directionally.

11. Culture system for the generation of cellularized medical implants characterized in that it comprises a bioreactor for the generation of cellularized medical implants, an external chamber (1,2) containing one of the various kinds of internal matrices (3,4,5,6,7), connected to a culture medium reservoir (10) by tubes connected to its tubular structures (8) and an additional connection for the entry and exit of gases which are purified by an air filter (11) .

8. Statement under article 19(1)

The expression "rapid prototyping" refers to a set of technologies used to manufacture physical objects directly from source data generated by computer-aided design systems (commonly referred to as C.A.D.). With this type of manufacturing process, the physical objects are produced not only at the same time, but also physically together.

This technical feature of simultaneous fabrication of a matrix and a bioreactor with a shape adapted to matrix to be cellularized is a technical characteristic of the invention, by allowing the manufacture of the external culture chamber simultaneously with the implant to be cellularized, the manufacturing of a

culture chamber with a external shape adapted to the shape of the implant to be cellularized and also by allowing the sterility of the implant because, since it is made, it is always kept inside the external culture chamber (simultaneously manufactured) until the moment of implantation (when the outer chamber is cut in order to extract the cellularized implant).

Therefore, the product obtained depends mainly on its manufacture method because only with said method it is possible to ensure the sterility of the implant, since it is always maintained within the external culture chamber, since its manufacture until the moment of its implantation.

Its manufacturing process also allows the simultaneous manufacture of the matrix and of a bioreactor with a shape adapted to matrix to be cellularized. Therefore the bioreactor is again characterized by its manufacturing process.

Regarding to point V of the ISR, mentioning that the manufacture characteristics of the matrix and the matrix camera simultaneously are only functional characteristics and only relevant to define the manufacturing process of the bioreactor, it is important to highlight the 4.12 Part F - Chapter IV- 15 of the EPO Guidelines which reads as follows:

Claims for products defined in terms of a process of manufacture are allowable only if the products as such fulfil the requirements for patentability, i.e. inter alia that they are new and inventive... "

As regards novelty, when a product is defined by its method of manufacture, the question to be answered is whether the product under consideration is identical to known products the modification of the process parameters results in another product, for example by showing that distinct differences exist in the properties of the products...

According to Art. 64(2), if the subject-matter of a European patent is a process, the protection conferred by the patent extends to the products directly obtained by such process...

Due to the presented reasons, the bioreactor of the present invention possesses technical features derived from its method of manufacture, which have advantages (cited above) compared to other known bioreactors. Therefore, this claim should be considered as a "product-by-process" claim.

9. Figures

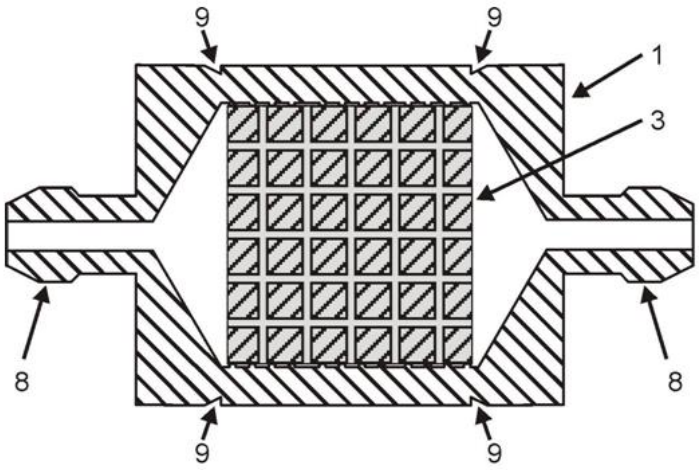

Figure 3.1 - Longitudinal section of the device containing a simple three-dimensional porous structure in its interior.

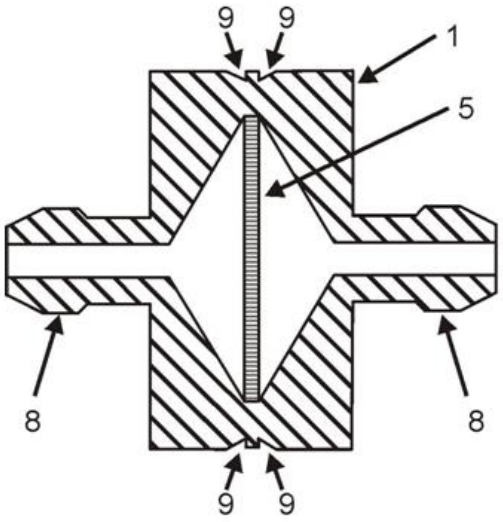

Figure 3.2 - Longitudinal section of the device containing a bi-dimensional porous structure in its interior.

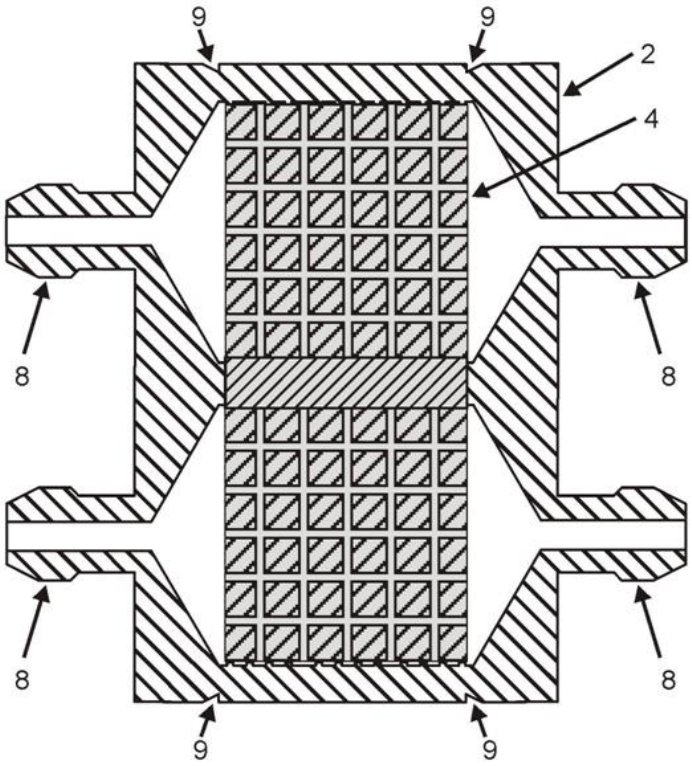

Figure 3.3 - Longitudinal section of the device containing a double three-dimensional porous structure in its interior.

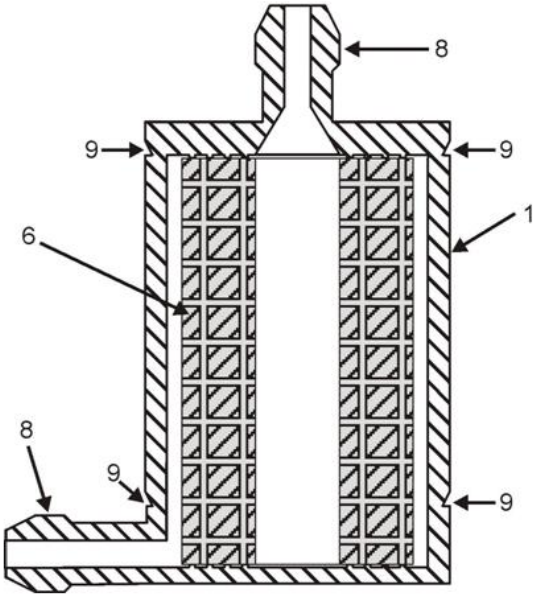

Figure 3.4 - Longitudinal section of the device containing a tubular three-dimensional porous structure in its interior.

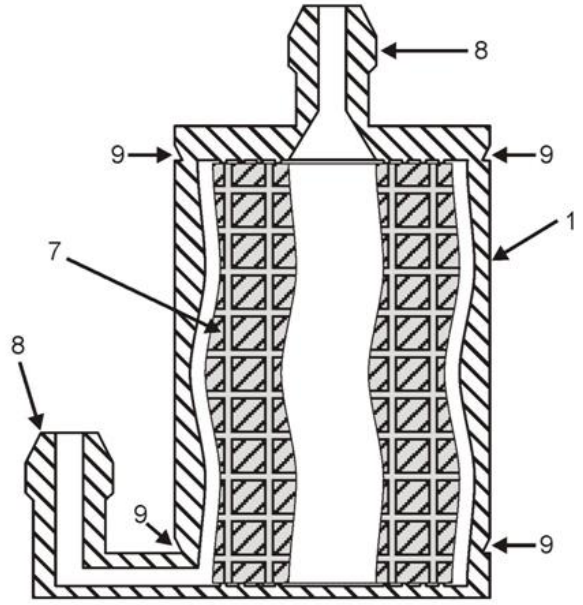

Figure 3.5 - Longitudinal section of the device containing a complex tubular three-dimensional porous structure, manufactured using a three-dimensional model obtained from computerized tomography or magnetic resonance analysis of a tissue or organ.

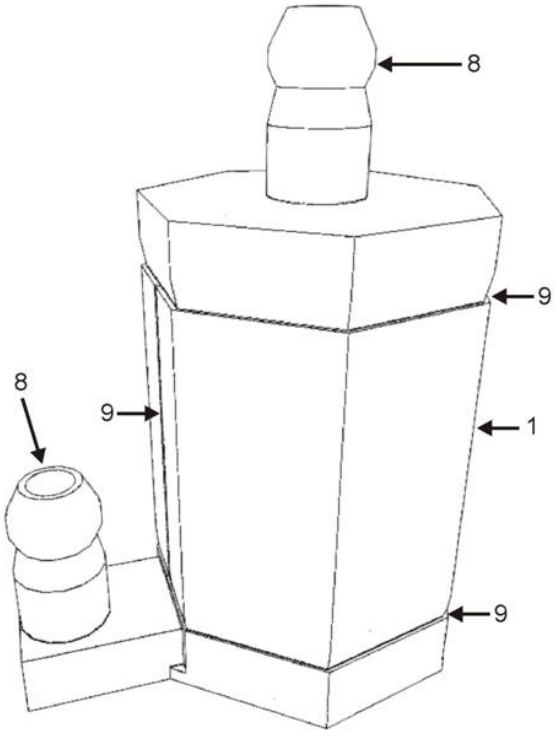

Figure 3.6 - Device in isometric view.

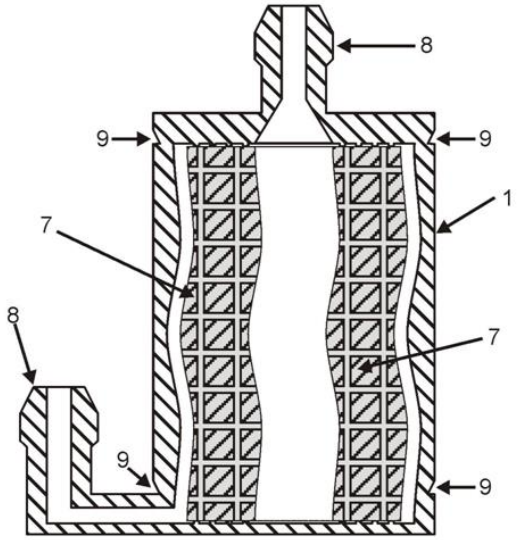

Figure 3.7 - Longitudinal section of the device.

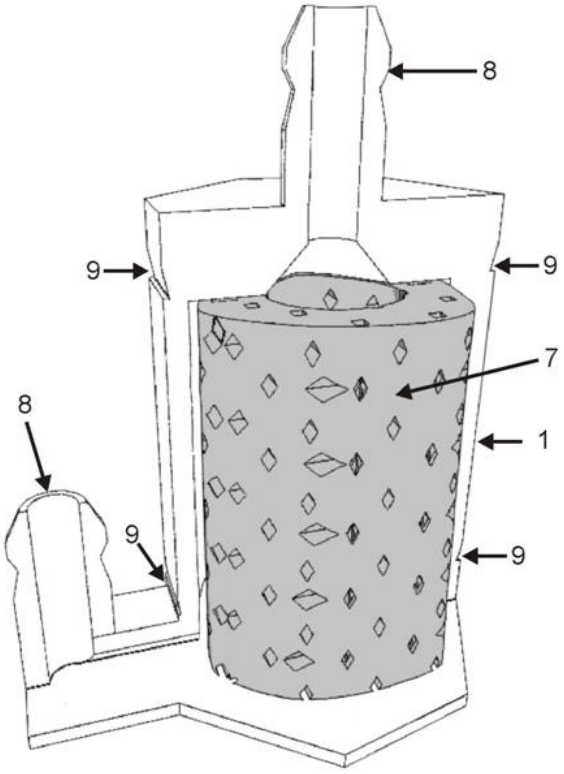

Figure 3.8 - Partial section of the device in isometric view.

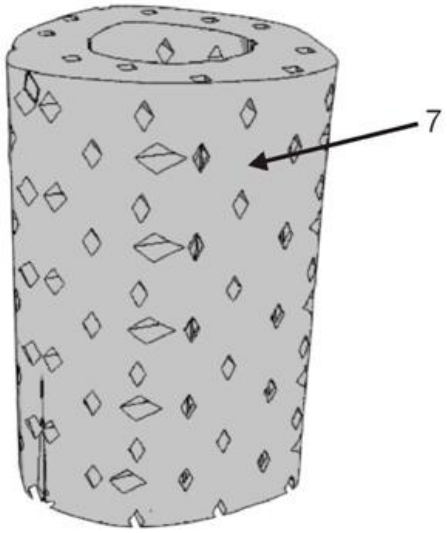

Figure 3.9 - Implant after removal of the external enclosure in isometric view.

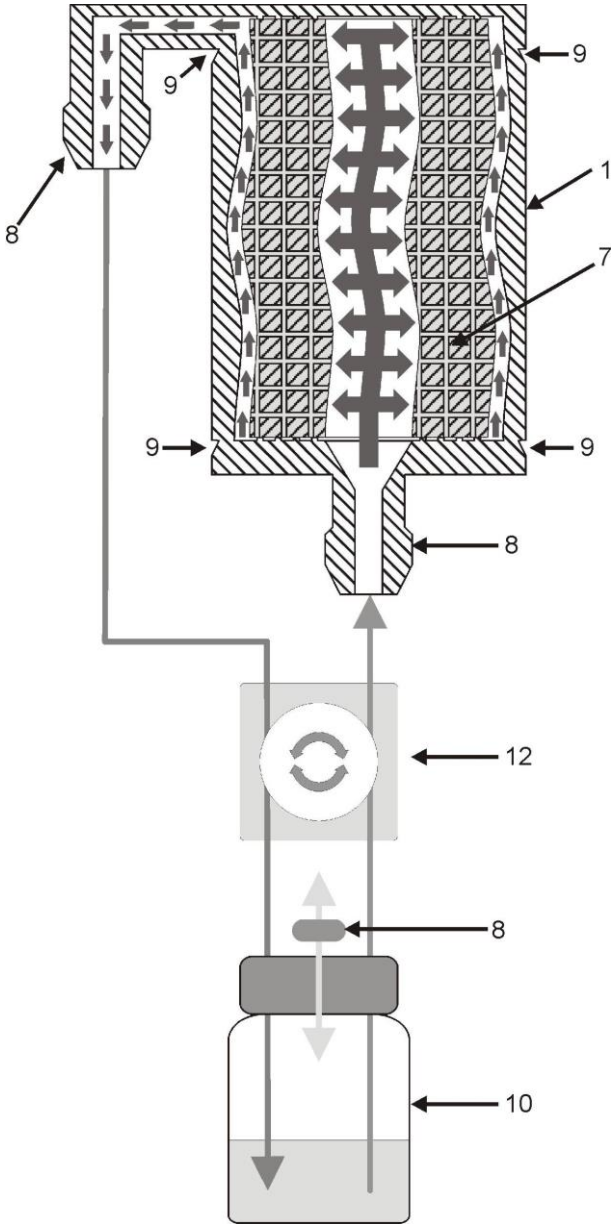

Figure 3.10 - Device described in figures 3.6 and 3.9 integrated into a dynamic perfusion cell culture system.

Chapter 4

Biofabrication of customized bone grafts by combination of additive manufacturing and bioreactor technologies

Abstract

This study reports on an original concept involving additive manufacturing for the fabrication of customized tissue engineered constructs, offering the possibility of concomitantly manufacturing a scaffold and a bioreactor chamber to any size and shape. As a proof of concept towards the development of anatomically relevant tissue engineered constructs, additive manufacturing was utilized for the design and fabrication of a sheep-tibia scaffold around which a bioreactor chamber of similar shape was simultaneously constructed. The morphology of the resulting device was investigated by micro-computed tomography and scanning electron microscopy (SEM) confirming the porous architecture of the internal scaffold as opposed to the non-porous nature of the bioreactor chamber. Additionally, this study demonstrates that both the shape, as well as the inner architecture of the device can significantly impact the perfusion of fluid within the scaffold. Indeed, fluid flow modelling revealed that this was of significant importance for controlling the nutrition flow pattern within the scaffold and the device, avoiding the formation of stagnant regions detrimental for in vitro tissue development. The device was further seeded with human primary osteoblasts and cultured under bidirectional perfusion for 2 and 6 weeks. Primary human osteoblasts were observed homogenously distributed throughout the scaffold, and were viable for the 6 weeks culture period. This work demonstrates a novel application for additive manufacturing in the development of scaffolds and bioreactors. Given the intrinsic flexibility of this technology, more complex culture systems can be fabricated which would contribute to the advancement of customized tissue engineering strategies for a wide range of applications.

This chapter is based on the following publication:

Costa P.F., Vaquette C., Baldwin J., Gomes, M.E., Reis R.L., Theodoropoulos, C., Hutmacher D.W., 2013, Biofabrication of customized bone grafts by combination of additive manufacturing and bioreactor technologies, *Biofabrication*, Submitted.

1. Introduction

Personalized medical therapy is an emerging practice of medical treatment offering tailored solutions to each individual. This approach is envisioned to revolutionize healthcare, with cost-effectiveness, efficiency and improved patient outcomes. Currently, the pharmaceutical industry is investing heavily in this approach through the development of personalized medicine supported by the advancement in molecular and genomic technologies [1]. To some extent, the field of tissue engineering is following a similar path with increasing attention given to the development of customized tissue engineered products that would meet the patient-specific requirements for replacing organs or tissues.

Additive manufacturing (AM) is one of the many engineering technologies that have been utilized in tissue engineering, and is central for the fabrication of customized implants. Additive manufacturing builds objects in a layer-by-layer manner by gradual deposition of materials in an organized fashion, permitting the fabrication of three-dimensional (3D) objects of highly complex architecture [2]. However, the development of customized constructs of large dimensions and their subsequent cell culture remained challenging because of the requirements for appropriate oxygen and nutrient diffusion throughout the entire construct. By utilizing bioreactors, rather than traditional static cultures, enhanced fluid diffusion within the scaffold can be achieved, permitting *in vitro* culture under highly controlled conditions [3]. Bioreactors are usually designed to meet specific requirements for a standardized scaffold size and shape, type of perfusion, desired fluid flow pattern, type of applied stimulatory factors (biochemical or biomechanical), and integrated sensorial probes [4-10]. These points exemplify the degree of complexity achieved in traditional bioreactors, as well as, the lack of versatility when anatomical scaffolds are considered for tissue engineering applications. Indeed, this represents a major limitation to the generalized use of bioreactors in personalized tissue engineering strategies as any modifications of a standardized bioreactor chamber engender considerable additional engineering steps and therefore result in significantly increased labour and cost.

Control over the fluid flow pattern within the construct is a crucial parameter for the proliferation and survival of cultured cells in 3D. Shear stress resulting from fluid perfusion is known to influence cell behaviour and more importantly perfusion is able to positively impact on cell survival by avoiding the formation of regions where culture media is stagnant [11-17]. This suggests that the architecture of the bioreactor should be similar to that of the scaffold for achieving homogeneous fluid perfusion and alleviating the aforementioned issues. A significant advance towards the development of anatomically shaped bioreactor chambers was performed by Grayson *et al* [10] who fabricated a scaffold resembling

a bovine temporomandibular joint (TMJ) condylar bone and cultured the resulting construct in a bioreactor of similar dimensions. The anatomically shaped bioreactor's chamber was produced by casting polydimethylsiloxane (PDMS) around a TMJ-like mould, inserted into a cylindrical tube which was utilized to hold the scaffold for achieving appropriate fluid transfer to the construct's most central portions. This technique required multiple steps and lacked versatility for facilitating the addition of new bioreactor features such as additional inlets and variation in scaffold dimension. Although promising, this approach still requires the revision of the bioreactor design when tailoring to suit anatomically different samples, indicating that even though scaffolds can be easily fabricated into an array of unique but specific anatomical dimensions, it is not necessarily the case for bioreactor chambers.

Based on this background, we hypothesized that additive manufacturing could be utilized to simultaneously fabricate both the scaffold and the bioreactor chamber and provide sufficient flexibility for rapidly manufacturing devices with various anatomical shapes. This concept inherits a high degree of process automation, hence enabling the fabrication of high quality personalized tissue engineered constructs in a reproducible manner and at an efficient cost and speed. This study reports on a proof of concept that additive manufacturing involving a commercial inexpensive dual polymer extrusion system is capable of fabricating anatomical complex devices, comprising of an ovine tibia scaffold, and a bioreactor chamber in one single step.

2. Materials and Methods

2.1. Design and fabrication concept

The general design methodology employed in this study begins with the generation of a 3D numerical model for any tissue or organ by micro-computed tomography (micro-CT) imaging which is then converted into a three-dimensional replica with pre-determined porosity. An outer shell, referred herein as bioreactor chamber, possessing inlets/outlets is then designed around the replica in order to manufacture, in one step, an anatomically shaped device comprising of an anatomically-optimized scaffold inserted into a customized bioreactor chamber. This allows for the perfusion of the resulting scaffold during *in vitro* culture, while better controlling the flow and shear stress in the system. As a proof of concept, we scanned a 3 cm ovine tibia section by micro-CT to create a numerical 3D model which was subsequently imported into 3Ds Max (Autodesk, USA) software. The 3D model was vertically re-oriented and both extremities of the tibial model were trimmed for obtaining horizontal flat surfaces

and resulted in the final model having a total length of 2.5 cm. The 3D design tool, extrusion, was then used to generate a shell wall around the lateral and top outer surfaces of the 3D model. The generated wall was 1 mm thick and 1 mm-spaced from the 3D scaffold model's outer surfaces. The top part of the shell was converted to a tubular conical shape possessing a slope angle of 55° in order to be self-supportive. This part of the shell was designed to enable an adequate fluid flow on the interior of the device, and to provide sufficient space for containing extra culture medium. The top end of this conical medium reservoir had a slope angle of 90° creating an inlet/outlet structure with an inner diameter of 2mm onto which tubing could be connected. The bottom corners of the chamber were additionally chamfered by 2 mm with a slope angle of 45° to improve the hydrodynamic design. On the bottom part of the device, a plate containing a 1 mm-wide mini channel was designed, allowing connectivity of the centre of the plate to a lateral 2 mm diameter inlet/outlet. Furthermore, by using the same extrusion design tool, a plain column was also generated for filling the empty space located in the centre of the tibia-shaped model.

2.2. Fluid flow modelling

A computational fluid dynamics approach was used to simulate the flow pattern of the media in various device architectures. The studied architectures diverged in three main aspects: utilization of rectangular/chamfered chamber bottom corners, presence/absence of a central filler column for filling the void space inside the tibia model, and utilization of wide/narrow top inlets/outlets. Given the high complexity of the device, a simplified model consisting of two-dimensional sections was created in Design Modeler 13.0 software (Ansys, USA). A profile corresponding to the section of a tubular scaffold with a length of 2.5 cm, an outer diameter of 13 mm and inner diameter of 6 mm was considered. The thickness of the simplified section was 0.1mm while the maximum face size of the resulting mesh was 0.2 μm. The fluid flow velocity profiles were calculated using Fluent 13.0 software, within Ansys Workbench 13.0 platform (Ansys, USA). The pressure at the device's outlet was assumed to be zero and the scaffold and bioreactor chamber were considered rigid and impermeable. We assumed that the viscosity and the density of the culture media at 37°C were η = 1.45·10^{-3} Pa.s) and (ρ = 1000 kg.m^{-3}) respectively.

2.3. Conversion, slicing and prototyping of 3D models

Fluid flow modelling permitted the selection of an optimized device design which was subsequently utilized in the rest of the study. The device's 3D model was then sliced and converted to a G-Code file. The volume corresponding to the 3D tibia to be converted to a porous scaffold was processed using the open source software Reprap (Online Reprap Community). The 3D tibia model was sliced into 0.27 mm layers composed of deposition path lines with a spacing of 1.5 mm. On the other hand, the volume corresponding to the outer shell device was sliced and converted to G-Code files by using the open source software ReplicatorG (Online ReplicatorG Community). The conversion was performed using 2 shells, a slice thickness of 0.27 mm, an object infill of 100%, a feed rate of 20 mm/s and a travel feed rate of 55 mm/s as parameters. The G-Code generated through RepRap and ReplicatorG were then merged together in order to generate one single G-Code file.

The prototyping of the devices was performed using an open source dual extrusion rapid prototyping machine (Replicator, Makerbot Industries, USA). The materials used were poly(lactic) acid (PLA) Ingeo 4043D (NatureWorks LLC, USA) for the porous scaffolds and acrylonitrile butadiene styrene (ABS) (Makerbot industries, USA) for the bioreactor chamber. The temperature used for fusing both materials in their corresponding nozzles was 220°C. Both materials were deposited through coordinated and alternating operation of the nozzles.

2.4. Bioreactor surface treatment

In order to ensure that fluid leakage could not occur during subsequent cell culture, a post-treatment coating of ABS was applied to the outer bioreactor wall surfaces for closing any porosity. In brief, after capping all inlets/outlets, the devices were immersed for 2 seconds in an ABS/acetone 60 mg/mL solution and then air-dried at room temperature for 30 min. This procedure was performed twice. Finally, the devices were washed in distilled water to remove residual solvent.

2.5. Scaffold surface treatment

Given the hydrophobic nature of PLA, which could hinder appropriate and homogeneous fluid perfusion through the device, alkaline etching was performed using a 2M sodium hydroxide (NaOH) solution. The devices were rinsed in 100 % ethanol solution under vacuum for one hour to pre-wet the scaffold fibre

surfaces. After the removal of ethanol, sodium hydroxide solution was perfused through the device until the bioreactor was entirely filled. The devices were incubated for 30 minutes at room temperature under vacuum prior to a secondary incubation at 37°C for 60 minutes. Finally, the devices were washed several times with distilled water and then air-dried. In order to assess the efficacy of the NaOH treatment, the same protocol was performed onto 8 mm cubic scaffolds having similar architecture but not inserted in the device. Images of fluid infiltration within the construct prior and after NaOH treatment were taken using a digital camera.

2.6. Micro computerized tomography analysis (Micro-CT)

The devices were analyzed by micro-CT (µCT40, SCANCO Medical AG, Brüttisellen, Switzerland) at a resolution of 12 µm, a voltage of 55 kVp, and at a current of 175 µA. Three-dimensional images were reconstructed from the scans by the micro-CT system software.

2.7. *In vitro* study

Cell culture took place over 6 weeks and was performed under bidirectional perfusion. A 1 mL sterile syringe was connected to the device's medium inlet using sterile silicone tubing. This apparatus was mounted on a multi-syringe adapter placed on an Aladdin syringe pump (World Precision Instruments, USA). A total of 6 devices (each with a dedicated syringe) were simultaneously cultured in this system. The devices were first sterilized by perfusion with 50% ethanol solution for 20 minutes and dried in a sterile biohazard safety cabinet for 2 hours. The devices were manually filled with 4 mL of basal medium and bidirectionally perfused overnight at a flow rate of 0.4 mL/min and flow direction inversion every 100 seconds using the syringe system. This hydration step aimed at promoting the pre-adsorption of proteins to the scaffold surfaces and hence, facilitating subsequent cell attachment. In order to ensure the sterility of the device during the culture period while still allowing gas exchange with the incubator's environment, a 0.2 µm pore size filter (13 mm diameter) (Pall, USA) was connected to the outlet positioned at the top of the device.

Primary human osteoblasts were collected from a patient undergoing hip surgery. Ethics approval for the use of human osteoblasts in this experiment was granted from The Prince Charles Hospital ethics committee (ethics clearance number: EC2310) and Queensland University of Technology ethics committee (ethics clearance number 0600000232). The osteoblasts were expanded in basal alpha

MEM modified medium (Gibco, USA) supplemented with 10% foetal calf serum and 1% penicillin/streptomycin and used at passage 2. When reaching confluence, the cells were trypsinized and $1x10^6$ osteoblasts in 250 µl of media were injected into the devices through silicone tubes. The devices were bi-directionally perfused for 24 hours at a flow rate of 0.4 mL/min in order to allow cell attachment. The perfusion direction was automatically inverted every 100 seconds utilizing an external microcontroller connected to the syringe pump.

After 24 hours, the culture medium was replaced by fresh medium and the flow rate was increased to 0.8 mL/min whereas the flow inversion frequency was reduced to 50 seconds. The medium was changed weekly and the scaffolds were collected for analysis at 2 and 6 weeks post-seeding.

The scaffold collection was performed as follows: the devices were detached from the syringe pump by removing the silicone tubings and placed in a sterile biohazard safety cabinet. The scaffolds were retrieved from the interior of the bioreactor chamber by manually sectioning the bioreactor walls using sterile tweezers and scissors. The collected scaffolds were processed for either 3-(4,5-dimethylthiazol-2-yl)-2,5-diphenyltetrazolium bromide (MTT) staining, live/dead assay, confocal laser scanning or electron microscopy.

2.8. Metabolic activity staining

Metabolically active cells were visualized by using a 1 mg/mL 3-(4,5-dimethylthiazol-2-yl)-2,5-diphenyltetrazolium bromide (MTT) solution. Following retrieval, the scaffolds were washed in PBS and then immersed into MTT solution for 30 min. Images were captured by a digital camera mounted on an Eclipse TS100 microscope (Nikon, Tokyo, Japan).

2.9. Live/dead assay (FDA/PI)

Cell viability was assessed using a live/dead assay. The scaffolds were washed twice in PBS, incubated for 5 minutes at 37°C in PBS containing 0.67 µg/mL fluorescein diacetate (FDA) and 5 µg/mL propidium iodide (PI) (both Invitrogen) and washed again in PBS. The cellularised scaffolds were analysed using a confocal laser scanning microscope (Leica TCS SP5, Leica Microsystems, GmbH). The excitation/emission wavelengths used for imaging the FDA and PI stainings were respectively 488/518-568 nm and 561/598-795 nm. A semi-quantitative analysis of the cellular viability was performed using ImageJ software to quantify living cells (green colour) and dead cells (red colour). A total of seven

images from multiple regions of interest of the constructs were captured and analysed for each time point.

2.10. Scanning electron microscopy (SEM)

Osteoblast morphology and distribution in the scaffold was assessed at 2 and 6 weeks post-seeding by scanning electron microscopy. In brief, samples were fixed in 3% glutaraldehyde, washed in 0.1 M cacodylate buffer, post-fixed in 1 % osmium tetroxide in cacodylate buffer for 1 hour, prior to dehydration through sequential graded series of ethanol concentrations. Finally, samples were immersed in hexamethyldisilazane for 60 min, air dried, mounted onto aluminium stubs and gold coated. Samples were observed on a FEI Quanta 200 Environmental SEM operating at 10 kV. Scaffolds without cells were gold coated prior to imaging.

3. Results and discussion

The purpose of this study was to develop and assess an innovative biofabrication-rooted technology for simultaneously generating anatomically shaped scaffolds and bioreactor chambers for bone tissue engineering. Additive manufacturing is commonly used for fabricating scaffolds for tissue engineering, however it is rarely utilized for manufacturing bioreactors. This study is, to our knowledge, the first report on the utilization of rapid prototyping for designing anatomically shaped bioreactors and scaffolds in one process. The versatility provided by additive manufacturing technologies enables the production of highly complex scaffolds which raise a realm of new possibilities, but also new challenges strongly related to the *in vitro* culture methods. Indeed, seeding methods are yet to be developed for homogenously distributing the cells through large constructs such as the ones utilized in the present study. Also, adequate supply of nutrients and oxygen throughout the entire construct is another parameter of importance for the generation of viable tissue substitutes. Unlike small and regular-shaped constructs, the seeding and the culture of anatomically relevant constructs with large dimensions requires a greater degree of complexity in their design for achieving appropriate *in vitro* tissue development. In the context of personalized regenerative strategies, highly versatile manufacturing platforms are required for their fabrication and the methodology developed in this work intends to circumvent the abovementioned challenges while still being economically competitive.

3.1. Fluid flow modelling

The control over the fluid pattern within perfused scaffolds is essential for achieving effective *in vitro* culture conditions. Homogenous fluid velocities and absence of stagnant zones are among the main features defining an optimal culture system. Therefore, multiple architectural configurations were tested in order to define the most fluid dynamic-efficient design by varying several parameters such as the utilization of rectangular or chamfered chamber bottom corners, presence or absence of an inner filler column and wide (same diameter as the scaffold) or narrow top (2 mm diameter) inlet/outlet. Figure 4.1a) depicts the velocity profile of the media perfused in these devices as obtained by numerical modelling. It was observed that chamfered geometries were the most efficient in avoiding low velocity sites, in contrast to rectangular geometries where fluid velocities in the vicinity of the rectangular lower corners dropped to under 2.5% of the inlet fluid velocity. Hidalgo-Bastida *et al* utilized computational fluid dynamics for predicting and comparing fluid patterns into rectangular or circular bioreactor chambers. It was shown that a circular geometry was the most suitable for avoiding both the formation of stagnant zones in the peripheral regions of the scaffolds and high fluid velocity near the chamber's inlets/outlets [18]. However, the regions located between the scaffold and the chamber's inlets/outlets were not taken into account despite potential media accumulation in these areas. Figures 4.1a1-4.1a3 clearly show that rectangular bottom corners are prone to the formation of stagnant regions and this is of particular relevance for vertically oriented perfusion chambers and can induce cell apoptosis caused by lack of nutrients and oxygen. However, this is eliminated to a large extent by the chamfered geometry of the bioreactor chamber as demonstrated in figures 4.1a4-4.1a6 where fluid velocities were always kept 2.5% above initial fluid velocity. The design was further optimized by adding an ABS porous support structure at the base of the bioreactor (figures 4.1a3-4.1a6), which proved highly efficient at placing the scaffold away from both stagnant and high fluid velocity regions.

The design of a column internal to the scaffold's void central part, allowed to efficiently steer the media towards the central region of the scaffold (figures 4.1a3, 4.1a4 and 4.1a6). This contributed also to increasing the fluid velocity in the scaffold to 15-20% of the initial value and resulted in establishing a more homogeneous fluid velocity. This is in contrast to the design without ABS column where the fluid velocity was much lower (5 to 7.5%) and highly heterogeneous (figures 4.1a5 and 4.1a6). Taking into consideration that the initial flow rate was 0.8 mL/min, this column design resulted in an homogeneous flow rate of 0.12-0.16 mL/min in the scaffold, which is similar to what was found in previous studies

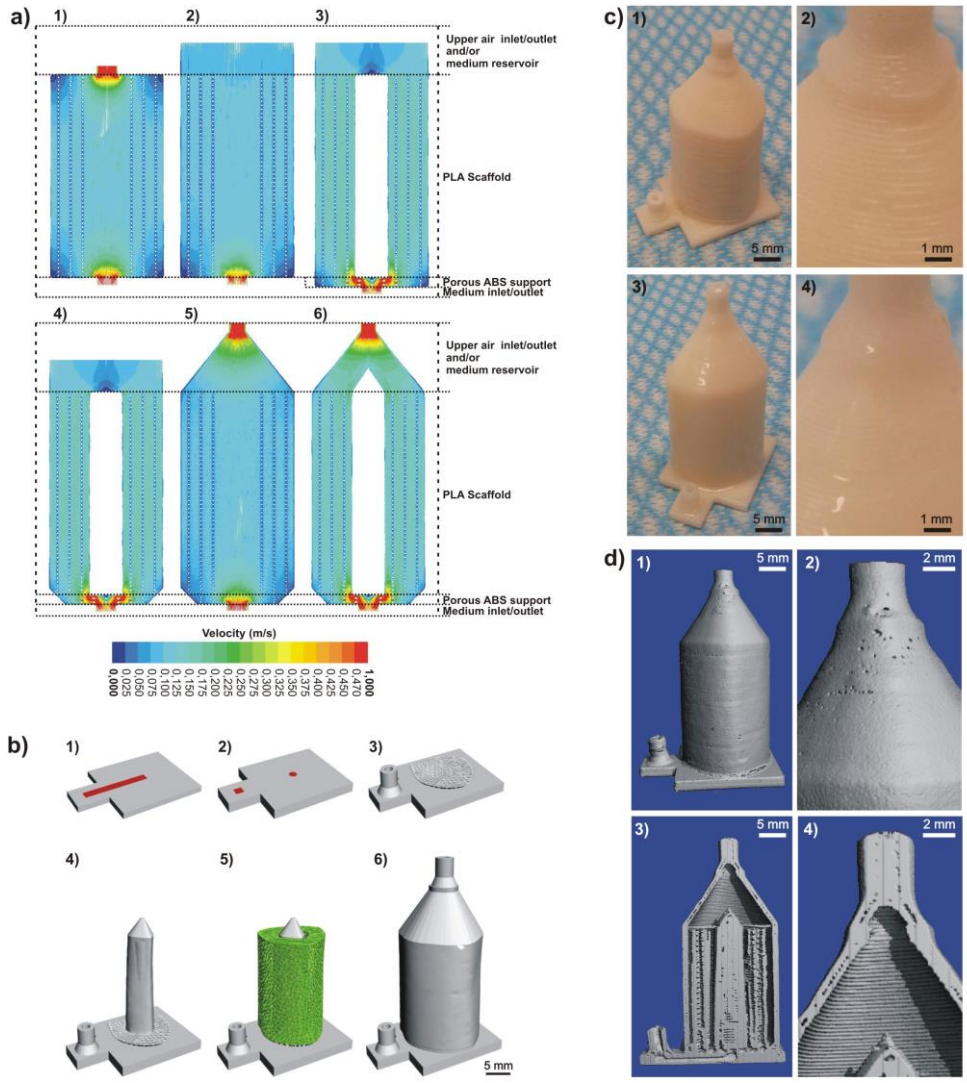

Figure 4.1 – a) Fluid flow modelling of various device inner architectures. a1) Rectangular device with narrow top outlet. a2) Rectangular device with wide top outlet. a3) Rectangular device with a support structure (located at the bottom) and a filler column centrally positioned in regard to the scaffold. a4) 2 mm-chamfered chamber with support structure, filler column and wide outlet. a5) 2 mm-chamfered chamber with support structure, conical outlet but without filler column. a6) 2 mm-chamfered chamber with support structure, filler column and conical outlet. b) Elements of the device to be prototyped. b1) Base of the device consisting in a lower plate designed with a mini channel for supplying culture medium (red) which is covered by another plate containing two holes b2). b3) Medium inlet/outlet and porous structure positioned over the holes. b4) Filler column centrally positioned in regard to the scaffold. b5) Tailor-made porous scaffold (green) positioned around the filler column. b6) Bioreactor chamber surrounding the scaffold. c) Fabrication and post-processing of the device. c1 and c2) Device after rapid-prototyping. c3 and c4) Device after treatment with ABS/acetone solution. d) Micro-CT reconstruction of device. d1 and d2) Reconstruction depicting the smooth outer ABS-made surface of the device which was treated with ABS/acetone solution. d3) Cross-section depicting the structure of the device containing an NaOH-treated PLA scaffold and a central ABS filler column. d4) Morphology of the bioreactor chamber which is characteristic of a layer-by-layer deposition suggesting that the ABS-acetone post-treatment did not affect the inner wall of the bioreactor chamber (in contrast to the outer wall shown in d2)).

where flow rates within this range positively influenced cellular proliferation and development while at the same time avoiding cell detachment caused by high shear stress [11, 19].

Also, we observed that the utilization of a wide or narrow inlet/outlet configuration at the top of the device did not significantly affect the flow pattern in the device, however the narrow outlet configuration (Figure 4.1a6) was selected for the subsequent *in vitro* culture, as it would effectively reduce the risk of contamination by permitting the attachment of a sterile air filter.

3.2. Design, fabrication and post-processing of the device

Taking into consideration the results obtained from the fluid flow modelling and considering the specific needs for the development of a perfusion bioreactor, an optimized device design was achieved by 3D modelling in the 3Ds Max Software (Figure 4.1b). The bottom part of the device consisted of a base plate into which a mini channel was integrated (figures 4.1b1 and 4.1b2) for supplying the culture media in the device. For this purpose, a tubular structure was added at one end of the channel for connecting the chamber to the culture medium reservoir. As already described in the previous section, a porous ABS structure was placed at the bottom of the device for allowing homogenous fluid distribution (Figure 4.1b3). This porous support was 1 mm thick and possessed a cross-section similar to the one found in the anatomically shaped scaffold. Figure 4.1b4 shows the filler column utilized to steer the media towards the central portions of the scaffold and reduce the volume of medium necessary for the cell seeding and subsequent culture. A 1 mm spacing was maintained between the column and the scaffold for permitting fluid circulation in these locations (Figure 4.1b5). Finally, an outer bioreactor chamber was designed around the scaffold and its porous support (Figure 4.1b6). This chamber was positioned at a 1 mm distance from the scaffold and matched the anatomical shape of the scaffold. While further reducing the volume of media utilized during the *in vitro* culture, this also enabled higher control over the fluid flow pattern. Indeed, a bioreactor chamber that follows accurately the shape of the scaffold ensures effective circulation of the culture medium through the interior of the construct, not only around its periphery. As seen in the fluid flow simulations, the hydrodynamic design provided by both the inner column and the bioreactor chamber resulted in homogenous fluid patterns throughout the interior of the scaffold. Commercially available bioreactor culture systems such as the U-Cup (Cellec Biotek AG, Switzerland) have shown that bidirectional perfusion enhances cell seeding efficiency and distribution and results in more reproducible bone formation [5, 20]. In contrast to our device, the U-Cup is only capable of culturing small cylindrical constructs and hence lacks the versatility

required for tailor-made applications in which the construct's shape and architecture need to be optimized on a case-to-case basis.

The final design (Figure 4.1b6) was saved as an STL file, converted to G-Code using RepRap and ReplicatorG softwares and finally prototyped in the Makerbot dual extrusion fused deposition prototyping machine. The time necessary for fabricating each device was 45 minutes. As some open porosity remained within the bioreactor chamber, a post-treatment with an ABS solution was utilized in order to close these pores, hence ensuring that no leaking would occur during the subsequent cell culture. As shown in Figure 4.1d, the treatment reduced the outer surface roughness of the bioreactor chamber and all interlayer micro-gaps were eliminated. This significantly affected the appearance of the chamber's outer wall as shown in Figure 4.1c as the post-treated material appeared smoother and with a glossy finish. Acetone-based solutions are commonly used as cements for repairing, welding and smoothing, as well as for waterproofing structures made of ABS [21, 22].

In contrast to this, the NaOH post-treatment on the PLA scaffold resulted in high surface roughness and consequently higher hydrophilicity when compared to untreated samples (Figure 4.2) which was in accordance with a previous study [23]. This post-treatment exemplifies the fact that other types of surface modification can be performed on the scaffold by simply perfusing fluids within the device such as simulated body fluid for a biomimetic coating [24-26].

The high versatility provided by additive manufacturing combined with the concept we have developed in this study, permits and facilitates the optimization of numerous devices with different shapes and sizes where various design features such as additional inlet/outlet can be incorporated. Indeed, unlike traditional bioreactors, one major advantage of this culture platform is that both culture chamber and scaffold designs can be freely modified and optimized according to the intended tissue engineering application without any additional engineering steps or increased costs.

Although in this study a rather simple scaffold architecture [27] was utilized, which mimicked an ovine tibia, and hence relatively basic in its shape and design, other scaffolds with more complex and heterogeneous architectures could be fabricated with the method described in this study. This high versatility in the design and manufacturing of both the scaffold and the culture chamber is the main characteristic that distinguishes this technology platform from other currently existing devices. For instance, a comparison with the strategy developed by Grayson *et al* [10], clearly shows the superior properties of our concept in regard to the design and the manufacturing. Indeed, the fabrication of the devices is performed in one single step while permitting the maintenance of a high degree of accuracy in the architecture and the shape of the scaffold or the bioreactor chamber.

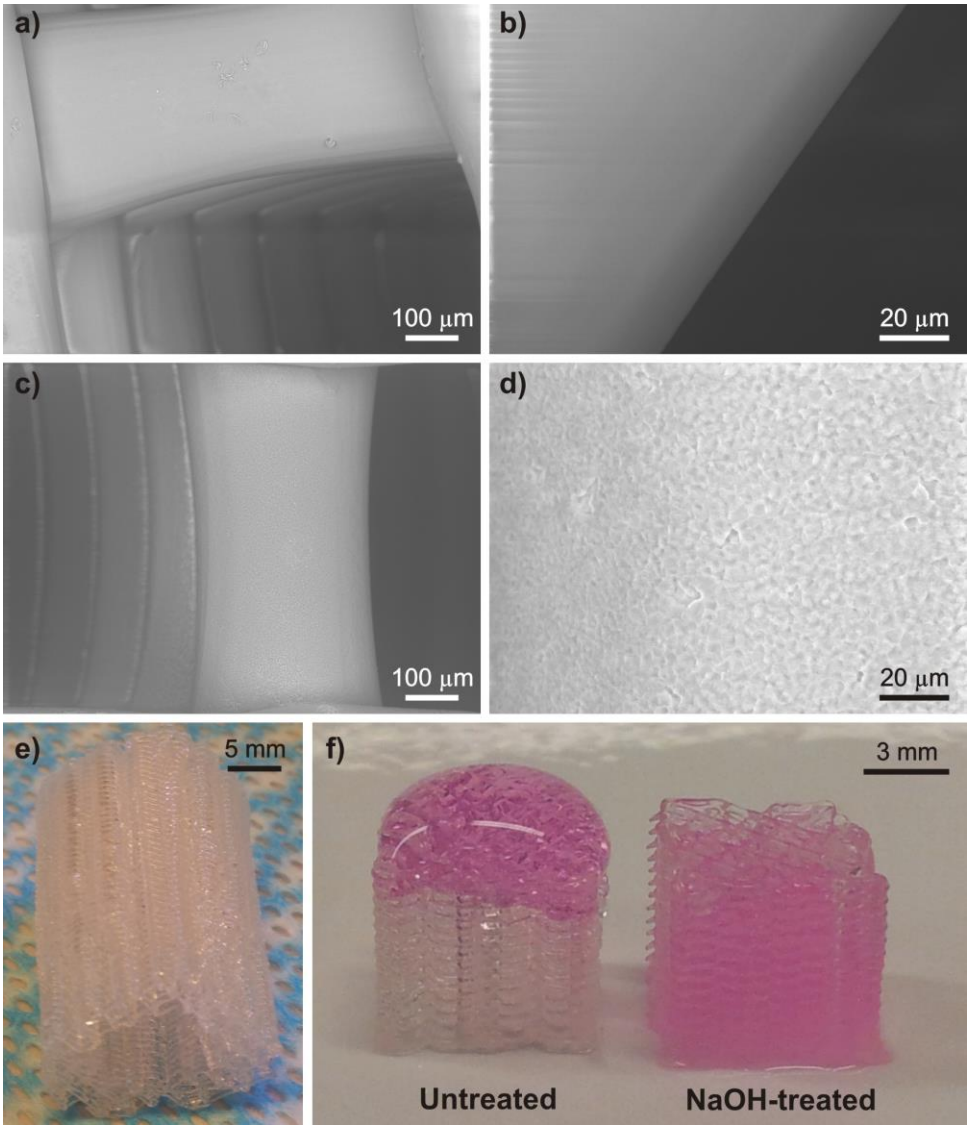

Figure 4.2 - Effect of NaOH treatment. a and b) Scanning electron micrographs obtained from the surface of untreated, a) and b) and NaOH-treated scaffold c) and d). e) Scaffold retrieved from the device. f) Increased hydrophilicity resulting from the NaOH treatment, untreated (left) and NaOH-treated test scaffolds (right) when hydrated with culture medium.

3.3. Perfusion cell culture

The perfusion bioreactor was composed of various devices with their top air inlet/outlets capped with syringe filters (Figure 4.3a2) and connected to individual syringes mounted into one single syringe pump by means of a multi-syringe adapter (Figure 4.3a1). After an overnight incubation of the scaffold in culture media, the cell suspension was injected into the device and the bidirectional perfusion was applied for achieving a homogeneous seeding. After 2 and 6 weeks of culture, the scaffolds were collected by manually opening the devices utilizing sterile scissors and tweezers as depicted in Figure 4.3b. The MTT staining revealed the distribution of viable cells at 2 and 6 weeks (Figure 4.4a). Indeed

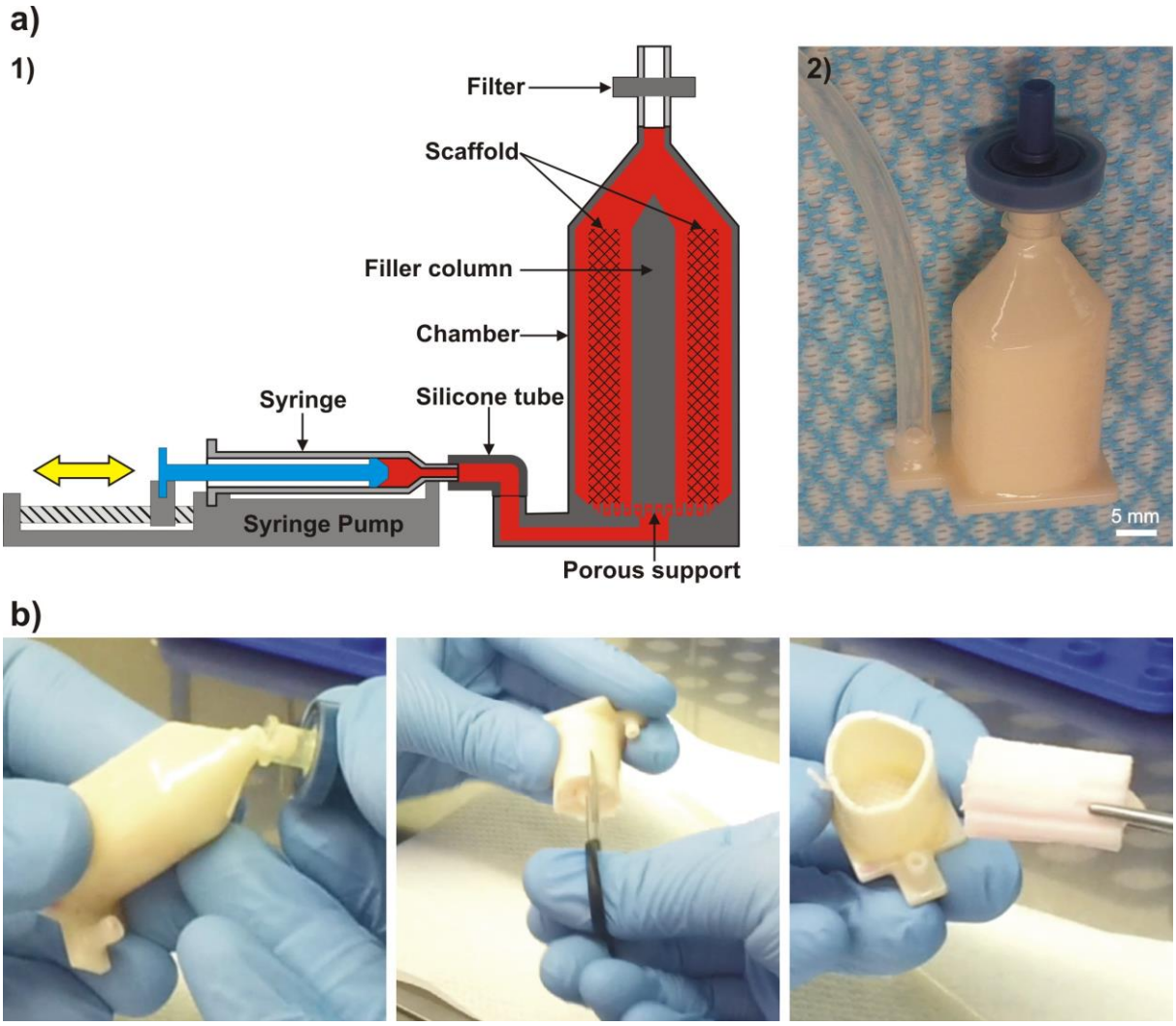

Figure 4.3 – a) Structure of the cell culture apparatus. a1) Schematic representation of the device being bidirectionally perfused with culture medium using a syringe mounted onto a syringe pump. a2) Device with upper inlet capped with a syringe filter for preserving sterility and for gas exchange. A silicone tube is connected to the lower inlet/outlet for bidirectional circulation of culture medium. b) Procedure for retrieving the construct from the culture device by manually breaking and cutting with the aid of sterile scissors and tweezers.

cells were well distributed throughout the length of the scaffold, and also on the outer and inner portions of the architecture confirming that appropriate *in vitro* culture conditions were achieved. The MTT staining observations were corroborated by SEM analysis (Figure 4.4b) which showed homogeneous cell distribution and intimate attachment onto the scaffold. Also it was observed that the cells were covering the polymer struts of the scaffold, although this was more pronounced at 6 weeks post-seeding. In some cases cells were capable of spanning the nearby struts as shown in Figure 4.4b. FDA/PI staining and confocal laser scanning microscopy confirmed the homogeneity of the cell distribution while assessing their viability (Figure 4.4c) despite the technical challenges encountered

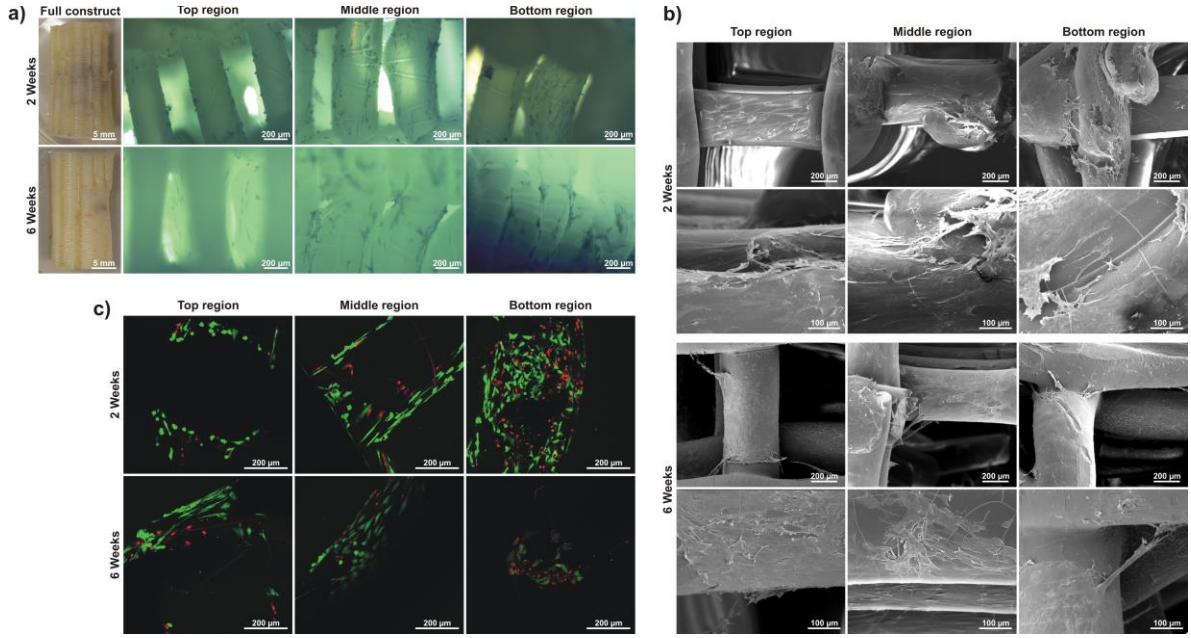

Figure 4.4 – a) MTT staining of human osteoblast-cultured scaffolds at 2 and 6 weeks culture timepoints. b) Scanning electron micrographs of human osteoblast-cultured scaffolds at 2 and 6 weeks culture timepoints. c) FDA/PI viability staining of human osteoblast-cultured scaffolds at 2 and 6 weeks culture timepoints showing viable cells in green and dead cells in red.

when imaging large dimension samples. Therefore, the scaffolds were divided in three zones - top, middle and bottom region - similarly to what was performed in the rest of this study. This revealed that, despite the presence of some dead cells (stained in red), the vast majority of the cells were alive (green). No significant difference in cell viability was observed when semi-quantitatively comparing the various sites of the construct. Although a slight increase in dead cells at the bottom region was observed, it did not reach statistical significance. The percentage of living cells at 2 and 6 weeks was 70% ± 10 and 74% ± 18 respectively (Table 4.1). These results demonstrate that nutrients were able to homogeneously diffuse throughout the entire construct, resulting in an even distribution of viable cells in the scaffold and validating the fluid flow model predicting a homogenous flow pattern inside the device.

Table 4.1 - Statistical analysis of percentage of live cellular content in cultured samples.

	2 Weeks	6 Weeks
Percentage of live cells (%)	70.15 ± 10.14	74.29 ± 18.45

4. Conclusions

In this study, we have developed a unique concept based on additive manufacturing for the integrated and simultaneous manufacturing of anatomically shaped scaffolds and customized bioreactor chambers. As a proof of concept, a tailor-made critical size bone tissue substitute was generated by manufacturing a scaffold mimicking the shape of a sheep tibia section into which osteoblasts were seeded and cultured. We foresee that this innovative concept will represent a significant advancement in further implementing the currently available biofabrication toolbox towards the development of automated customisation of tissue engineered products.

5. Acknowledgements

This work was supported by the NHMRC, the Australian Research Council. Pedro Costa acknowledges the Portuguese Foundation for Science and Technology for his PhD grant (SFRH/BD/62452/2009).

6. References

[1] Bates S 2010 Progress towards personalized medicine *Drug Discov. Today*. **15** 115-120.

[2] Grylls R 2003 Intricate parts from the inside out *Machine Design*. **75** 56-62.

[3] Martin I, Wendt D and Heberer M 2004 The role of bioreactors in tissue engineering *Trends Biotechnol*. **22** 80-86.

[4] Bancroft G N, Sikavitsas V I and Mikos A G 2003 Design of a flow perfusion bioreactor system for bone tissue-engineering applications *Tissue Eng*. **9** 549-554.

[5] Wendt D, Marsano A, Jakob M, Heberer M and Martin I 2003 Oscillating perfusion of cell suspensions through three-dimensional scaffolds enhances cell seeding efficiency and uniformity *Biotechnol. Bioeng*. **84** 205-214.

[6] Costa P F, Martins A, Neves N M, Gomes M E and Reis R L 2009 Multichamber bioreactor with bidirectional perfusion integrated in culture system for tissue engineering strategies: European Patent Application 09009863.

[7] Orr D E and Burg K J L 2008 Design of a modular bioreactor to incorporate both perfusion flow and hydrostatic compression for tissue engineering applications *Ann. Biomed. Eng*. **36** 1228-1241.

[8] Schulz R M, Wuestneck N, van Donkelaar C C, Shelton J C and Bader A 2008 Development and Validation of a Novel Bioreactor System for Load- and Perfusion-Controlled Tissue Engineering of Chondrocyte-Constructs *Biotechnol. Bioeng.* **101** 714-728.

[9] Janssen F W, Oostra J, van Oorschot A and van Blitterswijk C A 2006 A perfusion bioreactor system capable of producing clinically relevant volumes of tissue-engineered bone: In vivo bone formation showing proof of concept *Biomaterials*. **27** 315-323.

[10] Grayson W L, Frohlich M, Yeager K, Bhumiratana S, Chan M E, Cannizzaro C, Wan L Q, Liu X S, Guo X E and Vunjak-Novakovic G 2010 Engineering anatomically shaped human bone grafts *P. Natl. Acad. Sci. USA*. **107** 3299-3304.

[11] Goncalves A, Costa P, Rodrigues M T, Dias I R, Reis R L and Gomes M E 2011 Effect of flow perfusion conditions in the chondrogenic differentiation of bone marrow stromal cells cultured onto starch based biodegradable scaffolds *Acta Biomater*. **7** 1644-1652.

[12] Bancroft G N, Sikavitsast V I, van den Dolder J, Sheffield T L, Ambrose C G, Jansen J A and Mikos A G 2002 Fluid flow increases mineralized matrix deposition in 3D perfusion culture of marrow stromal osteloblasts in a dose-dependent manner *P. Natl. Acad. Sci. USA*. **99** 12600-12605.

[13] Cartmell S H, Porter B D, Garcia A J and Guldberg R E 2003 Effects of medium perfusion rate on cell-seeded three-dimensional bone constructs in vitro *Tissue Eng*. **9** 1197-1203.

[14] Goldstein A S, Juarez T M, Helmke C D, Gustin M C and Mikos A G 2001 Effect of convection on osteoblastic cell growth and function in biodegradable polymer foam scaffolds *Biomaterials*. **22** 1279-1288.

[15] Grayson W L, Bhumiratana S, Cannizzaro C, Chao P H G, Lennon D P, Caplan A I and Vunjak-Novakovic G 2008 Effects of Initial Seeding Density and Fluid Perfusion Rate on Formation of Tissue-Engineered Bone *Tissue Eng. Pt. A*. **14** 1809-1820.

[16] Meinel L, Karageorgiou V, Fajardo R, Snyder B, Shinde-Patil V, Zichner L, Kaplan D, Langer R and Vunjak-Novakovic G 2004 Bone tissue engineering using human mesenchymal stem cells: Effects of scaffold material and medium flow *Ann. Biomed. Eng*. **32** 112-122.

[17] Sikavitsas V I, Bancroft G N, Holtorf H L, Jansen J A and Mikos A G 2003 Mineralized matrix deposition by marrow stromal osteoblasts in 3D perfusion culture increases with increasing fluid shear forces *P. Natl. Acad. Sci. USA*. **100** 14683-14688.

[18] Hidalgo-Bastida L A, Thirunavukkarasu S, Griffiths S, Cartmell S H and Naire S 2012 Modeling and design of optimal flow perfusion bioreactors for tissue engineering applications *Biotechnol. Bioeng*. **109** 1095-1099.

[19] Alvarez-Barreto J F, Linehan S M, Shambaugh R L and Sikavitsas V I 2007 Flow perfusion improves seeding of tissue engineering scaffolds with different architectures *Ann. Biomed. Eng*. **35** 429-442.

[20] Scherberich A, Galli R, Jaquiery C, Farhadi J and Martin I 2007 Three-dimensional perfusion culture of human adipose tissue-derived endothelial and osteoblastic progenitors generates osteogenic constructs with intrinsic vascularization capacity *Stem Cells*. **25** 1823-1829.

[21] Galantucci L M, Lavecchia F and Percoco G 2009 Experimental study aiming to enhance the surface finish of fused deposition modeled parts *Cirp. Ann-Manuf. Techn*. **58** 189-192.

[22] Galantucci L M, Lavecchia F and Percoco G 2010 Quantitative analysis of a chemical treatment to reduce roughness of parts fabricated using fused deposition modeling *Cirp. Ann-Manuf. Techn*. **59** 247-250.

[23] Yang J, Wan Y Q, Tu C F, Cai Q, Bei J Z and Wang S G 2003 Enhancing the cell affinity of macroporous poly(L-lactide) cell scaffold by a convenient surface modification method *Polym. Int*. **52** 1892-1899.

[24] Kokubo T, Kushitani H, Sakka S, Kitsugi T and Yamamuro T 1990 Solutions Able to Reproduce Invivo Surface-Structure Changes in Bioactive Glass-Ceramic a-W3 *J. Biomed. Mater. Res*. **24** 721-734.

[25] Kokubo T, Ito S, Huang Z T, Hayashi T, Sakka S, Kitsugi T and Yamamuro T 1990 Ca, P-rich layer formed on high-strength bioactive glass-ceramic A-W *J. Biomed. Mater. Res*. **24** 331-343.

[26] Vaquette C, Ivanovski S, Hamlet S M and Hutmacher D W 2013 Effect of culture conditions and calcium phosphate coating on ectopic bone formation *Biomaterials*. **34** 5538-5551.

[27] Reichert J C, Wullschleger M E, Cipitria A, Lienau J, Cheng T K, Schutz M A, Duda G N, Noth U, Eulert J and Hutmacher D W 2011 Custom-made composite scaffolds for segmental defect repair in long bones *Int. Orthop*. **35** 1229-1236.

Chapter 5

Additive manufacturing for high throughput screening of 3D tissue engineered constructs in dynamic culture

Abstract

The utilisation of high throughput screening (HTS), in a pharmaceutical, toxicity on top of a tissue engineering and regenerative medicine context, relies on the ability to test large arrays of cell and biomaterial combinations in 3D environments. Here, we report on the development of a highly versatile and up-scalable method based on additive manufacturing for the fabrication of arrays of scaffolds enclosed in individualised perfusion chambers. This technique allowed the simultaneous in vitro culture of 96 scaffolds under controlled bi-directional perfusion. The methodology developed in this work exemplifies the applicability of additive manufacturing as a tool for achieving further automation of HTS in the field of biomedical science and biotechnology.

This chapter is based on the following publication:

Costa P.F., Hutmacher D.W., Theodoropoulos C., Gomes M.E., Reis R.L., Vaquette C., 2013, Additive manufacturing for high throughput screening of 3D tissue engineered constructs in dynamic culture, *Nature Materials*, Submitted.

1. Introduction

Tissue engineering is based on the combination of cells and three-dimensional (3D) porous scaffolds to facilitate the replacement and regeneration of damaged tissues.[1] As such, scaffolds should enable both the maintenance of sufficient oxygen diffusion and nutrient supply *in vitro,* and provide mechanical support and space maintenance to allow the formation of new tissue and appropriate vascularisation *in vivo*. Further, these scaffolds with a tailored composition/architecture when combined with cells of interest and any necessary biochemical and physical cues, are essential for the successful development of tissue-engineered constructs (TEC) with desirable *in vivo* properties[2, 3]. This is generally achieved through an extensive and time consuming optimisation process.

High throughput screening (HTS) enables a large number of optimisation tests under automated and highly controlled conditions to be conducted simultaneously. This methodology is widely utilised for screening compounds for drug discovery purposes [4] and has been also proposed for screening three-dimensional structures for tissue engineering applications.[5-11] However in the majority of existing HTS devices, several drawbacks remain when screening biomaterials and more specifically 3D scaffolds. One of the main limitations is the mostly two-dimensional nature of the protocols utilised for investigating cellular response and behaviour, which may not necessarily be relevant in 3D environments.[12-15] Fluid diffusion and associated nutrient and oxygen supply within a given construct along with cell-material and cell-cell interactions are also crucial parameters, which greatly influence *in vitro* cellular maturation. These aspects are particularly critical when considering the use of large dimension constructs close to that required in the target application and when the cell culture is performed statically, as is the case in the vast majority of HTS devices. Flow perfusion bioreactors are traditionally utilised to circumvent these aforementioned issues in scaffolds with significantly larger dimensions. Perfusion improves nutrient supply and distribution and therefore avoids cell death in the most central regions of the scaffolds.[16-28] However, the lack of versatility in current perfusion bioreactor systems does not permit user-friendly design modifications such as incorporating additional culturing chambers and the flexibility in a short period of time to utilise scaffolds of various sizes. In some flow perfusion bioreactors, sub-optimal fluid flow distribution allows media to flow around the scaffold but does not necessarily perfuse though the construct when the scaffold dimension is significantly different to that of the bioreactor chamber.[25] These design limitations greatly impede the fabrication and testing of large arrays of scaffolds with multiple characteristics (such as architecture, dimensions, shape etc.) in a high throughput manner.

Additive manufacturing technologies such as fused deposition modelling, offer the possibility to rapidly generate arrays of porous 3D constructs with different shapes and architectures in a highly controlled and reproducible manner.[29-33] In a previous report,[34] we utilised this technology for fabricating an anatomically relevant device comprising a porous scaffold replica of an ovine tibia around which a bioreactor chamber of similar shape was simultaneously built. We hypothesised that this concept could be further utilised in HTS while circumventing the aforementioned issues associated with the use of HTS and traditional bioreactors.

As a proof of concept, a device was designed to simultaneously accommodate 8 cubical scaffolds 8 mm in width. These scaffolds were made of polylactic acid (PLA) and composed of 400 µm diameter struts spaced 1.5 mm horizontally in a 0-90 degree orientation. Fluid flow modelling was used to optimise the design of the individual culture chambers in the HTS device. The main requirements considered during this optimisation were: 1) homogeneous fluid velocities throughout the entire scaffold and 2) the elimination of any stagnant fluid regions. Homogeneous fluid distribution ensures a constant and uniform supply of nutrients and oxygen within the construct. When similar culture conditions are achieved throughout the scaffolds, high reproducibility can be achieved. To this end, a number of different configurations of the culture chamber and geometry of the top outlet (Figure 5.1) were tested.

The geometry of the top outlet was shown to significantly impact on the flow pattern as demonstrated in

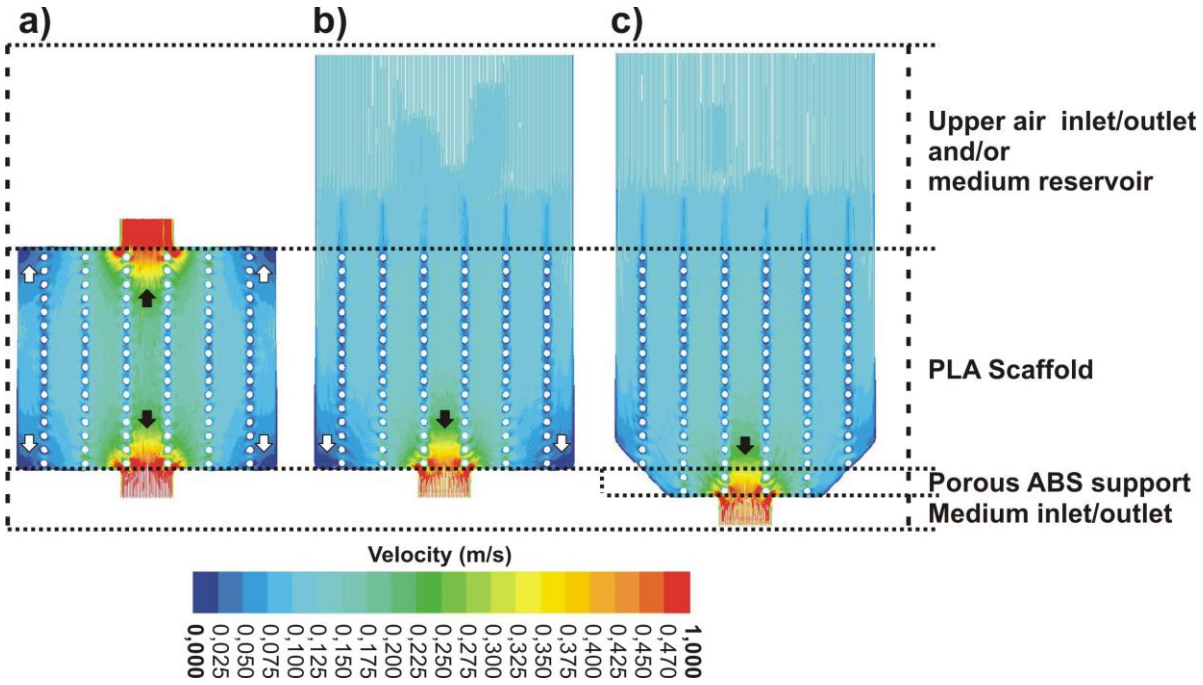

Figure 5.1- Fluid flow modelling of various device inner architectures. a) Rectangular device with narrow top outlet. b) Rectangular device with wide top outlet. c) 2mm-chamfered chamber with support structure and wide top outlet. White arrows indicate stagnant zones and black arrows indicate high velocity zones.

Figure 5.1a and b. Indeed an open outlet (Figure 5.1b) was found to significantly reduce the formation of both low and high velocity zones in the upper portion of the scaffold when compared to a closed outlet configuration (Figure 5.1a). Taking into consideration results obtained in a previous study,[35] the design of the chamber was modified to prevent the formation of regions with heterogeneous fluid velocity located at the base of the scaffold. To this end, a porous acrylonitrile butadiene styrene (ABS) structure supporting the PLA scaffold was inserted at the bottom of the chamber. This resulted in positioning the scaffold away from the high velocity regions (represented in yellow and red and highlighted by the black arrows in Figure 5.1) located in the vicinity of the inlet/outlet. The chambers were chamfered 2 mm with an angle of 45° (Figure 5.1c) to eliminate low fluid velocity regions (white arrows in Figure 5.1a-b) as our demonstrated in our previous work.[34].

This configuration combining the ABS support structure and the chamfered chambers maintained a homogeneous fluid flow velocity throughout the scaffold ranging from 10% to 15% of the initial flow rate (Figure 5.1c). At the inlet of each individual chamber, the flow rate was 0.1 mL/min and therefore the flow rate in the scaffold ranged from 0.01-0.015 mL/min (Figure 5.1c), which is in agreement with optimal flow rates reported in other studies.[16, 36]

This optimised design of an individual bioreactor chamber was then utilised to fabricate the HTS device. 3Ds Max software was used to design a multi-chamber device which could simultaneously accommodate 8 scaffolds (Figure 5.2a). Figure 5.2a shows the different elements utilised to create the numerical 3D model. The base of the device integrated a network of 1 mm wide fluidic channels connecting each of the eight culture chambers to one single medium inlet/outlet (Figure 5.2a1-5.2a2). Based on the fluid flow modelling analysis, the bottom of each chamber was chamfered by 2 mm along an angle of 45° (Figure 5.2a2) onto which a 1 mm thick porous ABS structure (Figure 5.2a3) was added to support the PLA scaffold represented in green in Figure 5.2a4. Each scaffold was surrounded by a 10 mm wide square chamber with 1mm thick walls and positioned at a distance of 1mm from the sides of the scaffolds (Figure 5.2a5). This chamber was 18 mm high to create a reservoir for the subsequent cell culture as shown in Figure 5.2a6. Two pyramidal structures were then placed over each group of 4 chambers to fully enclose the device. The final model of the device (Figure 5.2a7) was saved as an STL file, converted to G-Code using RepRap and ReplicatorG software and finally prototyped in a Makerbot dual extrusion fused deposition prototyping machine (Figure 5.2b1 and 5.2b2) (Supplementary Video 1). The time necessary for fabricating each device was 40 minutes.

As some open porosity remained within the bioreactor chamber, surface treatment with an ABS solution was used in order to close these pores ensuring that no leaking would occur during the subsequent cell

culture. As a result of this treatment, the outer surfaces of the device became smoother and glossier (Figure 5.2b5 and 5.2b6) than non-treated surfaces (Figure 5.2b3 and 5.2b4) due to the elimination of the roughness and the interlayer gaps. A more detailed analysis was performed using micro-CT which confirmed that most of the porosity initially contained in the bioreactor walls was either fully closed or removed by the ABS treatment (Supplementary Figure 5.1a1). This analysis also demonstrated that the inner walls and the scaffolds were not affected by the ABS/acetone treatment (Supplementary Figure 5.1a2-5.1a4) as shown by the presence of the original interlayer gaps.

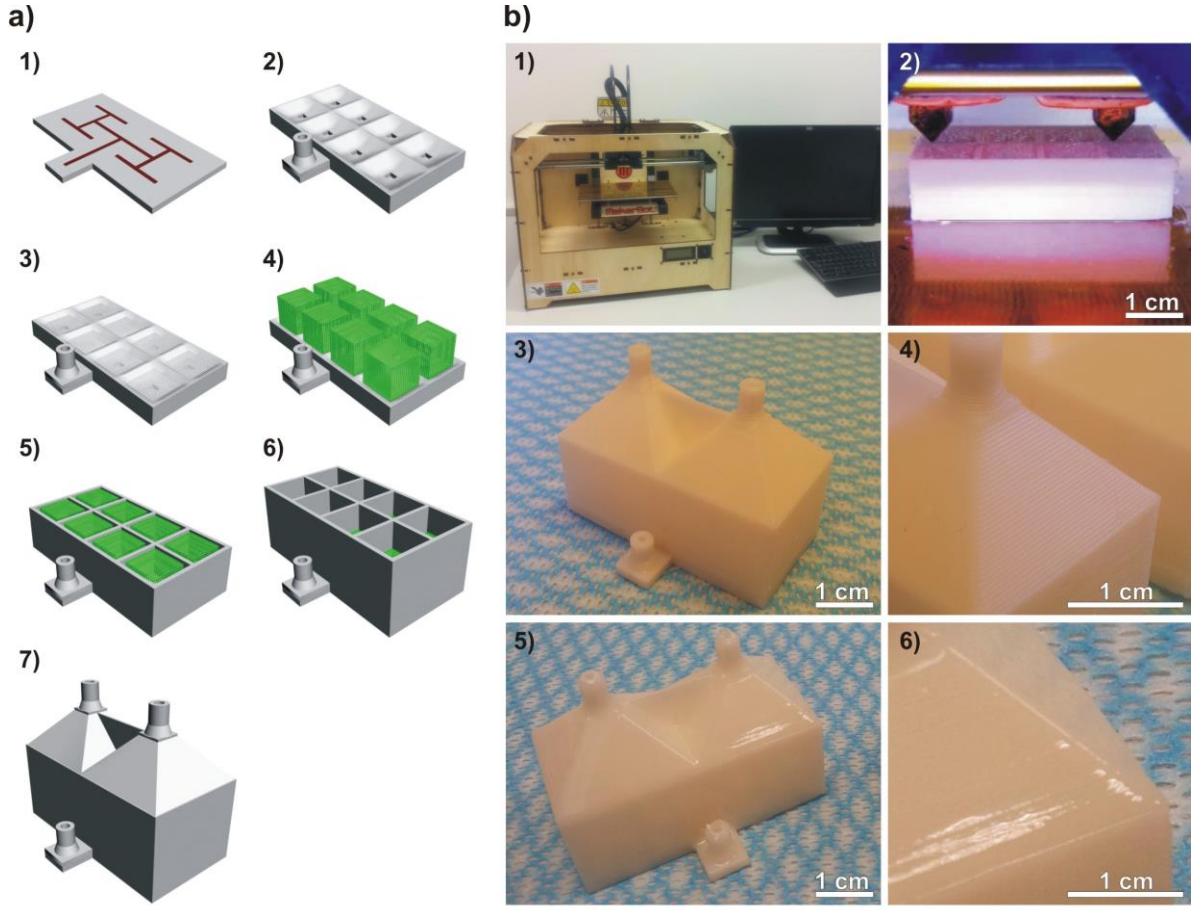

Figure 5.2- a) Elements of the device to be prototyped. a1) Base of the device consisting of a lower plate designed with a mini channel network for supplying culture medium (red) to the eight culture chambers. a2) The channel network is covered by a perforated layer which defines the chamfered bottom of the culture chambers as well as a lateral inlet/outlet. a3) Porous support structures positioned over the chamber bottoms. a4) Scaffolds positioned over the porous support structures on the bottom of each culture chamber. a5) Walls designed around and in between the scaffolds. a6) Walls extended upwards in order to create an upper reservoir over the scaffolds. a7) Two covers designed on the top part of the device to enclose the culture chambers. The top of each cover possesses an inlet/outlet for air circulation. b) Fabrication and post-treatment of device. b1) Dual extrusion prototyping machine. b2) Close-up view of device being fabricated in the prototyping machine by dual extrusion of ABS (left extruder) and PLA (right extruder). b3-b4) Device after rapid-prototyping. b5-b6) Device after post-treatment with ABS/acetone solution.

The ability to fabricate high throughput culture devices directly from numerically designed 3D models by additive manufacturing offers significant advantages: it reduces costs and human intervention in the fabrication process, while permitting a high degree of control over the size and the architecture of the scaffolds. Generally, the fabrication of high throughput culture devices involves the utilisation of highly specific technologies and equipment such as clean room facilities, spin coaters, mask aligners or micro-moulding and laser ablation machines [37, 38] which are not necessarily commonly available in a research laboratory and moreover, not as economically viable as additive manufacturing. Furthermore, inherent limitations of these fabrication technologies, such as the need to fabricate one or multiple master moulds, result in a time consuming, expensive and largely manual manufacturing process.

HTS devices manufactured in such a way have indeed been employed [20, 37] in order to culture simple-shaped cylindrical scaffolds albeit of smaller dimensions than those developed in the present study. Unlike conventional HTS where insights are mainly provided at a cellular and hence microscopic level, the HTS device developed in this study shows the ability to provide further knowledge at a more macroscopic / tissue level, hence enabling more clinically realistic *in vitro* assessment. Further, a broad range of materials can be utilised for fabricating scaffolds and therefore contribute to the development of a scaffold materials library. The polymer melt-based deposition process permits the fabrication of objects from a wide array of materials such as aliphatic polyesters, polyurethane, etc.

To further demonstrate the versatility of our strategy, the PLA scaffolds were coated with a calcium phosphate layer by successively filling the individual culture chambers with NaOH and simulated body fluid (SBF). Treatment with NaOH increases the hydrophilicity of the scaffold by increasing roughness (as shown by the micro-porosity in Supplementary Figure 5.1b1-5.1b2) and is also known to increase the density of carboxylic acid on the surface of the polymeric struts, which has a significant impact on cell adhesion.[39, 40] The SBF treatment resulted in the deposition of biomimetic calcium phosphate crystals. However this deposition was not entirely homogenous as agglomerations of CaP spherical particles were found in many locations of the scaffold as shown in Supplementary Figure 5.1b3-5.1b4, unlike what was reported in another study utilising a perfusion system for coating scaffolds of similar architecture.[41] The heterogeneity in the CaP coating probably comes from the relatively short exposition time and the reduced volume of SBF solution utilised, which did not enable the formation of a continuous CaP layer. The NaOH post-treatment was performed to obtain a single phase of CaP as a previous study, although performed on a different scaffold, demonstrated that a highly soluble CaP phase (brushite) was removed by the gentle etching, leaving a unique carbonate hydroxylapatite

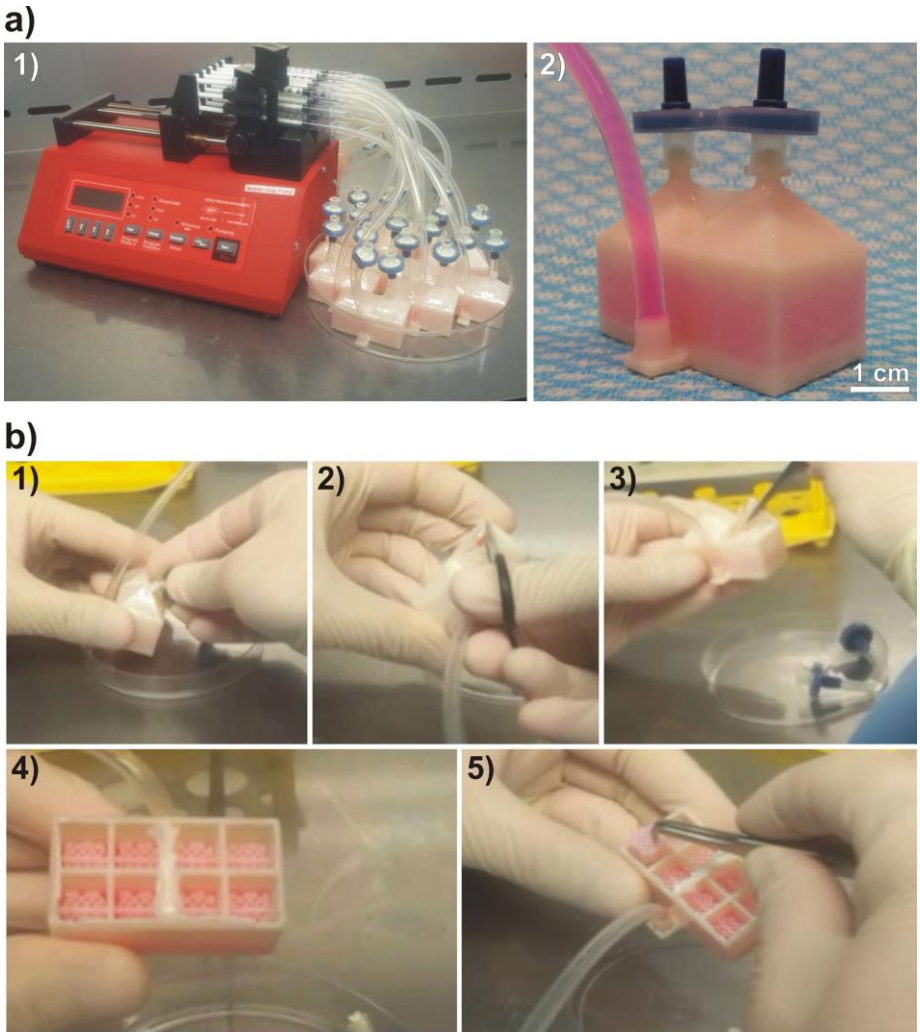

Figure 5.3- a) Culture system apparatus. a1) multiple culture devices connected to one single syringe pump for bi-directional perfusion. a2) device being perfused with culture medium through silicone tubing connected to the lower medium inlet/outlet and with upper air inlets/outlets capped with filters. b) Procedure for retrieving the constructs from the culture device by manually breaking and cutting with the aid of sterile scissors and tweezers.

layer.[42] These two treatments (NaOH etching and CaP coating) demonstrate that our device also enables the screening of functionalised scaffolds.

Another important aspect of the technology we have developed is that it enables the *in vitro* culture of the scaffold under bi-directional perfusion. The perfusion apparatus was assembled by connecting a syringe to the bottom inlet/outlet of each device using sterile silicone tubing. To preserve the sterility of the device, the top outlets were capped with sterile 0.22 μm filters (Figure 5.3a2). Each silicone tube was then connected to an individual syringe placed onto a multi-syringe adapter (Figure 5.3a1) which was mounted into one single syringe pump. The devices were then filled with culture medium and the scaffolds incubated overnight to enable protein adsorption. The following day, cell suspensions were injected into the devices through the silicone tubing and bi-directionally perfused to allow homogeneous

cell seeding (Supplementary Video 2). Scaffolds were collected after 24 hours, 2 weeks and 4 weeks of culture using sterile scissors and tweezers according to the method shown in Figure 5.3b and Supplementary Video 3.

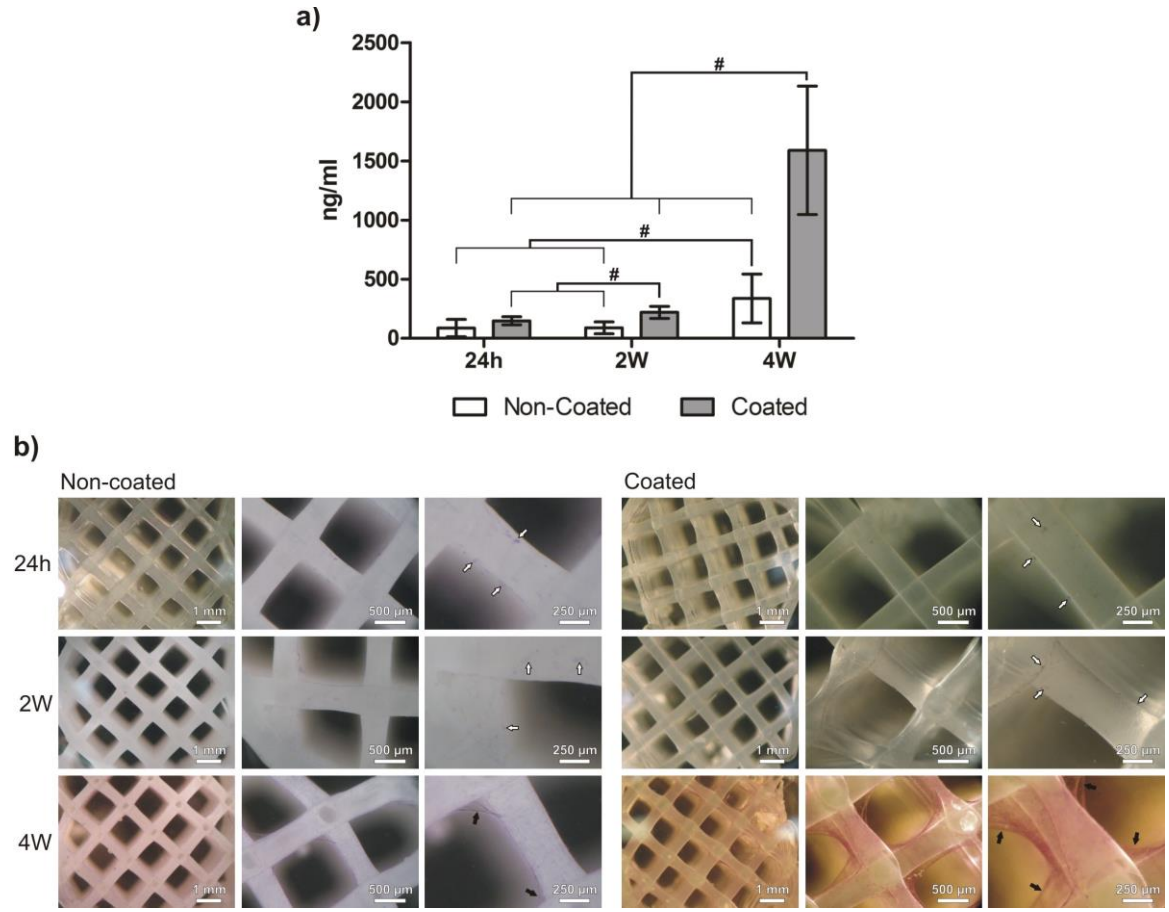

Figure 5.4- a) DNA content in non-coated and CaP-coated scaffolds after 24 hours, 2 weeks and 4 weeks of culture. # shows statistically different values ($p<0.05$). b) MTT staining of coated and non-coated samples seeded with osteoblasts after 24 hours, 2 weeks and 4 weeks of culture. At the 4 weeks time-point non-coated scaffolds struts were covered by a dense layer of single cells while CaP-coated scaffolds were covered by thick sheets of cells. White arrows indicate isolated adhered cells while black arrows indicate cellular bridging between struts.

DNA quantification revealed that the device supported cell adhesion and proliferation in all types of scaffold as shown in Figure 5.4a although these parameters were significantly higher in the CaP-coated specimens. Indeed, the DNA content increased 4-fold for the non-coated samples between 24 hours and 4 weeks post-seeding, whereas it increased 11-fold for the CaP coated specimens within the same time period. This finding is supported by several studies which reported a significant increase in the cell proliferation on CaP coated scaffolds. [43, 44] This is explained by the release of Ca^{2+} ions into the culture media from the CaP coating which stimulates cell growth. The scaffolds were stained with MTT to assess the cell distribution within the scaffold. Despite low staining efficacy, at the earliest time points

metabolically active cells had homogeneously infiltrated the scaffolds regardless of the surface treatment (coated and non-coated) as shown in Figure 5.4b. This shows that the chamber design was effective in homogeneously distributing the cells (highlighted by white arrows) throughout the scaffold and hence validates the fluid flow simulation analysis.

After 4 weeks of culture, the struts of non-coated scaffolds were covered by a dense layer of single cells while CaP-coated scaffolds were covered by thick sheets of cells (in red) bridging multiple struts (highlighted by black arrows in Figure 5.4b). SEM microscopy confirmed the homogeneous cell distribution in both types of scaffolds and also showed that the cells gradually covered the polymeric struts and were capable of bridging adjacent struts and partially filling the pores of the scaffold at 4 weeks post-seeding as shown in Figure 5.5.

The distribution and viability of cells in several locations of the scaffolds was also assessed by FDA/PI-staining and confocal laser microscopy (Figure 5.5). Despite the presence of some dead cells (red) the great majority of cells were alive (green) at the 4 weeks culture period showing that sufficient nutrient supply was provided throughout the entire scaffold. This was further shown in the semi-quantitative analysis in which both coated and non-coated samples displayed a percentage of live cells above 85% at the 4 weeks culture period (Table 5.1).

Table 5.1- Statistical analysis of percentage of live cellular content in CaP-coated and non-coated constructs after 24 hours, 2 weeks and 4 weeks of culture.

Culture period	Non-coated	Coated
24 hours	97.53 ± 4.28	93.64 ± 9.88
2 weeks	95.44 ± 6.34	96.80 ± 2.00
4 weeks	85.67 ± 8.22	94.73 ± 3.69

The present study demonstrates that additive manufacturing can be applied to the fabrication of complex cell culture devices for screening large three-dimensional tissue engineered constructs in a high throughput manner under highly controlled conditions. As design and testing is performed at the numerical level and then carried out by the same single automated equipment, the integration of additive manufacturing in high throughput screening demonstrates the advantage of generating arrays of three-dimensional scaffolds in a highly reproducible manner while also facilitating possible design modifications (scaffold number, dimension and architecture). The highly three-dimensional nature of the device represents a significant advancement in the field as most HTS systems tend to have reduced three-dimensionality and/or *in vitro* cell culture is performed under static conditions.[45-47] Also the

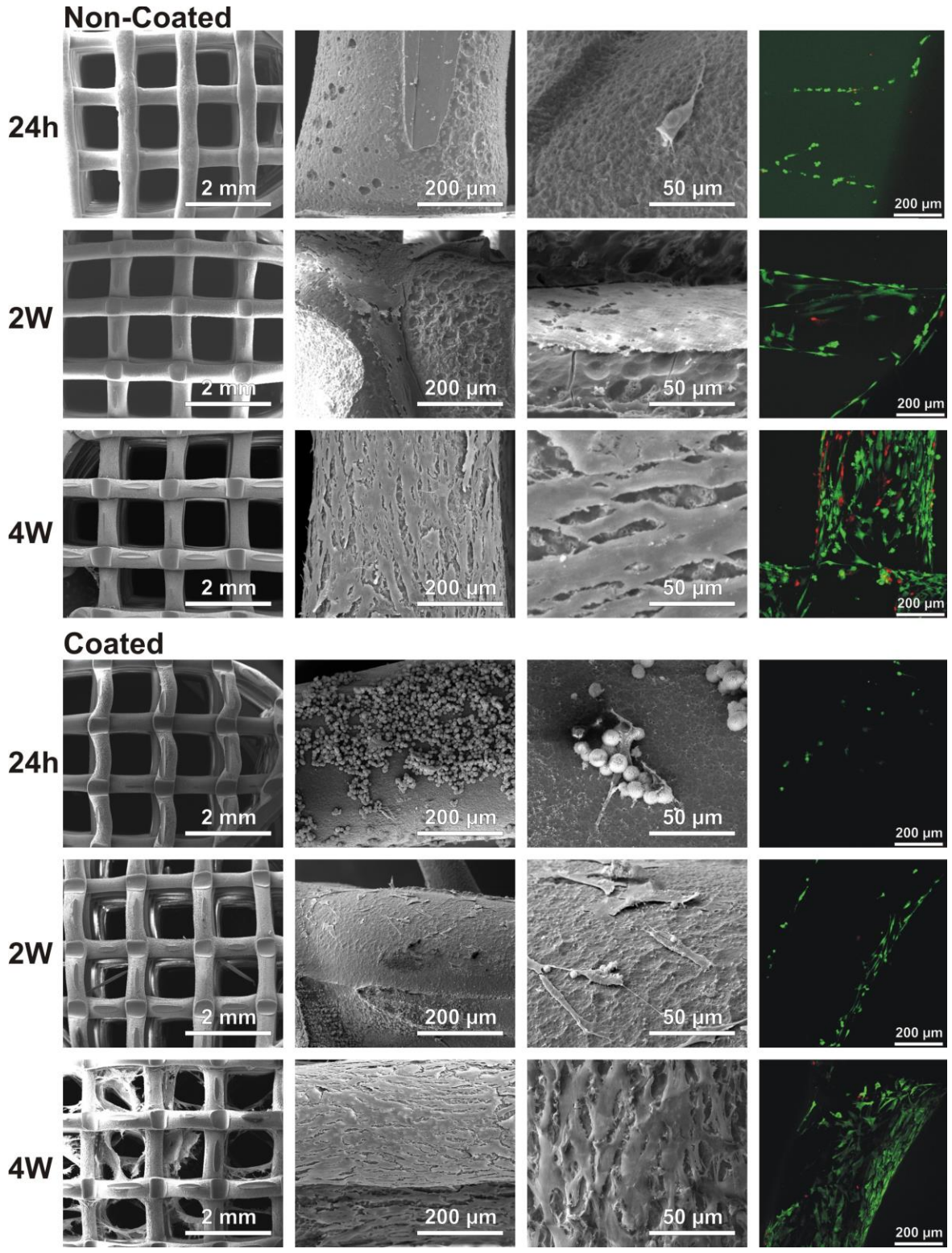

Figure 5.5- SEM and confocal microscopy (right column) micrographs of non-coated and CaP-coated scaffolds seeded with osteoblasts after 24 hours, 2 weeks and 4 weeks of culture. Samples observed through confocal microscopy were stained with FDA/PI showing live cells in green and dead cells in red.

automation of the scaffold fabrication along with the bidirectional perfusion enables the systematic assessment of the performance in a more standardised and highly controlled manner and at an effective cost and speed. It also reduces variations inherent to manual cell culture, such as differences in manual cell seeding efficacy, potential contamination due to frequent media change, as well as variability in volume of media utilised which can affect oxygen diffusion and therefore result in disparities within samples. Moreover, most bioreactors can test only a few samples at any one time and therefore systematic assessments involving large number of specimens are highly time consuming and labour-intensive.[48, 49] This is in contrast to the technology proposed in the present study which is unprecedented in the literature as it was capable of testing a large number of large 3D samples under bidirectional perfusion. Indeed, even in a simplified 4 by 2 configuration, 96 three-dimensional scaffolds contained in 12 separated culture devices were simultaneously cultured demonstrating the high throughput ability. This utilisation of additive manufacturing provides a new tool for allowing a higher level of automation of HTS in tissue engineering under three-dimensional and highly controlled dynamic environments.

2. Experimental

2.1. Design and fabrication concept

Devices targeting HTS applications are required to contain multiple samples for simultaneous testing and handling. This is usually achieved by using versatile test platforms and by process automation. The device utilised in this study was designed to be modular and to allow for up-scaling according to the number of scaffolds required. As a proof of concept, a device was designed to simultaneously accommodate 8 cubical scaffolds (8 mm width) composed of 400 µm diameter struts 1.5 mm horizontally spaced in a 0-90 degree orientation. Device design was performed in 3Ds Max (Autodesk, USA) software and consisted of building individualised bioreactor chambers by placing 1 mm thick walls around each of the 8 scaffolds, which were organised in a rectangular 2 by 4 configuration. The walls were positioned 1 mm from the scaffolds and were 10 mm taller than the scaffolds in order to create a reservoir for the culture medium. The top of every 4 chambers (in a square configuration) was covered by a pyramidal structure ending in a 2 mm diameter outlet used for attaching sterile filters during subsequent cell culture. A symmetrical mini-fluidic channel network connected to a 2mm diameter inlet/outlet was designed for homogenously distributing the culture medium through the various individual chambers.

2.2. Fluid flow modelling

Computational fluid dynamics was used to simulate the flow pattern of the media in various device architectures. The studied architectures differed in two main aspects: the use of either rectangular or chamfered chamber bottom corners and the use of either wide or narrow top inlets/outlets. Given the high complexity of the device, a simplified model consisting of two-dimensional sections was first created in Design Modeler 13.0 software (Ansys, USA). The profile corresponding to the section of an 8 mm wide cubic porous scaffold surrounded by a 10 mm wide bioreactor chamber was considered. The thickness of the simplified section was 0.1 mm and the maximum face size of the generated model mesh was 0.2 µm. The fluid flow velocity profiles were calculated using Fluent 13.0 software within Ansys Workbench 13.0 platform (Ansys, USA). The pressure at the device's outlets was assumed to be zero and the scaffold and the bioreactor chamber were considered rigid and impermeable. We assumed that the viscosity and the density of the culture media at 37°C were $\eta = 1.45.10^{-3}$ Pa.s) and ($\rho = 1000$ kg.m^{-3}) respectively.

2.3. Conversion, slicing and prototyping of 3D models

The device design displaying the most homogenous fluid flow pattern was selected for further experiments. The device's 3D model was then sliced and converted to a G-Code file. The volumes corresponding to the 8 cubes to be converted to porous scaffolds were processed using the open source software Reprap (Online Reprap Community). The cubes were sliced into 0.27 mm layers composed of deposition path lines with a spacing of 1.5 mm. On the other hand, the volume corresponding to the outer shell device was sliced and converted to G-Code files by using the open source software ReplicatorG (Online ReplicatorG Community). The conversion was performed using 2 shells, a slice thickness of 0.27 mm, an object infill of 100%, a feed rate of 20 mm/s and a travel feed rate of 55 mm/s as parameters. The G-Codes generated through RepRap and ReplicatorG were then merged together in order to generate one single G-Code file. The prototyping of the devices was performed using an open source dual extrusion rapid prototyping machine (Replicator, Makerbot Industries, USA). The materials used were poly(lactic) acid (PLA) Ingeo 4043D (NatureWorks LLC, USA) for the porous scaffolds and acrylonitrile butadiene styrene (ABS) (Makerbot industries, USA) for the bioreactor chamber. The temperature used for fusing both materials in their corresponding nozzles was 220°C. Both materials were deposited through coordinated and alternated operation of the nozzles.

2.4. Bioreactor surface treatment

In order to ensure that fluid leakage could not occur during subsequent cell culture, a post-treatment coating of ABS was applied to the outer bioreactor wall surfaces to close any remaining porosity. In brief, after capping all inlets/outlets, the devices were immersed for 2 seconds in an ABS/acetone 60 mg/mL solution and then air-dried at room temperature for 30 min. This procedure was performed twice. Finally, the devices were washed in distilled water to remove residual solvent.

2.5. Scaffold surface treatment

Given the hydrophobic nature of PLA which could hinder appropriate and homogeneous fluid perfusion through the device, alkaline etching was performed using a 2M sodium hydroxide (NaOH) solution. The devices were rinsed in 100 % ethanol under vacuum for one hour to pre-wet the scaffold fibre surfaces. After the removal of ethanol, sodium hydroxide solution was perfused through the device until the bioreactor was entirely filled. The devices were incubated for 30 minutes at room temperature under vacuum prior to a secondary incubation at 37°C for 60 minutes. Finally, the devices were washed several times with distilled water and then air-dried prior to proceeding to the deposition of a calcium phosphate biomimetic coating on the PLA filaments.

2.6. Biomimetic coating of scaffolds

The deposition of the calcium phosphate coating was performed by filling the chambers with a total of 8 mL of 10x Simulated Body Fluid (SBF) solution at pH 6 (solution preparation described elsewhere [42, 50]) for 30 min at 37°C and followed by perfusion with a 0.5 M sodium hydroxide solution for 30 min at 37°C. Finally the coated scaffolds were rinsed five times with ultrapure water and air-dried.

2.7. Micro computerised tomography analysis (Micro-CT)

The devices were analysed by Micro-CT (μCT40, SCANCO Medical AG, Brüttisellen, Switzerland) at a resolution of 12 μm, a voltage of 55 kVp and at a current of 175 μA. Three-dimensional images were reconstructed from the scans by the micro-CT system software.

2.8. *In vitro* study

The cell-seeded scaffolds were cultured up to 4 weeks under bi-directional perfusion. To this end, a 1 mL sterile syringe was connected to each device's medium inlet using sterile silicone tubing. This apparatus was mounted on a multi-syringe adapter placed on an Aladdin syringe pump (World Precision Instruments, USA). A total of 12 devices (each with a dedicated syringe) were simultaneously cultured in this system and therefore 96 scaffolds were cultured at one time. The devices were first sterilised by perfusion with 50% ethanol solution for 20 minutes and dried in a sterile hood for 2 hours. Each device was then manually filled with a total of 8 mL of basal medium and bi-directionally perfused overnight at a flow rate of 0.4 mL/min with flow inversion occurring every 100 seconds. This hydration step aimed to promote the pre-adsorption of proteins onto the scaffold and hence facilitate subsequent cell attachment. In order to ensure the sterility of the device during the culture period while still allowing gas exchange with the incubator's environment, 0.2 µm pore size filters (13 mm diameter) (Pall, USA) were connected to the outlets positioned at the top of the devices.

Primary human osteoblasts were collected from a patient undergoing hip surgery. Ethics approval for the use of human osteoblasts in this experiment was granted from The Prince Charles Hospital ethics committee (ethics clearance number: EC2310) and Queensland University of Technology ethics committee (ethics clearance number 0600000232). The osteoblasts were expanded in basal alpha MEM modified medium (Gibco, USA) supplemented with 10% fetal calf serum and 1% penicillin/streptomycin and used at passage 2. When reaching confluence, the cells were trypsinised and 250 µL cell suspensions containing $1x10^6$ osteoblasts were injected into the devices through the silicone tube connecting the devices. Since the mini-fluidic channel network diverted the fluid into eight individual chambers, each scaffold was theoretically seeded with 125,000 cells. The devices were bi-directionally perfused for 24 hours at a flow rate of 0.4 mL/min (resulting in a 0.05 mL/min flow rate per chamber) in order to allow cell attachment. The perfusion direction was automatically inverted every 100 seconds utilising an external microcontroller connected to the syringe pump.

After 24 hours, the culture medium was replaced with fresh medium and the flow rate was increased to 0.8 mL/min (0.1 mL/min/chamber) whereas the flow inversion frequency was reduced to 50 seconds. The medium was changed weekly and the scaffolds were collected for further analysis at 24 hours, 2 weeks and 4 weeks post-seeding.

The scaffold collection was performed as follows: the devices were detached from the syringe pump by

removing the silicone tubing and placed in a sterile biohazard safety cabinet. The scaffolds were retrieved from the interior of the bioreactor chambers by manually sectioning the bioreactor walls using scissors and tweezers. The collected scaffolds were processed for DNA content quantification, 3-(4,5-dimethylthiazol-2-yl)-2,5-diphenyltetrazolium bromide (MTT) staining, live/dead assay, confocal laser and scanning electron microscopy examination.

2.9. DNA content quantification

For cellular DNA content analysis, the cell-scaffold constructs were frozen at -80°C for at least 48 hours. The cell membrane and the extracellular matrix were disrupted in 300 µL of 0.5 mg/mL Proteinase K in phosphate buffered EDTA (PBE) at 37°C overnight and then transferred into 1.5 mL eppendorf tubes and further incubated for 24 hours at 60°C. 100 µL of the diluted (1/50 in PBE) lysate was aliquoted into black 96-well plates with 100 µL of PicoGreen (P11496, Invitrogen) working solution according to the manufacturer's instructions. After 5 min incubation in the dark the fluorescence (excitation 485 nm, emission 520 nm) was measured using a fluorescence plate reader. A standard curve was also constructed using known concentrations of λ DNA provided with the kit. The standards ranged from 10 ng/mL to 1 µg/mL λ DNA and were used to calculate the final DNA content of the sample.

2.10. Metabolic activity staining

Metabolically active cells were visualised by using a 1mg/mL 3-(4,5-dimethylthiazol-2-yl)-2,5-diphenyltetrazolium bromide (MTT) solution. Following retrieval, the scaffolds were washed in PBS and then immersed into MTT solution for 30 min. Images were captured by a digital camera mounted on an Eclipse TS100 microscope (Nikon, Tokyo, Japan).

2.11. Live/dead assay (FDA/PI)

Cell viability was assessed using a live/dead assay. For this purpose, the cell-scaffold constructs were washed twice in PBS, incubated for 5 min at 37°C in PBS containing 0.67 µg/mL fluorescein diacetate (FDA) and 5 µg/mL propidium iodide (PI) (both Invitrogen) and washed again in PBS. The cellularised scaffolds were then analysed using a confocal laser scanning microscope (Leica TCS SP5, Leica

Microsystems, GmbH). The excitation/emission wavelengths used for imaging the FDA and PI stainings were respectively 488/518-568 nm and 561/598-795 nm. A semi-quantitative analysis of the cellular viability was performed using ImageJ software to quantify living cells (green colour) and dead cells (red colour). At least two images from different areas of the constructs were captured and analysed for each condition/time-point.

2.12. Scanning electron microscopy

Osteoblast morphology and distribution in the scaffolds was assessed at 24 hours, 2 weeks and 4 weeks post-seeding by scanning electron microscopy. In brief, samples were fixed in 3% glutaraldehyde, washed in 0.1 M cacodylate buffer, post-fixed in 1 % osmium tetroxide in cacodylate buffer for 1 hour, prior to dehydration through sequential graded series of ethanol concentrations. Finally, samples were immersed in hexamethyldisilazane for 60 mins, air dried, mounted onto aluminium stubs and gold coated. Samples were observed on a FEI Quanta 200 Environmental SEM operating at 10 kV. Scaffolds without cells were gold coated prior to imaging.

3. Acknowledgments

This work was supported by the NHMRC, the Australian Research Council. Pedro Costa acknowledges the Portuguese Foundation for Science and Technology for his PhD grant (SFRH/BD/62452/2009).

4. Supplementary information

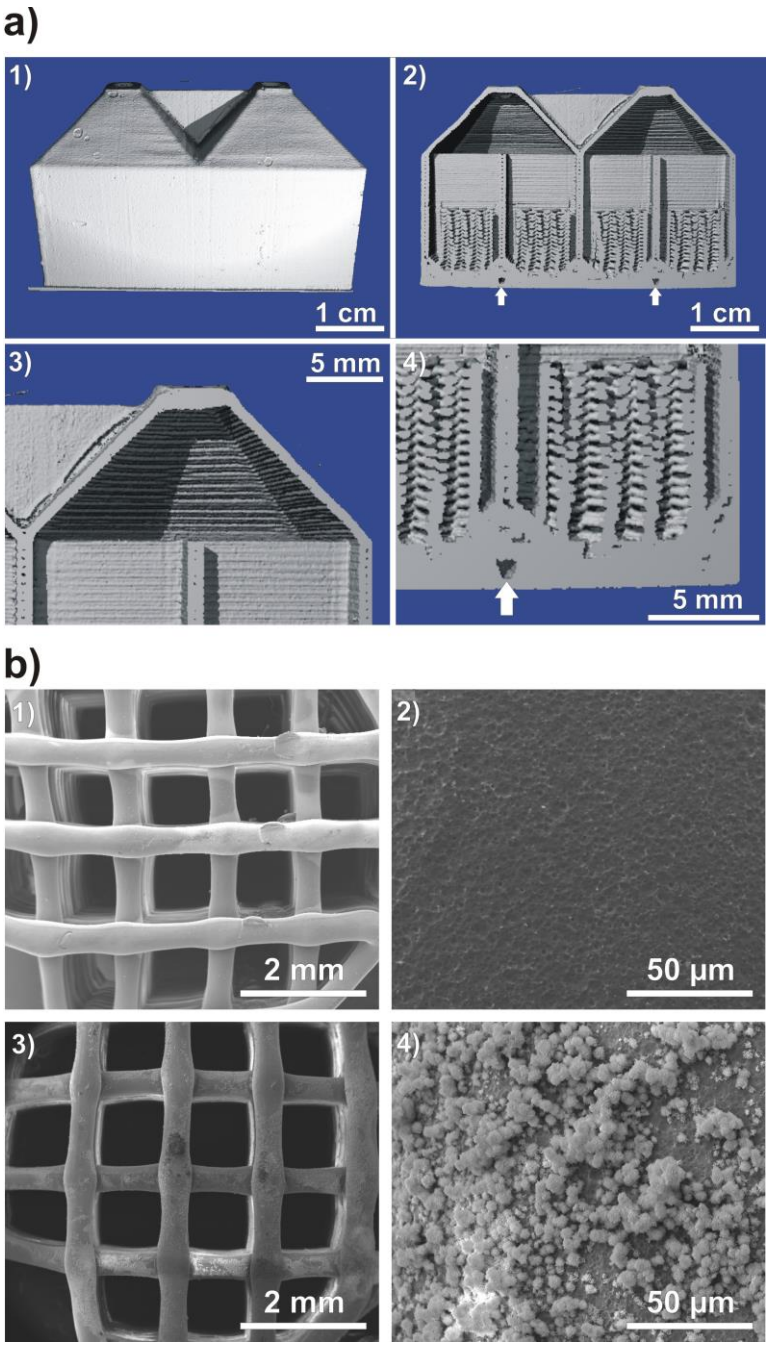

Supplementary Figure 5.1- a) Micro-CT reconstruction of device. a1) 3D reconstruction featuring the smooth ABS external wall of the device after post treatment with an ABS/acetone solution. a2) Cross-section depicting the structure of the device containing the PLA scaffolds. a3) Morphology of the inner surface of the bioreactor chamber which is characteristic of a layer-by-layer deposition suggesting that the ABS-acetone post-treatment did not affect the inner wall of the bioreactor chamber. a4) close-up view depicting scaffold architecture and the bottom part of device. Arrows indicate sections of mini-fluidic channels. b) SEM micrographs of scaffolds before (b1-b2) and after CaP coating (b3-b4).

5. References

1. Langer, R. and J.P. Vacanti, *Tissue Engineering.* Science, 1993. **260**(5110): p. 920-926.

2. Hutmacher, D.W., *Scaffold design and fabrication technologies for engineering tissues - state of the art and future perspectives.* Journal of Biomaterials Science-Polymer Edition, 2001. **12**(1): p. 107-124.

3. Martin, I., D. Wendt, and M. Heberer, *The role of bioreactors in tissue engineering.* Trends in Biotechnology, 2004. **22**(2): p. 80-86.

4. Pereira, D.A. and J.A. Williams, *Origin and evolution of high throughput screening.* British Journal of Pharmacology, 2007. **152**(1): p. 53-61.

5. Simon, C.G., et al., *Fabrication of combinatorial polymer scaffold libraries.* Review of Scientific Instruments, 2007. **78**(7).

6. Zapata, P., et al., *Quantitative high-throughput screening of osteoblast attachment, spreading, and proliferation on demixed polymer blend micropatterns.* Biomacromolecules, 2007. **8**(6): p. 1907-1917.

7. Nakajima, M., et al., *Combinatorial protein display for the cell-based screening of biomaterials that direct neural stem cell differentiation.* Biomaterials, 2007. **28**(6): p. 1048-1060.

8. Albrecht, D.R., et al., *Photo- and electropatterning of hydrogel-encapsulated living cell arrays.* Lab on a Chip, 2005. **5**(1): p. 111-118.

9. Simon, C.G., et al., *Combinatorial screening of cell proliferation on poly(D,L-lactic acid)/poly(D,L-lactic acid) blends.* Biomaterials, 2005. **26**(34): p. 6906-6915.

10. Kohn, J., *New approaches to biomaterials design.* Nature Materials, 2004. **3**(11): p. 745-747.

11. Anderson, D.G., S. Levenberg, and R. Langer, *Nanoliter-scale synthesis of arrayed biomaterials and application to human embryonic stem cells.* Nature Biotechnology, 2004. **22**(7): p. 863-866.

12. Cukierman, E., et al., *Taking cell-matrix adhesions to the third dimension.* Science, 2001. **294**(5547): p. 1708-1712.

13. Sun, T., et al., *Culture of skin cells in 3D rather than 2D improves their ability to survive exposure to cytotoxic agents.* Journal of Biotechnology, 2006. **122**(3): p. 372-381.

14. Birgersdotter, A., R. Sandberg, and I. Ernberg, *Gene expression perturbation in vitro - A growing case for three-dimensional (3D) culture systems.* Seminars in Cancer Biology, 2005. **15**(5): p. 405-412.

15. Hutmacher, D.W., *Biomaterials offer cancer research the third dimension.* Nature Materials, 2010. **9**(2): p. 90-93.

16. Goncalves, A., et al., *Effect of flow perfusion conditions in the chondrogenic differentiation of bone marrow stromal cells cultured onto starch based biodegradable scaffolds.* Acta Biomaterialia, 2011. **7**(4): p. 1644-1652.

17. Bancroft, G.N., et al., *Fluid flow increases mineralized matrix deposition in 3D perfusion culture of marrow stromal osteloblasts in a dose-dependent manner.* Proceedings of the National Academy of Sciences of the United States of America, 2002. **99**(20): p. 12600-12605.

18. Cartmell, S.H., et al., *Effects of medium perfusion rate on cell-seeded three-dimensional bone constructs in vitro.* Tissue Engineering, 2003. **9**(6): p. 1197-1203.

19. Goldstein, A.S., et al., *Effect of convection on osteoblastic cell growth and function in biodegradable polymer foam scaffolds.* Biomaterials, 2001. **22**(11): p. 1279-1288.

20. Grayson, W.L., et al., *Effects of Initial Seeding Density and Fluid Perfusion Rate on Formation of Tissue-Engineered Bone.* Tissue Engineering Part A, 2008. **14**(11): p. 1809-1820.

21. Han, Y.F., et al., *Mechanotransduction and strain amplification in osteocyte cell processes.* Proceedings of the National Academy of Sciences of the United States of America, 2004. **101**(47): p. 16689-16694.

22. Marolt, D., et al., *Bone and cartilage tissue constructs grown using human bone marrow stromal cells, silk scaffolds and rotating bioreactors.* Biomaterials, 2006. **27**(36): p. 6138-6149.

23. Meinel, L., et al., *Bone tissue engineering using human mesenchymal stem cells: Effects of scaffold material and medium flow.* Annals of Biomedical Engineering, 2004. **32**(1): p. 112-122.

24. Martin, I., T. Smith, and D. Wendt, *Bioreactor-based roadmap for the translation of tissue engineering strategies into clinical products.* Trends in Biotechnology, 2009. **27**(9): p. 495-502.

25. Sikavitsas, V.I., G.N. Bancroft, and A.G. Mikos, *Formation of three-dimensional cell/polymer constructs for bone tissue engineering in a spinner flask and a rotating wall vessel bioreactor.* Journal of Biomedical Materials Research, 2002. **62**(1): p. 136-148.

26. Sikavitsas, V.I., et al., *Mineralized matrix deposition by marrow stromal osteoblasts in 3D perfusion culture increases with increasing fluid shear forces.* Proceedings of the National Academy of Sciences of the United States of America, 2003. **100**(25): p. 14683-14688.

27. van den Dolder, J., et al., *Flow perfusion culture of marrow stromal osteoblasts in titanium fiber mesh.* Journal of Biomedical Materials Research Part A, 2003. **64A**(2): p. 235-241.

28. Frohlich, M., et al., *Bone Grafts Engineered from Human Adipose-Derived Stem Cells in Perfusion Bioreactor Culture.* Tissue Engineering Part A, 2010. **16**(1): p. 179-189.

29. Hollister, S.J., *Porous scaffold design for tissue engineering.* Nature Materials, 2005. **4**(7): p. 518-524.

30. Melchels, F.P.W., et al., *Additive manufacturing of tissues and organs.* Progress in Polymer Science, 2012. **37**(8): p. 1079-1104.

31. Hutmacher, D.W. and S. Cool, *Concepts of scaffold-based tissue engineering-the rationale to use solid free-form fabrication techniques.* Journal of Cellular and Molecular Medicine, 2007. **11**(4): p. 654-669.

32. Hutmacher, D.W., M. Sittinger, and M.V. Risbud, *Scaffold-based tissue engineering: rationale for computer-aided design and solid free-form fabrication systems.* Trends in Biotechnology, 2004. **22**(7): p. 354-362.

33. Grylls, R., *Intricate parts from the inside out.* Machine Design, 2003. **75**(17): p. 56-62.

34. Costa, P.F., et al., *Biofabrication of customized bone grafts by combination of additive manufacturing and bioreactor technologies.* Biofabrication, 2013: p. SUBMITTED.

35. Hidalgo-Bastida, L.A., et al., *Modeling and design of optimal flow perfusion bioreactors for tissue engineering applications.* Biotechnology and Bioengineering, 2012. **109**(4): p. 1095-1099.

36. Alvarez-Barreto, J.F., et al., *Flow perfusion improves seeding of tissue engineering scaffolds with different architectures.* Annals of Biomedical Engineering, 2007. **35**(3): p. 429-442.

37. Figallo, E., et al., *Micro-bioreactor array for controlling cellular microenvironments.* Lab on a Chip, 2007. **7**(6): p. 710-719.

38. Gottwald, E., et al., *A chip-based platform for the in vitro generation of tissues in three-dimensional organization.* Lab on a Chip, 2007. **7**(6): p. 777-785.

39. Yang, J., et al., *Enhancing the cell affinity of macroporous poly(L-lactide) cell scaffold by a convenient surface modification method.* Polymer International, 2003. **52**(12): p. 1892-1899.

40. Tsuji, H., T. Ishida, and N. Fukuda, *Surface hydrophilicity and enzymatic hydrolyzability of biodegradable polyesters: 1. Effects of alkaline treatment.* Polymer International, 2003. **52**(5): p. 843-852.

41. Oliveira, A.L., et al., *Nucleation and growth of biomimetic apatite layers on 3D plotted biodegradable polymeric scaffolds: Effect of static and dynamic coating conditions.* Acta Biomaterialia, 2009. **5**(5): p. 1626-1638.

42. Vaquette, C., et al., *Effect of culture conditions and calcium phosphate coating on ectopic bone formation.* Biomaterials, 2013. **34**(22): p. 5538-5551.

43. Arafat, M.T., et al., *Biomimetic composite coating on rapid prototyped scaffolds for bone tissue engineering.* Acta Biomaterialia, 2011. **7**(2): p. 809-820.

44. Araujo, J.V., et al., *Surface controlled biomimetic coating of polycaprolactone nanofiber meshes to be used as bone extracellular matrix analogues.* Journal of Biomaterials Science-Polymer Edition, 2008. **19**(10): p. 1261-1278.

45. Unadkat, H.V., et al., *An algorithm-based topographical biomaterials library to instruct cell fate.* Proceedings of the National Academy of Sciences of the United States of America, 2011. **108**(40): p. 16565-16570.

46. Lutolf, M.P., et al., *Perturbation of single hematopoietic stem cell fates in artificial niches.* Integrative Biology, 2009. **1**(1): p. 59-69.

47. Mei, Y., *Microarrayed materials for stem cells.* Materials Today, 2012. **15**(10): p. 444-452.

48. Jaasma, M.J., N.A. Plunkett, and F.J. O'Brien, *Design and validation of a dynamic flow perfusion bioreactor for use with compliant tissue engineering scaffolds.* Journal of Biotechnology, 2008. **133**(4): p. 490-496.

49. Janssen, F.W., et al., *A perfusion bioreactor system capable of producing clinically relevant volumes of tissue-engineered bone: In vivo bone formation showing proof of concept.* Biomaterials, 2006. **27**(3): p. 315-323.

50. Yang, F., J.G.C. Wolke, and J.A. Jansen, *Biomimetic calcium phosphate coating on electrospun poly (epsilon-caprolactone) scaffolds for bone tissue engineering.* Chemical Engineering Journal, 2008. **137**(1): p. 154-161.

Chapter 6

Advanced Tissue Engineering Scaffold Design for Regeneration of the Complex Hierarchical Periodontal Structure

Abstract

Aim: This study investigated the competence of an osteoinductive biphasic scaffold to simultaneously regenerate alveolar bone, periodontal ligament and cementum.

Materials and Methods: A biphasic scaffold was built by attaching a fused deposition modeled bone compartment to a melt electrospun periodontal compartment. The bone compartment was coated with a calcium phosphate layer for increasing osteoinductivity, seeded with osteoblasts and cultured *in vitro* for 6 weeks. The resulting constructs were then complemented with the placement of PDL cell sheets on the periodontal compartment, attached to a dentin block and subcutaneously implanted into rats for 8 weeks. Scanning electron microscopy, x-ray diffraction, alkaline phosphatase and DNA content quantification, confocal laser microscopy, micro computerized tomography and histological analysis were employed to evaluate the scaffold's performance.

Results: The *in vitro* study showed that alkaline phosphatase activity was significantly increased in the CaP coated samples and they also displayed enhanced mineralization. In the *in vivo* study, significantly more bone formation was observed in the coated scaffolds. Histological analysis revealed that the large pore size of the periodontal compartment permitted vascularization of the cell sheets, and periodontal attachment was achieved at the dentin interface.

Conclusions: This work demonstrates that the combination of cell sheet technology together with an osteoinductive biphasic scaffold could be utilized to address the limitations of current periodontal regeneration techniques.

This chapter is based on the following publlication:

Costa P.F., Vaquette C., Zhang Q., Reis R.L., Ivanovski S., Hutmacher D.W., 2013, Advanced tissue engineering scaffold design for regeneration of the complex hierarchical periodontal structure, *Journal of Clinical periodontology*, Accepted for Publication.

1. Introduction

Periodontal disease is a chronic inflammatory condition which, if untreated, may ultimately result in tooth loss due to the destruction of the surrounding soft and hard tissues [1]. Periodontal regeneration following surgical treatment requires the reconstitution of the complex structure of the periodontium, which includes formation of periodontal ligament fibers and their insertion into newly formed cementum on the root surface, as well as regeneration of the adjacent alveolar bone.

Guided Tissue Regeneration (GTR) [2, 3] has emerged as the most widely used regenerative procedure, and relies on the fulfillment of three main principles: wound stabilization, space maintenance and selective cell repopulation of the defect. This technique consists of the placement of an occlusive barrier membrane over the periodontal defect. By this means, cells capable of regenerating the periodontium, namely periodontal ligament cells as well as osteoblasts and their progenitors, are permitted to infiltrate the defect, while cell types unable to support regeneration, such as gingival and epithelial cells, are excluded from the regenerating periodontal defect. By selectively allowing competent cells into the defect, GTR-based therapy results in a more effective healing when compared to non-selective procedures, where a poorly or non-organized collagenous scar tissue is observed, characterized by epithelial downgrowth along the root surface which prevents the formation of periodontal attachment. However, GTR-based procedures are generally considered unpredictable given the great variability found in clinical outcomes [4]. Relying merely on the use of a barrier membrane for selectively repopulating the diseased sites, GTR is greatly constrained by the amount and quality of pre-existing or remaining healthy tissues in the vicinity of the defect. Similarly, other currently available regenerative procedures are clinically unpredictable [5], and hence there is a need for new approaches.

Various preclinical studies have shown that tissue engineering concepts incorporating the broad principles of GTR can achieve enhanced regeneration of the periodontal complex [6-9]. In these studies, several cell types, such as periodontal ligament fibroblast or mesenchymal precursor cells, were cultured *in vitro* in order to form a cell sheet which could be easily harvested with the help of a carrier. A thick cell layer was obtained by superimposing several cell sheets that were thereafter positioned onto the root surface in rat or dog models [6, 7, 10-14] or placed onto a dentin block and subcutaneously implanted in an immuno-compromised rat model [10, 13]. Despite the evidence of histologically substantiated regeneration in most cases, the handling, placement and visualization of the cell sheets was found to be difficult and resulted in a lack of biomechanical stability. Indeed, Iwata et al. suggested

that the healing process could have been hindered by significant displacement of the implanted cell sheet, which subsequently compromised the regeneration of the periodontium complex [7].

In our previous work, this issue was successfully addressed by developing a biphasic scaffold made of a Fused Deposition Modeling (FDM) scaffold (bone compartment) and a solution electrospun membrane (for the periodontal compartment) which demonstrated significant improvement in the cell sheet biomechanical stability. The enhanced stability provided by the biphasic scaffold promoted the attachment of a periodontal-like tissue onto an ectopically implanted dentine block in a rodent model [15]. Despite the good outcome for periodontal attachment formation, the bone compartment did not support sufficient bone ingrowth. Owing to the highly hierarchical architecture of the periodontal tissues, it is necessary that the regenerative events occur in a timely manner so that the ligamentous tissue can insert into the new cementum on the root surface, as well as the newly formed bone. To this end, the bone compartment requires enhancement in order to circumvent the aforementioned limitation.

In the early nineties Kokubo at al. developed a solution called Simulated Body Fluid (SBF) which was utilized for depositing a biomimetic calcium phosphate (CaP) coating on the surface of devices and implants [16, 17]. This approach has been shown to increase bone related gene expression in various cell types [18-22] and enhance ectopic bone formation in a rat model [23]. Therefore we report herein the development of a second generation of biphasic scaffolds designed to incorporate an osteoinductive bone compartment by the means of a calcium phosphate coating. We further modified the original concept design by replacing the solution electrospun membrane previously used for the periodontal compartment with a thin melt electrospun scaffold comprising larger pores adequate for improving cellular and tissue interaction, especially from a vascularization point of view. The goal of this approach was to improve the inter-connectivity between the bone and periodontal ligament compartments, ultimately guiding the perpendicular orientation of newly formed periodontal fibres between regenerated alveolar bone and root cementum. The performance of this second generation of biphasic scaffold was evaluated *in vitro* and *in vivo* in an athymic rat subcutaneous model.

2. Materials and Methods

2.1. Biphasic scaffold fabrication

2.1.1. Bone compartment

Medical grade polycaprolactone (PCL) containing β-tricalcium Phosphate (β-TCP, 20% wt) was utilized to fabricate composite scaffolds via Fused Deposition Modeling (FDM, Osteopore Inc., Singapore). The scaffolds measured 100x100x2 mm^3 and had 100% interconnectivity, 70% porosity and a 0/90 degrees lay-down pattern. Prior to use the FDM scaffold block were sectioned with a sharp scalpel blade into 5x5x2 mm^3 specimens.

The FDM scaffolds were submitted to a calcium phosphate coating process by successive immersion into specific reagents and solutions. The procedure consisted of the following steps: immersion in 100% ethanol for 15 minutes under vacuum, immersion in sodium hydroxide 2 M for 30 min at 37°C, multiple rinse-immersions in ultrapure water until a water pH of 7 is reached, immersion in a 10x simulated body fluid (SBF) solution (solution preparation described elsewhere [24] for 30 min at 37°C and immersion in a 0.5 M sodium hydroxide solution for 30 min at 37°C. Finally the coated scaffolds were rinsed with ultrapure water and stored in a desiccator until use.

2.1.2. Periodontal compartment

Medical grade polycaprolactone (PCL, Lactel, USA) was electrospun using an in-house melt electrospinning device [25, 26]. Polymer pellets were loaded into a 2 mL syringe and electrospun at a temperature of 80°C at a feed rate of 20 μL/h, at 7 kV and at a 4 cm tip to collector distance. Circular membranes with 8 mm diameter were produced by electrospinning the molten PCL for periods of 4 min onto aluminum foil-covered glass slides placed over the collector.

2.1.3. Assembly of the biphasic scaffold

The assembly of the biphasic scaffolds was performed accordingly to the protocol utilized in our previous study [15]. Briefly the FDM component was placed 1 cm from a hot plate heated to 300°C for

4 seconds and then quickly press-fitted for 10 seconds onto the PCL melt-electrospun membrane. This heat treatment partially melted the first layer of the FDM component enabling it to strongly bind to the electrospun scaffold upon cooling and solidification.

2.2. Biphasic scaffold characterization

2.2.1. Scanning electron microscopy (SEM)

SEM was used to assess the scaffold morphology as well as to evaluate the cohesion of the two compartments. The scaffolds were immersed in liquid nitrogen for 5-10 min and a sharp razor blade was used to section the structures. The samples were gold coated for 3 min and observed with a FEI Quanta 200 Environmental SEM operating at 10 kV.

2.2.2. X-ray diffraction

The CaP coating was characterized by X-ray diffraction using a PANalytical X'Pert MPD Powder X-ray Diffractometer, a Cobalt anode and a 2 theta step size of 0.001.

2.3. *In vitro* study

2.3.1. Cell isolation and culture

Osteoblast and periodontal ligament explants were obtained from Merino sheep (ovis aries). Animal ethics approval for this study was granted by the Animal Ethics Committee of the Queensland University of Technology.

2.3.2. Osteoblasts

Compact bone samples were collected under sterile conditions from the mandible under general anesthesia with a trephine drill (5 mm diameter), minced, washed with phosphate buffered saline (PBS) and vortexed 5 times. Bone samples were then incubated with 10 mL of 0.25% trypsin/EDTA for 3 min at 37°C in a 5% CO_2 atmosphere. After trypsin inactivation, samples were washed once again with PBS

and transferred in basal culture media (DMEM containing 10% FBS, 1% of penicillin/streptomycin) into 175 cm^2 tissue culture flasks. Outgrowth of osteoblasts was observed after 5-7 days. Cells were expanded and used at the third passage (P3).

2.3.3. Periodontal ligament cells

Two incisors were extracted and placed into a 50 mL tube containing DMEM with 2% penicillin/streptomycin and 4 μg/mL fungizone. The middle third of the periodontal ligament (PDL) was subsequently gently removed from the root surface with a scalpel and further sectioned into approximately 1x1 mm^2 pieces. The PDL tissues were placed into a 25 cm^2 culture flask which was left standing upright in an incubator at 37°C and 5% CO_2 atmosphere for 30 min to allow tissue adhesion. After this incubation period, 3 mL of DMEM containing 10% FBS, 1% of penicillin/streptomycin and 0.1 μg/mL fungizone were added and the flask was carefully laid down in the incubator. The first media change occurred 4 days post extraction. After one week of culture, cells started migrating outwards from the PDL tissues and reached confluence after 2-3 weeks of culture. The cells were passaged using 0.25% trypsin and further expanded until P3.

2.3.4. Biphasic scaffold seeding and culture

Osteoblasts (200,000 cells in 40 μL of media) were seeded onto the FDM component and allowed to adhere for 4 hours at 37°C in a 5% CO_2 atmosphere before the well was filled with media. The biphasic scaffolds were then turned upside down with the periodontal compartment facing upwards in order to minimize cell infiltration into the electrospun component. Biphasic scaffolds were further cultured for 6 weeks either in osteogenic media (50 μg/mL ascorbate-2-phosphate, 10 mM β-glycerophosphate, 0.1 μM dexamethasone) or in basal media. The biphasic scaffolds were entirely covered by the medium. Four groups were created: Non-coated with osteoblasts in basal media (N-N), or in osteogenic media (N-O), CaP coated scaffold with osteoblasts in basal media (CaP-N), or in osteogenic media (CaP-O). Osteoblast proliferation and alkaline phosphatase activity were measured at 2, 4 and 6 weeks post seeding according to the procedure described in the following section.

2.3.5. Alkaline phosphatase activity and DNA content

ALP activity was measured from the media in triplicate at different time-points (2, 4 and 6 weeks) after a 24 hours release period as described in the supplementary information. DNA content was measured utilizing the Picogreen kit after matrix digestion in a solution of proteinase K (more details can be found in the Supplementary Information). For the ALP and DNA analyses, 4 biological replicates per group were used.

2.3.6. Scanning electron microscopy (SEM)

Osteoblasts morphology and distribution into the biphasic scaffold were assessed at 2, 4 and 6 weeks post-seeding. Samples were fixed in 3% glutaraldehyde until processing. Samples were treated by sequentially immersing them into 0.1 M cacodylate buffer, 1 % osmium tetroxide in cacodylate buffer, rinsed in ultrapure water and then dehydrated by immersion into increasingly higher concentration ethanol solutions. Finally, samples were immersed in hexamethyldisilazane for 60 min, air dried, mounted onto stubs and gold coated. Samples were observed on a FEI Quanta 200 Environmental SEM operating at 10 kV.

2.3.7. Confocal laser microscopy

Cellular morphology and orientation were assessed by confocal laser microscopy at 2, 4 and 6 weeks post-seeding. Samples were washed in PBS and fixed overnight in 4% (w/v) paraformaldehyde (PFA)/PBS. Samples were then washed in PBS and permeabilized with 0.2 % Triton X100/PBS for precisely 5 minutes and again washed twice with PBS. F-actin filaments and nuclei were then stained for 45 minutes with 0.8 U/mL rhodamine 415-conjugated phalloidin and 5 μg/mL 4′-6-diamidino-2-phenylindole (DAPI) respectively in PBS. Immunofluorescence was visualized and z-stacks acquired using a confocal microscope (SP5, Leica).

2.4. Micro-CT analysis

The effect of the CaP coating along with the *in vitro* culture conditions upon mineralization was quantitatively assessed 6 weeks post seeding by micro-computed tomography. Prior to cell seeding each biphasic scaffold was assigned a number to allow sample tracking. They were thereafter scanned in a micro-computed tomography (micro-CT) scanner (μCT40, SCANCO Medical AG, Brüttisellen, Switzerland) at a resolution of 12 μm, a voltage of 45kVp and a current of 177 mA in order to obtain the signal originating from the scaffold only (called herein scan 1). At the end of the *in vitro* culture (6 weeks post-seeding) these samples were fixed in 4% paraformaldehyde solution overnight at room temperature and then washed in PBS and scanned again according to the same parameters in order to measure the mineralization volume (referred to as scan 2). The true mineralization was quantitatively determined by subtracting the corresponding initial signal (scan 1) from the mineralization volume at the end of the culture (scan 2).

2.5. *In vivo* study

The ability of the biphasic scaffold to facilitate periodontal regeneration including simultaneous bone, periodontal ligament and cementum regeneration was assessed following insertion in ectopic (subcutaneous) sites in rats. The osteoblast loaded scaffolds were cultured for 6 weeks and then three PDL ligament cell sheets were successively placed onto the melt electrospun PCL membrane, thus creating the periodontal compartment. The following sections describe the cell sheet harvesting along with the animal implantation.

2.5.1. Harvesting of cell sheets

PDL cells were seeded at 10,000 cells/cm^2 in a 24-well plate. The cells were cultured in osteogenic media and as the cell sheet matured (after 7 days of culture), it started to contract and detach from the well. Following a procedure used in previous work [15], three PDL cell sheets were then harvested using the electrospun component of the biphasic scaffold (see Supplementary Information).

2.5.2. Dentin slices and scaffold assembly

One millimeter thick dentin slices were prepared from sheep teeth and adjusted to the size of the biphasic scaffolds. The assembly of the biphasic scaffolds onto dentin blocks was performed under sterile conditions and sutures were used to keep the biphasic scaffold on top of the dentin slice. Thereafter the samples were immersed in media for 2 hours in order to allow for cell sheet adhesion onto the dentin surface. Notches on the dentin slices were created in order to prevent the sutures from sliding off, thus ensuring high stability of the scaffold.

2.5.3. Subcutaneous implantation

Animal ethics approval for the use of athymic nude rats in this experiment was granted by the Animal Ethics Committee of Griffith University. Five 8-week old male rats (Animal Resources Centre, Canning Vale, WA, Australia) were used. The animals were anaesthetized with isoflurane. Six small incisions were made longitudinally along the central line of the shaved dorsal area, approximately 2 cm apart, and subcutaneous pockets were made with surgical scissors. Six different groups of biphasic scaffolds were implanted for 8 weeks. The groups consisted of 1) non coated biphasic scaffolds combined with cell sheets (n=5) or 2) without cell sheets (n=5); 3) non-coated biphasic scaffolds with osteoblasts cultured in basal media (n=5) or 4) in osteogenic media (n=5); 5) CaP-coated scaffolds with osteoblasts cultured in basal media (n=5) or 6) in osteogenic media (n=5). Each individual pocket held one scaffold and the incisions were closed with 5/0 silk sutures. Therefore, 4 groups out of 6 did not receive the CaP coating. The animals were sacrificed after eight weeks and the implants were retrieved and fixed in 4% paraformaldehyde in PBS at pH 7.4 for further analysis.

2.5.4. Micro-CT analysis

To determine the efficacy of the biphasic scaffold in regard to mineralized tissue formation, the retrieved samples were analyzed by micro-CT according to the parameters described in section 2.3. Here again the intrinsic signal originating from the scaffold was measured prior to *in vitro* culture and subtracted from the signal obtained when scanning the samples 8 weeks post implantation. This permitted the precise measurement of the amount of newly formed bone. To validate the *in vivo* mineralization within the PCL scaffold, the attached dentin block was excluded from the scan and the average density of

mineralization against a hydroxyapatite standard (supplied by Scanco) was measured by the micro-CT system software.

2.5.5. Histology

Samples were decalcified in 10% EDTA at pH 7.4 for 3 months at 4 °C with a weekly change of solution and subsequently embedded in paraffin. Sections near the central area of the implants were used for the haematoxylin and eosin (H&E) staining. We defined periodontal-like attachment as direct contact of the connective tissue (or cell sheets) with the dentine slice. The number of specimens demonstrating periodontal-like attachment in each group (with or without cell sheets) was calculated and compared to the total number of samples within the same group.

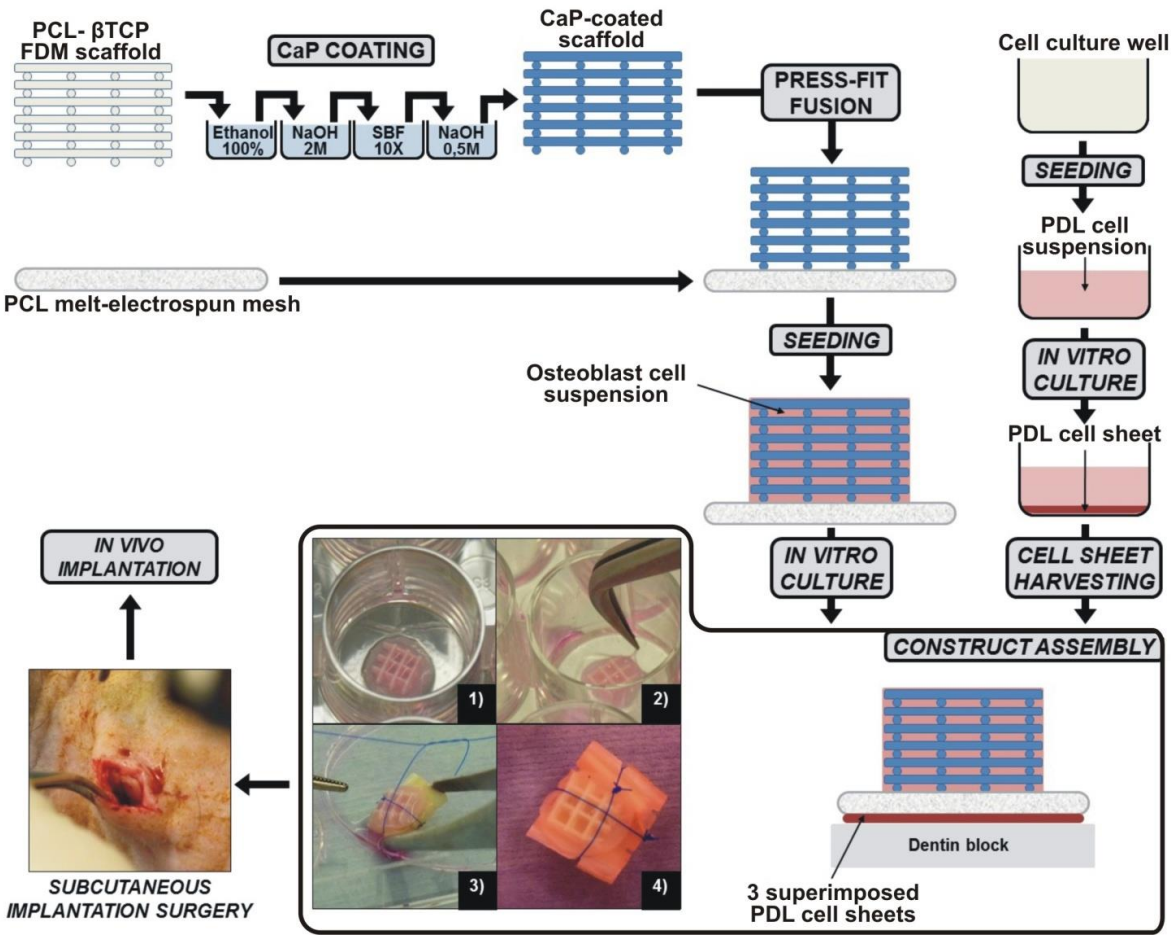

Figure 6.1 – Graphical illustration of the biomimetic coating procedure, the fabrication of the biphasic scaffold, cell seeding, subsequent *in vitro* culture and *in vivo* implantation of the cellular constructs. a) and b) harvesting and placement of cell sheets on the periodontal compartment. c) and d) positioning of the construct to a dentin block.

2.6. Statistical analysis

The statistical analysis was performed using a Shapiro-Wilk normality test and one-way ANOVA followed by a Tukey HSD post-hoc test. $p< 0.05$ was considered as statistically significant.

3. Results

3.1. Scaffold morphology

Figure 6.1 depicts the global strategy developed in this study from the scaffold fabrication and assembly to the *in vivo* implantation. The bone compartment was coated with a layer of calcium phosphate homogenously distributed on the polymer struts. This surface modification displayed the typical features of biomimetic calcium phosphate coating, that is formation of cauliflower-like structures as seen in Figure 6.2.b. The NaOH pre-treatment resulted in exposure of the β-TCP particles on the surface of the PCL struts. This enabled the creation of specific nucleation sites for the deposition of the CaP coating. Indeed, the calcium phosphate preferentially nucleated onto the TCP particles (probably due the higher affinity and the lower surface energy) and then spread over the surface on the PCL strut. The resulting CaP coating was composed of a mixture of Di-Calcium Phosphate Dihydrate (DCPD) and carbonate apatite, however the NaOH post treatment was capable of removing the more soluble phase (DCPD). Indeed, the XRD analysis (Figure 6.2.e.) revealed that the intensity of the peaks corresponding to DCPD was reduced after the post-treatment while the intensity of the peaks corresponding to carbonate hydroxylapatite was increased. This indicates that the CaP deposits on the polymeric strut had good physical stability, which is necessary for osteogenesis.Upon sectioning of the bone compartment, it was possible to access the approximate thickness of the coating. The SBF immersion resulted in the deposition of a 600-800 nm coating.

The periodontal compartment consisted of a melt electrospun scaffold composed of randomly orientated PCL fibers. As seen in Figure 6.2.d, fiber fusion occurred at different locations, which created a concentric ring pattern during the fabrication process. The fiber diameter was around 10 to 15 µm which resulted in the formation of a fully interconnected porous structure, with pore sizes ranging from 100 to 400 µm (as estimated by SEM). The assembly of the biphasic scaffold was performed through a press-fit methodology by compressing the partially fused CaP coated bone compartment (FDM scaffold) onto the periodontal compartment (melt electrospun mesh) for several seconds. Upon solidification of

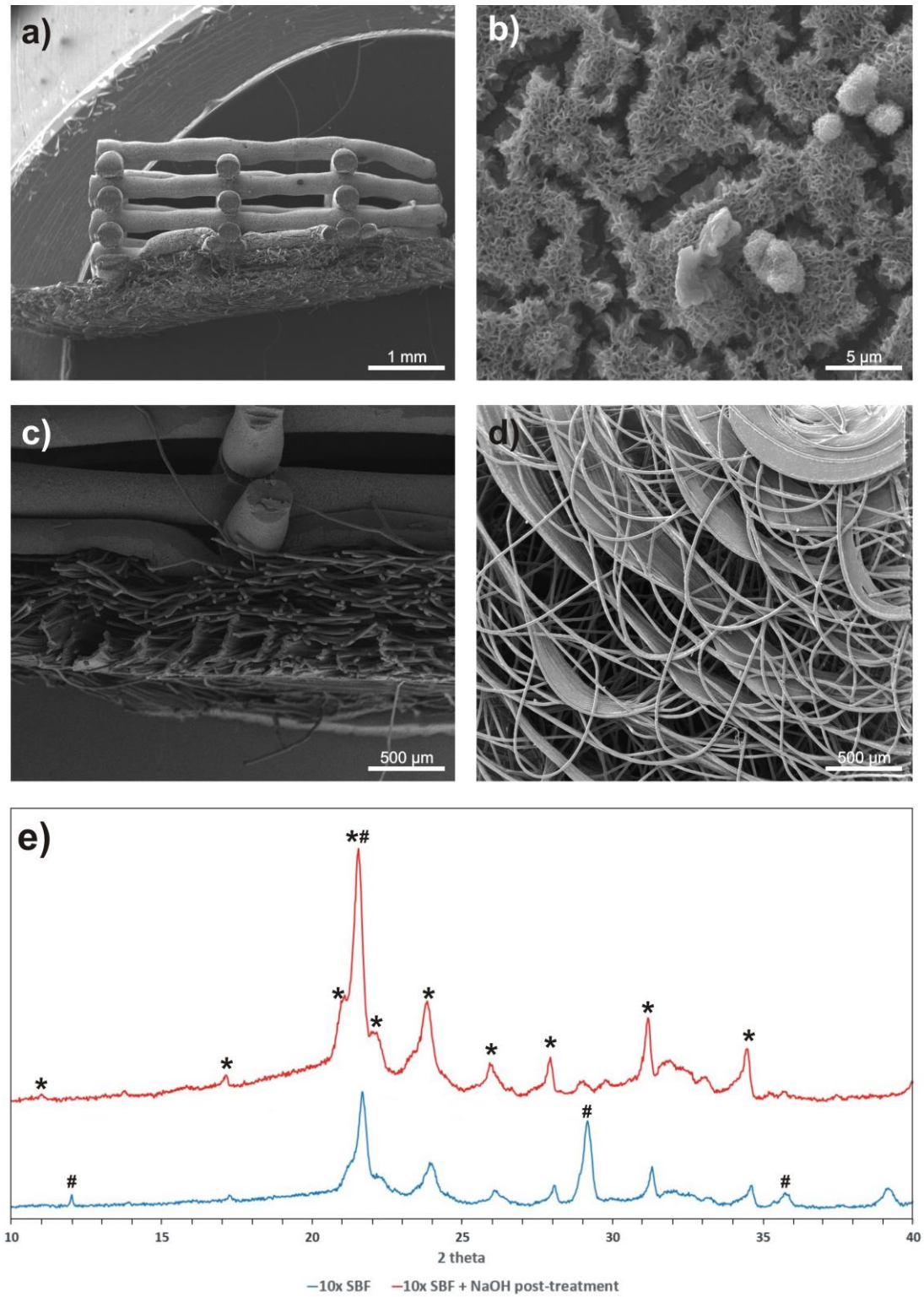

Figure 6.2 – Scanning Electron Microscopy and X-ray diffraction analysis of scaffolds. a) and c) Cross-sectional views of scaffolds. b) CaP-coated surface of FDM scaffold. d) Melt electrospun mesh. e) X-ray diffraction analysis of surface of non-coated and CaP-coated scaffold strut. * is hydroxyapatite and # is DCPD.

the partially molten bone compartment, both scaffold remained fused and firmly attached together. As seen in Figure 6.2 the scaffold assembly was not detrimental to the physical integrity of each individual component.

3.2. *In vitro* study

3.2.1. Cell imaging

Osteoblasts were seeded and cultured *in vitro* in the biphasic scaffold's bone compartment for a total period of 6 weeks. Confocal laser microscopy and SEM imaging (Figure 6.3 and Supplementary Figures 6.1 and 6.2) revealed that 2 weeks post-seeding cells were homogenously distributed around the bone compartment's polymer struts and acquired a spindle-like shape. Noticeable differences were observed between osteoblasts grown in the groups cultured in basal media (N-N and CaP-N) and the ones under osteogenic induction (N-O and CaP-O) as the latter were capable of spanning between the polymer struts and therefore started filling the macroscopic pores of the bone compartment. Notably, the periodontal compartment was also infiltrated by the osteoblasts as early as 2 weeks post seeding regardless of the culture conditions. The cells entirely filled the melt electrospun pores after 2 weeks of osteogenic induction and formed a dense cell layer on the surface of the periodontal compartment. A similar effect was observed for the cell in basal media albeit at a later time point (6 weeks post seeding). Scanning Electron Microscopy also revealed that the osteoblasts accumulated at the interface of both compartments when cultured under osteogenic induction (second and fourth column).

3.2.2. DNA content and Alkaline Phosphatase activity

Cell proliferation was assessed by DNA quantification. At two weeks post-seeding, a significantly higher amount of DNA was found in the groups under osteogenic induction but this effect was less pronounced for the two later time points (Figure 6.4.A.). It was also observed that the osteoblasts in basal media, seeded onto the non-coated scaffold (N-N group) supported significant cell proliferation at 6 weeks post-seeding, whereas the DNA remained constant for the other experimental groups excepted for the N-O group in which a gradual but significant decrease was observed (Figure 6.4.B.). The reason for this finding is unclear but it may be linked to a lack of diffusion of oxygen and nutrient in the depth of the

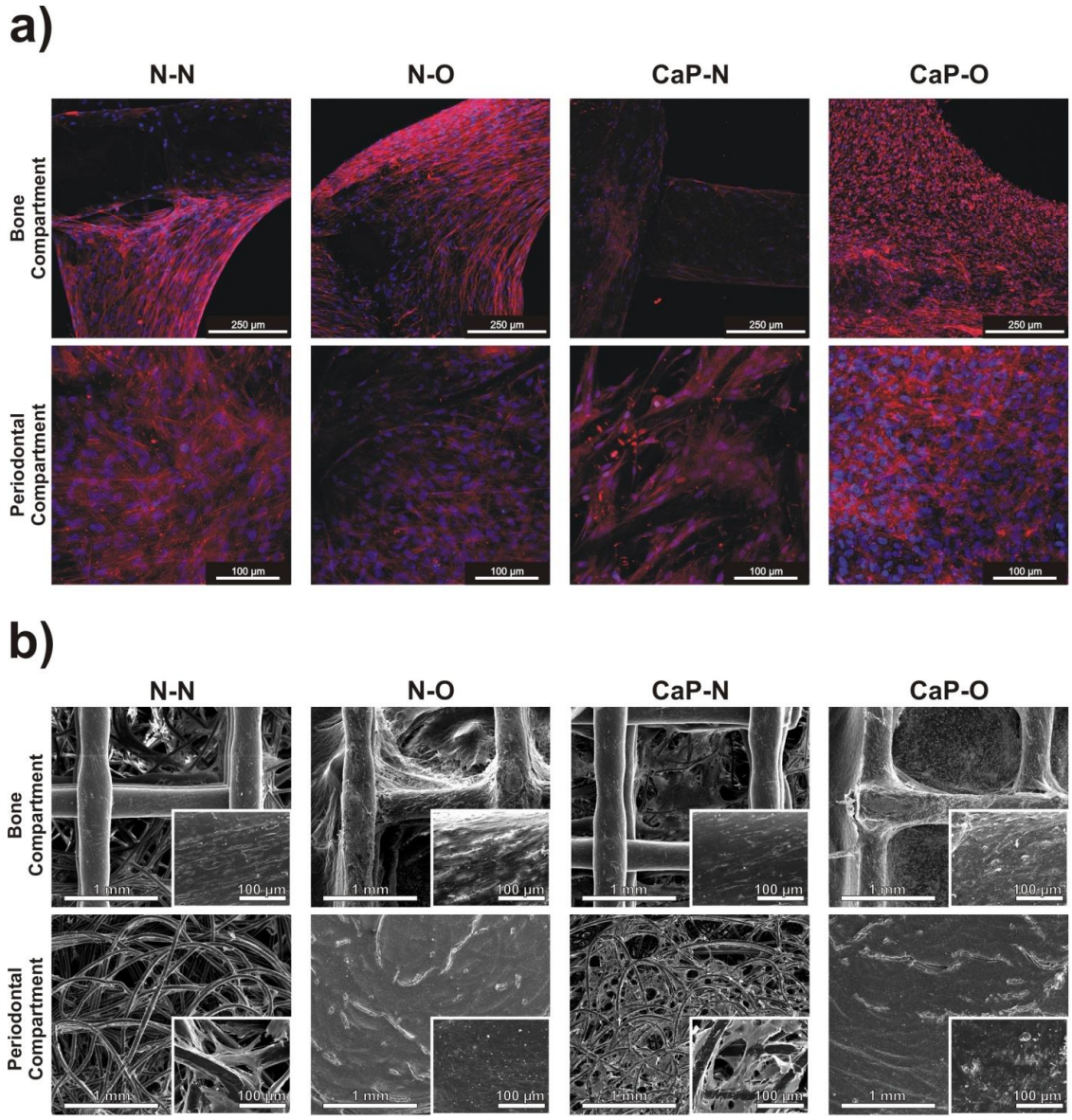

Figure 6.3 – Confocal laser microscopy a) and scanning electron microscopy images b) of the seeded scaffolds after 6 weeks of in vitro culture under four different conditions.. N-N - non coated scaffold cultured in basal medium, N-O - non coated scaffold cultured in osteogenic medium, CaP-N – calcium phosphate-coated scaffold cultured in basal medium, CaP-O – calcium phosphate-coated scaffold cultured in osteogenic medium

scaffold due to the formation of a thick cellularized tissue at the periodontal/bone compartment's interface which may have caused, to some extent, unexpected cell death.

An ALP quantification assay was used to measure the osteogenic activity of the osteoblasts seeded into the biphasic scaffold at 2 week intervals over 6 weeks of *in vitro* culture. At 2 weeks post seeding, the CaP coating resulted in significantly enhanced ALP activity in the group CaP-N (cultured in basal media, Figure 6.4.C.). A noticeable increase in ALP expression was observed in the osteo-induced samples (N-O and CaP-O) although it did not reach statistical significance. Notably, the CaP-N group displayed

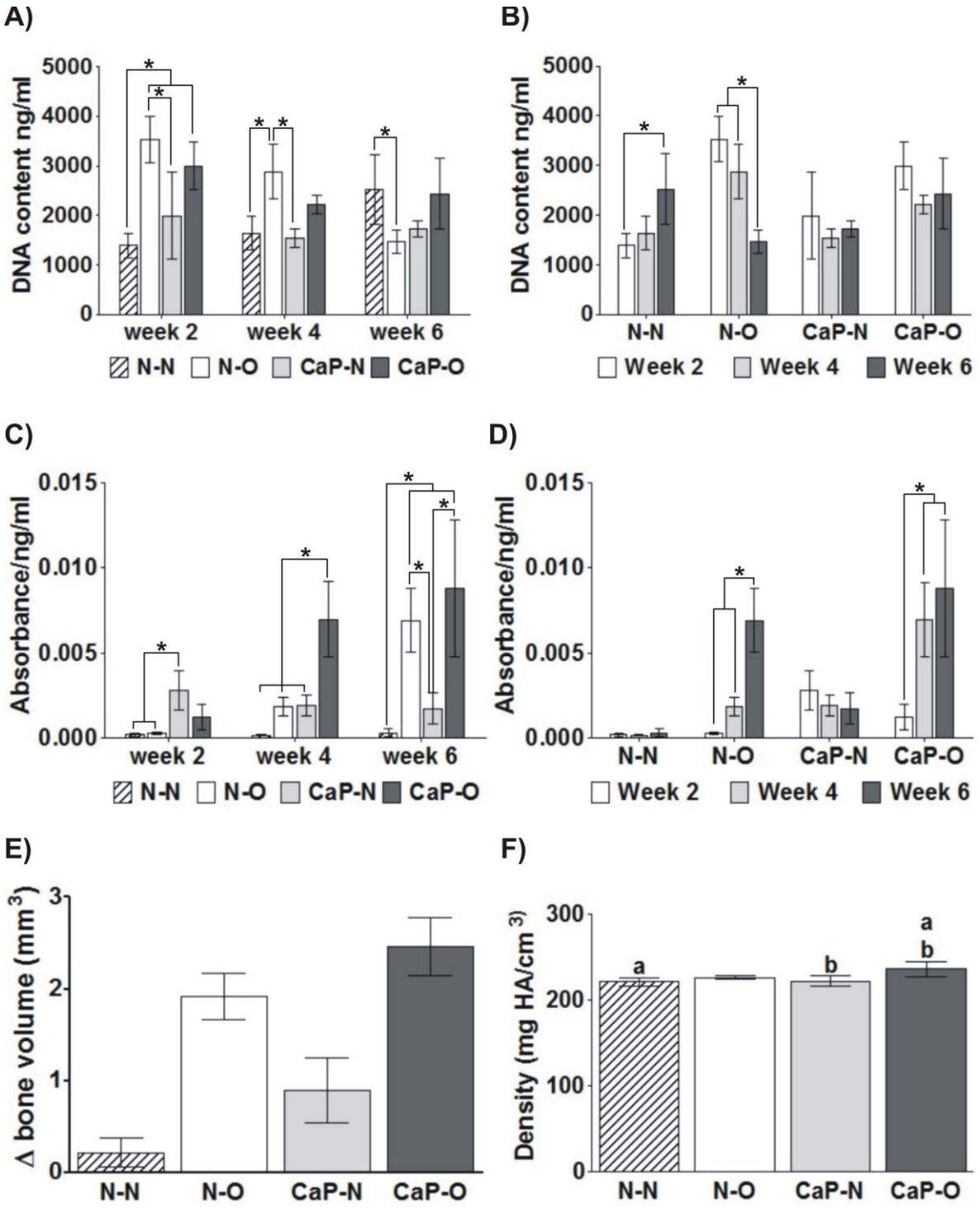

Figure 6.4 - Biological characterization. A) DNA content versus time in culture. B) DNA content versus experimental groups. C) Normalized ALP activity versus time in culture. D) Normalized ALP activity versus experimental groups. E) *In vitro* volume of mineralization as measured by micro-CT analysis F) Mineralization density. a, b and * indicate statistical significance ($p<0.05$). In graph E) all values are statistically different ($p<0.05$). N-N: non coated scaffold cultured in basal medium, N-O: non coated scaffold cultured in osteogenic medium, CaP-N: calcium phosphate-coated scaffold cultured in basal medium, CaP-O: calcium phosphate-coated scaffold cultured in osteogenic medium.

higher ALP expression at 2 weeks post seeding than the osteoblasts cultured in osteogenic media, exemplifying the efficacy of the CaP coating at enhancing ALP activity. The synergetic effect of the coating and the osteogenic induction was more pronounced at 4 weeks post seeding where the CaP-O group induced significantly higher ALP expression than any other groups. ALP activity was significantly up-regulated at 6 weeks post-seeding in both groups with osteogenic media when compared the samples in basal media (N-N and CaPN). However no statistical difference was found between N-O and CaP-O at this time point. Figure 6.4.D. depicts ALP activity for each group throughout the time course of the *in vitro* culture, and it can be observed that ALP activity remained constant in the samples cultured in basal media whereas the osteogenic induction resulted in a gradual and significant increase in this parameter.

3.2.3. Micro-computed tomography

The volume of mineralized matrix deposited by the cells during the 6 weeks of *in vitro* culture was quantified by micro-CT and is shown in Figure 6.4.E. It was observed that the CaP coating clearly resulted in enhanced mineralization within the scaffolds regardless of the culture conditions. More importantly, it showed that osteogenic induction was the most potent signal for secreting mineralized matrix as both, N-O and CaP-O groups displayed much higher mineralization volume than the corresponding groups cultured in basal media. Indeed, mineralization in N-N samples remained within the noise level, whereas 1.9 and 2.5 mm^3 of mineralized matrix was produced for N-O and CaP-O respectively. This corroborated the ALP activity profile observed in these groups and confirmed the beneficial effect of CaP coating on the deposition of mineralized matrix. The average mineralization density, as assessed from the micro-CT scan, provided insights into the mineralized matrix maturation, whereby higher density is associated with a more mature matrix. However no significant differences were observed between CaPO and NO suggesting that the mineralized matrix was equivalent “quality”.

3.3. *In vivo* study

After an uneventful 8 weeks post-operative period, the animals were sacrificed and the constructs collected. Good tissue integration into the subcutaneous pocket was observed and no acute foreign body reaction or infections were observed.

The amount of newly formed bone in the constructs was analyzed using micro CT (Figure 6.5.A.). The

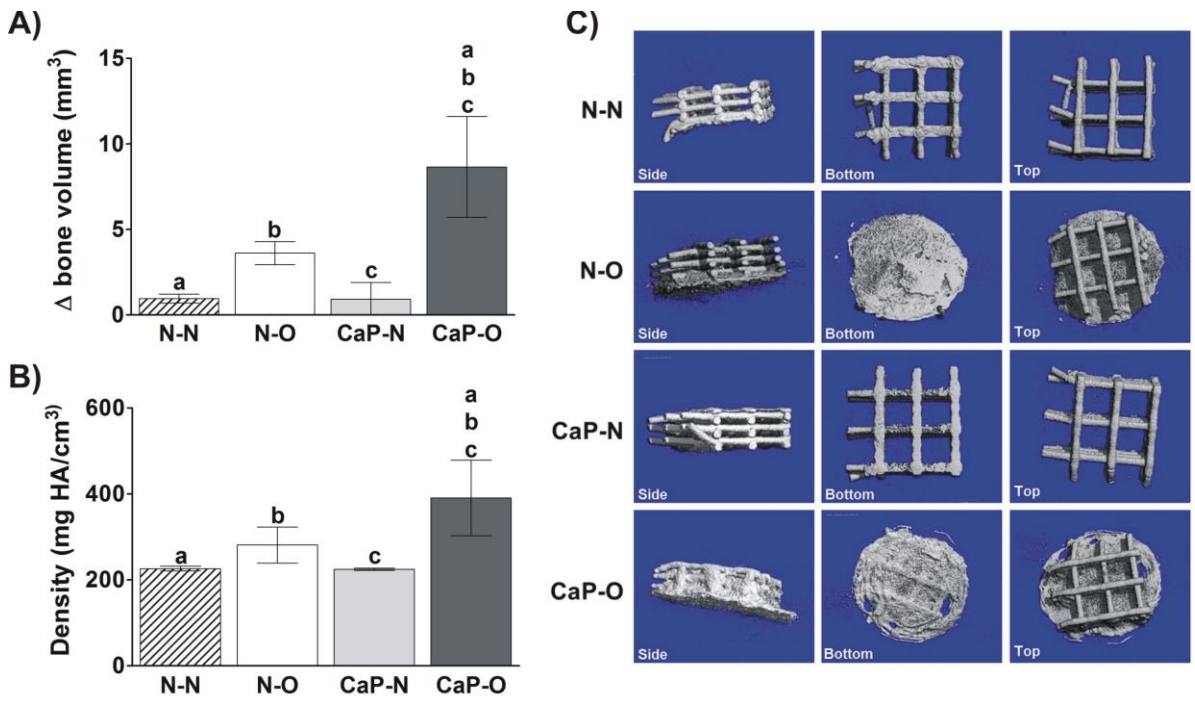

Figure 6.5 - Micro-CT analysis 8 weeks post-implantation. A) Bone volume and B) bone density. Same letters indicate statistical significance between the groups ($p<0.05$). C) Representative reconstruction of constructs from each group. N-N: non coated scaffold cultured in basal medium, N-O: non coated scaffold cultured in osteogenic medium, CaP-N: calcium phosphate-coated scaffold cultured in basal medium, CaP-O: calcium phosphate-coated scaffold cultured in osteogenic medium.

results showed that the samples cultured in basal media did not form any bone, with the signal remaining at the background level. In contrast, the samples cultured in osteogenic media resulted in bone formation and CaP-O displayed the highest level of bone (Figure 6.5.A.). Figure 6.5.B. displays the density of the newly formed bone and it was observed that CaP-O specimens featured the highest density when compared to all other groups. This indicates that the bone formed in the CaP coated scaffold was denser and therefore more mature. By performing 3D reconstructions (Figure 6.5.C.) of the analyzed constructs, it was observed that a significant amount of new bone was located at the periodontal/bone compartment's interface. This was confirmed by the histology as shown in Figure 6.6 and Supplementary Figure 6.3. Bone formation solely occurred in samples previously cultured in an osteoinductive environment (Figure 6.6.b. and Supplementary Figure 6.3.b.). Histological analysis of the periodontal compartment revealed that the host tissue had entirely colonized the melt electrospun scaffold. It was also observed that the constructs with cell sheets (Figure 6.6.b. and Supplementary Figure 6.3.a.) had attached more frequently onto the dentin block compared to the constructs without cell sheets (Figure 6.6.a.). Despite signs of connective tissue adhesion on the dentin in the constructs without cell sheets, this attachment was not functional and was not sufficiently strong to withstand

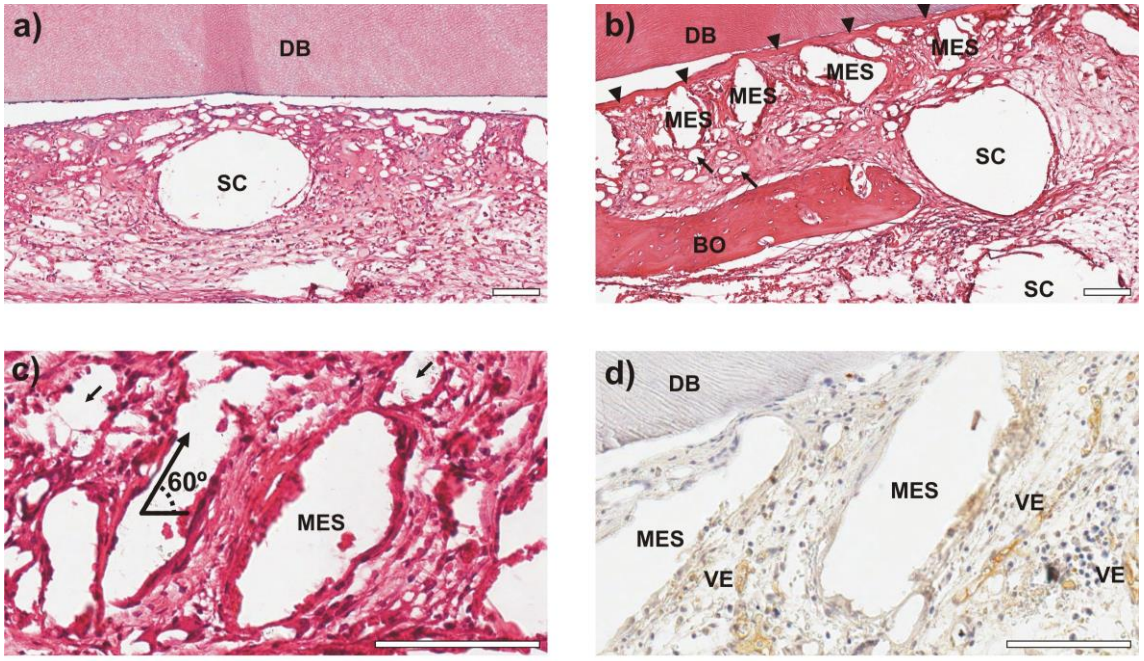

Figure 6.6 - Representative H&E (a-c) and immune (d) staining images of implanted biphasic scaffolds. a) Reduced tissue attachment on the dentin without cell sheets. b) Bone formation in the CaP-coated samples cultured in osteogenic media prior to implantation. d) Representative section depicting the vascularization in the periodontal compartment. c) Tissue orientation provided by the periodontal compartment architecture. DB- dentin block, BO- bone, VE- vessel, SC- Spaces formed by FDM scaffold's struts, MES indicates melt electrospun scaffold and thin arrows indicate single melt electrospun fibers. Triangular arrows indicate periodontal ligament. Scales are 100 μm.

histological processing and sectioning hence generating a space between these two elements. The percentage of attachment for each condition was calculated (Table 6.1) and showed that most of the constructs with cell sheets (4/5-80%) were able to attach as opposed to 1/5-20% for the constructs without cell sheets. Blood vessels penetrated not only throughout the bone compartment (FDM scaffold) (Supplementary Figure 6.3.c. and e.), but also throughout the periodontal compartment (Figure 6.6.d. and Supplementary Figure 6.3.d.). Blood vessels were found in close vicinity of the implanted cell sheets (Figure 6.6.d. and Supplementary Figure 6.3.d.), which may have a significant impact on cell sheet survival and subsequent tissue remodeling. It is also noteworthy that, due to the intrinsic architecture of the melt electrospun scaffold, which consisted of superimposed concentrically oriented

Table 6.1 - Quantification of tissue attachment on the dentin block showing that attachment to the dentin block is more effective in the presence (80%) than in absence (20%) of cell sheet.

	With Cell sheet (%)	**Without Cell sheet (%)**
Percentage of samples showing attachment to dentin	**80**	**20**

rings, some level of tissue organization was observed as shown in Figure 6.6.c. This tissue was obliquely orientated in regard to the dentin block and formed an angle of approximately 60 degrees.

4. Discussion

The objective of this study was to optimize the design and the material properties of a biphasic construct for periodontal regeneration via a strategy that simultaneously delivers tissue engineered bone and periodontal ligament tissue into the periodontal defect. The design of a biphasic scaffold previously described by our group [15] was modified in order to enhance the osteoconductive properties by the addition of a calcium phosphate coating, along with the utilization of a large pore size membrane fabricated by melt electrospinning for improving the integration between the bone and periodontal ligament compartments. This had an effect on the *in vivo* outcomes as significant higher bone formation was observed in the CaP coated scaffolds when compared to our previous scaffold design. Further, the incorporation of a larger pore size membrane into the bi-phasic scaffold design permitted both improved fiber orientation and blood vessel ingrowth, important for achieving functional attachment and sustaining the viability of the new periodontal ligament formed by the cell sheets.

Scaffolds produced by rapid prototyping have been increasingly used for bone regeneration [27-29] and are envisioned as good candidates for periodontal tissue engineering as they fulfill key requirements for this type of application, namely facilitating wound stabilization and space maintenance. Owing to the adaptability of the manufacturing method, they can be fabricated in any shape, pore size and porosity. Another important feature of these scaffolds is that their mechanical properties can be tailored to specific requirements based on the host environment, through the selection of specific material and architecture [30] to provide appropriate structural and biomechanical stability to newly formed tissues.

Our group has recently shown that FDM scaffolds could be combined with electrospun membranes for permitting simultaneous periodontal fibroblast cell sheet delivery and space maintenance for bone regeneration in the context of periodontal regeneration [15]. Although this approach was conceptually sound, it fell short of achieving appropriate bone regeneration in an ectopic site.

To circumvent this, the bone compartment was surface-modified with a layer of CaP according to a protocol described by Yang et al. [24]. CaP implants have been shown to initiate and enhance bone formation in various implantation sites [31-34] and CaP biomimetic deposition is known to significantly impact on cell and tissue behavior [35-39].

The findings reported in the present study clearly showed that the CaP coating resulted in increasing Alkaline Phosphatase Activity in a time dependent manner. Notably, only scaffolds coated with CaP displayed high ALP activity at 2 weeks post-seeding but this was gradually reduced over the time course of the study. This is in accordance with observations by De Jong et al. [40], who demonstrated that CaP-coated titanium discs were capable of enhancing ALP activity for an initial period of 12 days in culture, however the expression was reduced during the later stages of culture. We also demonstrated that osteogenic induction plays an important role in stimulating ALP activity, along with the deposition of mineralized ECM. Indeed, cells cultured under osteoinductive conditions were capable of depositing mineralized ECM visible under light microscopy from 4 weeks post seeding. However, a synergetic effect was observed in the CaP coated samples under osteogenic induction as enhanced ALP activity was detected at 4 weeks post-seeding, combined with increased mineralization. Micro-CT analysis was also in agreement with the ALP measurement in regard to the deposition of mineralized ECM. Indeed, osteoblast seeded CaP coated scaffolds cultured under osteoinductive conditions displayed the highest level of mineralization. Taken together, these results corroborate well with a study from our group [23] investigating the conditions influencing ectopic bone formation, albeit in a different scaffold. Indeed, this study demonstrated a synergetic effect of CaP coating and osteoinduction in melt electrospun scaffolds when implanted in a similar rat model [23]. In a different strategy, involving the incorporation of calcium phosphate particles into a macroporous poly-L-lactide-co-glycolide acid (25/75) foam fused onto an occlusive membrane of similar composition, Carlo-Reis et al. [41] obtained significant bone formation, thus exemplifying the importance of calcium phosphate for bone regeneration. In this strategy utilizing a bi-layered construct, the membrane was used to protect the defect from fibrous tissue infiltration while the macroporous component was utilized to maintain space for permitting adequate healing. This approach proved successful for both bone formation and new ligament attachment onto the root surface. It was nevertheless noted that only partial regeneration of the periodontal complex was achieved because of the rapid degradation of the polymer scaffold. Indeed, the space maintenance property of the construct was lost upon degradation, which resulted in fibrous tissue infiltration impeding the regeneration of some areas of the defect This was the rationale for selecting a slower degrading polymer for the present study in order to achieve higher stability of the scaffold and hence enabling sufficient time for osteogenesis and periodontal attachment to occur. Furthermore, a stable biomaterial surface is essential for bone formation to occur; a rapid degrading polymer might compromise bone regeneration and subsequent remodeling.

In the present study, the majority of new bone was located at the interface of the two compartments, indicating that the accumulation of osteoblasts in this zone during the *in vitro* culture played a significant role in initiating bone formation. Indeed, other studies have shown that a minimum critical cell density is necessary for osteogenesis to occur and this was preferentially achieved at the interface between the two compartments in our study. The presence of vasculature connecting the bone and periodontal compartments was observed, which would have ensured sufficient supply of nutrients and oxygen for the regenerative events and subsequent remodeling to occur. This is of particular importance, as vascularization is known to strongly impact on bone formation and remodeling.

During periodontal regeneration, ligament formation and new bone ingrowth should occur in an orderly manner in order to facilitate the attachment of the PDL fibers into cementum and newly formed bone. Therefore, it is essential that ligament attachment and integration into bone is facilitated. To enhance this, the biphasic scaffold included a melt electrospun mesh with a macroscopic interconnected pore network favored vascularization and ultimately tissue formation, so that an integrated interface between the periodontal tissue and bone was achieved. This effect was already seen *in vitro* as osteoblasts colonized the electrospun mesh comprising the periodontal compartment, which indicates that these cells would have intimately interacted with the PDL cell sheets that were placed on the electrospun mash prior to implantation. The *in vivo* study confirmed this excellent tissue integration between both compartments as they had merged together forming a tissue structurally resembling native periodontal tissues. Our previous study [15] reported full colonization of the periodontal compartment (composed of a solution electrospun membrane), however this tissue was not as organized as the one obtained in the present study. Indeed, the new scaffold architecture resulted in the orientation of the periodontal tissue towards the dentin at an angle of about 60 degrees, in contrast to the first generation membrane where the tissue oriented parallel to the dentin surface [15]. This is of significance as obliquely oriented ligament fibers are necessary for periodontal regeneration. Indeed, Park et al. successfully addressed this requirement by manufacturing complex fiber-guiding scaffolds using solid freeform fabrication methods [42]. Using aligned micro-channels placed in the vicinity of the dentin, functional ligament attachment was obtained.

As described in previous studies [10, 15], the addition of periodontal fibroblast cell sheets was crucial for efficient attachment onto the dentin block. Indeed, several reports in the literature describe the use of cell sheets from various cell sources (PDL, or MSC) in order to facilitate periodontal regeneration. For example, Iwata et al. [7] reported successful periodontal regeneration in a canine 3-wall intrabony defect by using 3-layered PDL cell sheets and they demonstrated both periodontal attachment into

newly formed cementum and enhanced bone regeneration. The methodology adopted by Iwata et al. consisted in applying 3-layered PDL cell sheets supported by a thin poly-glycolic acid (PGA) membrane onto the exposed root [7]. Subsequent to cell sheet placement, the defect was filled with β-TCP particles. In comparison, the utilization of a single construct for simultaneous cell sheet delivery and space maintenance, as presented in the present study, will not only greatly enhance the biomechanical stability of the cell sheet, but also simplify the surgical technique. However, the clinical translation potential of this technique is constrained by the need for time consuming and costly cell culture requirements. Therefore cell culture automation would be required to significantly reduce the cost of this strategy and make it commercially viable. Based on the positive results further studies are planned in a clinically relevant large animal model to confirm the performance of the biphasic design.

The number of samples that exhibited attachment from the groups with and without cell sheets remained consistent to that observed in our previous study (4/5=80% and 1/5=20% respectively). This was achieved despite the larger pore size of the periodontal compartment, which could have compromised appropriate cell sheet attachment and allowed tissue colonization from the bone compartment, thus preventing the formation of attachment to the dentin surface.

5. Conclusions

The biphasic scaffold design studied in this work displayed suitable properties for periodontal regeneration based on faultless tissue integration of both compartments, high levels of vascularization and tissue orientation in both the bone and most importantly periodontal compartment, which is of high significance for fiber attachment formation.

6. Acknowledgements

The authors thank Dr. Leonore de Boer for assistance with the confocal laser microscopy and Dr. Christina Theodoropoulos for assistance with the scanning electron microscopy. This study was funded by a grant from the Australian National Health and Medical Resaerch Council. Pedro Costa acknowledges the Portuguese Foundation for Science and Technology for his PhD grant (SFRH/BD/62452/2009).

7. Supplementary information

7.1. ALP and DNA analysis:

Briefly, samples were first immersed for 5 min in DMEM without phenol red and this was repeated three times. They were then transferred to a new 24-well plate and 1000 µL of this media was added before the samples were placed back in the incubator for precisely 24 hours. ALP activity was measured using the SigmaFASTTM kit, as per the manufacturer's instructions. 100 µL of p-Nitrophenyl phosphate in Tris-base buffer was added to 100 µL of the culture media in a 96-well plate, and incubated at 37°C and 5% CO2 for another 24 hours. At the end of the second incubation period, the plate was brought back to ambient temperature (20 °C) for 5 min and the absorbance was read at 405 nm using a plate reader (Benchmark PlusTM microplate spectrophotometer, BIO RAD). The ALP absorbance was normalized by the DNA content of each sample. For cellular DNA content analysis, the remaining media was removed from the wells and the samples were frozen at -80 °C for at least 48 hours. The scaffolds were then placed in 1.5 mL Eppendorf tubes containing 500 µL of Proteinase K (Invitrogen) (Proteinase K/phosphate buffered EDTA (PBE) 0.5 mg/ml), at 60°C for 12 hours. The solution was thereafter diluted at a ratio of 1/50 in Phosphate Buffered EDTA PBE, and 100 µL was aliquoted in triplicates into black 96-well plates, and 100 µL of PicoGreen (P11496, Invitrogen) working solution was added. After 5 min incubation in the dark, the fluorescence (excitation 485 nm, emission 520 nm) was measured using a fluorescence plate reader. A standard curve of known λ DNA concentrations ranging from 10 ng/ml to 1 µg/mL was used to calculate the final DNA content of the sample.

7.2. Harvesting of cell sheets:

The scaffold was positioned in the centre of the well and thereafter the first cell sheet was folded over the edge of the electrospun mat using sterile needle sharp forceps. Once the cell sheet was harvested, the biphasic scaffold was placed into a 6 well plate with the periodontal compartment facing upright. The bone compartment underneath was filled with media. 15 µL of media were added onto the top of the cell sheet to prevent the cells from drying out. The biphasic scaffolds were placed back into the incubator and the cell sheet was hydrated every 10 min with media. The cell sheet was allowed to

adhere onto the electrospun substrate for 30 min before another cell sheet was harvested. This procedure was repeated until 3 cell sheets were placed onto the biphasic scaffold.

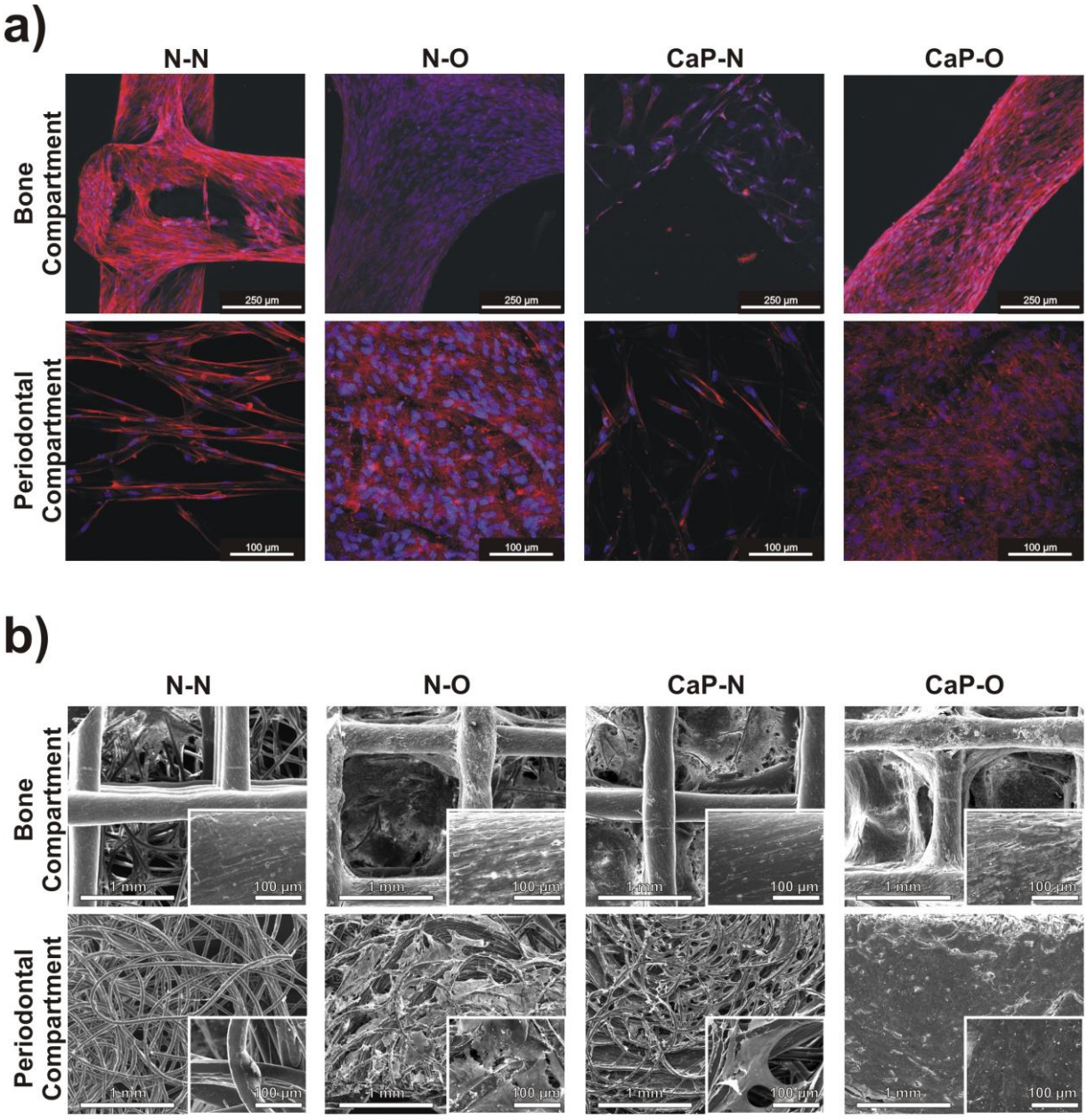

Supplementary Figure 6.1 – Confocal laser microscopy a) and scanning electron microscopy images b) of the seeded scaffolds after 2 weeks of *in vitro* culture under four different conditions. N-N - non coated scaffold cultured in basal medium, N-O - non coated scaffold cultured in osteogenic medium, CaP-N – calcium phosphate-coated scaffold cultured in basal medium, CaP-O – calcium phosphate-coated scaffold cultured in osteogenic medium.

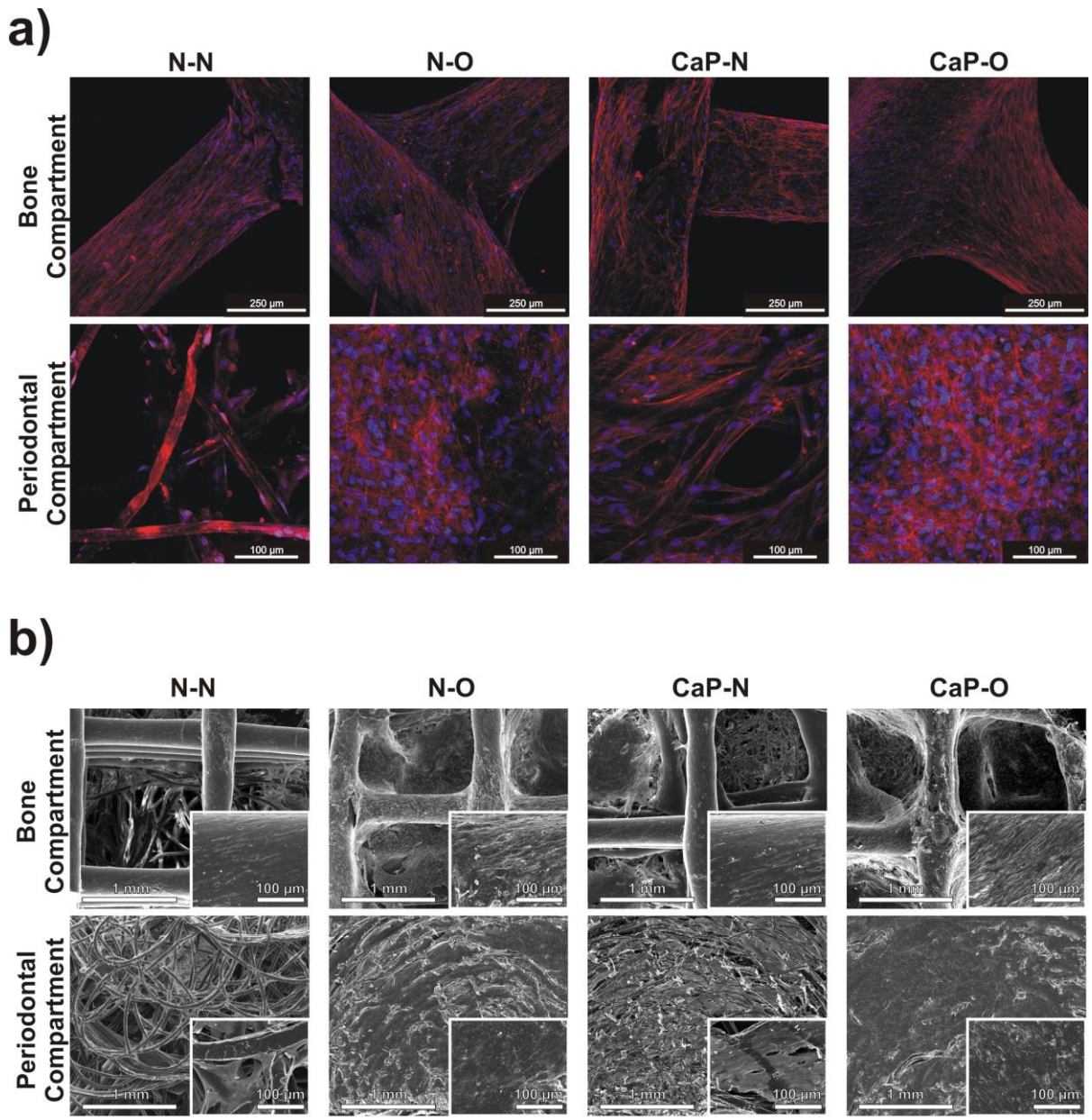

Supplementary Figure 6.2 – Confocal laser microscopy a) and scanning electron microscopy images b) of the seeded scaffolds after 4 weeks of *in vitro* culture under four different conditions. N-N - non coated scaffold cultured in basal medium, N-O - non coated scaffold cultured in osteogenic medium, CaP-N – calcium phosphate-coated scaffold cultured in basal medium, CaP-O – calcium phosphate-coated scaffold cultured in osteogenic medium.

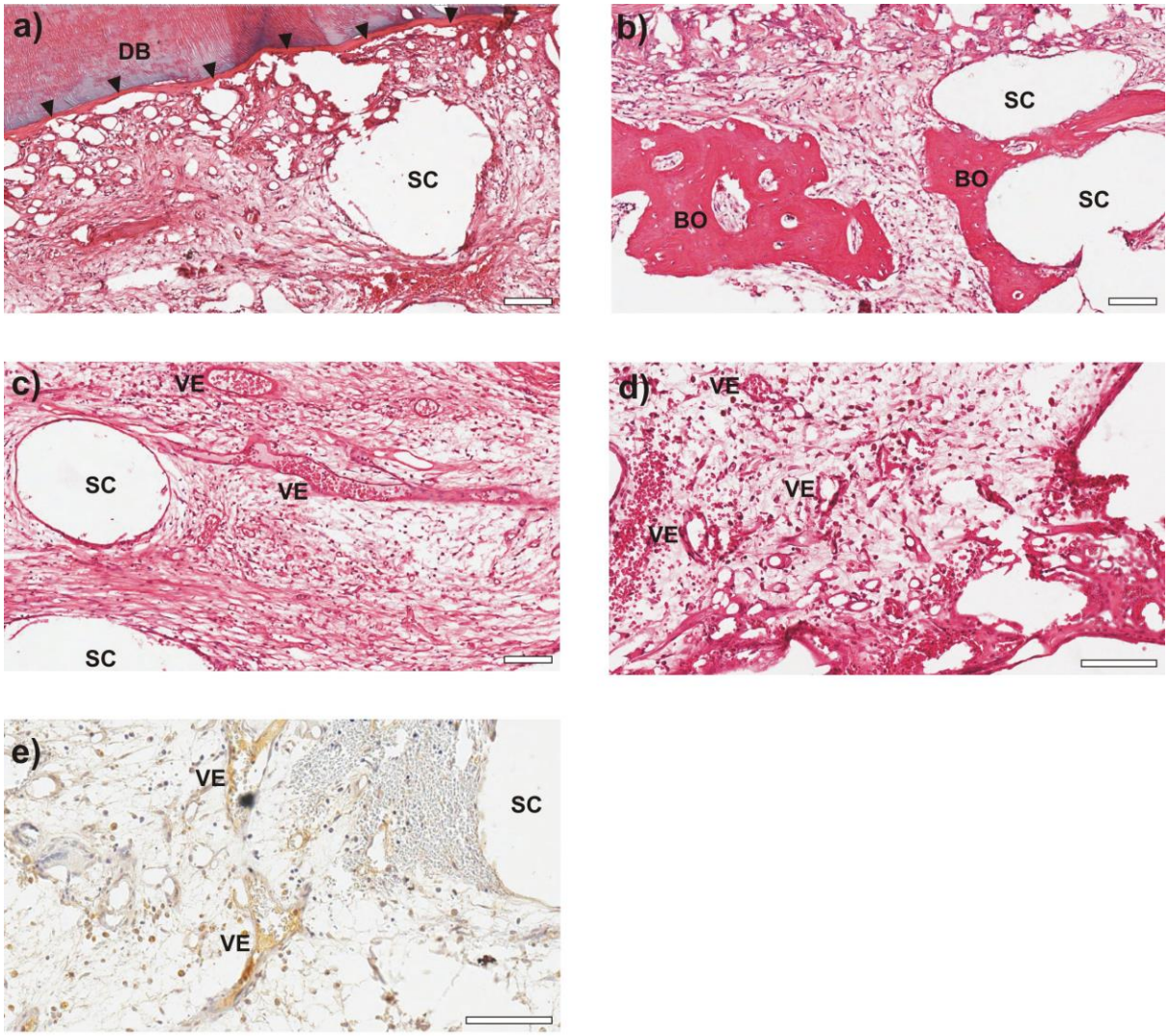

Supplementary Figure 6.3 - Representative H&E (a-d) and immune (e) staining images of implanted biphasic scaffolds. a) Tissue attachment on the dentin with cell sheets. b) Bone formation in the samples cultured in osteogenic media (N-O) prior to implantation. Representative sections depicting the vascularization in the bone (c and e) and in the periodontal compartment (d). DB- dentin block, BO- bone, VE- vessel, SC- Spaces formed by scaffold's struts. Arrows indicate periodontal ligament. Scales are 100 μm.

8. References

1. Armitage, G.C., *Development of a classification system for periodontal diseases and conditions.* Ann Periodontol, 1999. **4**: p. 1-6.

2. Gottlow, J., et al., *New attachment formation in the human periodontium by guided tissue regeneration. Case reports.* J Clin Periodontol, 1986. **13**: p. 604-16.

3. Gottlow, J., T. Karring, and S. Nyman, *Guided tissue regeneration following treatment of recession-type defects in the monkey.* J Periodontol, 1990 **61**: p. 680-5.

4. Needleman, I., et al., *Guided tissue regeneration for periodontal infra-bony defects.* Cochrane Database of Systematic Reviews, 2006. **2**.

5. Ivanovski, S., *Periodontal Regeneration.* Aust Dent J, 2009. **54**: p. S118-S128.

6. Akizuki, T., et al., *Application of periodontal ligament cell sheet for periodontal regeneration: a pilot study in beagle dogs.* J Periodontal Res, 2005. **40**: p. 245-251.

7. Iwata, T., et al., *Periodontal regeneration with multi-layered periodontal ligament-derived cell sheets in a canine model.* Biomaterials 2009. **30**: p. 2716-2723.

8. Vaquette, C. and J. Cooper-White, *The use of an electrostatic lens to enhance the efficiency of the electrospinning process.* Cell and Tissue Research, 2012. **347**(3): p. 815-826.

9. Dan, H., et al., *The influence of cellular source on periodontal regeneration using calcium phosphate coated polycaprolactone scaffold supported cell sheets.* Biomaterials, 2014. **35**(1): p. 113-122.

10. Gomez Flores, M., et al., *Cementum–periodontal ligament complex regeneration using the cell sheet technique.* J Periodontal Res, 2008. **43**: p. 364-371.

11. Hasegawa, M., et al., *Human periodontal ligament cell sheets can regenerate periodontal ligament tissue in an athymic rat model.* Tissue Eng, 2005. **11**: p. 469-478.

12. Ishikawa, I., et al., *Cell sheet engineering and other novel cell-based approaches to periodontal regeneration.* Periodontol 2000, 2009. **51**: p. 220-238.

13. Iwata, T., et al., *Validation of human periodontal ligament-derived cells as a reliable source for cytotherapeutic use.* J Clin Periodontol, 2010. **37**: p. 1088-1099.

14. Gomez Flores, M., et al., *Periodontal ligament cell sheet promotes periodontal regeneration in athymic rats.* J Clin Periodontol, 2008. **35**: p. 1066–1072.

15. Vaquette, C., et al., *A biphasic scaffold design combined with cell sheet technology for simultaneous regeneration of alveolar bone/periodontal ligament complex.* Biomaterials, 2012. **33**(22): p. 5560-5573.

16. Kokubo, T., et al., *Ca, P-rich layer formed on high-strength bioactive glass-ceramic A-W.* Journal of Biomedical Materials Research, 1990. **24**(3): p. 331-343.

17. Kokubo, T., H. Kushitani, and S. Sakka, *Solutions able to reproduce in vivo surface-structure changes in bioactive glass-ceramic A-W3.* Journal of Biomedical Materials Research, 1990. **24**: p. 721-734.

18. Al-Munajjed, A.A., et al., *Development of a Biomimetic Collagen-Hydroxyapatite Scaffold for Bone Tissue Engineering Using a SBF Immersion Technique.* Journal of Biomedical Materials Research Part B-Applied Biomaterials, 2009. **90B**(2): p. 584-591.

19. Arafat, M.T., et al., *Biomimetic composite coating on rapid prototyped scaffolds for bone tissue engineering.* Acta Biomaterialia, 2011. **7**(2): p. 809-820.

20. Araujo, J.V., et al., *Surface controlled biomimetic coating of polycaprolactone nanofiber meshes to be used as bone extracellular matrix analogues.* Journal of Biomaterials Science-Polymer Edition, 2008. **19**(10): p. 1261-1278.

21. Liu, Y., et al., *Influence of calcium phosphate crystal assemblies on the proliferation and osteogenic gene expression of rat bone marrow stromal cells.* Biomaterials, 2007. **28**(7): p. 1393-1403.

22. Lu, Z.F., et al., *Bone biomimetic microenvironment induces osteogenic differentiation of adipose tissue-derived mesenchymal stem cells.* Nanomedicine-Nanotechnology Biology and Medicine, 2012. **8**(4): p. 507-515.

23. Vaquette, C., et al., *Effect of culture conditions and calcium phosphate coating on ectopic bone formation.* Biomaterials, 2013. **34**(22): p. 5538-5551.

24. Yang, F., J.G.C. Wolke, and J.A. Jansen, *Biomimetic calcium phosphate coating on electrospun poly(ε-caprolactone) scaffolds for bone tissue engineering.* Chemical Engineering Journal, 2008. **137**: p. 154–161.

25. Brown, T.D., P.D. Dalton, and D.W. Hutmacher, *Direct writing by way of melt electrospinning.* Adv Mater, 2011. **23**: p. 5651–5657.

26. Dalton, P.D., et al., *Electrospinning and additive manufacturing: converging technologies.* Biomaterials Science, 2013. **1**(2): p. 171-185.

27. Hutmacher, D.W., et al., *Mechanical properties and cell cultural response of polycaprolactone scaffolds designed and fabricated via fused deposition modeling* Journal of Biomedical Materials Research, 2001. **55**: p. 203–216.

28. Reichert, J.C., et al., *Custom-made composite scaffolds for segmental defect repair in long bones.* Int Orthop, 2011. **35**: p. 1229–1236.

29. Park, S., et al., *Scaffolds for bone tissue engineering fabricated from two different materials by the rapid prototyping technique: PCL versus PLGA.* Journal of Materials Science: Materials in Medicine, 2012. **23**(11): p. 2671-2678.

30. Moroni, L., J.R. de Wijn, and C.A. van Blitterswijk, *3D fiber-deposited scaffolds for tissue engineering: Influence of pores geometry and architecture on dynamic mechanical properties.* Biomaterials, 2006. **27**(7): p. 974-985.

31. Chai, Y.C., et al., *Mechanisms of ectopic bone formation by human osteoprogenitor cells on CaP biomaterial carriers.* Biomaterials, 2012. **33**(11): p. 3127-3142.

32. Hartman, E.H.M., et al., *Ectopic bone formation in rats: the importance of the carrier.* Biomaterials, 2005. **26**(14): p. 1829-1835.

33. Kruyt, M.C., et al., *Analysis of ectopic and orthotopic bone formation in cell-based tissue-engineered constructs in goats.* Biomaterials, 2007. **28**(10): p. 1798-1805.

34. Kruyt, M.C., et al., *Bone tissue engineering in a critical size defect compared to ectopic implantations in the goat.* Journal of Orthopaedic Research, 2004. **22**(3): p. 544-551.

35. Vehof, J.W.M., P.H.M. Spauwen, and J.A. Jansen, *Bone formation in calcium-phosphate-coated titanium mesh.* Biomaterials, 2000. **21**(19): p. 2003-2009.

36. Mavis, B., et al., *Synthesis, characterization and osteoblastic activity of polycaprolactone nanofibers coated with biomimetic calcium phosphate.* Acta Biomaterialia, 2009. **5**(8): p. 3098-3111.

37. Nandakumar, A., et al., *Calcium Phosphate Coated Electrospun Fiber Matrices as Scaffolds for Bone Tissue Engineering.* Langmuir, 2010. **26**(10): p. 7380-7387.

38. Polini, A., et al., *Osteoinduction of Human Mesenchymal Stem Cells by Bioactive Composite Scaffolds without Supplemental Osteogenic Growth Factors.* PLoS ONE, 2011. **6**(10): p. e26211.

39. Whited, B.M., et al., *Pre-osteoblast infiltration and differentiation in highly porous apatite-coated PLLA electrospun scaffolds.* Biomaterials, 2011. **32**(9): p. 2294-2304.

40. de Jonge, L.T., et al., *In vitro responses to electrosprayed alkaline phosphatase/calcium phosphate composite coatings.* Acta Biomaterialia, 2009. **5**(7): p. 2773-2782.

41. Carlo-Reis, E.C., et al., *Periodontal regeneration using a bilayered PLGA/calcium phosphate construct.* Biomaterials, 2011. **32**: p. 9244-9253.

42. Park, C.H., et al., *Tissue engineering bone-ligament complexes using fiber-guiding scaffolds.* Biomaterials, 2012. **33**: p. 137-145.

Chapter 7

Cryopreservation of cell/scaffold tissue engineered constructs

Abstract

The aim of this work was to study the effect of cryopreservation over the functionality of tissue engineered constructs, analysing the survival and viability of cells seeded, cultured and cryopreserved onto 3D scaffolds. Furthermore, it was also evaluated the effect of cryopreservation over the properties of the scaffold material itself since these are critical for the engineering of most tissues and in particular tissues such as i.e. bone. For this purpose, porous scaffolds, namely fiber meshes based on a starch and poly(caprolactone) blend (SPCL) were seeded with goat bone marrow stem cells (GBMSCs) and cryopreserved for 7 days. Discs of the same material seeded with GBMSCs were also used as controls. After this period, these samples were analyzed and compared to samples collected before the cryopreservation process. The obtained results demonstrate that it is possible to maintain cell viability and scaffolds properties upon cryopreservation of tissue engineered constructs based on starch scaffolds and goat bone marrow mesenchymal cells using standard cryopreservation methods. In addition, the outcomes of this study suggest that the greater porosity and interconnectivity of scaffolds favor the retention of cellular content and cellular viability during cryopreservation processes, when comparing to nonporous discs. These findings indicate that it might be possible to prepare off-the-shelf engineered tissue substitutes and preserve them in order to be immediately available upon patient's needs.

This chapter is based on the following publlication:

Costa P.F., Dias A., Reis R.L., Gomes M.E., 2012, Cryopreservation of cell/scaffold tissue engineered constructs, *Tissue Engineering Part C: Methods*, 18(11): 852-858

1. Introduction

Tissue engineering is showing an increasing advancement as time goes by while cell-scaffold constructs are expected to find a growing number of applications in the regeneration of human tissues. As the first engineered tissue substitutes are concurrently undergoing clinical trials, and foreseeing a growing demand for cultured cells and tissues, the tissue engineering community is becoming increasingly worried about the challenge of providing sufficient amount of these products to the market.

One major such obstacle is related to preserving and storing "living" biomaterials. Maintaining large stocks of living tissues will become an important issue for manufacturers and/or distributors, in order for them to be able to ensure a steady supply of tissue substitutes. Hospitals will as well feel the need to create tissue banks due to unpredictable demand for specific tissues in clinical settings [1, 2].

Given that simple preservation techniques, such as refrigeration or tissue culture, have drawbacks including limited shelf-life, high cost, risk of contamination or genetic drift, cryopreservation becomes a more viable option. This approach is based on the principle that chemical, biological and physical processes are effectively "suspended" at cryogenic temperatures [2].

The process of developing tissue substitutes can as well require long time spans, as long as several weeks. Starting from the isolation of autogenous cells to the *in vitro* expansion followed by the seeding and culture of those cells on a scaffold and finally to implantation [3-7], there is a resulting excessively long incapacitation of patients. In order to overcome this problem, an alternative approach, facilitating the large-scale clinical use of engineered tissues, would be the cryopreservation of constructs, that is, the cryopreservation of cells previously seeded and cultured onto scaffolds. This would be a way to generate a reliable source of readily available and ready to implant engineered constructs, greatly reducing the incapacitation time of patients.

Nevertheless, very few studies have focused on this problem [8-12]. Thus, the present study aimed at analysing the effect of cryopreservation over cells while seeded and contained into porous and nonporous constructs as well as the effect of cryopreservation over the morphological and mechanical properties of the scaffold itself which are critical for the engineering of various tissues. Porosity and mechanical properties are important features in tissue engineering scaffolding, particularly for hard/structural tissues such as bone. Scaffolds intended to replace tissues such as bone must preferably possess highly and fully interconnected open pore geometry, providing large surface-area volume ratios and allowing for sufficient diffusion of nutrients and gases and removal of cellular metabolic waste for in vitro culture, but also to enable the tissue and vascularity ingrowth upon

implantation. Apart from being able to maintain the spaces required for cell in-growth and matrix production, scaffolds for bone tissue engineering should also *a priori* possess enough mechanical properties to provide structural support for neo-tissue formation upon implantation of the construct [13]. Taking all of this into consideration, we submitted cell-seeded and non seeded constructs to a standard cryopreservation procedure for a period of 7 days and then, after a short recovery period, compared their response, in terms of cell viability and proliferation as well as concerning the surface and mechanical material properties, to constructs collected immediately before cryopreservation.

2. Materials and Methods

2.1 Preparation of porous scaffolds and nonporous discs

Porous scaffolds and nonporous discs were produced using a polymeric mixture of corn starch and polycaprolactone (30/70 wt.%) designated by SPCL (Novamont, Italy). The nonporous discs were produced by injection moulding in a Klockner Ferromatic FM-20 machine using a mould that allowed obtaining discs with 8 mm diameter and 3 mm thickness. The porous scaffolds were produced through a pre-established fiber bonding methodology [14, 15], briefly consisting of bonding fibers previously obtained by melt spinning by heat and pressure, and then cut into 8 mm diameter and 3.5–4 mm thick samples. All samples were sterilized with ethylene oxide before cell culture studies.

2.2 Cell seeding and culturing onto porous scaffolds and nonporous discs

Goat bone marrow stromal cells (GBMSC) were harvested from the iliac crest of adult goats and isolated as described elsewhere [16] and then expanded in low-glucose Dulbecco's modified essential medium (DMEM; Sigma Chemical Co., St. Louis, MO, USA) supplemented with 1% antibiotic/antimycotic (Sigma) and 10% fetal bovine serum (FBS; Sigma). When confluence was reached, cells were trypsinized and ressuspended (at passage 4). From the obtained cell suspension, and given the difference in surface area available for cell attachment, two different cellular concentrations were prepared: one cell suspension to seed $5x10^5$ cells in 300 µl volumes, for the scaffolds, and the other in order to seed $1x10^5$ cells in volumes of 200 µl onto the surface of SPCL discs. The rationale used for the cell seeding density used in this work was based in previously performed studies [16] which showed that a ratio of 5:1 was appropriate for being able to seed a similar amount of these cells per surface

area in both porous and nonporous scaffolds and allowing for the formation of extracellular matrix and osteoblastic differentiation. All the scaffolds/discs were placed in 24 well non-adherent plates in order to perform the seeding.

After seeding, these samples were carefully transferred into the incubator and left there for three hours, before adding 1,5 ml of DMEM basal medium. The samples were cultured for 7 days, being the medium changed every 2 or 3 days. Scaffolds and discs without cells were kept in the same conditions to be used as experimental controls.

2.3 Cryopreservation of cell-seeded porous scaffolds and nonporous discs

After 7 days of culture, half of the previously seeded constructs, as well as unseeded scaffolds and discs, were collected for characterization assays, namely MTS, DNA quantification, SEM, micro-CT and mechanical analysis while the other half of the constructs was cryopreserved, along with some more unseeded scaffolds and discs. For the cryopreservation step, a cryopreservative solution composed of DMSO and FBS was used for suspending the seeded and unseeded scaffold and discs. The concentration of DMSO to use in the cryoprotective solution was determined by estimating the amount of cells in the scaffolds after 7 days of culture, using data obtained in previous studies [17]. A period of 7 days of cryopreservation was chosen taking into consideration previous studies performed in the field which state that the duration of the storage in liquid nitrogen (-196ºC) has a negligible impact on constructs. Those studies used even shorter cryopreservation periods (less than one day) [18].Thus, for each million of cells, a 10% concentration of DMSO was added to the cryopreservative solution. All seeded and unseeded scaffolds and discs were suspended in cryoprotective solution inside standard cryovials and placed inside a Statebourne Biosystem 24 cryogenic tank.

2.4 Thawing of cell-seeded porous scaffolds and nonporous discs after cryopreservation

After 7 days of cryopreservation, the constructs and unseeded scaffolds/discs were removed from the cryogenic tank and partially thawed in a 37°C waterbath, removed from the cryovials and placed in 24 well non-adherent plates. To each sample, a volume of cold DMEM basal medium with 20% FBS was added. The samples were further cultured for 9 days being the medium changed every 2 or 3 days in order to allow cells to recover from the cryopreservation step. Cells alone and tissues that are submitted

to cryopreservation always require a certain time to recover. Studies found in the literature have shown that, after thawing, cellular viability tends to decrease for a period of at least 7 days before stabilizing[19]. This recovery culture period also allowed for a more prolonged and more efficient leaching of toxic DMSO's residues, in particular from the porous constructs. The recovery culture period was not prolonged for longer than 9 days since the strategy involved in a medically oriented usage of these constructs would consist of applying these constructs into tissue defects as quickly as possible after thawing in order to reduce patient's immobilization time. After this time, all the remaining samples were used for characterization assays, namely MTS, DNA quantification, SEM, micro-CT and mechanical analysis.

2.5 Collection of cell-seeded porous scaffold and nonporous disc samples for biological analysis

After each culturing period, the collected cell-seeded cells/scaffolds samples were washed at least twice with 1ml of sterile PBS. In the case of the cells/scaffolds constructs to be used in DNA quantifications, each sample was transferred to a sterile tube with 1ml of ultra-pure water. After this procedure, the tubes with samples were kept at a temperature of -80°C until further analysis.

2.6 MTS quantification

Cellular viability was quantitatively assessed by the MTS [3-(4,5-dimethylthiazol-2-yl)-5-(3-carboxymethoxyphenyl)-2-(4-sulfophenyl)-2H-tetrazolium] assay (Promega, Madison, USA) [33]. Culture medium without FBS and phenol red was mixed with MTS in a ratio of 5:1 and added to wells containing the constructs to be analyzed. The constructs were incubated in this solution for 3 hours at 37°C in a 5% CO2 atmosphere. After the incubation period, the optical density (OD) was read in a microplate reader (Bio-Tek, Synergie HT, USA) at 490 nm. A total of 9 samples per study group/condition were analyzed being measurements made in triplicate. The obtained results were normalized to the surface area of each type of sample used (discs or scaffolds).

2.7 DNA quantification

The previously frozen samples were defrosted at room temperature and submitted to an ultrasound bath for about 15 minutes, to ensure the removal of all cell content from the scaffolds. Double-stranded DNA (dsDNA) content was then measured using a fluorimetric PicoGreen dsDNA Quantification Kit (P7589, Invitrogen, Molecular Probes, USA). Experimental samples and standards (0–2 μg/ml) were added to a white opaque 96-well plate. The procedure followed was based on the manufacturer instructions. Fluorescence was quantified using a microplate reader (Bio-Tek, Synergie HT, USA) at an excitation of A485/20 and at an emission of A528/20. A total of 9 samples per study group/condition were analyzed being measurements made in triplicate. The obtained results were normalized to the surface area of each type of sample used (discs or scaffolds).

2.8 Scanning electron microscopy (SEM)

Constructs to be observed on the scanning electron microscope (SEM) (Leica Cambridge S360, Leica Cambridge, UK), were fixated in a 2.5% glutaraldehyde solution (Sigma-Aldrich, Germany) for 1 hour at 4°C, dehydrated using an increasing concentration series of ethanol solutions (20%, 30%, 50%, 70%, 90% and 100% (v/v)), left to dry overnight at room temperature, and finally sputter-coated with gold in a Sputter Jeol JFC 1100 equipment. The controls (unseeded scaffolds/discs) were merely submitted to the sputter coating part of this procedure. A total of 6 samples per study group/condition were analyzed.

2.9 Micro computerized tomography (micro-CT)

Micro computerized tomography was performed in order to quantify the porosity of the several scaffolds produced as well as their surface area. For this analysis, a SkyScan 1072 equipment was used. The x-ray source was set up to 40KV, 248μA with a magnification of 23.29x and an exposure time of 1.8 seconds which resulted in a resolution of about 11.32 μm/pixel. The measurements were performed on a total of 9 samples per study group/condition. This analysis was not performed on discs since their porosity is negligible. The surface area of discs was calculated taking into consideration their height and diameter since these were composed of flat surfaces.

2.10 Atomic Force Microscopy (AFM)

The roughness of the samples (SPCL discs) surfaces was measured by AFM. The analysis was performed on 3 samples per study group/condition on at least three spots per sample using tapping mode in a multimode scanning probe microscope (Veeco, USA) connected to a NanoScope III (Veeco, USA) with non-contacting silicon nanoprobes (ca. 300 kHz, setpoint 2–3 V) (Nanosensors, Switzerland). All images were fitted to a plane using the 1st degree flatten procedure included in NanoScope software version 4.43r8.

2.11 Mechanical analysis

Scaffolds and discs were submitted to compression tests before and after cryopreservation for determining their compressive modulus, using a Universal tensile testing machine (Instron 4505 Universal Machine). The tests were performed under compression loading using a crosshead speed of 2 mm/min until 60% strain was reached. The compressive modulus was determined in the most linear region of the stress–strain curve using the secant method. A total of 10 samples per study group/condition were used for this analysis.

2.12 Statistics

DNA and MTS assays results are presented as means ± standard deviation. Statistical evaluation was performed using two-tailed paired Student t tests, to assess the statistical differences between groups at different time points. Statistical significance was defined as $p < 0.05$ for a 95% confidence interval.

3. Results

3.1 Viability, cellular content and morphology of GBMSCs on porous scaffolds and nonporous discs before and after cryopreservation

GBMSCs were successfully seeded and cultured under basal culture conditions on the porous scaffolds and nonporous discs for 7 days. Constructs were cryopreserved under standard conditions for 7 days, thawed and then cultured for a further period of 9 days to allow for full cellular recovery and efficient

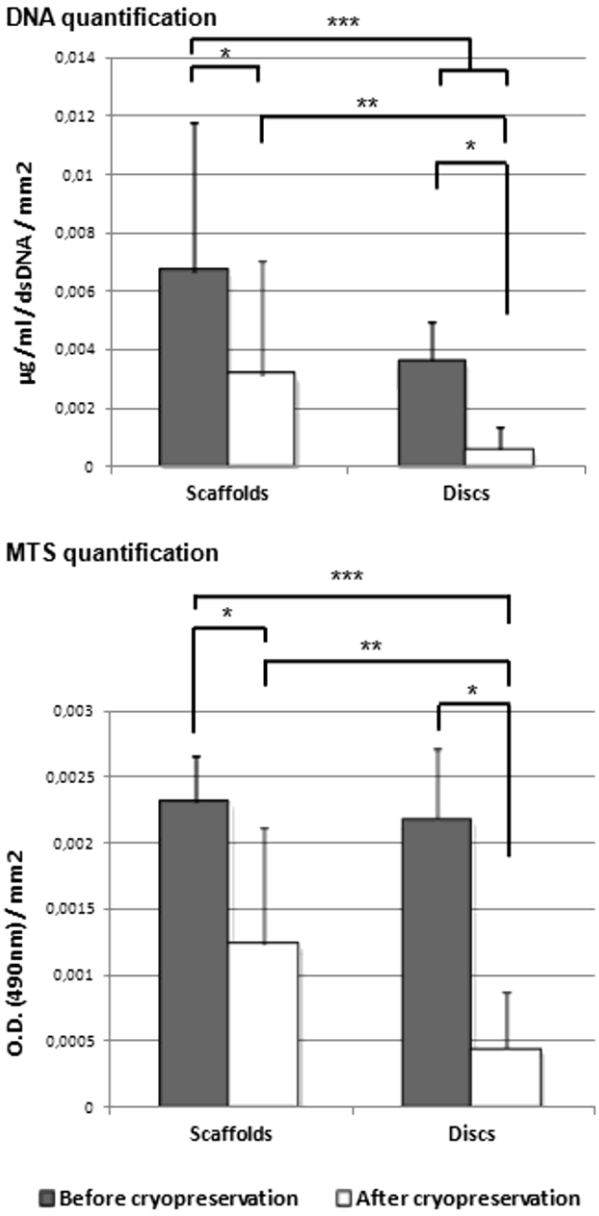

FIG. 7.1 - Quantification of cellular content by DNA quantification and cellular viability by MTS quantification normalized to surface area. *, ** and *** indicate statistical significance ($p<0,05$).

leaching of DMSO residues. By examining the results obtained from the MTS and DNA analysis (Fig. 7.1) performed on seeded scaffolds and discs before and after cryopreservation and by normalizing these values with the surface area of each of both systems it was possible to determine that, despite an expected decrease observed upon cryopreservation, constructs were able to maintain cellular content and cellular viability. It was also possible to notice that cellular viability and DNA content were more efficiently maintained in porous scaffolds than in nonporous discs. The percentage of DNA/cellular content maintained in the constructs after cryopreservation was 46% for porous scaffolds and 15% for nonporous discs while the percentage of cellular viability was 54% for porous scaffolds and 20% for nonporous discs, when comparing to values obtained before cryopreservation. This distinction between

the behavior of cells in porous scaffolds and discs was particularly visible in the MTS data which showed an evolution from statistically similar cellular viability between both groups before cryopreservation to a statistically and significantly higher cellular viability of cells in porous scaffolds after cryopreservation. These results corroborated our expectations that cells seeded in porous scaffolds would be better preserved given that the scaffold´s pores would retain the cryoprotectant more efficiently. As well, and also importantly, these results showed that, along with a prolonged recovery time for cellular viability stabilization, there was an effective removal of the cryoprotectant from the porous scaffold after cryopreservation. Cryoprotectants, in particular the one we used (DMSO), are known to be highly toxic for cells and, for this reason, it would be crucial not only to maintain the cryoprotectant inside the scaffold during cryopreservation but also to make sure it would be efficiently removed after cryopreservation. For the efficiency of the cryoprotectant's removal contributed the scaffold's specific porosity and architecture.

Through the SEM analysis (Fig. 7.2) it was possible to observe that the cellular morphology was not affected by the cryopreservation process and that cells remained well attached to the material's surfaces after thawing.

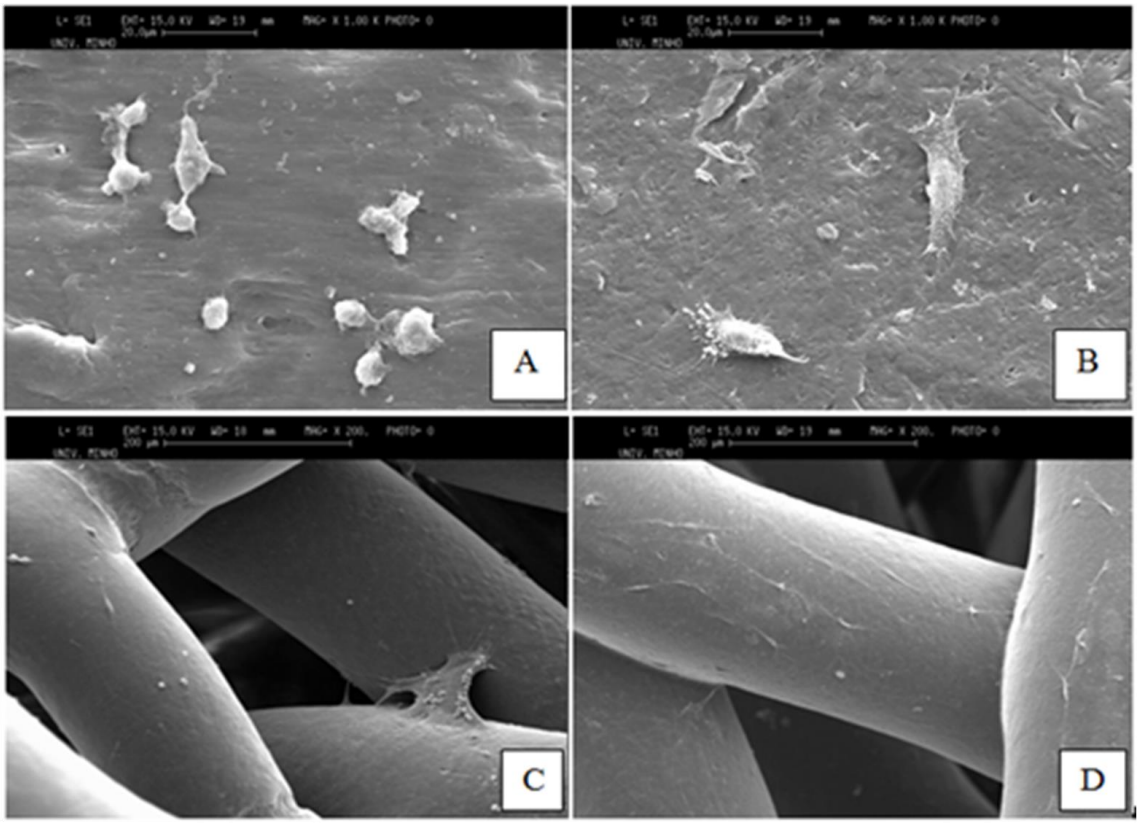

FIG. 7.2 - SEM micrographs of SPCL discs and scaffolds before and after cryopreservation at magnification 1000x. GBMC-seeded SPCL discs before A) and after B) cryopreservation (magnification 1000x); GBMC-seeded SPCL scaffolds before C) and after D) cryopreservation (magnification 200x)

3.2 Morphology, surface topography and architecture of porous scaffolds and nonporous discs before and after cryopreservation

By comparing the SEM micrographs (Fig. 7.2) before and after cryopreservation it was possible to observe that the cryopreservation process did not change the material's surface morphology. After cryopreservation, the surface of the fibers of porous scaffolds as well as the surface of the nonporous discs showed the same smooth topography as before cryopreservation. This was more accurately confirmed by performing an AFM analysis (Fig. 7.3) on the surface of nonporous discs which revealed

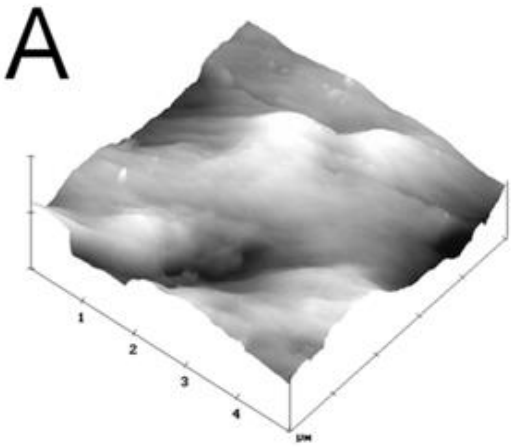

C

	Before Cryopreservation	After Cryopreservation
Average Roughness - Ra (nm)	52,75 ± 4,72	58,71 ± 4,32

FIG. 7.3 - AFM images of SPCL discs before A) and after B) cryopreservation and their average roughnesses C). Values of average roughness before and after cryopreservation were not significantly different (p>0,05).

no significant difference between sample's roughness before and after cryopreservation. It was not possible to perform the same AFM analysis over the porous scaffolds given the very irregular fibrous architecture. In the same way, a micro-ct analysis and reconstruction was performed on the porous scaffolds showing that the cryopreservation process did not alter the general architecture of scaffolds as well as its porosity as show in the performed micro-ct 3D reconstructions (Fig. 7.4A and B) and porosity quantitative analysis results (Fig. 7.4C).

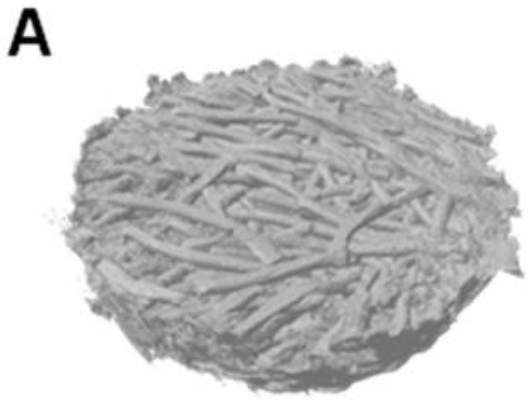

C

	Before Cryopreservation	After Cryopreservation
Average Porosity (%)	50,98 ± 3,98	50,09 ± 3,97

FIG. 7.4 - Micro-CT analysis of fiber bonded scaffolds before A) and after B) cryopreservation. No significant difference was found in terms of scaffold morphology. A quantitative analysis was also performed in order to compare the total porosity of scaffolds before and after cryopreservation C). The values of average porosity before and after cryopreservation were not significantly different ($p>0,05$).

3.3 Mechanical properties of porous scaffolds and nonporous discs before and after cryopreservation

Compression mechanical tests were performed on cryopreserved and non cryopreserved porous scaffolds and nonporous discs. The results showed that the cryopreservation process did not alter the mechanical compressive properties of scaffolds and discs since there was no significant difference found when comparing the values for young´s modulus before and after cryopreservation (Table 7.1).

TABLE 7.1 - Comparative compression mechanical analysis on scaffolds and discs before and after cryopreservation. Values of average Young's modules before and after cryopreservation were not significantly different (p>0,05).

Sample	Average Young's Modulus (Mpa)	
	Before Cryopreservation	After Cryopreservation
Scaffolds	30,46 ± 4,40	29,07 ± 3,62
Discs	83,04 ± 12,19	77,48, ± 3,43

4. Discussion

In this work we were able to show that it is possible to maintain cellular content and cellular viability into cell-seeded constructs in standard cryopreservation conditions as shown by the MTS, DNA and SEM results. Furthermore, we were able to show that the porosity and pore interconnectivity found in porous scaffolds may in fact beneficially influence the viability and retention of cells in constructs exposed to cryopreservation processes. This observation may be explained by a possible retaining and protective effect exerted by the scaffold over the cells contained inside the scaffold's pores against the intrinsic damaging effects of cryopreservation.

As for the morphology of scaffolds and discs, we were able to assess that it was not damaged or altered by the cryopreservation process both at a macroarchitectural level as also in terms of superficial topography. This is an important observation since scaffold's architecture and surface morphology are known to greatly influence the efficiency of cell adhesion and subsequent proliferation over material's surfaces.

Starch–polycaprolactone fiber mesh scaffolds have been extensively studied, demonstrating very promising results, both in vitro and in vivo, for applications in the tissue engineering field [16, 17, 20].

We were also able to assess that the cryopreservation process did not alter the mechanical compressive properties of SPCL based scaffolds and discs since there was no significant difference found when comparing the values for young´s modulus before and after cryopreservation. This means that it would be possible to accurately define construct's mechanical properties prior to cryopreservation aiming at specific tissue applications (in this case, given the mechanical properties of the studied scaffolds, mostly bone and cartilage) without having any detrimental effect caused by the cryopreservation process. The same principle applies to the architecture and surface topography of scaffolds which, as shown by the performed SEM, AFM and micro-CT analysis, are also not affected by the cryopreservation process.

Overall, the obtained results show that it is possible to maintain viable cells and scaffolds properties upon cryopreservation of tissue engineered constructs based on SPCL scaffolds and goat bone marrow mesenchymal cells using standard cryopreservation methods. Also, this study suggests that the architecture found in porous scaffolds favors the retention and viability of construct's cellular content during cryopreservation processes, when compared to nonporous structures. Finally, these findings indicate that it may be possible to prepare off-the-shelf engineered tissue substitutes and preserve them in order to be immediately available upon patient's need.

5. Acknowledgments

This work was partially supported by the European Network of Excellence EXPERTISSUES (NMP3-CT-2004-500283). It is also acknowledged the Portuguese Foundation for Science and Technology for the PhD grant of Pedro Costa (SFRH/BD/62452/2009) and the research grant of Ana Dias in the scope of the research project VivoTissue (PTDC/CVT/67677/2006).

6. References

1. Hirose, M., et al., *Osteogenic potential of cryopreserved human bone marrow-derived mesenchymal cells after thawing in culture.* Mater Sci Eng C, 2004. **24**(3): p. 355-359.

2. Karlsson, J.O. and M. Toner, *Long-term storage of tissues by cryopreservation: critical issues.* Biomaterials, 1996. **17**(3): p. 243-56.

3. Fleming, J.E., Jr., C.N. Cornell, and G.F. Muschler, *Bone cells and matrices in orthopedic tissue engineering.* Orthop Clin North Am, 2000. **31**(3): p. 357-74.

4. Hutmacher, D.W., *Scaffolds in tissue engineering bone and cartilage.* Biomaterials, 2000. **21**(24): p. 2529-43.

5. Kim, B.S. and D.J. Mooney, *Development of biocompatible synthetic extracellular matrices for tissue engineering.* Trends Biotechnol, 1998. **16**(5): p. 224-30.

6. Perka, C., et al., *Tissue engineered cartilage repair using cryopreserved and noncryopreserved chondrocytes.* Clin Orthop Relat Res, 2000(378): p. 245-54.

7. Vacanti, C.A. and L.J. Bonassar, *An overview of tissue engineered bone.* Clin Orthop Relat Res, 1999(367 Suppl): p. S375-81.

8. Miyoshi, H., et al., *Cryopreservation of Fibroblasts Immobilized Within a Porous Scaffold: Effects of Preculture and Collagen Coating of Scaffold on Performance of Three-Dimensional Cryopreservation.* Artificial Organs, 2010. **34**(7): p. 609-614.

9. Yin, H., et al., *Vitreous cryopreservation of tissue engineered bone composed of bone marrow mesenchymal stem cells and partially demineralized bone matrix.* Cryobiology, 2009. **59**(2): p. 180-187.

10. Rupf, T., et al., *Cryopreservation of Organotypical Cultures Based on 3D Scaffolds.* Cryoletters, 2010. **31**(2): p. 157-168.

11. Bernemann, I., M. Kuberka, and B. Glasmacher, *71. Adapted freezing and thawing procedures to improve the cryopreservation of cell seeded scaffolds.* Cryobiology, 2006. **53**(3): p. 397-398.

12. Kofron, M.D., et al., *Cryopreservation of tissue engineered constructs for bone.* Journal of Orthopaedic Research, 2003. **21**(6): p. 1005-1010.

13. Salgado, A.J., O.P. Coutinho, and R.L. Reis, *Bone Tissue Engineering: State of the Art and Future Trends.* Macromolecular Bioscience, 2004. **4**(8): p. 743-765.

14. Mendes, S.C., et al., *Evaluation of two biodegradable polymeric systems as substrates for bone tissue engineering.* Tissue Eng, 2003. **9 Suppl 1**: p. S91-101.

15. Gomes, M.E., et al., *Influence of the porosity of starch-based fiber mesh scaffolds on the proliferation and osteogenic differentiation of bone marrow stromal cells cultured in a flow perfusion bioreactor.* Tissue Eng, 2006. **12**(4): p. 801-809.

16. Rodrigues, M.T., et al., *Tissue-engineered constructs based on SPCL scaffolds cultured with goat marrow cells: functionality in femoral defects.* Journal of Tissue Engineering and Regenerative Medicine, 2011. **5**(1): p. 41-49.

17. Gomes, M.E., et al., *Effect of flow perfusion on the osteogenic differentiation of bone marrow stromal cells cultured on starch-based three-dimensional scaffolds.* J Biomed Mater Res A, 2003. **67**(1): p. 87-95.

18. Wen, F., et al., *Vitreous cryopreservation of nanofibrous tissue-engineered constructs generated using mesenchymal stromal cells.* Tissue Engineering - Part C: Methods, 2009. **15**(1): p. 105-114.

19. Lübke, C., et al., *Cryopreservation of Artificial Cartilage: Viability and Functional Examination after Thawing.* Cells Tissues Organs, 2001. **169**(4): p. 368-376.

20. Tuzlakoglu, K., et al., *Nano- and micro-fiber combined scaffolds: A new architecture for bone tissue engineering.* Journal of Materials Science: Materials in Medicine, 2005. **16**(12): p. 1099-1104.

Section III

General conclusions

Chapter 8

General conclusions and future work

1. Conclusions

Over the last two decades, tissue engineering has shown great promise in the regeneration of human tissues. Despite the clear evidences that tissue engineering can be applied to the replacement and regeneration of damaged tissues, its translation from the lab to clinical widespread application has experienced important obstacles. This can be mostly explained by the complexity of the majority of the human tissues, that requires labour-intensive procedures to achieve functional tissue-like substitutes and to the inability of tissue engineering companies to shift from these methodologies to industrial/mass production processes. Automation is therefore seen as an urgently required means for enabling this transition. Several automated tools and strategies have been adopted by tissue engineering over time, among them additive manufacturing and bioreactor technologies, which were the focus of the work presented in this thesis.

Therefore, the work described in this thesis, namely under chapters 3, 4 and 5 reports to the use of the additive manufacturing technology to develop advanced cell/tissue culture systems composed of scaffolds contained into specifically designed bioreactor chambers. In the work described in chapter 4, and by resorting to medical imaging technologies, the first application of this concept allowed to additively manufacture bone tissue replicas which were simultaneously and concomitantly manufactured with enclosing culture chambers. As a proof of concept, this technology was employed in the design and fabrication of a sheep-tibia scaffold around which a bioreactor chamber of similar shape was simultaneously constructed. The morphology of the resulting device was investigated by micro-computed tomography and scanning electron microscopy confirming the porous architecture of the internal scaffold as opposed to the non-porous nature of the bioreactor chamber. Additionally, this study demonstrated that both the shape, as well as the inner architecture of the device can significantly impact the perfusion of fluid within the scaffold. Indeed, fluid flow modelling revealed that this was of significant importance for controlling the fluid flow pattern within the scaffold and the device, avoiding the formation of stagnant regions detrimental for *in vitro* tissue development. The design of these culture chambers was optimized by resorting to fluid flow simulation models which allowed to predict the behavior of fluids resulting from the integration into a perfusion culture system. As a result, an optimal chamber design was achieved and multiple copies were additively manufactured for further

testing. The additive manufacturing fabrication of each of the culture devices utilized was completed within 45 minutes, being the inner scaffold further post-treated with sodium hydroxide for increased hydrophilicity and the outer chamber post-treated with an ABS solution for increased watertightness. Finally, to demonstrate the feasibility of the proposed approach/construct, osteoblast cells were seeded into the replica scaffold and cultured over a period of 6 weeks under flow perfusion. The perfusion culture was performed bidirectionally by means of a standard syring pump. After culture, and due to the proposed design of the culture chambers, the cultured scaffolds could be easily collected from the interior of the device by simply cutting the device's walls with sterile scissors and tweezers. The analysis of the extracted constructs showed that the cell seeding was homogeneous throughout the whole scaffolds despite their large dimensions. Furthermore, cells found throughout the full thickness of those same large constructs were viable during the full duration of the 6 week study. This work demonstrated a novel application for additive manufacturing in the development of scaffolds and bioreactors which would contribute to the advancement of customized tissue engineering strategies for a wide range of applications. Unlike the large majority of bioreactors utilized in tissue engineering, which typically only enable culturing small cylindrical constructs, the device herein developed can be easily adapted on the fly to any construct's shape and size. Furthermore, this technology allows developing bioreactors that can be specifically designed to optimize aspects such as medium volumes or medium fluid flow patterns which in turn can modulate cellular density, survival and development. This high degree of versatility enabled by the utilization of additive manufacturing also allows to freely design the inner scaffold itself, independently. Furthermore, the enclosure (bioreactor chamber) and the inner scaffold can be built from a wide array of materiais which are currently available as well as many more materials which can be developed/optimized in the future. Apart from the melt-based FDM additive manufacturing employed in the work described in this thesis, many other additive manufacturing technologies are already available, which are capable of utilizing materials as demanding as i.e. metals or ceramics, hence increasing even more the range of materials to use in the fabrication of tissue engineering bioreactors and scaffolds, meeting broader requirements. Furthermore, due to the enclosed nature of the developed bioreactor, it becomes now safer to culture tissue engineered constructs as well as to transport them to various environments (such as i.e. surgery rooms) since the exposure to external contaminants can be greatly reduced by the device's outer walls. To our knowledge, this new concept employs additive manufacturing in a way that has never been used before. Furthermore, and most importantly, this new concept enables the development and fabrication of highly tailored culture systems which are as well inexpensive, easy to build, easy to use and highly versatile.

In order to become commercially viable, tissue engineering must not only become an automated process but must be as well able to generate large amounts of tissue substitutes in a scenario of widespread utilization of tissue engineered products. High throughput screening is a methodology which greatly relies on automation for producing large amounts of samples which can afterwards be tested and analyzed through equally automated technologies. In a tissue engineering context, high throughput screening can be used for testing and optimizing the combination of tissue engineered constructs possessing variable properties with variable culture conditions being therefore an extreme case of mass production of tissue engineered constructs samples. In this sense, additive manufacturing was again utilized in chapter 5 of this thesis to optimize and produce an up-scalable perfusion-based culture device enabling to simultaneously seed and culture large amounts of scaffolds in its interior. The developed device was also designed to enable surface modification of scaffolds by perfusion with aqueous solutions. As a proof-of-concept, the developed device was utilized to deposit a calcium phosphate osteoinductive coating over the surface of scaffolds which were then seeded and cultured with osteoblast for a period of 4 weeks. The technique utilized allowed the simultaneous *in vitro* culture of a total of 96 scaffolds under controlled bi-directional perfusion. The analysis of the resulting constructs demonstrated that the developed device was able to promote homogeneous cell adhesion over the surface of scaffolds as well as cellular proliferation along the culture period as shown by DNA quantification assays. The presence of the calcium phosphate coating showed to further improve these results when comparing to non-coated scaffolds seeded and cultured under the same conditions. The methodology developed in this work exemplifies the applicability of additive manufacturing as a tool for achieving further automation of HTS in the field of biomedical science and biotechnology as well as the potential to enable mass production of large ammounts of tissue engineered constructs. The most important feature of the developed device is that it allows to easily add a third dimension to HTS, unlike the majority of currently existing HTS devices which are only capable of performing 2D cultures. In this way, more realistic screening can be achieved since it is well known that cells behave and develop differently depending on wether they are in a 3D or a 2D environment. By employing additive manufacturing to simultaneously build unlimited amounts of 3D culture environments, HTS is able to become more realistic and therefore more closely mimic events happening in natural living tissues. Furthermore, given that the developed platform is 3D and not 2D, it becomes possible to upscale and highly optimize the number of tests to device size ratio allowing to develop systems with large number of 3D test chambers contained into very small devices.

Additive manufacturing can as well be combined with other technologies to produce constructs with greater complexity. In the work described in chapter 6 we have been able to combine additively manufactured scaffolds with a melt electrospinning technology for producing single biphasic scaffolds for the regeneration of the bone-periodontal ligament-cementum interface. The additively manufactured part of the scaffold was further treated by adding an osteoinductive coating in order to promote the formation of bone tissue into that section of the scaffold upon implantation. The electrospun part of the scaffold was attached to the additively manufactured scaffold by means of a melt and press-fitting methodology. The porous additively manufactured part of the scaffold was then seeded with osteoblasts in order to generate a construct similar to the bone found anchoring teeth. On the other hand, the electrospun part of the scaffold served as a support for the deposition of periodontal ligament cell sheets which would later be responsible for the attachment of the scaffold's bone construct to a dentin block intended to simulate the surface of teeth. The biphasic construct was subcutaneously implanted in rats in order to assess the efficacy of this tissue engineered guided tissue regeneration strategy. The deposition of periodontal ligament cell sheets resulted in a greater degree of attachment at the bone-tooth interface after 8 weeks of *in vivo* implantation. The biomimetic coating was as well responsible for increasing the quality of the bone tissue formed at the additively manufactured part of the scaffold by accelerating its formation *in vivo* as well as during the preceding *in vitro* culture stage. In short, the biphasic scaffold design studied in this work was able to display suitable properties for periodontal regeneration based on faultless tissue integration of both compartments, high levels of vascularization and tissue orientation in both the bone and most importantly periodontal compartment, allowing for significant fiber attachment formation. Unlike many other suggested treatments for defects resulting from severe cases of periodontitis, the scaffold herein developed resulted as a single all-in-one solution since it was able to simultaneously fulfill three main principles, namely wound stabilization due to its mechanical properties, space maintenance due to the creation of integrated cavities and selective cell repopulation due to its biphasic nature. The ability of the developed scaffold to generate organized and oriented tissues is also an important feature which is rarely achieved in such a simple and straightforward way. Furthermore, given the ability of the developed device to serve as a template for the regeneration of the studied interface, it might also be be adapted to other tissue interfaces such as, for example, osteochondral or bone-ligament interfaces.

Finally, the mass production and usage of tissue engineering and regenerative medicine products would also be much benefited if an efficient way to store such constructs could be found and optimized. To that end, in the work described in chapter 7, we have evaluated a simple methodology to store tissue

engineered constructs by means of cryopreservation which is know to enable the suspension of chemical, biological and physical processes for long periods of time. This study consisted of a comparative study in which both porous scaffolds and non-porous discs were seeded with goat bone marrow stem cells and cryopreserved for 7 days. By comparing to non cryopreserved constructs it was possible to evaluate the effect of cryopreservation. The obtained results showed that it is possible to maintain viable cells and scaffolds properties upon cryopreservation of tissue engineered constructs based on SPCL scaffolds and goat bone marrow mesenchymal cells using standard cryopreservation methods. Futhermore, this study suggested that the architecture found in porous scaffolds may be able to favor the retention and viability of construct's cellular content during cryopreservation processes, when comparing to nonporous structures. Given that currently the process of developing tissue substitutes still requires long time spans (as long as several weeks) and that, if applied, such strategy would require excessively long incapacitation of patients, the concept of cryopreserved off-the-shelf tissue engineered products would definitely make a significant difference in patient's quality of life. Such products would also be of substantive value in situations of high demand (i.e. large scale disasters) to which currently there are no effective solutions. Finally, the device and method described in the patent in annex 1, was thought at solving a major obstacle in tissue engineering, which is vascularization. Very few tissues are able to survive without integrating a proper vascular network providing nutrition which can as well withstand a certain level of biomechanical constraints. The cellular construct achievable through the described method would allow to more quickly generate blood vessel substitutes since they would *a priori* possess such properties given their integrated electrospun mesh. Apart from the mechanical properties, and very importantly, this mesh enables as well an efficient way of segregating and placing each of the cellular types forming blood vessels (fibroblasts, endothelial and smooth muscle cells) into their respective locations in the vessel, hence more closely mimicking the natural structure of blood vessels.

As a final remark, we believe that the work developed in the scope of this PhD thesis has contributed to further unveil the high potential of additive manufacturing in tissue engineering applications, in particular when combined with other technologies such as electrospinning, biomimetic surface treatments and bioreactor technologies. Such combined technologies will in the future enable the application of substantial degrees of automation into the fabrication of tissue engineering products which will in turn become more accessible and more commonly considered as practical and viable solutions for tissue regeneration. Furthermore, and relating to the work developed in the final part of this thesis, we believe that it may become possible in the future to prepare off-the-shelf engineered

tissue substitutes and preserve them in order to be immediately available upon patient's need. Therefore, the concept of mass produced and pacient-specifc replacement body parts is becoming closer to reality, however much more technological development and process optimization is needed for it to become common practise.

2. Future work

The work developed in the scope of this PhD provides strong evidence of the enormous potential residing in the automation of tissue engineering and simultaneously opens the way to many other possible approaches that can be further explored in future.

For example, related to the work described in chapters 3 to 5 of this thesis, more complex culture devices could be developed in the future in order to enable the simultaneous culture of large amounts of tissue constructs either for mass production of tissue substitutes or for high throughput screening purposes. Given that the developed devices were duly validated, a scaleup of the devices and/or of the device systems would be the first logical step. In this way, devices able to seed and culture large ammounts of tissue substitutes under standardized, traceable, cost-effective, safe and regulatory-compliant conditions would facilitate the realization of a scenario of widespread adoption of tissue engineering-based therapies in which large amounts of tissue substitutes would need to be simultaneously produced in order to fulfil demands.

In a high throughput screening perspective, as shown in chapter 5 of this thesis, the developed device and its design process could as well be improved. The success of a high throughput screening technology resides mainly on its ability to simultaneously expose large amounts of samples to varying ranges of factors in short periods of time and space and therefore high throughput screening tends to test large batches of samples simultaneously into one single device. As the number of samples and variable factors to be tested in a single device increase so does the complexity of the utilized device hence, given that the design of the developed device is performed manually, the increase in device complexity would therefore demand for greater human intervention. Automation of the design process might provide the solution for that issue. In a methodology called parametric design, shapes and objects can be numerically designed by simple introduction of a reduced number of design parameters. By applying parametric design, devices would be automatically designed with reduced human intervention. Given that the developed devices are built by means of an equally automated process of additive manufacturing, a fully automated process could be implemented in which the operator would insert design parameters (such as number, size, shape of scaffolds) and as a result a fully functional

HTS device would be effortlessly fabricated. Furthermore, the same parametrical methodology could as well be applied to the generation of varying chamber and fluid network designs resulting in the generation of multiple culture conditions into individual culture chambers of one same device.

The device and methodology decribed in chapter 4 shows as well a great potential for improvement and optimization. Being the aim of that work to address tailor-made tissue engineering, a wide range of new applications can be envisioned. The developed strategy can be virtually applied to the regeneration of any kind of tissue and organ. Given the high versatility of additive manufacturing, the inner and outer architectures of scaffolds and constructs can be made more complex and optimized in order to closely resemble the ones found in native tissues.

The applicability to such wide range of structures would require as well the utilization of a wider range of materials which would be able to more closely mimick the distinct properties of various tissues. In the same way, the combination of multiple materials into the regeneration of tissues would allow for the generation of complex structures composed of multiple types of tissues. A probable first combination of materials would involve the merger of solid materials (such as the ones already used) with more soft and flexible materials such as hydrogels or ready-made structures such as the one described in annex 1 which would enable the combination of soft structures such as blood vessels and nervous networks into more solid structures replicating tissues such as bone. Furthermore, the functionality of materials composing additively manufactured tailor-made scaffolds could as well be enhanced by performing surface treatments such as the ones performed in the devices described in chapters 5 and 6.

The biphasic scaffold utilized in chapter 6 is in fact a good example of the regeneration of multiple kinds of tissues into one same device by combination of materials with diverging properties. Given its ability to simultaneously regenerate bone tissue and periodontal ligament into one single construct both *in vitro* and *in vivo* (in a subcutaneous rat model), further *in vivo* studies should be performed onto larger animal models and into more realistic jaw defects. The *in vitro* generation of such constructs could as well be facilitated or even improved by utilizing dynamic cell culture in a strategy similar to the ones described in chapters 3 to 5. Such culture devices could be designed to segregate the different cell types into their specific scaffold regions and in a way allowing to apply the intended guided tissue regeneration methodology prior to implantation.

Finally, regarding the cryopreservation of tissue engineered constructs studied in chapter 7 of this thesis, although it has been shown to be possible, its efficiency should be further improved in order to become a more viable storage option. Other cryopreservation methodologies and cryoprotectants should as well be studied and compared in a systematic way in order to assess the best methodology or

combination of methodologies. Multiple cell sources should also be tested in this same way in order to assess if cell survival varies according to cellular origin/type.

Annex 1

Single-step method and device for the generation of stratified tubular tissue substitutes

Abstract

Device and method for manufacturing stratified tubular tissue. The device comprises a lower rectangular part (3) over which a porous membrane (4) is centrally placed, a malleable part with a closed (5) or open (6) configuration, provide with tubular structures (9) and defining at least two contiguous cavities in its lower surface, placed over the lower rectangular part (3) and over specific zones of the porous membrane (4), and a third part (7) with screws (8), which compresses the malleable part (5 or 6) and particularly against the porous membrane (4).

This annex is based on the following publlication:

Costa P.F., Martins A., Vaquette C., Neves N.M., Gomes M.E., Hutmacher D.W., Reis R.L., Single-step method and device for the generation of stratified tubular tissue substitutes, World Patent Application WO2013/085404 A1.

1. Object of the invention

The present invention is related to the manufacturing of stratified and tubular tissue substitutes for the replacement/regeneration of composite animal or human tissues, which may have been previously damaged by means of disease or trauma. The present invention describes a device which enables the simultaneous culture of multiple and different cellular types into porous membranes, as well as the method to manufacture stratified tubular tissue substitutes from those porous membranes cultured with multiple different cellular types.

2. Background

Live tissues are assemblies of cells arranged in a specific organized fashion. In some cases, cells are all structurally and functionally alike, forming simple tissues (e.g. cartilage, epithelial and adipose tissues). However, most tissues in the human body contain a mixture of cells with distinctive functions, which may be termed compound tissues (e.g. bone, skin, nervous and vascular tissues. Cells that form tissues can be divided into parenchymal cells, which maintain tissues, and support cells, which provide the structural scaffolding of a tissue. Support cells comprise a set of highly developed cell types with complex metabolic functions and produce an extracellular matrix (ECM) , which largely defines the physical characteristics of a tissue. The support cells together with ECM are organized in an elaborate and hierarchical order to achieve multi-scale functions and to mutually regulate the cellular activity by soluble bioactive molecules, cell-cell direct contact, or cell-ECM interaction. This elaborate structure also provides individual cells with different microenvironments, where cells experience specific cues and show corresponding responses towards tissue function.

Tissue Engineering has been recognized, for some time, as a promising alternative to the use of autografts or allografts for tissue reconstruction and regeneration. This approach utilizes cells, biomaterial scaffolds and signaling molecules for the repair of diseased or damaged tissues. Despite the great progress in this field, development of clinically relevant size tissues with complex architecture remains a great challenge. This is mostly due to limitations of nutrient and oxygen delivery to cells and limited availability of scaffolds, which can mimic the complex live tissue architecture. Biomaterial scaffolds are designed to support cell and tissue growth, aiming at a macroscopic level to be compatible with the mechanical loading of the surrounding organs and tissues but without the need to

recreate the complexity and nanoscale detail observed in tissues and organs at the extracellular level. In a Tissue Engineering and Regenerative Medicine approach, the development of a synthetic ECM is a critical issue, since we need to learn from nature how to engineer biomaterials that will help in recapitulating the early events of morphogenesis that lead to the formation of the hierarchical organization of the ECM and drive the cells to build fully functional adult tissues. To maintain the proper cell phenotype in 3D tissue engineering one needs to achieve biomimetic design to replicate the ECM, seeding/infiltration of cells into a biomaterial scaffold and culturing the seeded scaffold with adequate nutrient supply.

The in vivo microenvironment for each cell type varies from tissue to tissue and from site to site, and this variation provides and conveys specific cues to cells for specific functions. Besides the recognized complex hierarchical organization, cells in tissues constantly experience mechanical stimuli. Therefore, culturing cells in the appropriate biochemical environment and in the presence of mechanical stimuli will provide a more realistic extracellular microenvironment and, consequently, will improve cell-cell and cell-matrix interactions. Various developed bioreactor systems introduce convective flow of the medium to perfuse in vitro-grown 3D tissue constructs, e.g. spinner flasks, rotary vessels or perfusion flow systems. The use of these bioreactor systems can allow a homogeneous cell seeding of the biomaterial scaffold, a good nutrient distribution through the scaffold, and an efficient removal of metabolites at the cellular and sub-cellular levels. Consequently, there is a huge scientific interest in obtaining the appropriate mechanical environments to improve the quality and functionality of the in vitro-generated hybrid constructs.

3. Description of the invention

The present invention describes a device, which enables the simultaneous culture of multiple and different cellular types into porous membranes as well as the method to fabricate stratified tubular tissue substitutes from those porous membranes cultured with multiple different cellular types.

The device herein described allows to separately seeding and culture multiple and different cell types into separate areas of one same porous membrane.

The device allows delimitating multiple watertight areas on the surface of porous membranes by compression of those same membranes over specific zones. This compression is carried out by placing the membrane in between a lower rectangular plate and a malleable part, which defines cavities on its lower surface. This malleable part is in turn compressed against the porous membrane and the lower rectangular plate by means of a third part which is screwed to the lower rectangular plate.

The malleable part, which is part of this device, can be closed, making the cavities that it delimitates closed, or open, making the cavities that it delimitates open to contact with the exterior by means of upper apertures. In order to enable the injection/removal of cellular suspensions and/or culture medium from and to the interior of the closed culture cavities, tubular structures are used, which pierce the walls of the malleable part and connect each of the cavities to the exterior.

This device, in particular in its closed configuration, can be integrated into a dynamic cell culture system able to automatically seed the porous membrane's separate areas, which are delimitated by the device' s culture cavities as well as to renew the culture medium inside those cavities.

Due to the transparency of most of the materials utilized in its construction, this device allows as well for the observation of the interior of the internal chambers through the walls of its parts.

Due to the characteristics of the materials utilized in its construction, the device can as well be easily sterilized by chemical or thermal methodologies.

The method herein described enables the construction of stratified tubular tissue substitutes by resorting to porous membranes possessing specific zones of their surfaces seeded with multiple and different cell types.

The method herein described consists of rolling a porous membrane, which is seeded with multiple and different cell types, around a porous rolling structure. This rolling is started in the extremity of the porous membrane containing the cell type that should be situated in the more internal layer of the stratified tubular tissue substitute and finalized in the extremity containing the cell type which should be located in the tissue substitute's most external layers.

The method herein described is finalized after a culture period, which allows for the adhesion of cells to the surfaces of adjacent membranes. By removing the tubular and porous rolling structure a stratified tubular tissue substitute is generated.

4. Brief description of the drawings

Figure A1 shows in exploded isometric view the device in closed configuration.

Figure A2 shows in isometric view the assembled device in closed configuration.

Figure A3 shows in isometric view a partial section of the assembled device in closed configuration.

Figure A4 shows a longitudinal section of the device in closed configuration.

Figure A5 shows a transversal section of the device in closed configuration.

Figure A6 shows in exploded isometric view the device in open configuration.

Figure A7 shows in isometric view the assembled device in open configuration.

Figure A8 shows in isometric view a partial section of the assembled device in open configuration.

Figure A9 shows longitudinal section of the device in open configuration.

Figure A10 shows a transversal section of the device in open configuration.

Figure A11 shows the device in closed configuration integrated into a complete dynamic cell culture system.

Figure A12 shows the porous membrane and rolling structure before rolling the porous membrane containing three different cellular populations over its surface in order to generate a stratified tubular structure.

Figure A13 shows the porous membrane partially rolled around the rolling structure in order to generate a stratified tubular structure.

Figure A14 shows the porous membrane totally rolled around the rolling structure.

Figure A15 shows a transversal section of the porous membrane rolled around the rolling structure and showing its inner stratified structure possessing different cellular populations located into different layers.

Figure A16 shows the stratified tubular tissue substitute after removal of the rolling structure.

5. Detailed description of the invention

This description refers to a preferential configuration of the invention resorting to the figures in this document in order to allow for a better understanding of the invention.

The device, which may possess a closed 1 or open 2 configuration, comprises a lower rectangular part 3, over which a porous membrane 4 is centrally placed. A malleable part, which can possess a closed 5 or open 6 configuration, defining three contiguous cavities on its lower surface, is placed over the lower rectangular part 3 and over specific zones of the porous membrane 4. By using a third part 7 and screws 8 the malleable part 5 or 6 is compressed against the porous membrane 4. Given that the malleable part 5 or 6 defines three cavities on its lower surface, only the extremities and zones situated in between cavities are compressed. In this way, the surfaces submitted to compression become watertight surfaces consequently generating three watertight cavities.

Tubular structures 9 are added to the closed type malleable part 5) , which pierce its lateral walls and are used for injection, removal and circulation of fluids such as cell suspensions and culture media from/to the interior of the cavities previously delimitated by the device. In this configuration, each device cavity should be connected to the exterior by at least two of these tubular structures 9, in a way to allow the entry of fluids and gases through one tubular structure and the simultaneous exit of excess fluids and gases through the other tubular structure. If desired, by simultaneously controlling the entry

and exit of fluids and gases, it is possible to exert positive or negative pressures to the interior of each cavity.

In case of open type malleable part 6, cell suspensions and culture media are simply placed, removed or circulated into the cavities through their upper apertures.

The lower rectangular part 3 is preferably manufactured from polycarbonate or glass. The preferential utilization of these materials in the manufacturing of this part is related with their chemical, mechanical and optical properties since they are biologically inert, extremely resistant to solvents, possess good dimensional stability and good resistance to high temperatures. The resistance to solvents and high temperatures confers great versatility in terms of the sterilization process to be used since it allows sterilization both through exposure to solvents and to high temperatures (autoclaving) . Additionally, these materials confer an advantage by being transparent, allowing for the content of each cavity to be visualized through the inferior and upper part of the device.

The malleable parts 5 and 6 are manufactured through a molding process, preferably from silicone. Like polycarbonate and glass, silicone is biologically inert, resistant to solvents and to high temperatures. Therefore, these parts can also be sterilized both by exposure to solvents and to high temperatures (autoclaving) . Due to the silicone transparency, these parts allow the content of each cavity to be visualized through its lateral walls, as well as, in the case of the closed malleable part 5, through its upper wall. Additionally, silicone is permeable to gases, enabling the exchange of gases between the culture cavities and the exterior. This feature is particularly important in the case of devices with closed configuration 1.

As for the compression part 7 and screws 8, as they do not come into direct contact with the interior of the culture cavities or the porous membrane 4, they do not need to be transparent or inert and can be manufactured from a greater variety of materials, as long as they are dimensionally stable and resistant to solvents and high temperatures.

The porous membrane 4 should preferably be manufactured from a material or combination of biocompatible and biodegradable materials, which can be processed by various methods, such as electrospinning. The size of the membrane pores should also be preferably less than the diameter of

cells to be cultured onto the membrane surface in order to enable an efficient retention of each specific cell type into specific layers of the tubular structure to be fabricated.

Although the devices herein described possess three cavities, these can vary both in number and in size, according to the intended application.

The devices herein described can simultaneously contain three different cell cultures (one in each cavity) , which can vary in various ways, such as cellular type and density or culture medium used.

In its closed configuration 1, the device can be integrated into a culture system illustrated in figure A11. This system comprises the device 1 connected to a culture medium reservoir 10 by tubes connected to its tubular structures 9. In addition to the connections for entry/exit of medium, the reservoir 10 also possesses a further connection for the entry and exit of gases which are purified by an air filter 11.

Briefly, the culture medium is collected from the culture medium reservoir 10, pumped by a peristaltic pump 12 to the culture cavity inside the device and finally pumped by the same pump 12 again to the culture medium reservoir 10. This process and apparatus is repeated for each one of the individual culture cavities.

For the circulation of culture medium, tubing made from formulations, such as silicone, should preferably used be since they are highly permeable to gases such as carbon dioxide and oxygen, increasing the gas exchange between circulating medium and surrounding atmosphere.

In order to keep a sterile environment, with stable and adequate temperature and humidity, the system is placed inside a cell culture incubator.

The culture system can be used not only for culture but as well as for the seeding of cells onto membranes for cellular growth. Given its small dimensions, this device requires very low volumes of culture medium. For this reason, it is possible to perform dynamic seeding procedures using highly concentrated cell suspensions without using extremely large amounts of cells. In this way, cells have a greater chance to adhere to the porous membrane's surfaces 4 since they are highly concentrated and

are circulated more often through the membrane's surfaces, making the seeding process more efficient.

After sterilization and assembly of the device in its closed 1 or open 2 configuration, containing in its interior an equally sterilized porous membrane by properly compressing its extremities and inter-cavity areas, the device is ready for the start of the cellular seeding over the porous membrane 4 surface.

Cellular seeding can be performed by different ways depending on the device's configuration. When an open configuration device 2 is used, a cell suspension can be simply transferred to the interior of the cavities, through their upper apertures, over the porous membrane's 4 surface. Since there are three contiguous independent cavities, it is possible to transfer suspensions composed of different cell types or combinations of cell types to each one of the cavities. The cell suspension should be of sufficient volume to cover the porous membrane' s surface delimitated by each cavity. After having cell suspensions transferred to the cavities, a lid should be placed over the device in order to avoid evaporation.

When using a closed configuration device 1, the cell suspension is injected into the cavities through one of the tubular structures 9, which connect the cavities to the exterior. The injection can be performed using a syringe attached to the external part of the tubular structure. In this case, the second tubular structure of each cavity should be kept open so that the air, and probably medium excess, are expelled from the chamber and so avoiding excessive pressure. After this procedure all tubular structures should be closed with lids.

When using a closed configuration 1 it is also possible to perform dynamic cellular seeding by means of perfusion using the culture system described in figure A11.

After connecting the system tubing to each cavity tubular structures 9, a cell suspension, previously transferred to the culture medium reservoir 10, is pumped and circulated through the interior of each one of the device cavities.

The required time for performing each one of the seeding methods is variable, depending on various factors such as the type of cells use and operator preferences.

After the cell seeding period, an additional culture medium volume is added to the interior of the cavities or, in case a dynamic seeding/culture system is used, to its culture medium reservoir 10. From this point on, the cell culture period is started. This period can be meant for expansion and/or differentiation, according to the type of supplements included into the culture medium, and can be kept for variable periods of time. During the culture period, culture medium should be regularly renewed, totally or partially, according to the intrinsic necessities of each cell type in culture and to the operator' s preferences. This renewal is performed using the same procedures and apparatus as in the seeding step, after total or partial removal of the culture medium contained into the culture cavities and/or dynamic culture fluidic circuit .

At the end of the cell culture period, culture medium is totally removed from the culture cavities and/or dynamic culture fluidic circuit and the device disassembled.

As a result, a porous membrane seeded 13 with cells in three separate areas of its surface is obtained. Each separate area contains one cell type or combination of cell types different from the ones found in the other seeded areas.

This seeded and cultured porous membrane 13 possessing three different cell types into separate areas of its surface is then rolled around a porous cylindrical or tubular rolling structure 14 in order to generate a stratified tubular structure 15 around that same rolling structure 15. The rolling should be initiated from the porous membrane extremity which is closer to the internal cellular colony 16, that is, the cellular colony which should be located in the more internal layers of the generated stratified tubular structure 15. After that, the intermediate cellular colony 17 is rolled, which shall be located in the intermediate layers of the stratified tubular structure 15, and finally the external cellular colony 18 which shall be located in the more external layers of the stratified tubular structure 18.

The rolling tubular structure 14 should preferentially be porous in order to actively or passively allow a more efficient nutrition of the internal 16 and intermediate 17 cellular colonies while rolled around the rolling structure 14.

After the rolling process, the stratified tubular structure 15 should preferably be kept for a certain period of time rolled around the rolling structure 14 and immersed in culture medium in order to allow the cells contained into the various layers to adhere to the surfaces of membranes in adjacent layers. Furthermore, some kind of biocompatible adhesive, such as, for example fibrin-base sealants, can be applied to the membrane superficial extremities in order to reinforce the formed stratified tubular structure 15 stability.

Finally, after a sufficient culture period over which a consistent cellular matrix can be generated into the stratified tubular structure 15, the tubular rolling structure 14 is removed from the interior of the stratified tubular structure 15. In this way, a ready-to-use stratified tubular tissue substitute 19 is obtained.

The porous rolling structure 14 should preferably be manufactured from politetrafluorethylene (PTFE) . The choice of PTFE for fabricating this structure is justified by its reduced friction coefficient, which facilitates the process of removing the structure from inside the stratified tubular structure 15 and so preventing from damage to the latter structure. Besides, PTFE is characterized by its excellent dimensional stability, constant mechanical properties, inertness and biocompatxbxlity. Finally, it shows also great resistance to solvents and to high temperatures being easily sterilizable by use of solvents or by autoclaving.

6. Claims

1. Device for the separate seeding and culture of multiple and distinctive cell types in separate areas of the same membrane, characterized in that it comprises a lower) rectangular part (3) over which is centrally placed a porous membrane (4) ; a malleable part, which can possess a closed (5) or an open (6) configuration, defining at least two watertight contiguous cavities on its lower surface, placed over the inferior rectangular part (3) and over specific zones of the porous membrane (4) ; and a third part (7) that, by the use of screws (8), compresses the malleable part (5 or 6) against the porous membrane (4) .

2. Device, according to claim 1, characterized in that it allows a closed (5) or an open (6) configuration.

3. Device, according to the previous claims, characterized in that at least two tubular structures (9) are added to the closed type malleable part (5)) , which penetrate its lateral walls and are used for injection, removal and circulation of fluids such as cell suspensions and culture media from/to the interior of the cavities previously delimitated by the device.

4. Device, according to the previous claims, characterized in that the malleable part with a closed (5) or open (6) configuration, which defines at least two contiguous cavities on its lower surface, causes that only the zones of the porous membrane (4) placed under its extremities and zones between cavities are compressed upon compression against the porous membrane (4) and the lower rectangular part (3), making the surfaces subject to watertight surfaces and generating two watertight cavities.

5. Device, according to the previous claims, characterized in that it allows the use of any cell type, from animal or human origin, cell lines or primary cells, in procedures of seeding, adhesion and/or culture.

6. Device, according to the previous claims, characterized in that the porous membrane (4) is preferentially manufactured from a biocompatible material and in that the size of the membrane pores is preferably smaller than the diameter of cells to be cultured onto the membrane surface.

7. Device, according to the previous claims, characterized in that the lower rectangular part (3) , the malleable parts (5) and (6) , the compression part (7) and the screws (8) are manufactured from materials resistant to solvents, possessing good dimensional stability and good resistance to high temperatures, preferentially polycarbonate, glass and silicone; the lower rectangular part (3) being manufactured from a biologically inert material preferably polycarbonate or glass; and the malleable parts (5) and (6) being manufactured from a biologically inert material and through a molding process preferably from silicone.

8. Device, according to the previous claims, characterized in that it is manufactured from transparent materials, preferentially polycarbonate, glass and silicone, able to be sterilized both by chemical and thermal methods.

9. Dynamic culture system using the device for the separate seeding and culture of multiple and distinctive cell types in separate areas of the same porous membrane, characterized in that it is

composed by the closed configuration of the device (1) connected to a culture medium reservoir (10) by tubes connected to its tubular structures (9); the reservoir (10) possesses one connection for the entry/exit of medium and an additional connection for the entry and exit of gases, which are purified by an air filter (11); the culture medium is collected from the culture medium reservoir (10), pumped by a peristaltic pump (12) to the culture cavity inside the device and finally pumped by the same pump (12) back into the culture medium reservoir (10) ; this process and apparatus being repeated for each one of the individual culture cavities contained into the device in its closed configuration (1) .

10. Dynamic culture system, according to claim 9, characterized in that the circulation of the cell seeding suspensions or the expansion or differentiation medium is continuous or discontinuous and performed unidirectionally or bidirectionally.

11. Dynamic culture system, according to the claims 9 and 10, characterized in that it uses tubings made from materials such as silicon, which are permeable to gases, such as carbon dioxide and oxygen, in order to increase the gas exchange between circulating medium and surrounding atmosphere.

12. Method for the generation of stratified tubular tissue substitutes, characterized in that it comprises a first phase of seeding cells on specific areas of the porous membrane (4) located inside and delimitated by internal cavities of a device with a closed (5) or open (6) configuration; followed by a second phase of expansion and/or differentiation of cells cultured at the surface of the porous membrane (4) ; followed by a third phase of rolling of the seeded and cultured porous membrane (13) around a rolling structure (14); and finally followed by a fourth phase of post-culture and removal of the tubular rolling structure (14) from the interior of the stratified tubular structure (15), generating a stratified tubular tissue substitute (19) .

13. Method for the generation of stratified tubular tissue substitutes according to claim 12, characterized by a rolling phase where, after disassembling of the device with a closed (5) or open (6) configuration used in the culture phase, the seeded and cultured porous membrane (13) generated in the interior of that device is rolled around a porous cylindrical or tubular rolling structure (14) initiated from the porous membrane' s extremity which is closer to the internal cellular colony (16), that is, the cell type which should be located in the more internal layers of the generated stratified tubular structure

(15) , and finalized in the external cell type (18) , which shall be located in the more external layers of the stratified tubular structure (18) , in which some kind of biocompatible adhesive can be applied to reinforce the stability of the formed stratified tubular structure.

14. Method for the generation of stratified tubular tissue substitutes according to claims 12 and 13, characterized by a post-culture phase, where the stratified tubular structure (15) is immersed in culture medium to allow the cells contained into the various layers to adhere to the surfaces of membranes in adjacent layers; then, the tubular rolling structure (14) is removed from the interior of the stratified tubular structure (15), generating a stratified tubular tissue substitute (19).

15. Method for the generation of stratified tubular tissue substitutes according to claims 12 to 14, characterized in that a porous rolling structure (14) is manufactured from a material with reduced friction coefficient, good dimensional stability, constant mechanical properties, inertness, biocompatibility, and with great resistance to solvents and to high temperatures, preferentially politetrafluorethylene (PTFE).

7. Amended claims

1. Method for the generation of stratified tubular tissue substitutes, characterized in that it comprises a first phase of seeding cells on specific areas of the porous membrane (4) located inside and delimitated by internal cavities of a device followed by a second phase of expansion and/or differentiation of cells cultured at the surface of the porous membrane (4) ; followed by a third phase of rolling of the seeded and cultured porous membrane (13) around a rolling structure (14); and finally followed by a fourth phase of post-culture and removal of the tubular rolling structure (14) from the interior of the stratified tubular structure (15), generating a stratified tubular tissue substitute (19) .

2. Method for the generation of stratified tubular tissue substitutes according to claim 1, characterized by a rolling phase where the seeded and cultured porous membrane (13) generated in the interior of a device is rolled around a porous cylindrical or tubular rolling structure (14) initiated from the porous membrane's extremity which is closer to the internal cellular colony (16), that is, the cell type which should be located in the more internal layers of the generated stratified tubular structure (15), and finalized in the external cell type (18), which shall be located in the more external layers of the stratified

tubular structure (18), in which some kind of biocompatible adhesive can be applied to reinforce the stability of the formed stratified tubular structure.

3. Method for the generation of stratified tubular tissue substitutes according to the previous claims, characterized by a post-culture phase, where the stratified tubular structure (15) is immersed in culture medium to allow the cells contained into the various layers to adhere to the surfaces of membranes in adjacent layers; then, the tubular rolling structure (14) is removed from the interior of the stratified tubular structure (15), generating a stratified tubular tissue substitute (19).

4. Method for the generation of stratified tubular tissue substitutes according to the previous claims, characterized in that a porous rolling structure (14) is manufactured from a material with reduced friction coefficient, good dimensional stability, constant mechanical properties, inertness, biocompatibility, and with great resistance to solvents and to high temperatures, preferentially politetrafluorethylene (PTFE).

5. Device for the separate seeding and culture of multiple and distinctive cell types in separate areas of a membrane according to claim 1, characterized in that it comprises a lower rectangular part (3) over which is centrally placed a porous membrane (4) ; a part, which can possess a closed (5) or an open (6) configuration, defining at least two watertight contiguous cavities on its lower surface, placed over the inferior rectangular part (3) and over specific zones of the porous membrane (4); and a third part (7) that, by the use of screws (8), compresses the part (5 or 6) against the porous membrane (4) .

6. Device, according to claim 5, characterized in that it allows a closed (5) or an open (6) configuration.

7. Device, according to claims 5 and 6, characterized in that at least two tubular structures (9) are added to the closed type part (5), which penetrate its lateral walls and are used for injection, removal and circulation of fluids such as cell suspensions and culture media from/to the interior of the cavities previously delimitated by the device.

8. Device, according to claims 5 to 7, characterized in that the part with a closed (5) or open (6) configuration, which defines at least two contiguous cavities on its lower surface, causes that only the zones of the porous membrane (4) placed under its extremities and zones between cavities are

compressed upon compression against the porous membrane (4) and the lower rectangular part (3), making the surfaces subject to watertight surfaces and generating two watertight cavities.

9. Device, according to claims 5 to 8, characterized in that it allows the use of any cell type, from animal or human origin, cell lines or primary cells, in procedures of seeding, adhesion and/or culture.

10. Device, according to claims 5 to 9, characterized in that the porous membrane (4) is preferentially manufactured from a biocompatible material and in that the size of the membrane pores is preferably smaller than the diameter of cells to be cultured onto the membrane surface.

11. Device, according to claims 5 to 10, characterized in that the lower rectangular part (3), parts (5) and (6), the compression part (7) and the screws (8) are manufactured from materials resistant to solvents, possessing good dimensional stability and good resistance to high temperatures, preferentially polycarbonate, glass and silicone; the lower rectangular part (3) being manufactured from a biologically inert material preferably polycarbonate or glass; and parts (5) and (6) being manufactured from a biologically inert material and through a molding process preferably from silicone.

12. Device, according to claims 5 to 11, characterized in that it is manufactured from transparent materials, preferentially polycarbonate, glass and silicone, able to be sterilized both by chemical and thermal methods.

13. Dynamic culture system using the device for the separate seeding and culture of multiple and distinctive cell types in separate areas of the same porous membrane, according to claims 1, 5 and 6, characterized in that it is composed by the closed configuration of the device (1) connected to a culture medium reservoir (10) by tubes connected to its tubular structures (9); the reservoir (10) possesses one connection for the entry/exit of medium and an additional connection for the entry and exit of gases, which are purified by an air filter (11) ; the culture medium is collected from the culture medium reservoir (10), pumped by a peristaltic pump (12) to the culture cavity inside the device and finally pumped by the same pump (12) back into the culture medium reservoir (10) ; this process and apparatus being repeated for each one of the individual culture cavities contained into the device in its closed configuration (1) .

14. Dynamic culture system, according to claim 13, characterized in that the circulation of the cell seeding suspensions or the expansion or differentiation medium is continuous or discontinuous and performed unidirectionally or bidirectionally .

15. Dynamic culture system, according to claims 13 and 14, characterized in that it uses tubings made from materials such as silicon, which are permeable to gases, such as carbon dioxide and oxygen, in order to increase the gas exchange between circulating medium and surrounding atmosphere.

8. Amended claims statement

In order to clarify the purpose of such amendments the applicant would like to make the following comments:

In the applicant's view, although both the device and the dynamic culture system for the separate seeding and culture of multiple and distinctive cell types in separate areas of the same membrane are new, the main feature of the present invention can be considered as the method for the generation of stratified tubular tissue substitutes.

The replacement of the previous set of claims intends to redirect the object of the present invention from the device and system for culture of multiple cell types in separate areas of the same membrane to a method for the generation of stratified tubular tissue substitutes.

With these amendments neither the description nor the drawings are affected.

In addition, referring to the remark Clarity in the ISR, the term "malleable" in former claim 1 (new dependent claim 5) was removed, as suggested by the examiner, since its purpose was just to clarify how two contiguous cavities can be watertight. The use of such a property is not strictly necessary to ensure the water tightness.

9. Figures

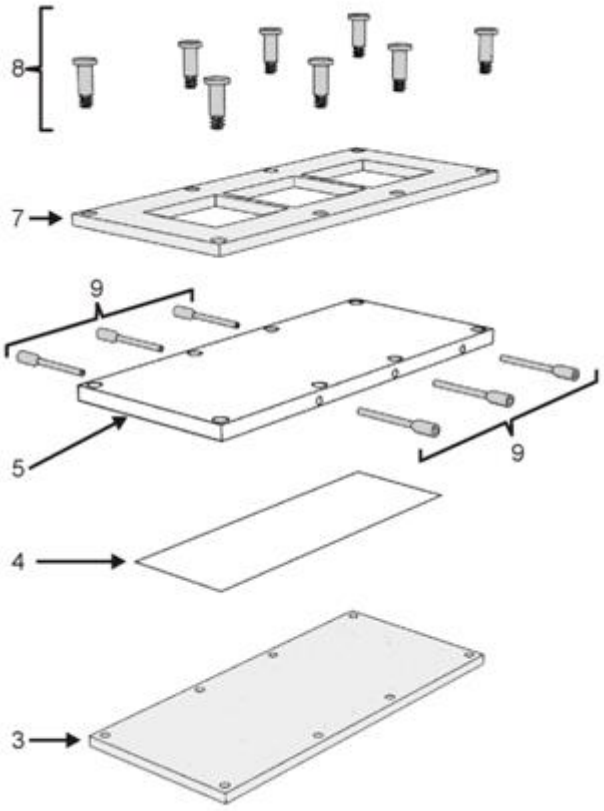

Figure A1- Exploded isometric view of the device in closed configuration.

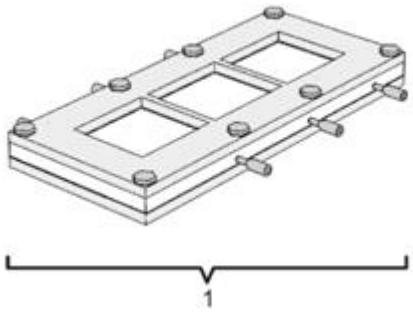

Figure A2 - Isometric view of the assembled device in closed configuration.

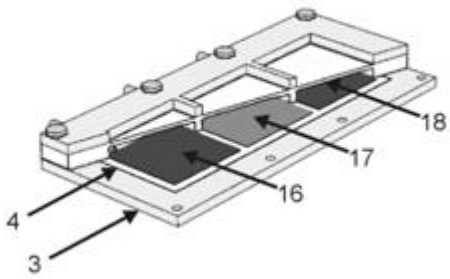

Figure A3 - Isometric view of a partial section of the assembled device in closed configuration.

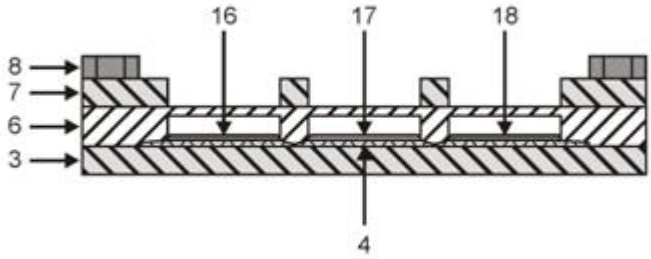

Figure A4 - Longitudinal section of the device in closed configuration.

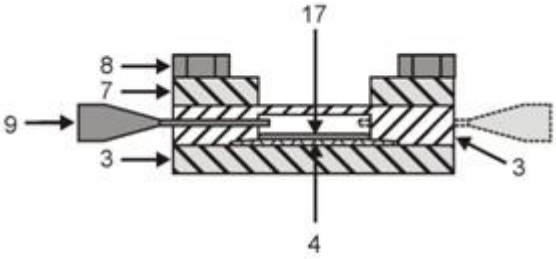

Figure A5 - Transversal section of the device in closed configuration.

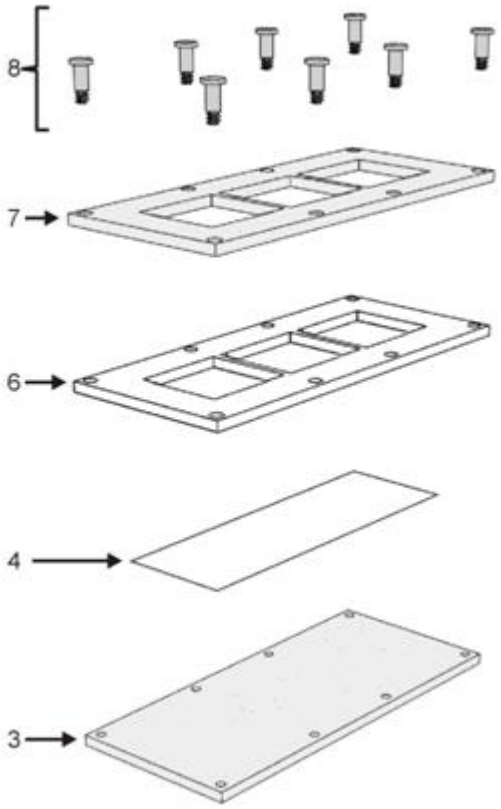

Figure A6 - Exploded isometric view of the device in open configuration.

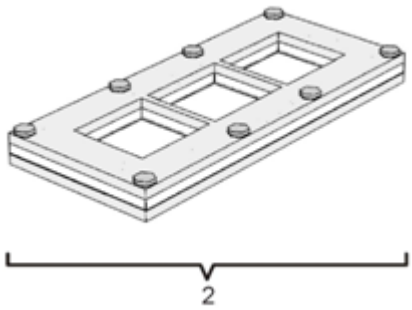

Figure A7 - Isometric view of the assembled device in open configuration.

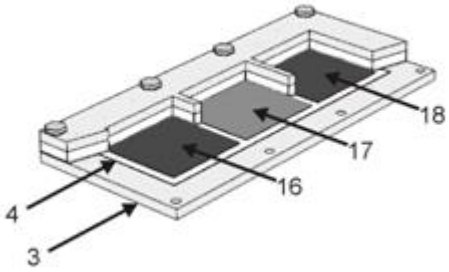

Figure A8 - Isometric view of a partial section of the assembled device in open configuration.

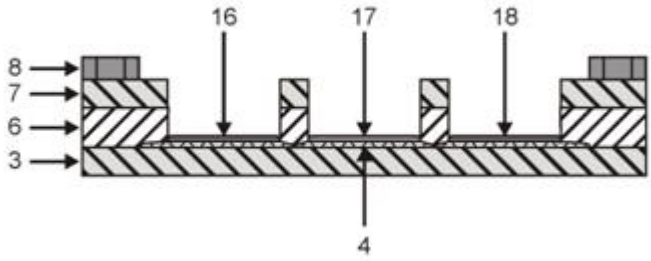

Figure A9 - Longitudinal section of the device in open configuration.

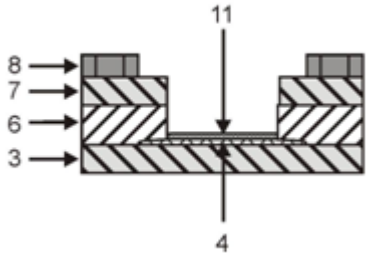

Figure A10 - Transversal section of the device in open configuration.

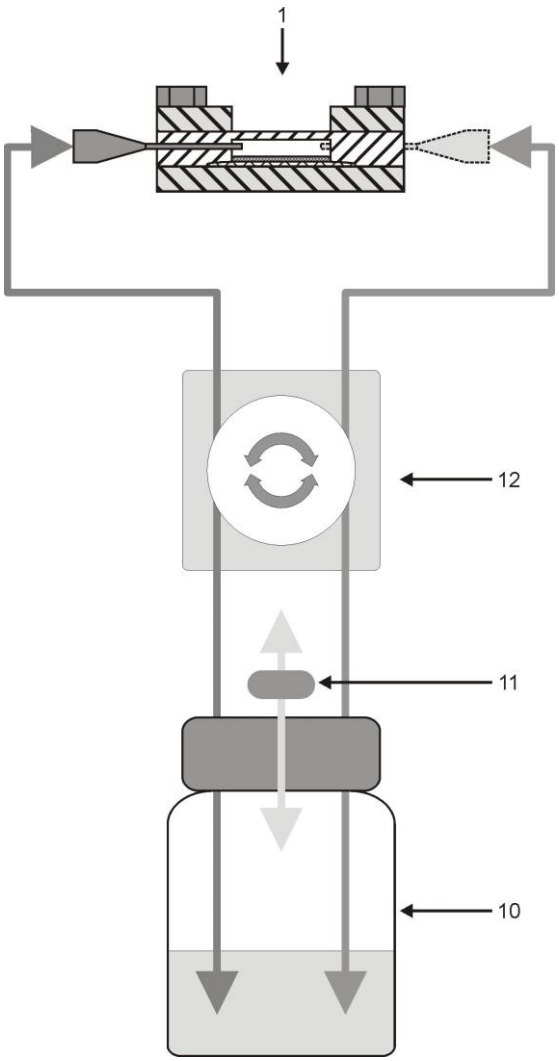

Figure A11 - Device in closed configuration integrated into a complete dynamic cell culture system.

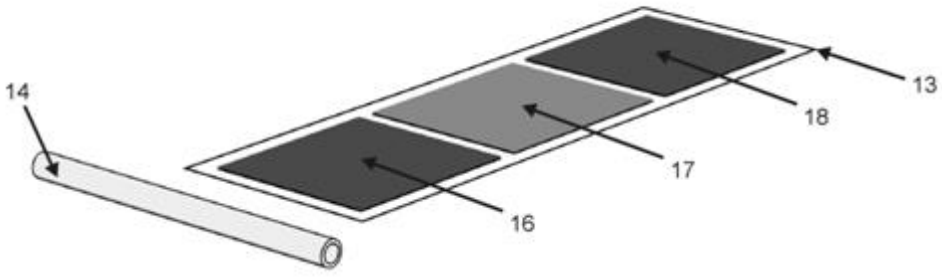

Figure A12 - Porous membrane and rolling structure before rolling the porous membrane containing three different cellular populations over its surface in order to generate a stratified tubular structure.

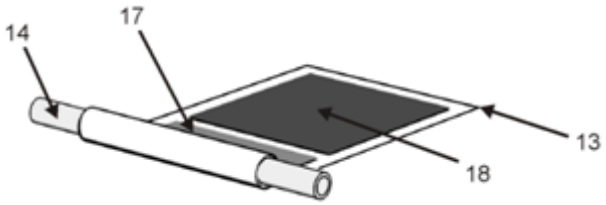

Figure A13 - Porous membrane partially rolled around the rolling structure in order to generate a stratified tubular structure.

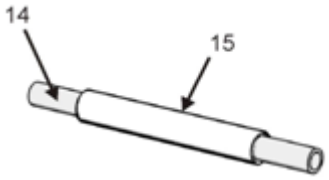

Figure A14 - Porous membrane totally rolled around the rolling structure.

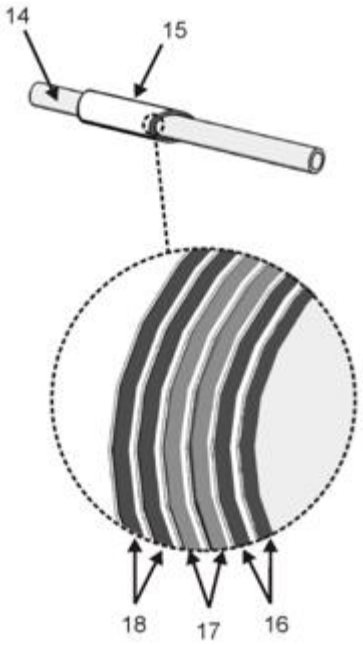

Figure A15 - Transversal section of the porous membrane rolled around the rolling structure and showing its inner stratified structure possessing different cellular populations located into different layers.

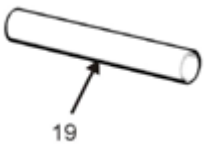

Figure A16 - Stratified tubular tissue substitute after removal of the rolling structure.